93122-01

ACSYNT Inner Loop Flight Control Design Study

NAS2-13701

Richard Bortins and John A. Sorensen

Prepared for:

The National Aeronautics and Space Administration
Ames Research Center
Systems Analysis Branch
Mountain View, California

Under:

Contract No. NAS 2-13701

July 1993

Table of Contents

1 Introduction 1

1.1 Background 1
1.2 ACSYNT Vision 2
1.3 Project Summary 3
1.4 Road Map to Report 4

2 Inner Loop Flight Control Module Functional Requirements 5

2.1 Inputs to the ILFCS Design Process 6
2.1.1 Default Parameter Sets 6
2.1.2 Inputs from the User 7
2.1.3 Inputs from ACSYNT 8
2.2 Outputs of the ILFCS Design Process 8
2.2.1 Outputs to the User 8
2.2.2 Outputs to ACSYNT 9
2.3 Conclusion 9

3 Control Effector Design 11

3.1 Effectors 11
3.1.1 Definition 11
3.1.2 Control Surface Design Considerations 11
3.1.3 Preliminary Control Surface Design Methodology 17
3.2 Control Derivatives 18
3.2.1 Air Worthiness Constraints 19
3.2.2 Design Inputs Required 22
3.2.3 DATCOM Methodology for Computing Control Derivatives 22
3.3 Conclusion 45

4 Inner Loop Control Design 47

4.1 Aircraft Dynamics 47
4.1.1 Decoupled Dynamics 48
4.1.2 Coupled Dynamics 49
4.1.3 Dynamics of Case Studies Aircraft 50
4.2 Actuators 51
4.3 Sensors 54
4.4 The FCS Design Algorithm 54
4.4.1 The Linear-quadratic Method 55
4.4.2 Enumeration of the Steps in the Algorithm 57
4.4.3 Discussion of Case Studies 58
4.5 Conclusion 62

5 Summary and Recommendations 63

5.1 Summary 63

5.1.1 FCS Design Requirements 63

5.1.2 Control Effector Design 63

5.1.3 Inner Loop Flight Control Design 64

5.2 Recommendations for Further Work 64

5.2.1 Immediate Tasks 64

5.2.2. Intermediate Tasks 65

References 67

Appendix 69

1 Introduction

The NASA Ames Research Center developed the Aircraft Synthesis (ACSYNT) computer program to synthesize conceptual future aircraft designs and to evaluate critical performance metrics early in the design process before significant resources are committed and cost decisions made. ACSYNT uses steady-state performance metrics, such as aircraft range, payload and fuel consumption, and static performance metrics, such as the control authority required for the takeoff rotation and for landing with an engine out, to evaluate conceptual aircraft designs. It can also optimize designs with respect to selected criteria and constraints.

Many modern aircraft have stability provided by the flight control system rather than by the airframe. This may allow the aircraft designer to increase combat agility, or decrease trim drag, for increased range and payload. This strategy requires concurrent design of the airframe and the flight control system, making trade-offs of performance and dynamics during the earliest stages of design.

ACSYNT presently lacks means to implement flight control system designs but research is being done to add methods for predicting rotational degrees of freedom and control effector performance. A software module to compute and analyze the dynamics of the aircraft, and to compute feedback gains and analyze closed loop dynamics is required. The data gained from these analyses can then be fed back to the aircraft design process so that the effects of the flight control system and the airframe on aircraft performance can be included as design metrics.

This report presents results of a feasibility study and the initial design work to add an inner loop flight control system (ILFCS) design capability to the stability and control module in ACSYNT. The overall objective is to provide a capability for concurrent design of the aircraft and its flight control system, and enable concept designers to improve performance by exploiting the interrelationships between aircraft and flight control system design parameters.

1.1 Background

The objective of aircraft conceptual design is to answer basic questions of configuration arrangement, size and weight, cost, and performance.[1] The goal is to work through the major choices available to aircraft designers rapidly, efficiently, and effectively to arrive at a configuration that satisfies the given requirements. Designers use rules of thumb, algorithms, design guidelines, history and projections of the capabilities of new technology to determine how best to satisfy many diverse and sometimes conflicting requirements. The conceptual design phase ends with specialists in disciplines such as aerodynamics, structures, propulsion and control systems using specialized tools to analyze their parts of the problem. At this point, the design effort fragments into specialized disciplinary efforts that may or may not stay in step with each other. The conceptual design phase is unique in that it is the only time the aircraft design resides in a single designer's mind or on a single computer.[2]

The ACSYNT program uses parameter studies, industry practices, and important trends to estimate the aerodynamic, structural, weight and balance, propulsion, stability and control, and economic characteristics of a conceptual design. It provides six ways to arrive at a final conceptual design:[3, 4]

- Converge to the appropriate fuel loading for a given design point
- Optimize a specified function with respect to specified constraints
- Compute the sensitivity of one or more specified functions to one or more design variables
- Analyze specified combinations of two design variables
- Compute the sensitivity when the design is optimized with respect to the remaining independent design variables
- Optimize using approximation techniques

Presently, ACSYNT evaluates longitudinal, steady-state flight performance at discrete design points.

1.2 ACSYNT Vision

ACSYNT continually evolves to account for technology advances, and to add precision and expanded capabilities in the aircraft disciplines of propulsion, aerodynamics, structures, and stability and control that are required to perform and evaluate design trades between the disciplines at the conceptual design level. This enables concept designers to improve the performance of their designs by exploiting the interrelationships between design parameters that are in the domains of these more specialized disciplines.

Figure 1.1 shows the software modules comprising ACSYNT and some of the organizations currently assisting NASA in this development.

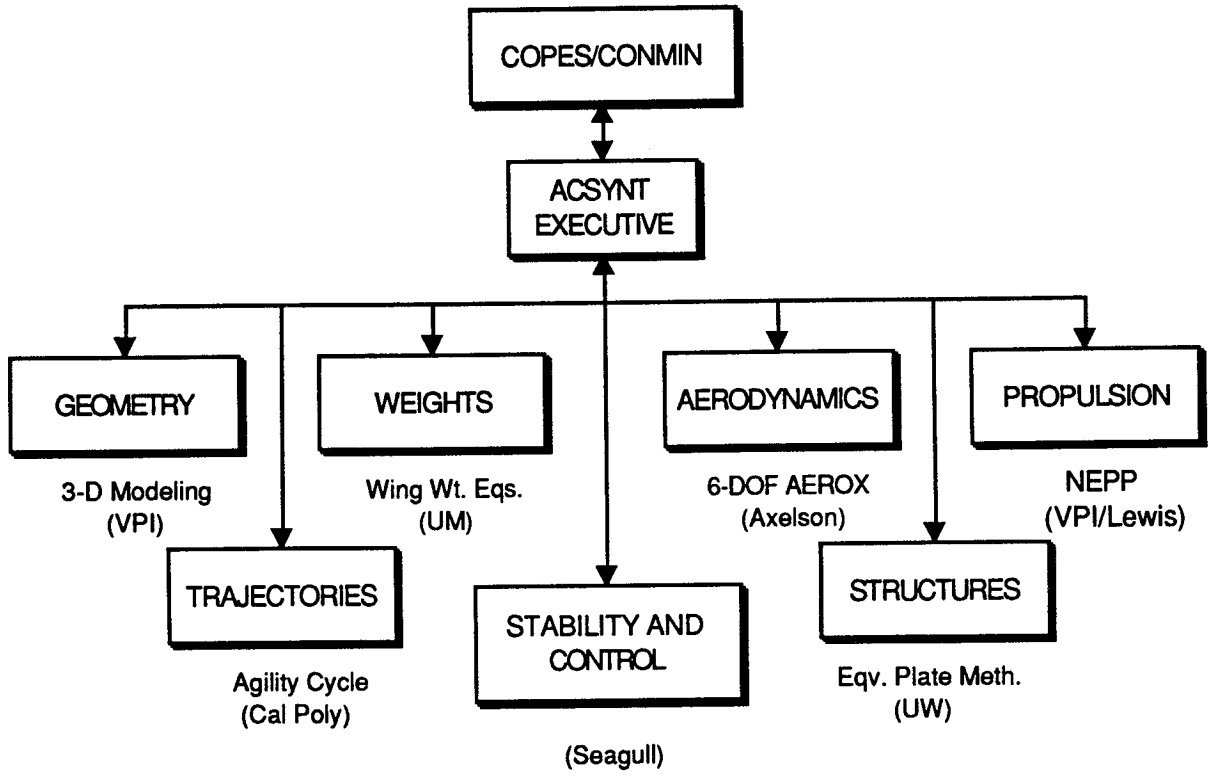

Figure 1.1: ACSYNT software modules

Enhancing ACSYNT capabilities must avoid increasing the number of required inputs excessively and adding such complexity in the specialized disciplines that the tool is no longer usable by aircraft concept designers. The objectives are to determine rapidly and efficiently the effect on total aircraft performance of design changes at high levels within these disciplines and to allow discipline specialists the opportunity to understand how their efforts affect other disciplines.

Each discipline has so many design parameters and performance metrics that only parameters and metrics of each discipline that have the most influence on aircraft performance must be identified and integrated into the concept design process. This integration should use formulations and approximations that promote rapid design iterations until more design details can be established.

A designer has many choices available. Adding additional level of detail to ACSYNT will increase the number of choices and the difficulty of comparing multiple concepts and the time required as more choices will have to be made without the aid of the ACSYNT tool. To enable a designer to focus on the effects on performance of specific aspects of the aircraft, initial designs that satisfy all constraints must be provided. Moreover, default constraints must also be provided. These defaults and initial designs provide a point of departure for the designer. The data for the defaults and initial designs can come from historical trends. Finally, warnings for convergence to atypical solutions and suggested remedies must be provided to the designer.

1.3 Project Summary

This project had the following goals:

- Determine what additional detail is required in ACSYNT to include an inner loop flight control system design capability
- Provide for the design of an inner loop of a flight control system (FCS) by determining the level of modeling fidelity and the importance of terms in the aircraft dynamics
- Evaluate the costs and benefits of including lateral/longitudinal coupling in the inner loop FCS control design
- Design an FCS architecture to support the conceptual design mission of ACSYNT
- Evaluate synthesis techniques for the FCS architecture and the design operating points
- Determine how to integrate the inner loop FCS design and performance evaluation parameters with ACSYNT

This report summarizes the progress made towards these goals.

ACSYNT must calculate rotational dynamics to implement an inner loop flight control system synthesis algorithm. Such an algorithm needs, as a minimum,

- Aircraft stability and control derivatives
- Aircraft mass properties such as mass, center of mass, and moments of inertia
- Flight condition data such as attitude, velocity and atmospheric density

Aircraft stability and control derivatives describe non-steady-state aerodynamics during linear control design. The control derivatives characterize force and moment generators and depend on their size, aerodynamic shape, and location. The mass properties are determined by weight and

configuration layout. The flight conditions are used to convert dimensionless derivatives to dimensioned derivatives and to compute output quantities such as angle of attack, α, and sideslip angle, β.

Control surface sizing and control derivative computation methods were found in references[5, 6, 7] and are summarized in this report. The design approach adopted for ACSYNT will use linearized aircraft dynamics at selected flight conditions within the flight envelope. The linear-quadratic method was chosen as the flight control system design algorithm because it accommodates linearized dynamics with lateral/longitudinal coupling and because it provides a "hands-off" way to compute feedback gains from design criteria. The linear-quadratic method uses the dynamics in state-space form, and the important stability derivatives to form these dynamics were identified. The state-space form has the advantages that many analytical, design, and simulation tools exist for dynamics in this form. The FCS architecture will assume that all aircraft state variables can be measured perfectly and fed back through a control law to the actuators to guarantee closed loop stability even when aircraft dynamics is open loop unstable.

Case studies comprising 3 aircraft, each at 3 flight conditions, were used to test the pole placement method and the linear-quadratic method. A single set of initial control design parameters were found to give acceptable results for the longitudinal dynamics. This provides a good starting point for automated control design iterations. We also tested the method on lateral/directional dynamics. A preliminary specification for an interface between ACSYNT and an inner loop control design module has been formulated.

1.4 Road Map to Report

This report summarizes the results, findings, conclusions and recommendations based on the work performed to date for contract NAS 2-13701. Technical details such as MATLAB scripts and plots, and notes and reprints from references have been assembled into the Appendices.

Section 1 contained the introduction, background, ACSYNT vision and project summary. Section 2 presents interface requirements for the addition of an inner loop flight control design module to ACSYNT. The requirements comprise what is needed by such a module from other ACSYNT modules and what results will be returned to the user and other ACSYNT modules. Section 3 discusses control surface sizing and control derivative computation. This reiterates methods found in Roskam and other references. Section 4 discusses flight dynamics, presents the inner loop flight control design algorithm and summarizes the results of the case studies. The last section summarizes our findings and presents recommendations for the continuing development of the ACSYNT stability and control module.

2 Inner Loop Flight Control Module Interface Requirements

This section discusses the inner loop control design interface with ACSYNT. Figure 2.1 is a top level diagram of the organization for an inner loop control design module.

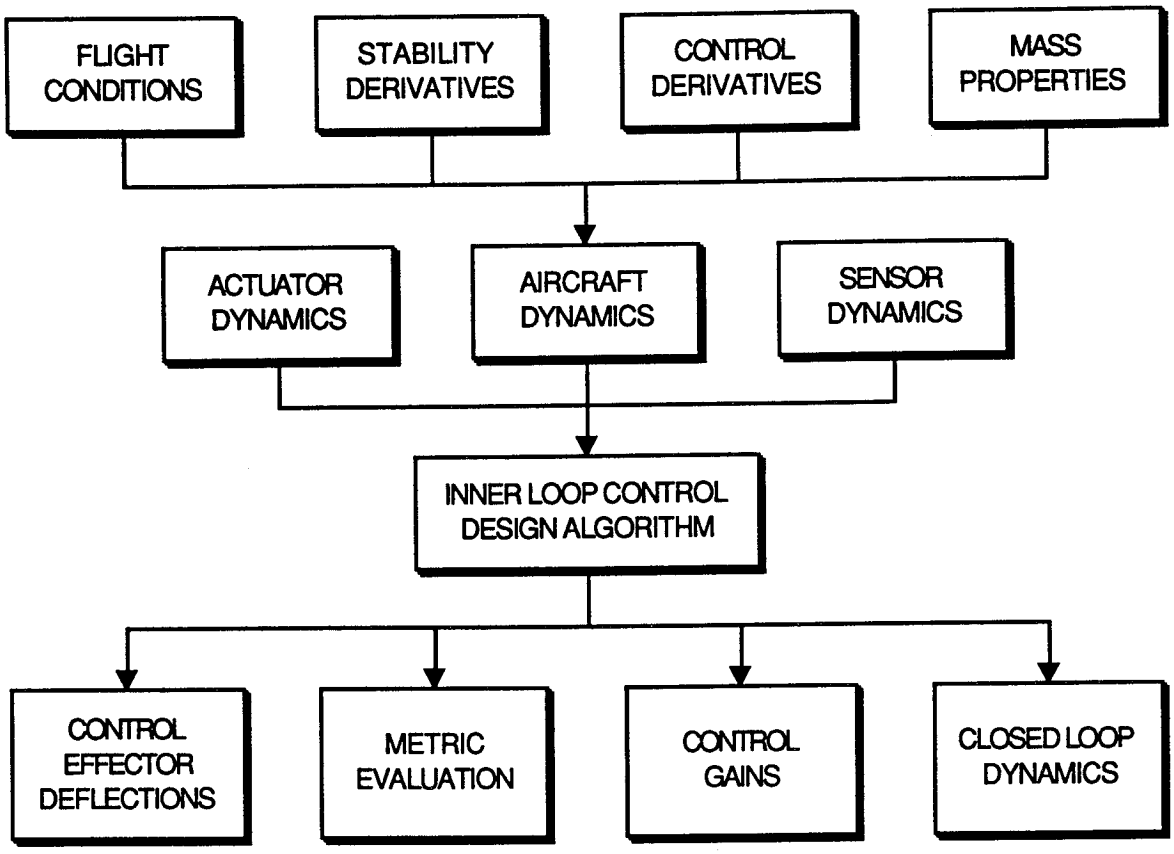

Figure 2.1: Schematic of the inner loop flight control system (ILFCS) design module

The elements in the top row are inputs to the inner loop control module from ACSYNT, default data sets, or user input. The flight conditions, stability derivatives, control derivatives, and mass properties are used to calculate the aircraft dynamics. Sensor and actuator dynamics and errors also affect flight control system performance. Section 4 gives a justification for assuming, for the purposes of conceptual design, that sensor dynamics are perfect. The methodology chosen does not preclude addition of sensor models in the future. Actuators will have first-order dynamics with time constants loaded from the default data sets. The composite of the aircraft and actuator dynamics is the main input to the inner loop control design algorithm. The algorithm produces a set of feedback gains that satisfy some design criteria. The closed loop dynamics are used to evaluate performance metrics in a simulation or are downloaded into a cockpit simulator for pilot evaluation. Data from control effector deflections that violate design constraints are fed back to the aircraft design modules to provide a basis for updating effector design parameters. The variation in feedback control gains over several flight conditions indicates the potential complexity of the ultimate flight controller; a high variation implies a complex controller that in turn implies a higher cost flight control computer.

The interface requirements for the ILFCS design module are discussed in two parts. Subsection 2.1 covers the necessary inputs to the ILFCS design process. Subsection 2.2 discusses the outputs that the ILFCS design process provides to the designer and as feedback to the ACSYNT design and optimization process.

2.1 Inputs to the ILFCS Design Process

There are three classes of inputs to the ILFCS design process.

- Default parameter sets
- Inputs from the user
- Inputs from ACSYNT

The default parameter sets provide initial estimates of flight control system parameters to minimize designer workload when the FCS is not the primary concern. The inputs from the user are made when the designer has special considerations, such as mission and flight conditions. The user can also override any default parameter. The inputs from ACSYNT are the data computed by other ACSYNT modules that are necessary to define the aircraft dynamics.

2.1.1 Default Parameter Sets

The purpose of the default flight control system design parameters is to provide an initial design that is a realistic point of departure for including the control design considerations without thought or effort. This is usually done early in the aircraft design process. The performance of this initial controller will be reasonable enough for initial studies. Ultimately, the algorithm will converge to a much better performing controller after starting with this initial design.

The default flight control system design parameter sets are organized by aircraft class. The MIL-F-8785C classification (Table 2.1) has been selected.

Table 2.1 MIL-F-8785 C Aircraft Classification

Class	Aircraft Type
I	small and light
II	medium weight and low to medium maneuverability
III	large, heavy and low to medium maneuverability
IV	high maneuverability

Most civilian aircraft can be mapped into the first three classes. The case studies presented in this report are from the last three classes. The methodology and data bases used to derive parameters are unique to these classes.

The default design parameter sets are the appropriate control system design specifications. There are three classes of specifications:

- Design objectives (*e.g.*, stability, no oscillation)
- Design constraints (*e.g.*, deflection and rate limits)
- Fixed design variables (*e.g.*, dynamics of sensors and actuators)

The usual design objective is to optimize a particular performance metric while staying within constraints on other performance metrics. Thus, the control design parameters in the default design parameter sets are the constraints on the metrics not optimized and designation of which metric is to be optimized. These design objectives are the defaults rather than, say feedback gains, because gains depend on the particular aircraft dynamics while the constraints and the metric to optimize depends more on the aircraft class. Useful measures of control system performance are:

- Percent overshoot
- Rise time
- Peak control surface deflection
- Peak vertical and lateral acceleration
- Percent steady-state error
- Closed loop natural frequencies
- Closed loop damping ratios

The first four metrics are transient, time-domain measures. They require a simulation capability to evaluate. The steady-state error can be evaluated analytically only when no nonlinearities are present; otherwise a simulation capability again is required. The last two metrics directly relate to aircraft handling qualities and can always be evaluated analytically.

2.1.2 Inputs from the User

The designer will select an aircraft class and an aircraft mission. The selection of a class loads the control design criteria appropriate for that class, as described in the previous subsection. The designer can override any of the default design parameter values. The aircraft mission determines the flight conditions used to compute the aircraft dynamics, and the stability and control derivatives. The flight conditions are made up of maneuvers such as

- Steady, level flight
- Steady, level turns
- Steady climbs or descents
- Steady rolls
- High angle of attack maneuvers
- One engine inoperative
- Take-off
- Approach

at various combinations of altitude and velocity. The first and last three flight conditions are applied to all classes of aircraft. The middle two are usually applied only to fighter aircraft in Class IV.

2.1.3 Inputs from ACSYNT

The primary data required from ACSYNT modules are

- Mass properties
- Stability derivatives
- Control derivatives

These are used to compute the aircraft dynamics. The mass properties include mass, center of mass, and the inertia matrix. The orientation of the body axes with respect to the stability axes is also needed if the inertias are defined with respect to the body frame. The stability and control derivatives are usually divided into longitudinal derivatives and lateral/directional derivatives because the aircraft dynamics decouples (Table 2.2).

Table 2.2: Stability and control derivatives

Longitudinal		Lateral	
C_D	C_{L_q}	C_{y_β}	C_{n_p}
C_{D_u}	C_{L_δ}	$C_{y_{\dot\beta}}$	C_{n_δ}
C_{D_α}	C_m	C_{y_r}	C_{l_β}
C_{D_δ}	C_{m_u}	C_{y_p}	$C_{l_{\dot\beta}}$
C_L	C_{m_α}	C_{y_δ}	C_{l_r}
C_{L_u}	$C_{m_{\dot\alpha}}$	C_{n_β}	C_{l_p}
C_{L_α}	C_{m_q}	$C_{n_{\dot\beta}}$	C_{l_δ}
$C_{L_{\dot\alpha}}$	C_{m_δ}	C_{n_r}	

At some flight conditions the dynamics are coupled, so other stability and control derivatives may be necessary.

2.2 Outputs of the ILFCS Design Process

Two kinds of outputs are required of the ILFCS design process. The first are the data provided to the user to show how well the process is converging, how good the final controller performs, and what might be done to improve performance. The second are data provided to ACSYNT modules (most likely the COPES/CONMIN optimization program) to integrate the ILFCS design process into ACSYNT's design optimization and sensitivity computation functions.

2.2.1 Outputs to the User

The main driver for the user outputs is that they be useful to an aircraft designer rather than a feedback control expert. Four types of data will be useful:

- Plots of time responses
- Performance metric values
- Design constraint values
- Iteration history

The plots of time responses are probably of the most use to an aircraft designer. The particular variables of interest will depend on the class of aircraft, and, consequently, the default design parameters. The designer will also be able to specify other variables. The performance metric values and the design constraint values indicate how well the control system performs and what might be limiting the performance when a constraint has been reached or violated. The iteration history will show how the control design algorithm arrived at its results.

2.2.2 Outputs to ACSYNT

The main driver for ACSYNT outputs is to integrate the control design process into the functionality that exists in ACSYNT for aircraft design. The primary data required by ACSYNT modules are

- Closed loop performance metric values
- Control system gains
- Actuator and sensor requirements for constraint definition
- Locally optimized FCS parameters
- Sensitivities to stability and control derivatives

The goal is to establish a capability to use the dependencies between aircraft and flight control design parameters to improve total aircraft performance. This can be done by brute force or by local optimization within the ILFCS design module. It is not clear at this point which way is more appropriate.

The brute force approach integrates the control design parameters and performance metrics with the COPES/CONMIN design optimization process. Integration into the sensitivity computations should be around the same level of difficulty. This integration is conceptually simple; the control parameters and metrics are just added to the ones COPES/CONMIN already handles. However, conceptually simple does not mean that it is practically simple.

The local optimization approach identifies ways to change stability and control derivatives to improve control system performance. This data can be fed back to the stability and control derivative computations to determine which aircraft parameters ought to be changed. The violation of control effector deflection or rate limits is the easiest to feed back. All that is required is an indication of how much to increase the control derivative magnitudes. Changes in the stability derivatives is another matter. This is much more conceptually difficult than the brute force method because it requires inverting some complex, difficult, and possibly singular computations. Dynamical approximations exist that give damping ratios and natural frequencies as simple functions of a few stability derivatives, but these approximations can be very inaccurate.

2.3 Conclusion

This section presented the interface requirements for adding an inner loop flight control system design module to the ACSYNT program. Both user interface and program module interface requirements were discussed. The next two sections give details on the functionality required.

3 Control Effector Design

This section outlines the procedures to add to the ACSYNT code to design flight control effectors and to compute the associated control derivatives. These must be added to ACSYNT when an ILFCS design module is added because the control derivatives are essential ingredients to flight control design.

3.1 Effectors

3.1.1 Definition

In the context of aircraft design, the control effectors are the mechanisms that are used to produce forces and moments for controlling the roll, pitch, and yaw orientation of the aircraft. Conventionally, these effectors have consisted simply of aileron, elevator and rudder for roll, pitch, and yaw control, respectively. These effectors are classified as "control surfaces" because they are movable surfaces on the wing and tail; they produce control moments by altering the basic lift forces and restoring moments produced by the aerodynamics of the wing and tail.

As aircraft designs have become more complex, different control surface designs and combinations of designs have appeared. These include elevons, carnardovators, stabilators, and spoilers. However, the design principles remain the same for each of these control surface variations.

For high performance aircraft or aircraft with special mission requirements, other force generators besides control surfaces have been developed. These consist of directed thrust forces from the propulsion system to allow special movements such as near vertical takeoff and hover, yaw without roll, control without need for a vertical tail, etc.

In the following, the design outline is limited to requirements for specifying and sizing control surface effectors. However, the ACSYNT logic development will be designed to be modular so that other force generators could be added as design options at a later date.

3.1.2 Control Surface Design Considerations

Three passes are made through the design cycle to determine the geometry of the control surfaces:

1. The baseline control surface geometry is selected subject to surface constraints determined by other design considerations, as discussed below. This selection is based upon historical average size and dimension for similar types of aircraft.
2. The control moment provided by the baseline design is checked against minimum static requirements that are stated as Military Specifications (Milspecs) or Federal Aviation Regulations (FARs). If necessary, the control surface area or the moment arm is increased to meet the requirements.
3. The control moment effectiveness is checked by examining the transient dynamic response of the aircraft with the flight control system (FCS) in place. If the transient performance can not meet requirements by FCS gain adjustment and design changes alone, then it may be necessary to increase the control surface size and moment arm further or to change the configuration geometry.

The next two subsections discuss the geometric constraints and historical data used during the first design pass.

3.1.2.1 *Geometric constraints*. This refers to constraints to the geometric dimensions of the control surface caused by the presence of other items or practical structural constraints.

a. Ailerons and elevons - Fig. 3.1 is a sketch of a wing planform with flap and aileron. The flap is designed first to give the appropriate slow speed lift characteristics for the landing or takeoff process. This sets the inner span boundary y_{ai} for most ailerons. The exception is for some jet transports where inner and outer sets of ailerons are used inside and outside of the flaps. For this case, the flaps also set the outer span boundary for the inner aileron. For delta wing aircraft, elevons are used for both roll and pitch control. The geometric constraints imposed by the flaps are the same, however. The outer limit of the aileron span y_{ao} is the wing half-span b. For inboard ailerons, the inner span boundary is some reasonable margin from the fuselage wall.

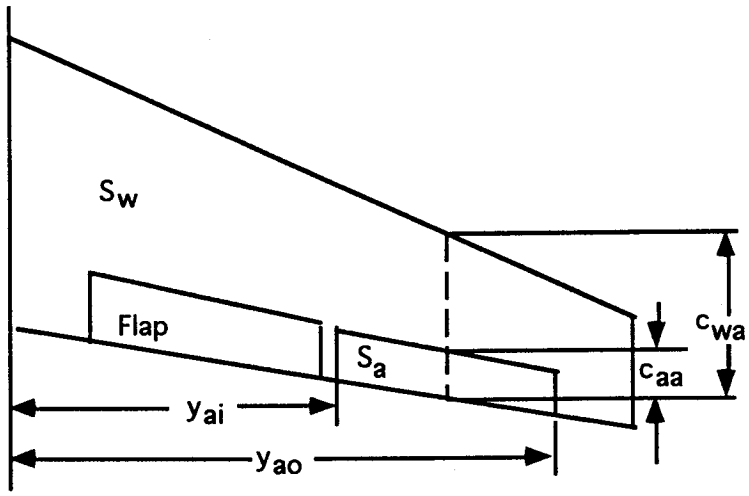

Figure. 3.1 Sketch of wing planform.

The other parameters that specify aileron size are the surface area S_a and the average chord dimension c_{aa}. The average chord dimension is measured at the average aileron span location. The aileron chord is often set by the location of the rear wing spar. That is, the aileron surface hinges are mounted to the rear wind spar. Thus, there is a structural limit to the chord dimension. For design practicality, the forward dimension of the aileron can be set equal to that of the flaps.

b. Rudder - The geometry of the rudder is dictated by the geometry of the vertical tail, the horizontal tail (in the case of a T tail), the fuselage, and possibly the presence of a mid-tail engine. Figure 3.2 shows examples of vertical tails[7]. The rudder would be specified to run a certain fraction of the span b_v of the tail. When the horizontal and vertical tail geometries and engine locations are specified within the ACSYNT design process, logic must be added to constrain the inner and outer rudder spanwise dimensions in compliance with the geometries. When the basic rudder geometry is computed, it is limited by the geometric constraints.

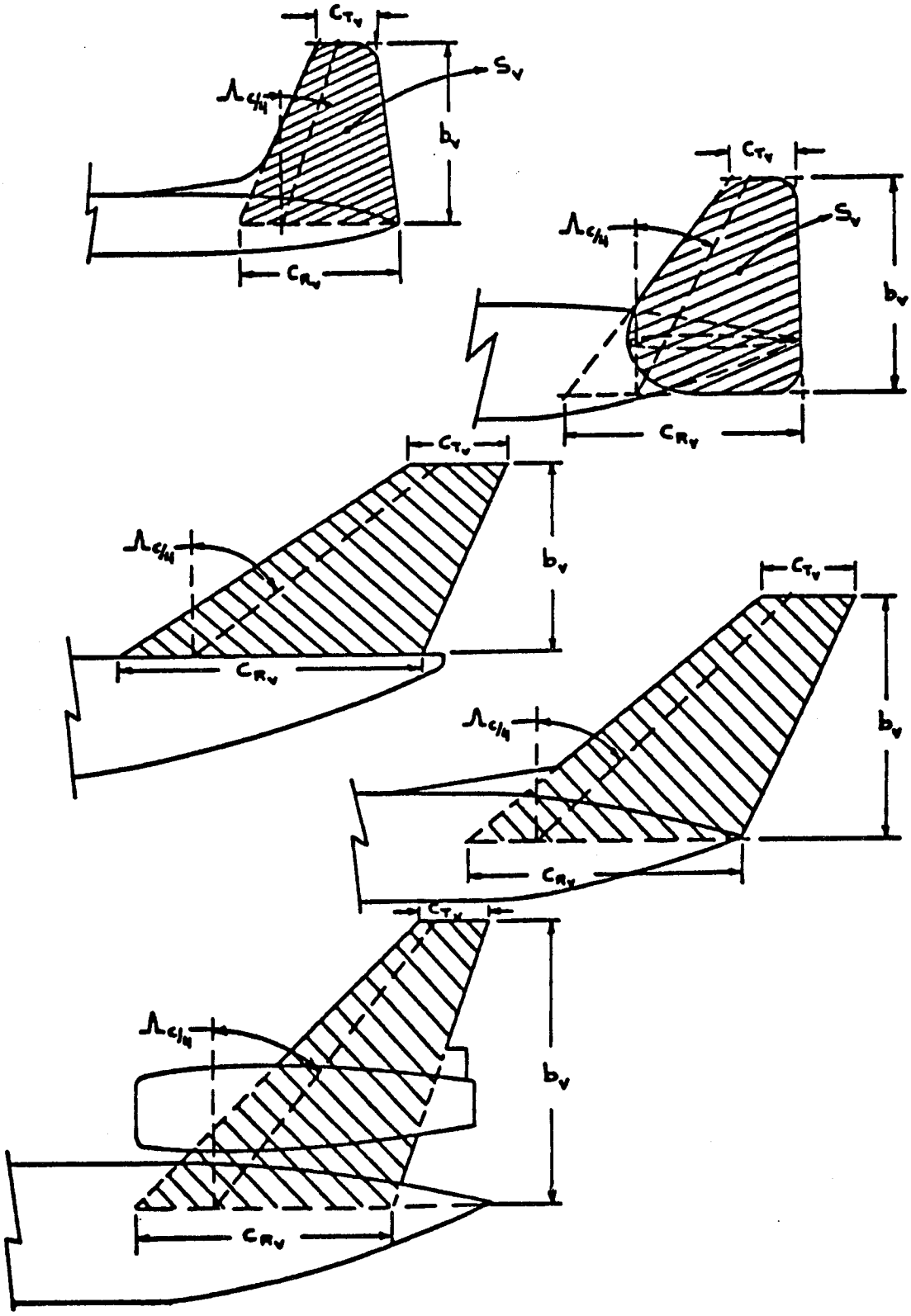

Figure 3.2 Examples of vertical tail geometries [Roskam[7]]

c. Elevator and stabilator - The elevator geometry is dictated by the geometry of the horizontal tail. Normally, the only constraint is the inner span location; this is dictated by the fuselage wall or the vertical tail wall for T-tail design. The inner span elevator dimension may be limited so as to not interfere with full rudder deflection. For a stabilator, the entire horizontal tail is both the horizontal stabilizer and the elevator; designing the stabilizer takes care of the stabilator design.

3.1.2.2 *Historical trends*. For the first design pass for aileron, rudder, and elevator geometry design, initial estimates of span, chord or surface area can be based on trends in historical data for the same parameters. The following Tables 3.1-3.3 summarize these parameters for three classes of aircraft - fighters, business jets, and jet transports. These data are repeated from Roskam[5] which contains larger tables and for several other types of aircraft.

Table 3.1 Fighter aircraft control surface parameters

	Elevator Data		Rudder Data		Aileron Data		
Type	S_e/S_h	fr. c_h	S_r/S_v	fr. c_v	S_a/S_w	fr. $b/2$	fr. c_w
Dassault Mir. IIIe	0	elevons	.20	.22/.29	.14	.18/1.0	.13/1.0
Mir. F1C	1.0	stabilator	.16	.21/.35	.031	.77/1.0	.23/.25
Mir. 2000	0	elevons	.16	.21/.34	.13	.19/1.0	.13/1.0
Super Et.	1.0	stabilator	.18	.25/.49	.053	.57/.81	.23/.27
FR A-10A	.32	.33	.28	.31/.34	.094	.58/.91	.42/.40
Grum. A6A	1.0	stabilator	.21	.28/.21			
Grum. F14A	1.0	stabilator	.29	.29/.33			
North. F5E	1.0	stabilator	.15	.26/.30	.050	.76/.99	.34/.33
Vought A7A	1.0	stabilator	.13	.21/.29	.053	.59/.90	.20/.24
McD D F-4E	1.0	stabilator	.20	.20/.29	.040	.63/.98	.23/.28
McD D F-15	1.0	stabilator	.25	.30/.50	.053	.60/.86	.25/.27
G D FB-111A	1.0	stabilator	.21	.25/.26			
G D F-16	1.0	stabilator	.25	.34/.33	.13	.30/.73	.21/.23
Cessna A37B	.25	.34/.31	.35	.37/.39	.061	.56/.91	.27/.32
Aermacchi MB339K	.29	.26/.37	.26	.26/.41	.069	.58/.90	.24/.26
MIG-25	1.0	stabilator	.15	.24	.053	.54/.79	.22/.21
Su-7BMK	1.0	stabilator	.26	.28/.25	.11	.62/.97	.29/.35

In the tables, the ratios of control surface area to wing, horizontal, or vertical tail areas are given as S_a/S_w, S_e/S_h, and S_r/S_v. The corresponding ratios of control surface chord to wing or tail surface chord are given as fr. c_w, fr. c_h, and fr. c_v. When two numbers are given, for chord ratios, this represents the inboard and outboard edges of the control surface. For the aileron data, the spanwise edges are specified as fractions of the half wing span, or fr. $b/2$.

For fighter aircraft, Table 3.1 shows that most types of aircraft use stabilators rather than the elevator. Two Mirage types use elevons to combine the functions of elevator and aileron into one surface; these are delta wing configurations. The rudder surface represents about 22% of the vertical stabilizer surface on the average with the chord dimension ranging from 20% to 50% of the total chord, depending on the configuration. For the fighter aircraft ailerons, the spanwise dimension ratio ranges from .18 to .77 inboard and from .73 to 1.0 outboard. The aileron surface area averages to about 7.6% of the wing surface area for the aircraft listed in Table 3.1.

Table 3.2 Business jet aircraft control surface parameters

	Elevator Data		Rudder Data		Aileron Data		
Type	S_e/S_h	fr. c_h	S_r/S_v	fr. c_v	S_a/S_w	fr. $b/2$	fr. c_w
Dassault Falcon 10	.20	.31/.29	.32	..34/.49	.051	.67/.95	.27/.31
Falcon 20	.22	.28/.31	.23	.25/.39	.057	.62/.92	.25
Falcon 50	.23	.31/.34	.12	.21/.32	.049	.68/.97	.27
Cessna Citation 500	.29	.32/.23	.36	.36	.096	.55/.94	.32/.30
Citation II	.36	..37/.35	.34	.35/.31	.078	.56/.89	.32/.30
Citation III	.34	.39/.42	.30	.37/.38		.70/.86	.21/.17
Gates Learjet 24	.26	.36/.26	.17	.23/.22	.050	.63/.89	.25/.23
Learjet 35A	.33	.33	.17	.26/.25	.066	.55/.79	.30/.27
Learjet 55	.32	.31/.35	.17	.26/.25	.062	.49/.71	.30
Canadair Challenger	.28	.30/.31	.26	.29/.31	.033	.73/.91	.23/.26
Aerospatiale SN-601	.42	.40/.44	.30	.36/.32	.033	.68/.91	.22/.20
Israel Airc.Astra	.25	.30/.32	.21	.33/.32	.040	.67/.95	26/.25
Westwind	.25	.29/.26	.18	.34/.44	.050	.59/.90	.21/.31
Brit. Aero. 125-700	.48	.37/.67	.22	.31/.37	.084	.66/1.0	.33/.46
G.A. III	.33	.33	.24	.28	.038	.66/.86	.24/.27
MU Diam.I	.37	.37	.25	.33/.28	.012	.86/.94	.20/.22

From Table 3.2 for business jets, all the designs are conventional with elevator, rudder and aileron surfaces. The average elevator area is 30.8% of the horizontal stabilizer area. The average rudder area is 24.0% of the vertical stabilizer area. The average aileron area is 5.3% of the wing area.

For jet transports, Table 3.3 shows that this class of aircraft has a conventional tail configuration. The exception is the L1011 which uses a stabilator. The average elevator surface area is 32.4% of the horizontal tail area. The average rudder surface area is 29.3% of the vertical tail area.

The roll control for jet transports uses both inboard and outboard ailerons and spoilers. Table 3.3 presents span and chord dimensions for all four surfaces. Typically, the inboard ailerons operate in all flight conditions, but the outboard ailerons operate with flaps down only. Spoilers are used

for both lateral control and as speed brakes. Of the 17 aircraft types in Table 3.3, the nine smaller aircraft (B737 etc.) do not have inboard ailerons. The exception is the A310 which does not have outboard ailerons. All configurations but the Fokker F-28 have inboard spoilers. Only four of the types have outboard spoilers. The average aileron surface area is 3.7% of the wing surface area. Thus, for conceptual design of jet transports, the roll control surface design can be primarily by means of inboard spoilers and outboard ailerons for "large" classification aircraft with inboard ailerons added for the "heavy" classification.

Table 3.3 Jet transport aircraft control surface parameters

	Elevator		Rudder		Inboard Aileron		
Type	S_e/S_h	fr. c_h	S_r/S_v	fr. c_v	S_a/S_w	fr. $b/2$	fr. c_w
Boeing 727-200	.25	.29/.31	.16	.29/.28	.043	.38/.46	.17/.24
737-200	.27	.30/.32	.24	.25/.22	.024	none	none
737-300	.24	.24/.34	.31	.26/.50	.021	none	none
747-200B	.24	.29	.30	.30	.040	.38/.44	.17/.25
747SP	.21	.32/.20	.27	.31/.34	.040	.38/.44	.17/.25
757-200	.25	.29/.38	.34	.35/.33	.027	none	none
767-200	.23	.30/.25	.35	.33/.36	.041	.31/.40	.23/.20
McD D DC-9-80	.34	.39/.38	.39	.49/.46	.030	none	none
DC-9-50	.38	.41/.47	.41	.45/.44	.038	none	none
DC-10-30	.22	.25/.30	.18	.35	.047	.32/.39	.20/.25
AIRBUS A300-B4	.26	.35	.30	.35/.36	.049	.29/.39	.23/.27
A310	.26	.33/.30	.35	.33/.35	.027	.32/.40	.23/.27
Lockheed L1011	1.0	stabilator	.23	.29/.26	.051	.40/.49	.22/.23
Fokker F-28	.20	.34/.33	.16	.29/.31	.034	none	none
BAC 111	.27	.41/.35	.28	.39/.37	.030	none	none
BAC 146-200	.39	.42/.44	.44	.29	.046	none	none
Tu-154	.18	.27/.25	.27	.37	.036	none	none

Table 3.3 Continued.

Type	Outboard Aileron		Inboard Spoiler		Outboard Spoiler	
	fr. *b/2*	fr. c_w	fr. b/2	fr. c_w	fr. *b/2*	fr. c_w
Boeing 727-200	.76/.93	.23/.30	.14/.37	.09/.14	.48/.72	.16/.20
737-200	.74/.94	.20/.28	.40/.66	.14/.18	none	none
737-300	.72/.91	.23/.30	.38/.64	.14	none	none
747-200B	.70/.95	.11/.17	.46/.67	.12/.16	none	none
747SP	.70/.95	.11/.17	.46/.67	.12/.16	none	none
757-200	.76/.97	.22/.36	.41/.74	.12/.13	none	none
767-200	.76/.98	.16/.13	.16/.31	.09/.11	.44/.67	.12/.17
McD D DC-9-80	.64/.85	.31/.36	.35/.60	.10/.08	none	none
DC-9-50	.78/.95	.30/.35	.35/.60	.10/.08	none	none
DC-10-30	.75/.93	.29/.27	.17/.30	.05/.06	.43/.72	.11/.16
AIRBUS A300-B4	.83/.99	.32/.30	.57/.79	.16/.22	none	none
A310	none	none	.62/.83	.16/.22	none	none
Lockheed L1011	.77/.98	.26/.22	.13/.39	.08/.12	.50/.74	.14/.14
Fokker F-28	.66/.91	.29/.28	none	none	none	none
BAC 111	.72/.92	.26	.37/.68	.06/.11	none	none
BAC 146-200	.78/1.0	.33/.31	.14/.70	.22/.27	none	none
Tu-154	.76/.98	.34/.27	.43/.70	.14/.20	none	none

3.1.3 Preliminary Control Surface Design Methodology

This section outlines a procedure to follow in the ACSYNT geometry design code for specification of the dimensions of the control surfaces. This begins by picking average geometry and specifying the constraints if the control surface has to be changed to produce more control power. Average geometry is based on fractions of wing and tail span and chord dimensions. These terms are maintained within the default parameter data base within ACSYNT. The user has the option to override these default values for a particular design configuration.

The following is limited to three classes of aircraft – fighters, business jets, and jet transports. It can be expanded to include other aircraft classes using the basic methodology of this study.

3.1.3.1 *Ailerons and spoilers*. These two surfaces are designed after the wing planform and flap have been specified. The flap chord dimension defined by the leading edge of the flap is extended to define the leading edge and chord of the aileron. Also, the inboard span dimension of the flap defines the outboard span dimension limit of inboard ailerons. The outboard span dimension of the flap defines the inboard span dimension limit of outboard ailerons. Thus, choice of the average aileron surface area is used to define the rest of the aileron details.

a. Fighter aircraft. Assume that fighter aircraft only have outboard ailerons. Use the average aileron surface area to be 7.6% of the half wing area. Follow the following steps:
   1. Set the chord dimension by that of the flap surface chord.
   2. Solve for the aileron span to produce the desired surface area, taking into account the wing taper.
   3. Solve for the outboard aileron span dimension. Determine that this is within the wing half span limit.

b. Business jet aircraft. Assume that business jets only have outboard ailerons. Use the average aileron surface area to be 5.3% of the half wing area. Follow the same steps as for fighter aircraft.

c. Jet transport aircraft. Assume that large category transports have only outboard ailerons and spoilers. Use the average aileron surface area to be 3.0% of the half wing area. Then follow the same steps as for the fighter aircraft in designing the aileron. For the spoilers, use the average span and chord dimensions from aircraft with inboard spoilers only to position and dimension the spoilers.

For heavy category transports, add an additional 1.0% surface area to cover the inbound aileron design. Then follow the same steps as for the outbound aileron except for Step 3. Instead, assume the inbound aileron runs from the inner flap edge inward. Solve for the inner aileron span dimension to produce the desired area. Determine that this is beyond the fuselage wall distance from the aircraft centerline.

3.1.3.2 *Rudder*. It is assumed that the vertical stabilizer planform has been previously specified and that any constraints such and engine and horizontal stabilizer geometry have been noted. Use the remaining trailing edge of the vertical stabilizer to define the rudder span. Then use average rudder surface areas to pick the chord dimension.

For fighter and business jet aircraft, assume that 22% of the vertical tail is used for the rudder. For jet transports, assume that 29% of the vertical is used for the rudder.

3.1.3.3 *Elevator*. For fighter aircraft, assume a stabilator design so that the pitch control surface is the same as that of the horizontal stabilizer. For business jet and transport aircraft, assume that the previously designated trailing edge is available for elevator design. Assume an elevator surface area of 30% of the horizontal stabilizer. Solve for the chord dimension that will produce this area, taking into account the taper of the stabilizer surface.

3.2 Control Derivatives

The control derivatives are the parameters in the aircraft equations of motion that multiply the control inputs to determine overall control effectiveness or power. They are the terms that multiply the control surface deflections in Eqs. (4.1-2) and that form the B matrix of Eq. (4.7). These terms are used along with the stability derivatives that appear as parameters in the A matrix of Eq. (4.7) as primary input to the flight control system design. They are computed as functions of the control surface geometry and many other parameters as discussed below.

The control derivatives are evaluated to determine if they produce adequate control effectiveness for two sets of criteria. The first is to determine if the control surfaces produce sufficient steady state torque for specific flight conditions, as documented in the Milspecs or FARs. The second is to determine if the aircraft has appropriate responsiveness during certain dynamic maneuvers

when the actions of the flight control system are taken into account. The former is referred to as air worthiness constraints. The latter is referred to as flight control performance requirements. It includes pilot handling qualities, gust response, wing load alleviation, passenger comfort, maneuver agility, and basic stability augmentation performance measures. The choice of the prevailing performance requirements depends heavily upon the type of aircraft and its mission.

After the control surfaces are designed, the associated control derivatives or control torque effectiveness measures need to be checked to determine that the air worthiness criteria are met. These criteria are described below. This is followed by a summary of the input data required to compute the control derivatives. Then, the method that can be followed by ACSYNT to computed the control derivatives is summarized.

3.2.1 Air Worthiness Constraints

It is convenient to refer to these constraints in terms of attitude angular moments required of the aircraft; i.e., pitch moment for longitudinal control and roll-yaw moments for lateral-directional control. These moments are produced by elevator and aileron-rudder deflections, respectively.

3.2.1.1 *Elevator produced moments.* Roskam[6] gives a procedure for checking for the required pitching moment from the elevator or combination elevator-canard surfaces. Raymer[1] discusses the moment equation for pitch with the requirement that sufficient rotation torque is available for takeoff at 80% takeoff speed with the most-forward c.g. This is summarized below.

The equation that governs the pitching moment about the c.g. is

$$C_{mcg} = C_L(X_{cg} - X_{acw}) - \eta\, S_h\, C_{Lh}(X_{ach} - X_{cg})/S_w + \text{other terms} \qquad (3.1)$$

In Eq. (3.1), the first and second terms account for the change in the c.g. location on the pitching moments caused by the wing and horizontal tail. The second term includes the effective tail moment arm $(X_{ach} - X_{cg})$ and the change in tail lift due to elevator deflection in the term C_{Lh}. The other terms include other moments caused by the free wing, flap deflection effect, fuselage, engine thrust, and other engine rotor effects. For takeoff rotation, additional moment terms must be added due to the upward force of the ground on the main landing gear (accounting for partial lift) and the backward force due to rolling friction. In normal trimmed flight, Eq. 3.1 must equal zero. For adequate takeoff rotation torque, the moment due to added lift from full elevator deflection must counter the other terms.

In addition to providing adequate torque, the angle of attack must be adjusted for a given elevator deflection so that the total lift force is zero. This can be expressed as

$$C_{Ltotal} = C_{L\alpha}(\alpha + i_w) + \eta\, S_h\, C_{Lh}/S_w \qquad (3.2)$$

The process for assuring that adequate control power is available from the elevator to provide pitching moment torque while maintaining trimmed lift breaks down further into the following:

a. Determine the governing regulation. Here, we are assuming it is the requirement for rotation control during takeoff.
b. Tabulate the range of flight conditions that may prevail that must be handled. This includes c.g. location, flap position, weight, altitude, temperature, etc. that may affect the terms in the trim equations. A typical weight-c.g. envelope is shown in Fig. 3.3.

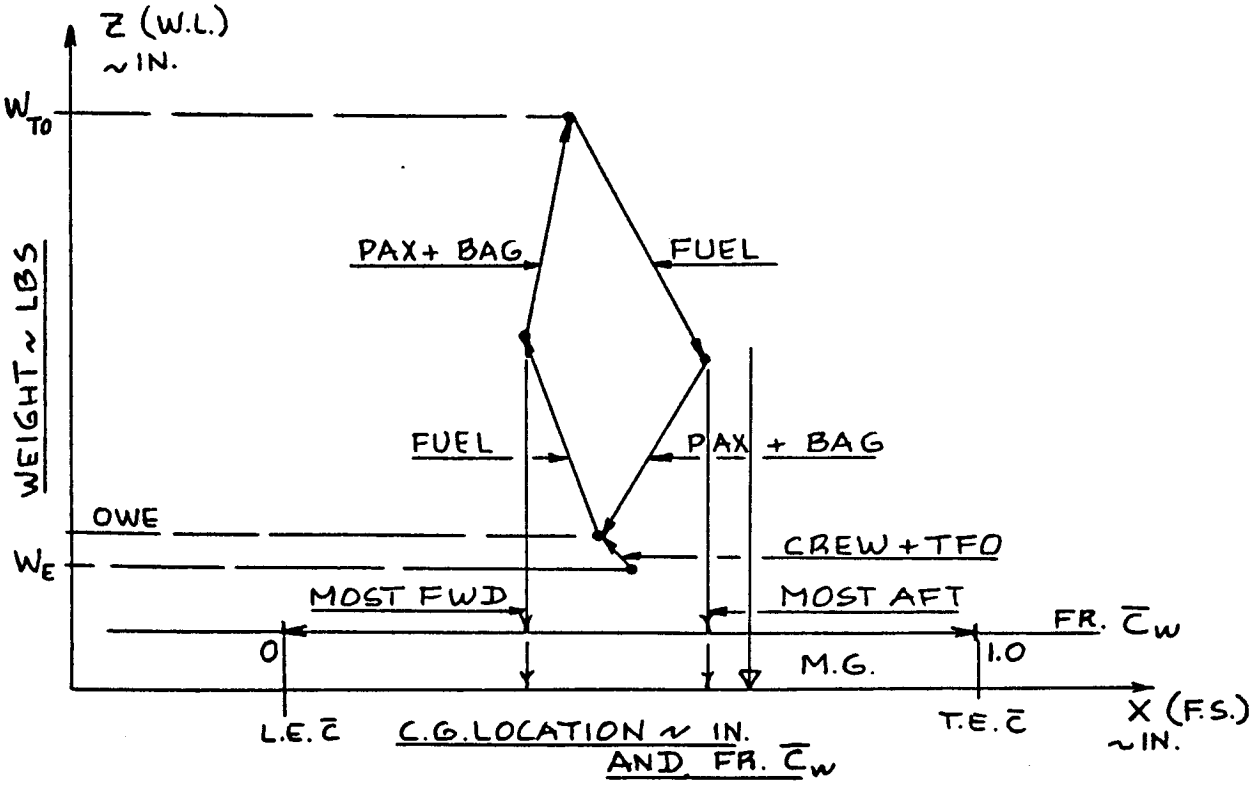

Figure 3.3 Example of weight/c.g. envelope [Roskam[7]]

c. With the data collected in Step b, plot the aircraft trim diagram. An example is shown in Fig. 3.4. The steps to generate this plot are detailed in Roskam.[7] However, from Fig. 3.4, it is evident that the boundaries shown require the zero pitching moment as a function of lift coefficient for the maximum forward and aft c.g. locations plus the lift coefficient at maximum angle of attack for each of the elevator deflection settings. This requires that the control derivative $C_{L\delta e}$ be known; its computation is discussed in Section 3.2.3.

d. From the trim diagram, determine if equilibrium flight is possible for the flight conditions of interest. Criteria for acceptance include that the control surface deflection is within the range designed into the aircraft, the angle of attack is below airplane stall, and the tail (or canard) are not stalled within the trim-triangle.

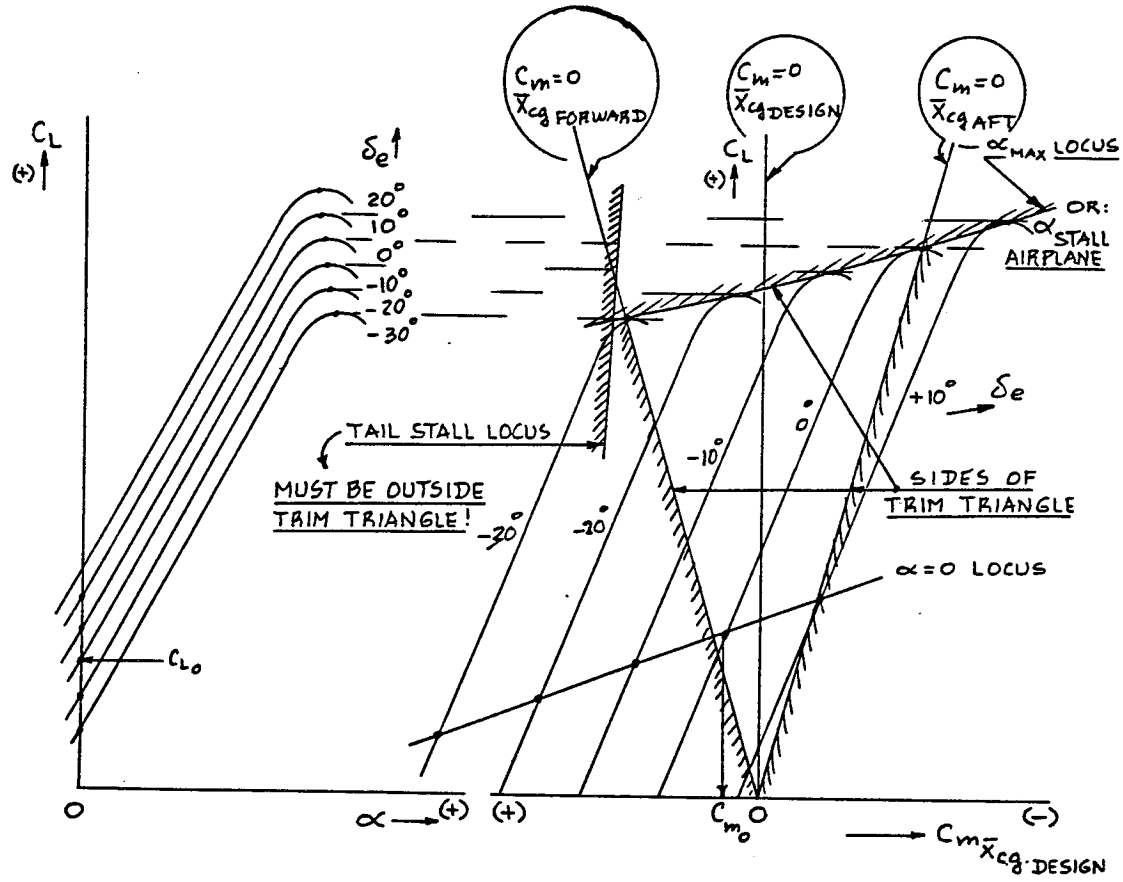

Figure 3.4 Example trim diagram for conventional aircraft [Roskam]

3.2.1.2 *Aileron produced moments*. The aileron effectiveness is established by the requirement to roll the aircraft at a certain rate, depending upon the aircraft mission. For military applications, the roll requirements come from the Milspecs; see Table 3.4.

Table 3.4 MIL-F-8785 B roll requirements [Raymer[7]]

Class	Aircraft Type	Required Roll
I	Light utility, observation, primary trainer	60° in 1.3 s
II	Medium bomber, cargo, transport, ASW, recon.	45° in 1.4 s
III	Heavy bomber, cargo, transport	30° in 1.5 s
IV A	Fighter-attack, interceptor	90° in 1.3 s
IV B	Air-to-air dogfighter	90° in 1.0 s 360° in 2.8 s
IV C	Fighter with air-to-ground stores	90° in 1.7 s

For conceptual design it can be assumed that roll rate can be achieved instantaneously from constant aileron deflection. To solve for the steady rate, use

$$p = - (C_{l\delta a} / C_{lp}) \, \delta a \tag{3.3}$$

Here, p is the steady roll rate caused by the aileron deflection δa. The terms C_{lp} and $C_{l\delta a}$ are the damping-due-to-roll stability derivative and the roll power control derivative, respectively. To increase roll rate requires either increasing the aileron deflection or increasing the control derivative by enlarging the surface or moving it further out on the wing.

3.2.1.3 *Rudder produced moments*. The primary constraint that must be met by the rudder is the engine-out case at takeoff. The rudder must produce sufficient yawing moment to keep the aircraft at zero angle of sideslip at takeoff speed (1.1 times stall speed) with one engine out and at the aftmost c.g. location. Rudder deflection should be no more than 20° to allow additional deflection for control.

Another lateral trim condition which should be checked is the crosswind landing case. The aircraft must be able to operate in crosswinds equal to 20% of takeoff speed, which is equivalent to holding an 11.5° sideslip at takeoff speed.

This constraint is evaluated by examining the equation

$$C_n = N / q \, S_w \, b$$

$$= C_{n\delta a} \, \delta a + (C_{n\beta w} + C_{n\beta fus} + C_{n\beta v})\beta - (TY_p + DY_p + F_p(X_{cg} - X_p))/q \, S_w \tag{3.4}$$

where

$$C_{n\beta v} = C_{F\beta v} \, (\partial\beta v/\partial\beta) \, \eta_v \, S_v \, (X_{acv} - X_{cg}) / S_w \tag{3.5}$$

This latter term is the side force coefficient caused by the deflected rudder. It contains the yawing moment arm $(X_{acv} - X_{cg})$ and the change in vertical tail lift due to rudder deflection in the term $C_{F\beta v}$. To increase this force, one can increase the rudder chord or span or use a double-hinged rudder so that the maximum deflection can be greater.

3.2.2 Design Inputs Required

To compute the control derivatives requires input from several sources throughout the ACSYNT code. This includes the control surface geometry and moment arms from the "geometry" module, the lumped mass weights and their moment arms to compute moments of inertia from the "weights" module, and the lift curve slopes of the wing and tail surfaces with aileron, elevator, and rudder deflections. The computation of control derivatives also requires the computation of certain stability derivatives first. This is depicted in the program flowchart in Fig. 3.5.

3.2.3 DATCOM Methodology for Computing Control Derivatives

The DATCOM methodology can be found in Hoak.[8] It is summarized in Roskam[7] for subsonic flight. The following is a summary of computing the relevant control derivatives using this

procedure. The complete set of plots and charts for encoding this process are not presented here. However, the following is sufficient for outlining the associated ACSYNT code.

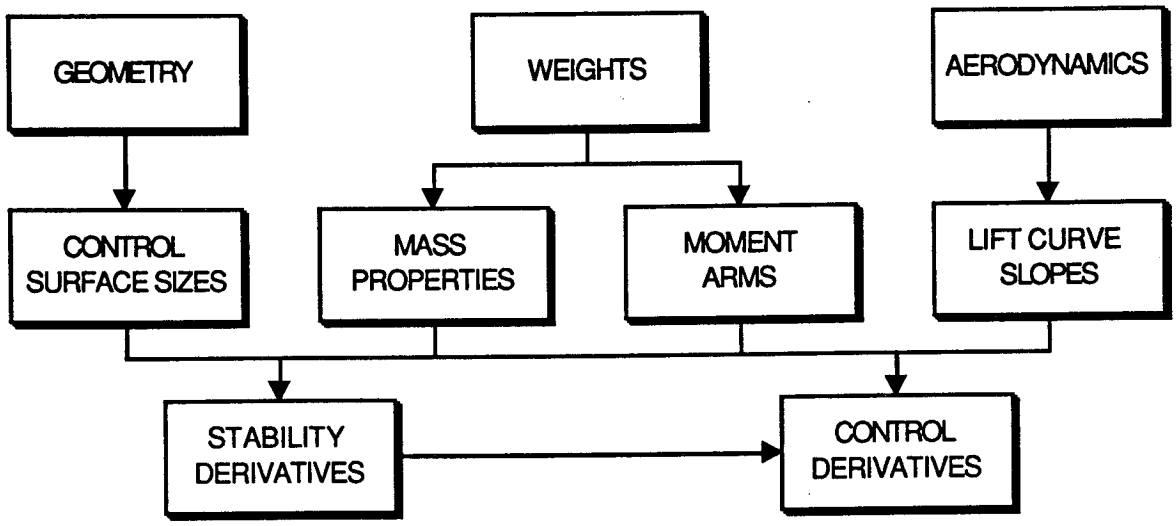

Figure 3.5 Flow chart of input required to compute control derivatives.

3.2.3.1 *Aileron/elevon derivatives.* The three coefficients associated with aileron deflection are $C_{y\delta a}$, $C_{l\delta a}$, and $C_{n\delta a}$. The side force term $C_{y\delta a}$ is normally zero except if the ailerons are close to the vertical tail, as in the F-106. It will be assumed zero here.

For subsonic flight, the rolling moment coefficient $C_{l\delta a}$ is computed using the following steps:

1. Compute the normalized full chord coefficient ($\beta C_{l\delta a}$ '/ κ) from the charts such as Fig. 3.6. The entire set of these charts are found in the DATCOM reference. Here, the coefficient is given as a function of taper ratio, sweep angle, and aspect ratio. Note that the independent axis is the location of the inner and outer span dimensions y of the aileron normalized by the half span. The coefficient value is found by taking the difference of the two values from the inner and outer span dimension.

   The coefficient uses the terms

$$\beta = (1 - M^2)^{0.5} \tag{3.6}$$

$$\kappa = (C_{l\alpha})_M \beta / 2\pi \tag{3.7}$$

   The term $(C_{l\alpha})_M$ is the lift curve slope of the airfoil at the mean geometric center of the part of the wing covered by the aileron. Also, the sweep angle term Λ_β is defined as

$$\Lambda_\beta = \tan^{-1}(\tan \Lambda_{c/4} / \beta) \tag{3.8}$$

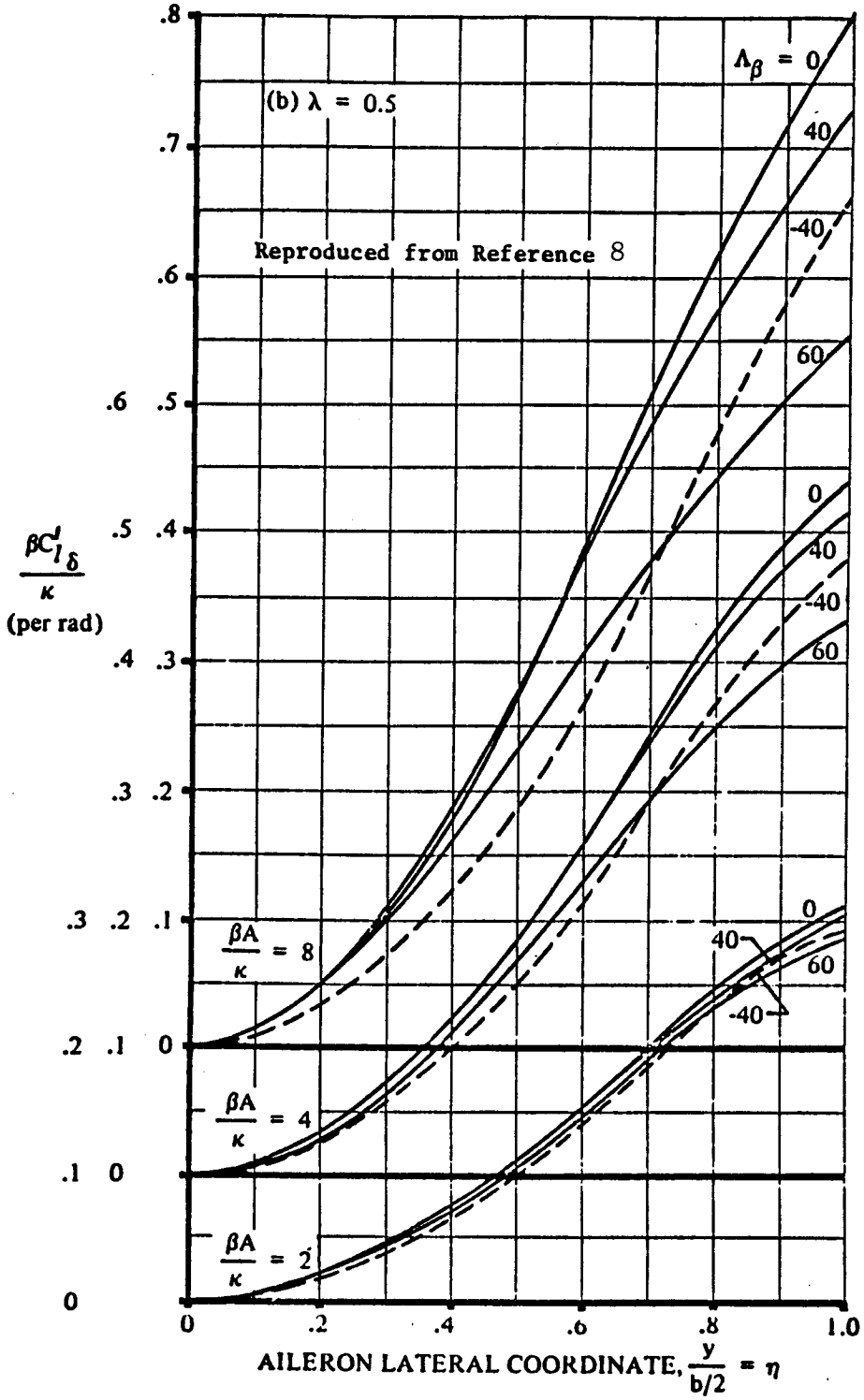

Figure 3.5 Aileron rolling moment parameter [DATCOM[8]]

2. Denormalize the coefficient by multiplying by κ and dividing by β.
3. Determine the effectiveness for partial-chord ailerons ($c_a/c < 1.0$) by the equation

$$C_{l\delta a} = |\alpha_{\delta a}|\, C_{l\delta a}{}' \tag{3.9}$$

Here,

$$\alpha_{\delta a} = [(C_{l\delta}/\, C_{l\delta\, theory})\, C_{l\delta\, theory}] \,/\, (C_{l\alpha})_a \tag{3.10}$$

The term $(C_{l\delta}/\, C_{l\delta\, theory})$ is found from Fig. 3.6 as a function of aileron chord to wing chord ratio. The lift curve slope ratio parameter in Fig. 3.6 is explained in Roskam; it is a function of the airfoil chosen.

The term $C_{l\delta\, theory}$ is found from Fig. 3.7.

The term $(C_{l\alpha})_a$ is computed from the lift curve slope at the mean aileron span as

$$(C_{l\alpha})_a = C_{l\alpha} \,/\, (1 - M^2)^{0.5}$$

4. The average aileron roll control power derivative is then found by averaging the derivative computed for the left and right wing. The aileron deflection used as the control input is the average of the deflections of the left and right wing ailerons.

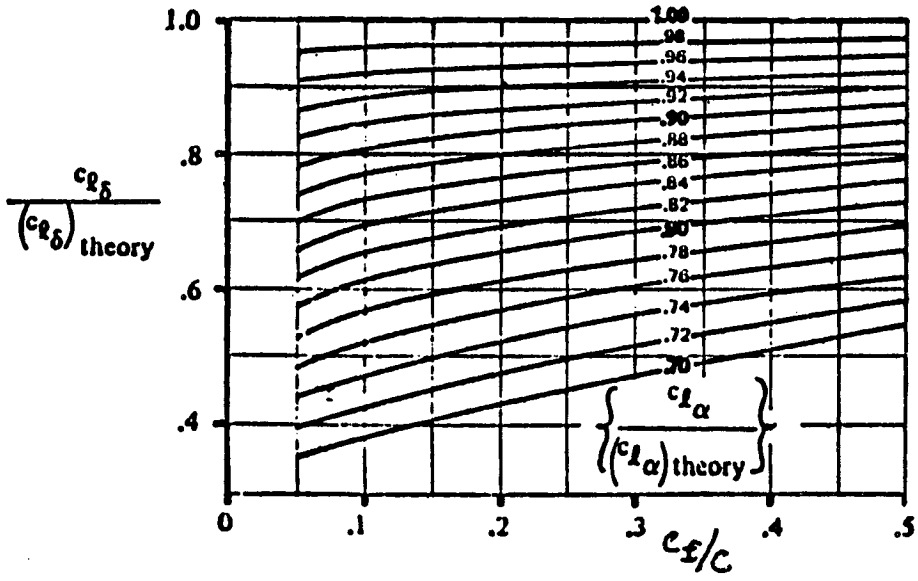

Figure 3.6 Correction factor for plain flap lift [DATCOM[8]]; use for aileron

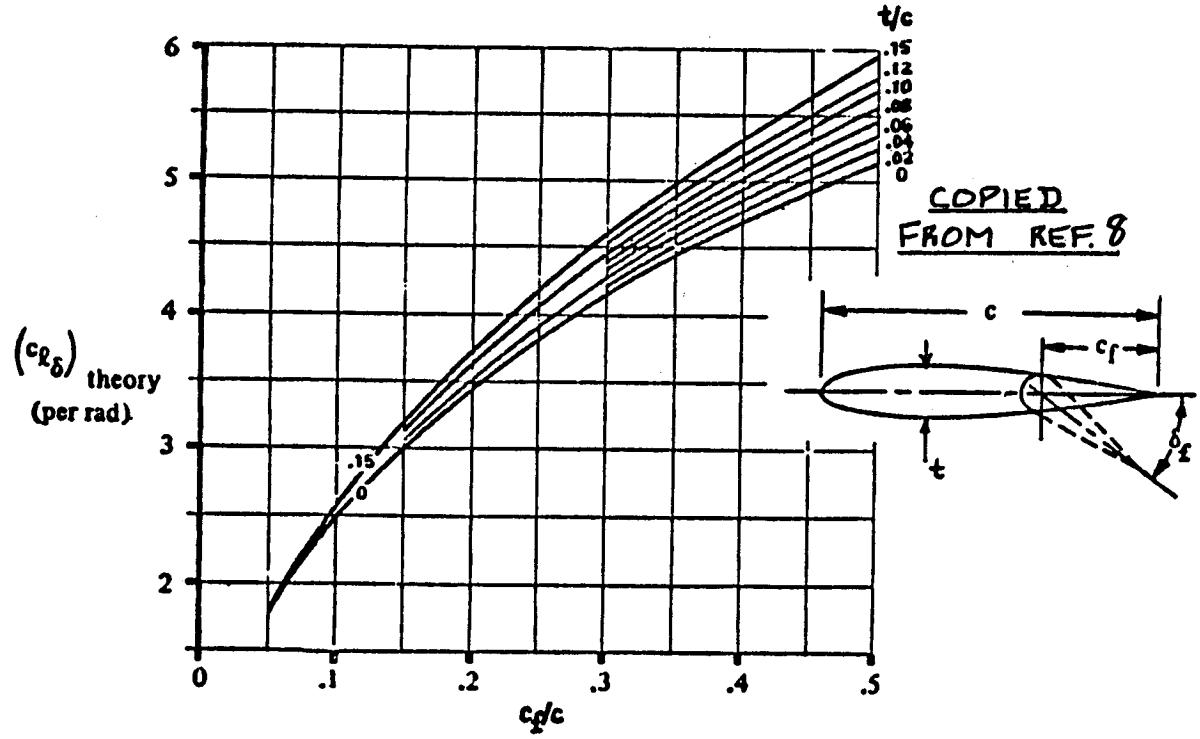

Figure 3.7 Lift effectiveness of a plain flap; use for aileron

The yawing moment coefficient $C_{n\delta a}$ is found as

$$C_{n\delta a} = K_a \, C_{Lw} \, C_{l\delta a} \tag{3.11}$$

where K_a is found from Fig. 3.8. The parameters are aspect ratio and wing taper. The independent variable is the average span location of the aileron. The term C_{Lw} in Eq. 3.11 is the wing lift coefficient.

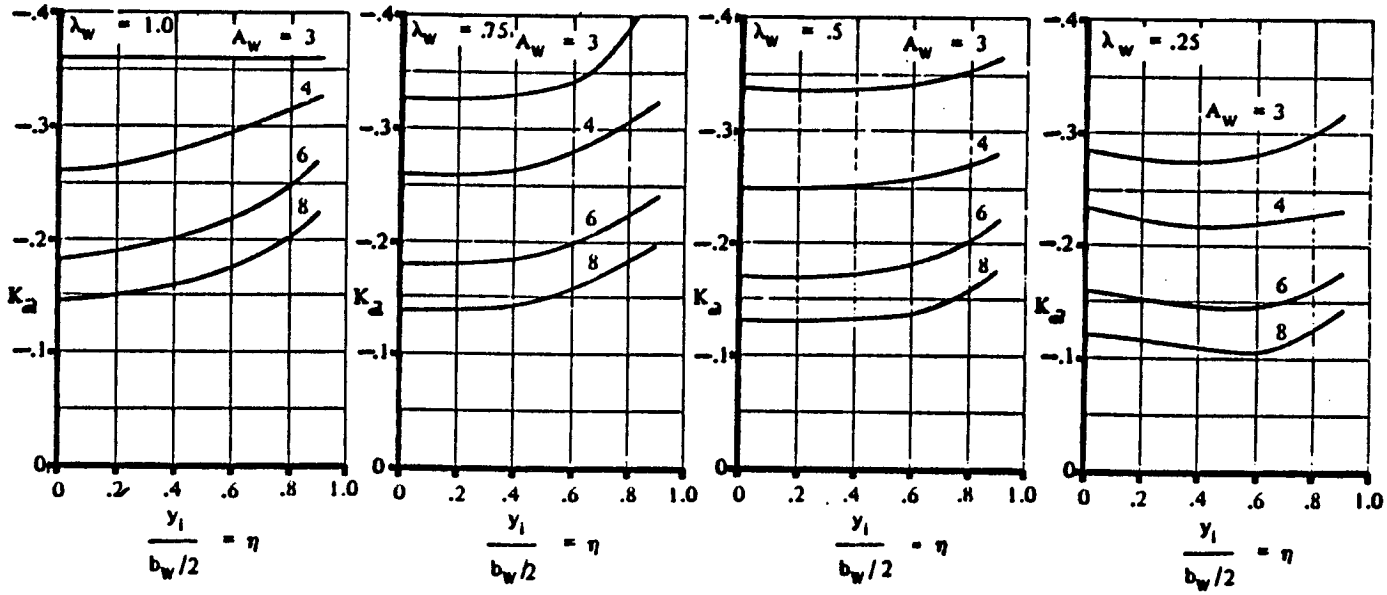

Figure 3.8 Correlation Constant for Yawing Moment due to Aileron Deflection.

To compute the rolling moment coefficient for when Mach number exceeds 1.0, the following data are taken directly from DATCOM:

Supersonic linear theory is used to derive conical-flow solutions for the rolling effectiveness of wing trailing-edge flap type control surfaces. The theory is based on the following assumptions (using Fig. 3.9):

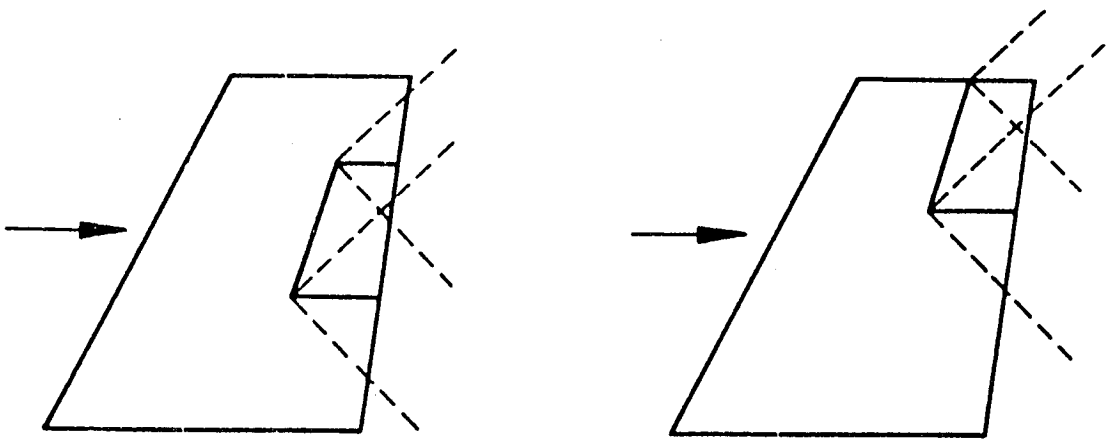

Figure 3.9 Sketch of wing flap geometrics in supersonic flight.

1. The leading (hinge line) and trailing edges of the control surface are supersonic (swept ahead of the Mach lines).

2. The control surfaces are located at the wing tip or are far enough inboard to prevent the outermost Mach lines from the control surface from crossing the wing tip.

3. The innermost Mach lines from the deflected control surface do not cross the root chord.

4. The root and tip chords of the control surfaces are streamwise.

5. Controls are not influenced by the tip conical flow from the opposite wing panel or by the interaction of the wing-root Mach cone with the wing tip.

The supersonic rolling effectiveness of plain trailing-edge flap-type controls is given by

$$C_{l_\delta}=\left(1-\frac{C_2}{C_1}\phi_{TE}\right)C'_{L_\delta}\frac{S_f}{S_w}\frac{1}{2}\left[\frac{y_i}{b_w}+\left(\frac{b_f}{2b_w}\right)\frac{C'_{l_\delta}}{C'_{L_\delta}}\right] \tag{3.12}$$

where

C_{l_δ} is the control-surface rolling effectiveness of one control surface deflected on one wing panel, based on the total wing area and span.

C'_{l_δ} is the theoretical rolling-moment derivative based on total control area S_f for thin wings for the following cases:

(a) Tapered control surfaces with outboard edge coincident with wing tip (use Fig. 3.10).

(b) Tapered control surfaces with outboard edge not coincident with wing tip (use Fig. 3.11).

(c) Untapered control surfaces with outboard edge coincident with wing tip (use Fig. 3.12a).

(d) Untapered control surfaces with outboard edge not coincident with wing tip (use Fig. 3.12b).

$\frac{S_f}{S_w}$ is the ratio of the total control area (both sides of the wing) to the total wing area

$\frac{b_f}{b_w}$ is the ratio of the total control span (both sides of wing) to the total wing span.

$\frac{y_i}{b_w}$ is the distance from the wing root chord to the control root chord in wing spans.

$\left(1-\frac{C_2}{C_1}\phi_{TE}\right)$ is a thickness correction factor to the supersonic flat-plate derivative.

$$C_1=\frac{2}{\sqrt{M^2-1}} \text{ (per radian)}$$

$$C_2=\frac{(\gamma+1)M^4-4(M^2-1)}{2(M^2-1)^2} \text{ (per radian)}$$

ϕ_{TE} is the trailing-edge angle in radians, measured normal to the control hinge line.

γ is the ratio of specific heats, $\gamma = 1.4$.

C'_{l_δ} is the lift-effectiveness of one symmetric, straight-sided control, based on the area of the control. This parameter is obtained from Figs. 3.13 for controls located at the wing tip, and from Fig. 3.14 for controls located inboard from the wing tip.

It should be noted that in applying this method the control deflection angle and all dimensions (with the exception of ϕ_{TE}) are measured in planes parallel and perpendicular to the plane of symmetry.

The yawing moment due to aileron deflection at supersonic speeds is found from Fig. 3.15 as a function of $C_{l\delta a}$ and aileron span dimensions.

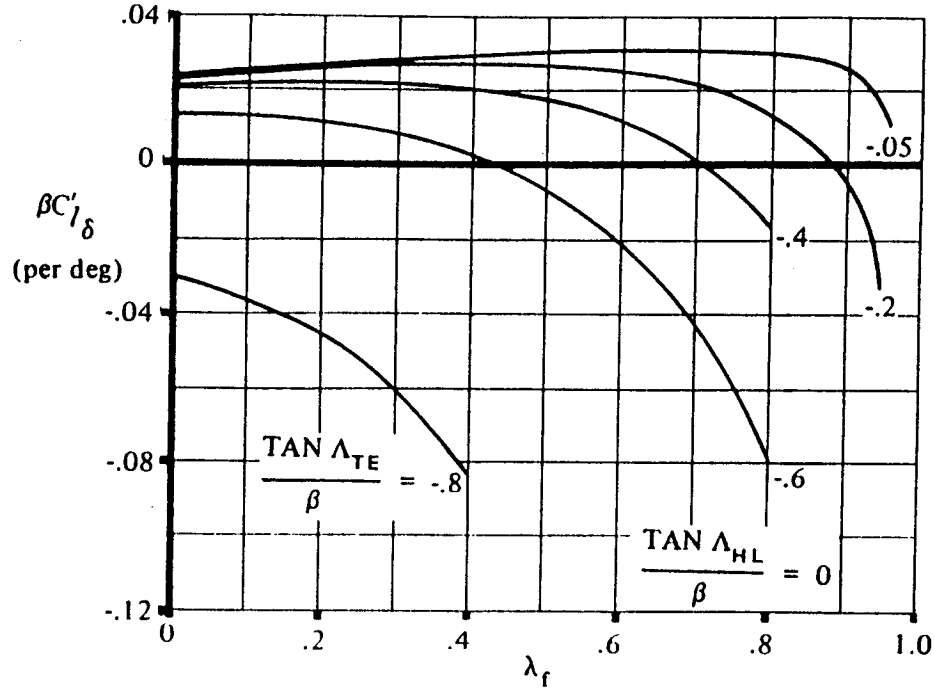

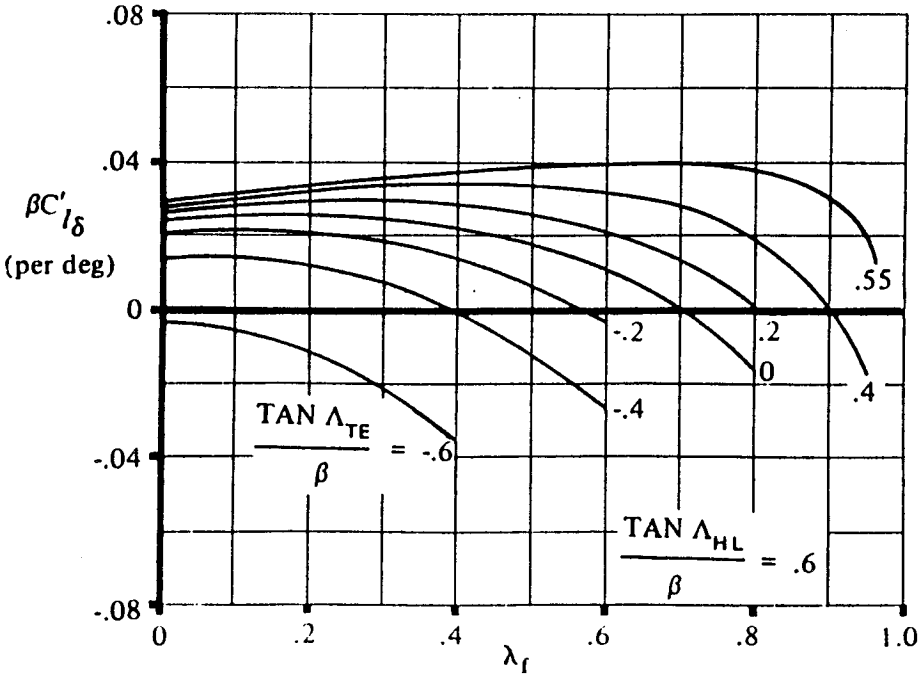

Figure 3.10 [DATCOM] Rolling moment derivative for tapered control surfaces having outboard edge coincident with wing tip

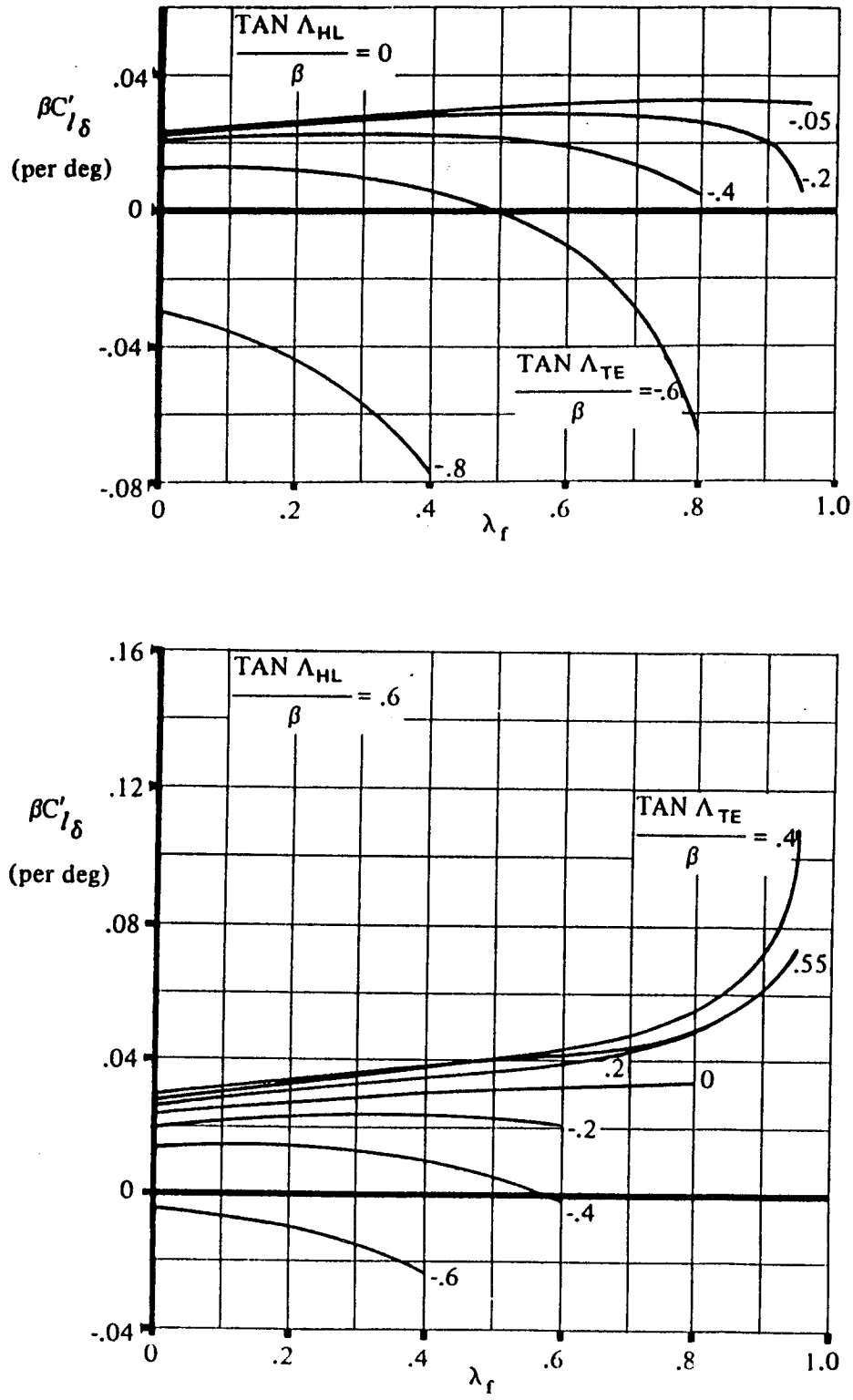

Figure 3.11 [DATCOM] Rolling moment derivative for tapered control surfaces having outboard edge not coincident with wing tip.

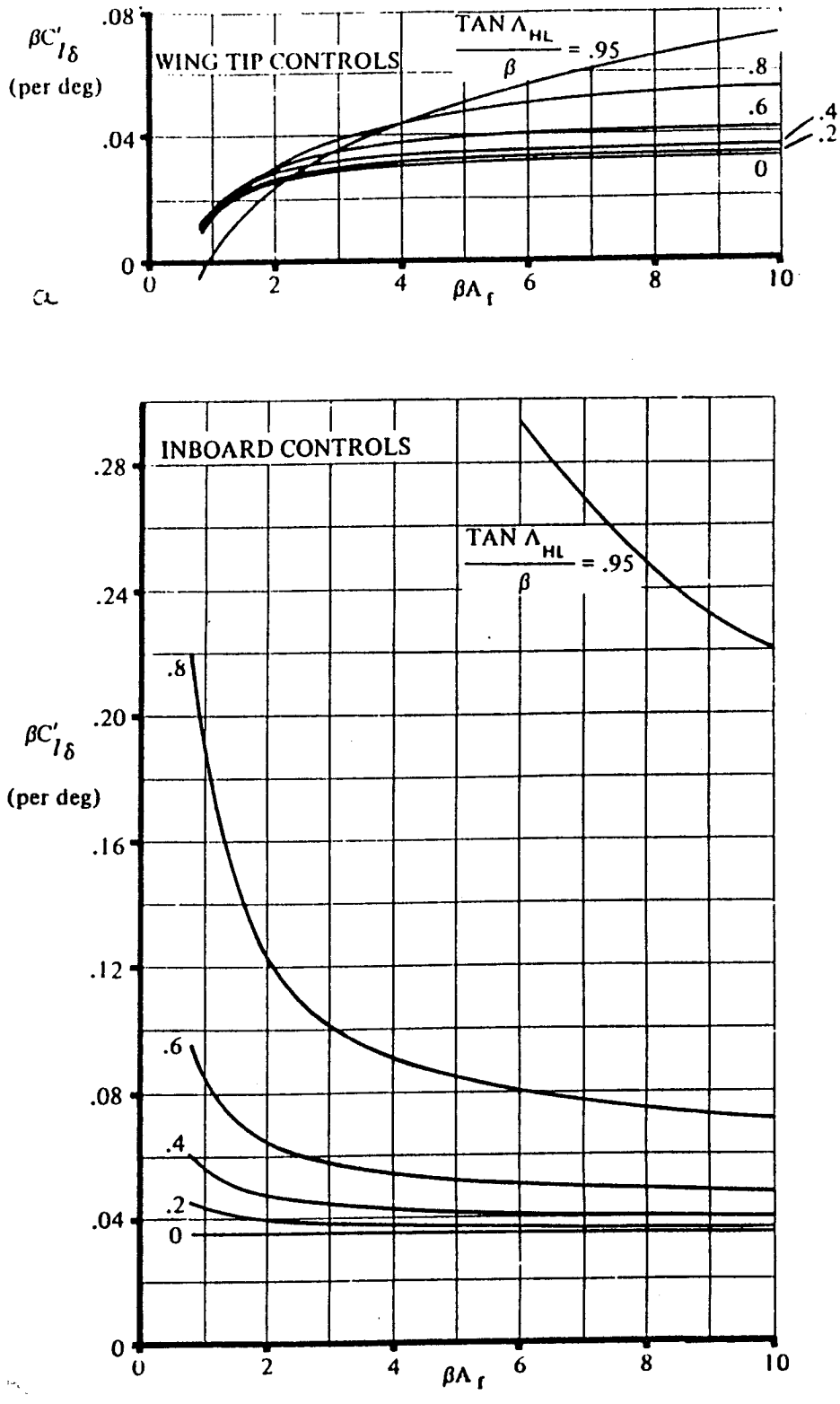

Figure 3.12 a and b [DATCOM] Rolling moment derivative for untapered control surfaces having outboard edge coincident (a) and not coincident (b) with wing tip

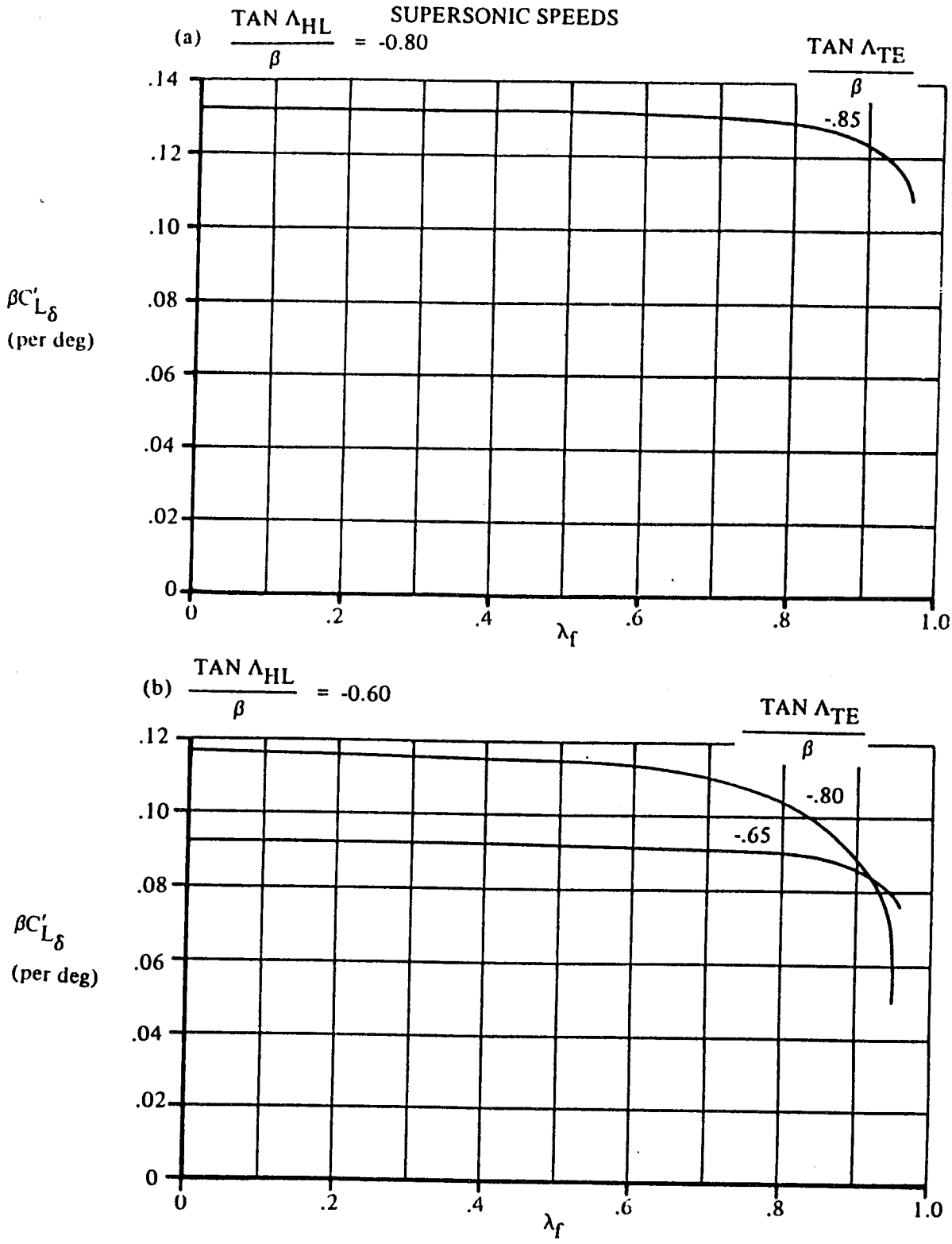

Figure 3.13 [DATCOM] Lift parameter for deflected trailing-edge flaps located at the wing tip

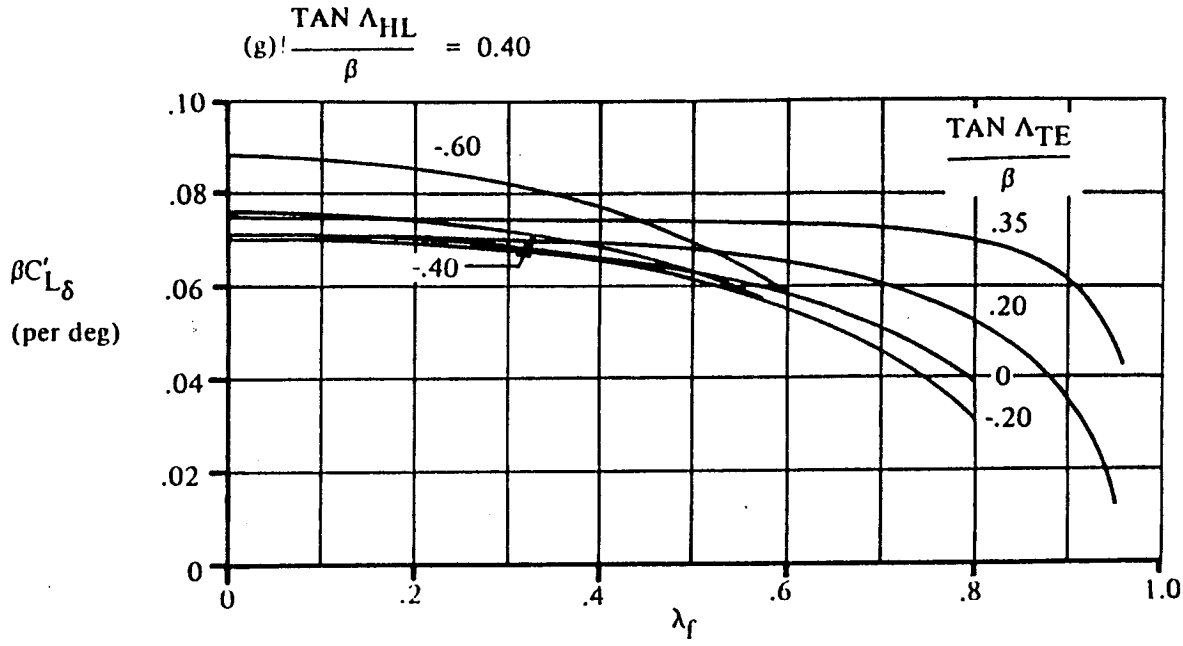

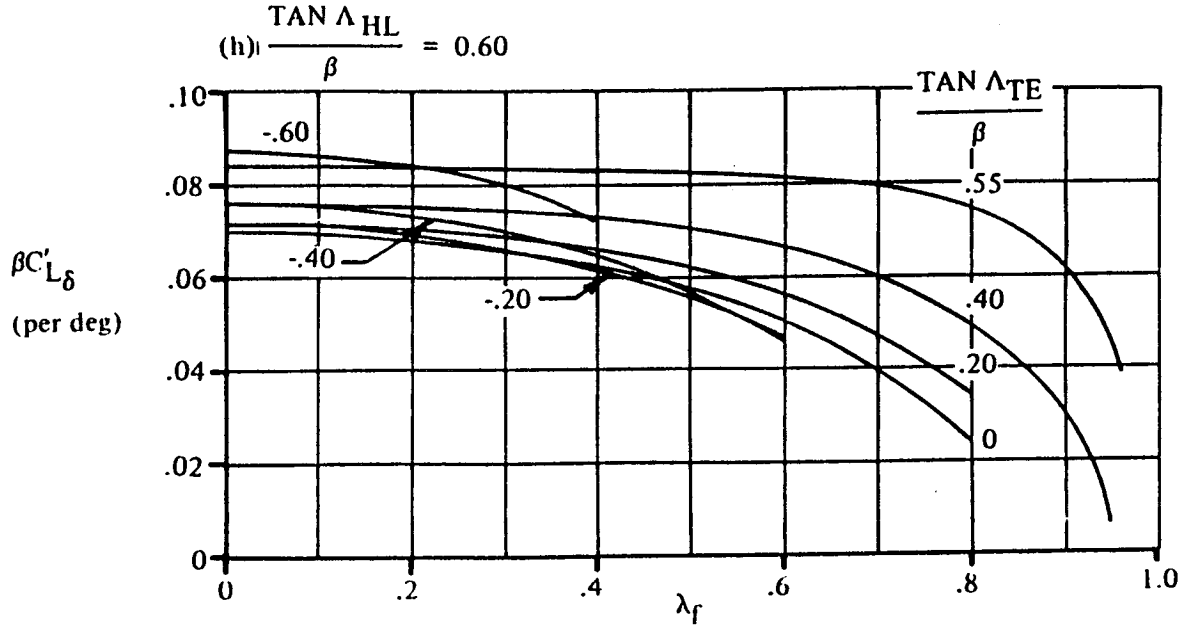

Figure 3.13 (cont'd.) [DATCOM]

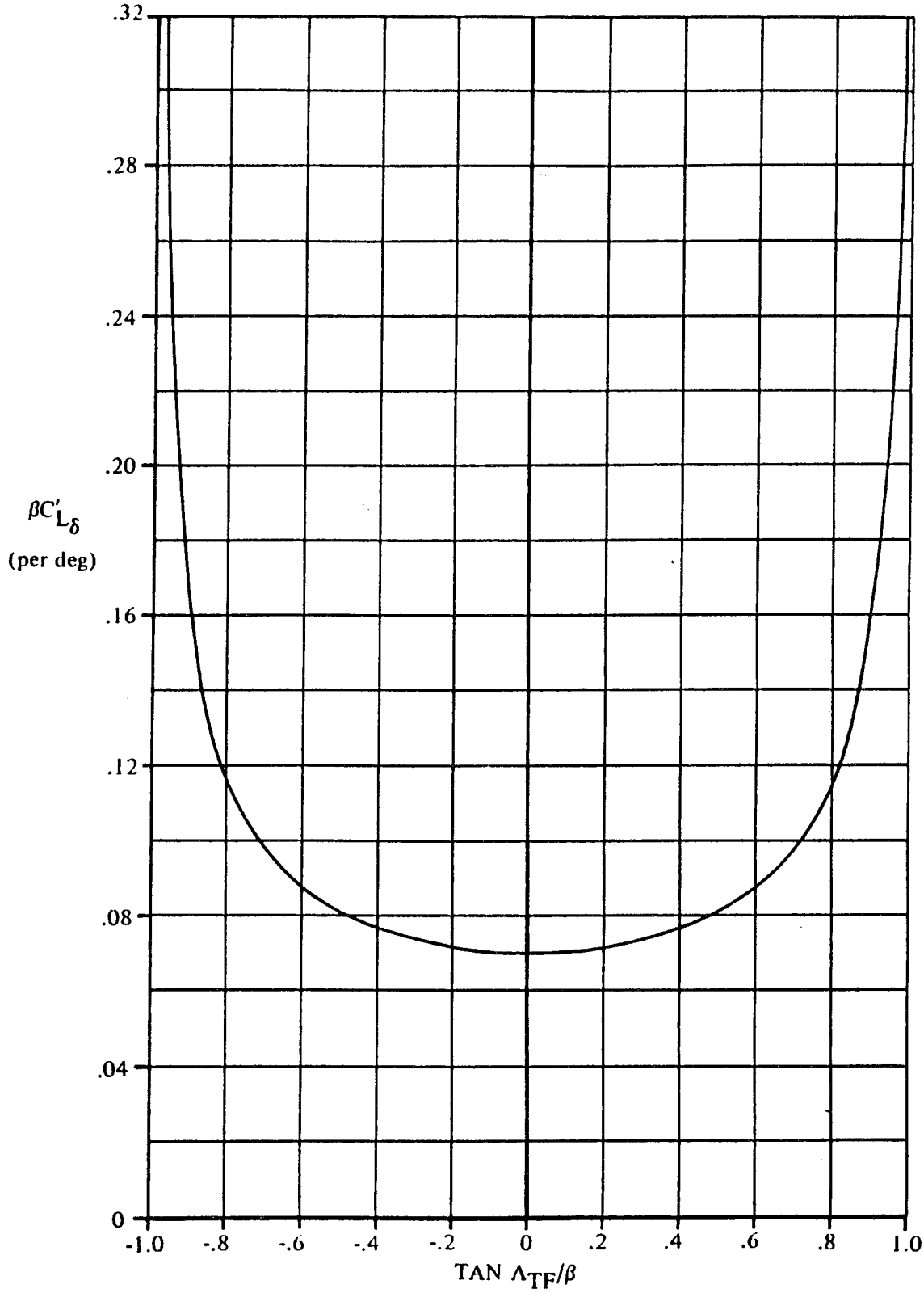

Figure 3.14 [DATCOM] Lift parameters for deflected trailing-edge flaps located inboard from wing tip

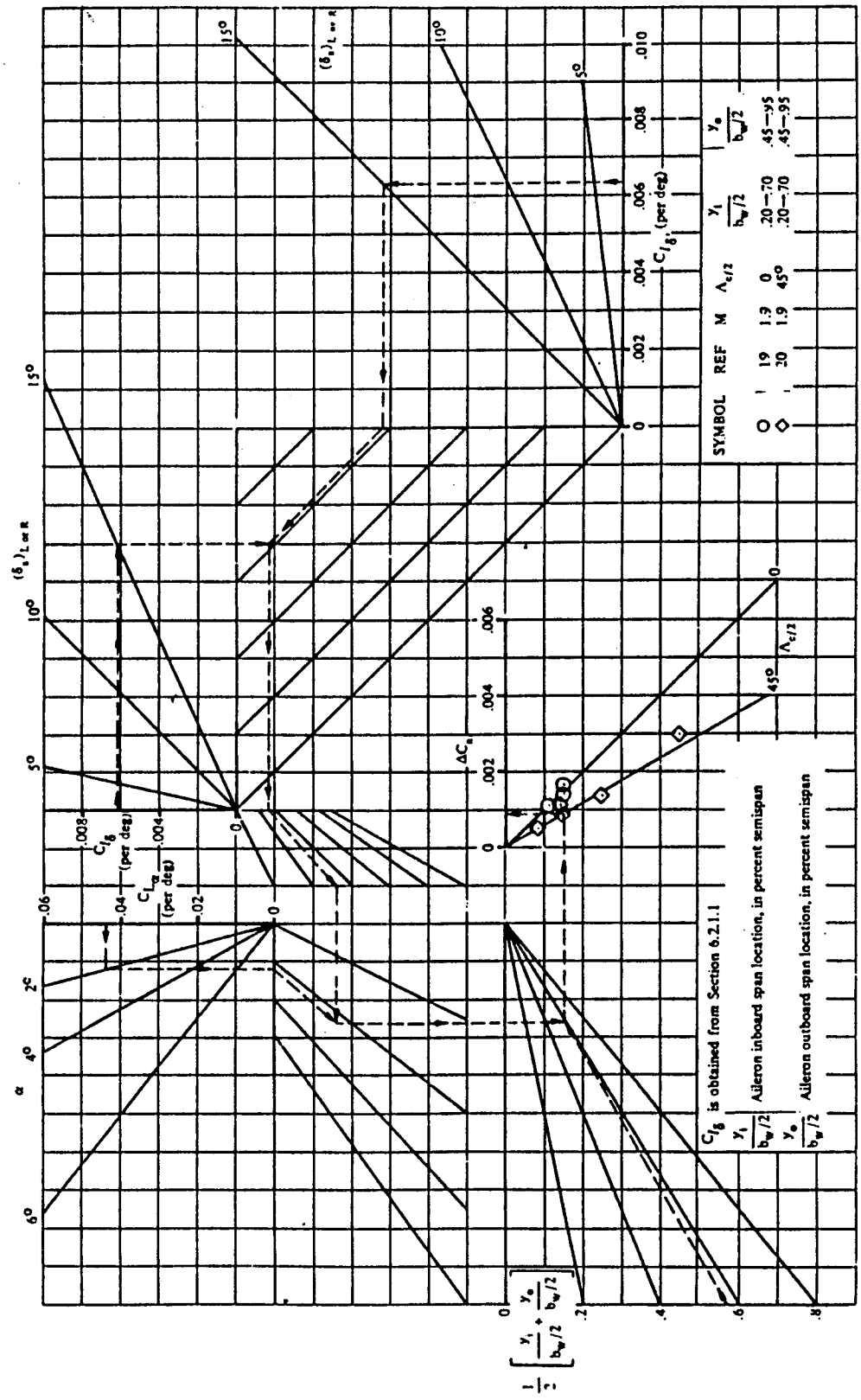

Figure 3.15 [DATCOM] Yawing moment due to aileron deflection at supersonic speeds

3.2.3.2 *Rudder derivatives.* The three coefficients associated with rudder deflection are $C_{y\delta r}$, $C_{l\delta r}$ and $C_{n\delta r}$. The side force coefficient is computed as follows:

$$C_{y\delta r} = C_{L\alpha v}\, k'\, K_b\, (C_{l\delta} / C_{l\delta\, theory})\, C_{l\delta\, theory}\, (S_v / S) \tag{3.13}$$

In Eq. (3.13), the terms are evaluated as follows:

a. $CL\alpha v$ is found from the following expression:

$$CL_{\alpha v} = 2\,\pi\, A_{eff} / [2 + \{A_{eff}^2\, \beta^2 / k^2\, (1 + \tan^2 \Lambda c/2\, / \beta^2) + 4\}^{0.5}] \tag{3.14}$$

$\beta = (1 - M^2)^{0.5}$ or $4(M^2 - 1)^{0.5}$

$k = C_{L\alpha}$ at M

$= C_{L\alpha}\,(1 - M^2)^{0.5}$ for $M < 1$ or

$= 4(M^2 - 1)^{0.5}$ for $M > 1$.

$\Lambda_c/2$ is semi-chord sweep angle.

$$A_{eff} = (A_{vf} / A_v)\, A_v\, [1 + K_{vh}\{(A_{vhf} / A_{vf}) - 1\}] \tag{3.15}$$

$A_v = b_v^2 / S_v$ from Fig. 3.2; these are for the effective tail area.

(A_{vf} / A_v) = ratio with and without the fuselage from Fig. 3.16

(A_{vhf} / A_{vf}) = ratio with and without horizontal tail from Fig. 3.17

K_{vh} = factor accounting for relative size of tail from Fig. 3.18.

b. k' accounts for rudder deflection from Fig. 3.19

c. K_b is the rudder span factor from Figs. 3.20 and 3.21

d. $(C_{l\delta} / C_{l\delta\, theory})$ is obtained from Fig. 3.6 as is the case for the aileron and flaps.

e. $C_{l\delta\, theory}$ is obtained from Fig. 3.7 as before.

f. S_v is the effective vertical tail area from Fig. 3.2.

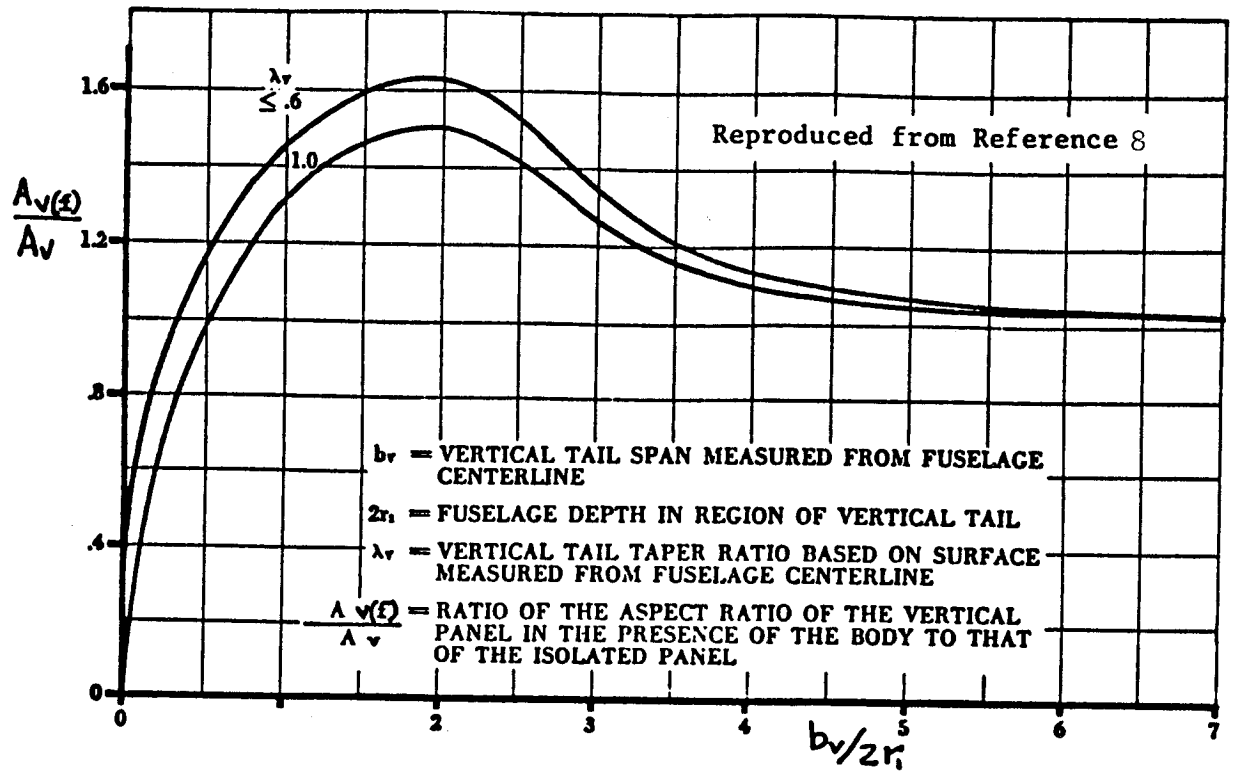

Figure 3.16 Ratio of vertical tail aspect ratio in presence of fuselage to that of isolated tail

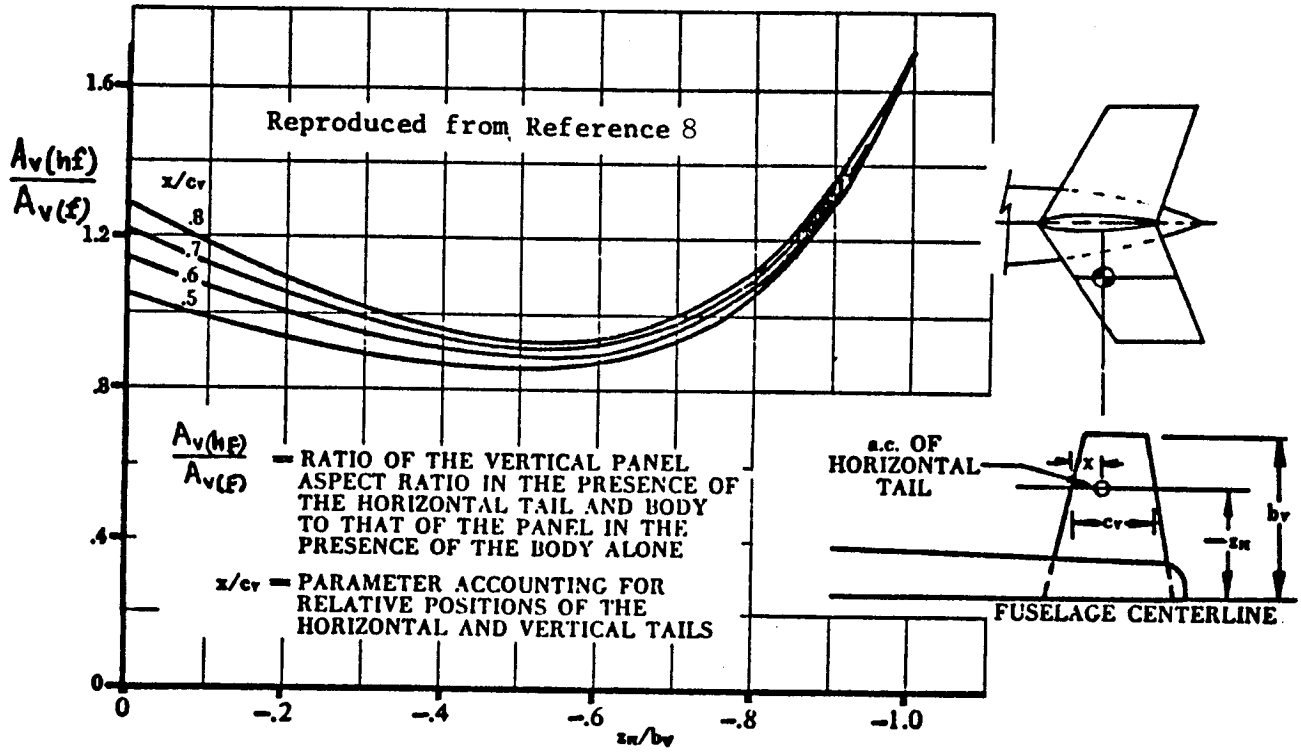

Figure 3.17 Ratio of vertical tail aspect ratio in presence of fuselage and horizontal tail to that in presence of fuselage alone

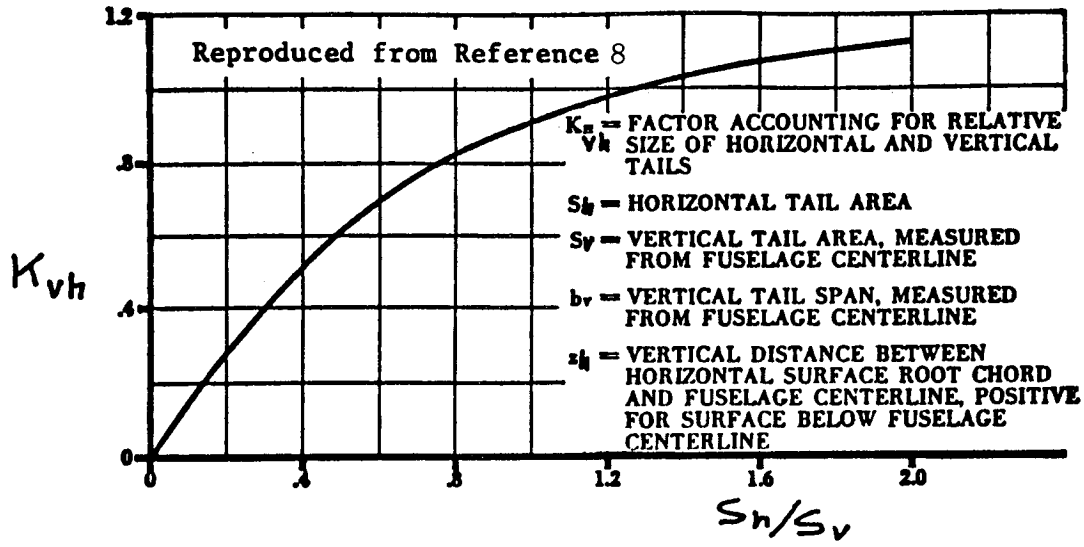

Figure 3.18 Factor which accounts for relative size of horizontal and vertical tail

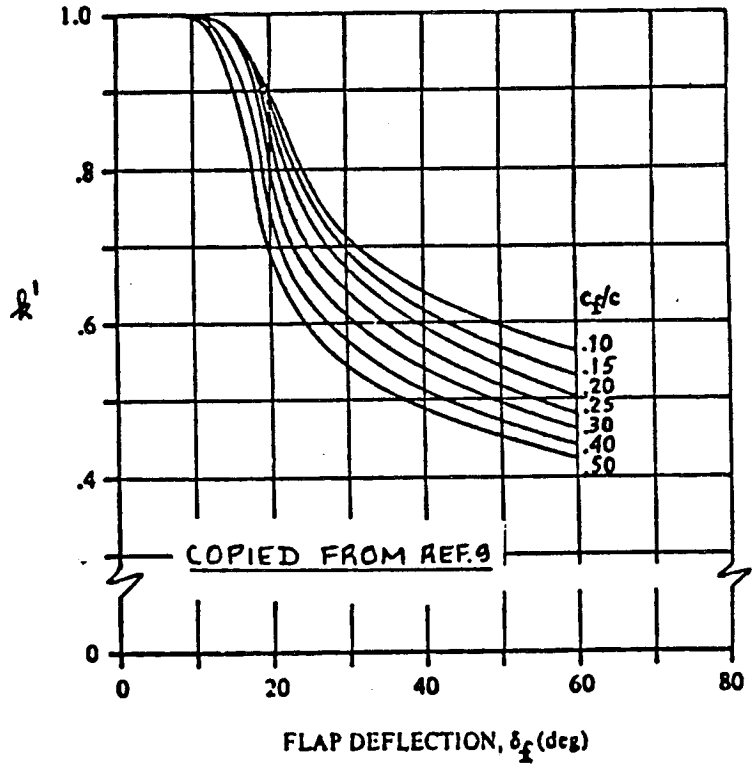

Figure 3.19 Correction factor for nonlinear lift behavior of plain flaps

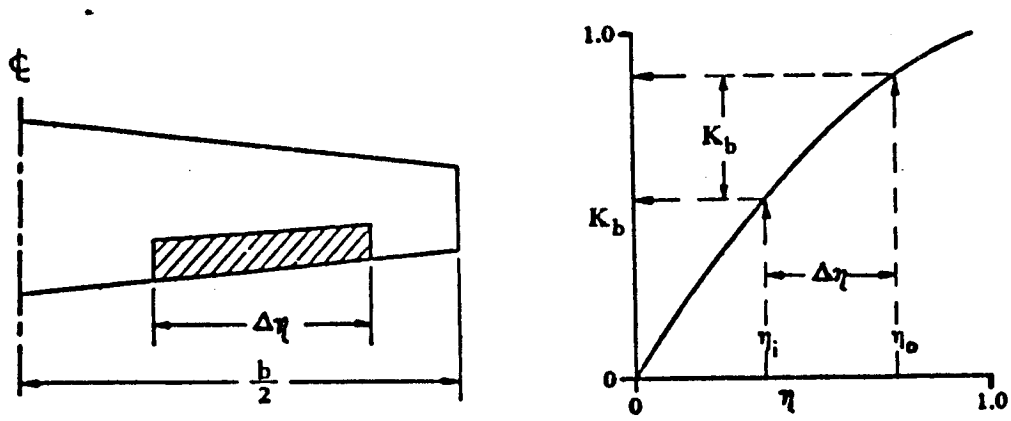

Figure 3.20 Procedure for estimating K_b

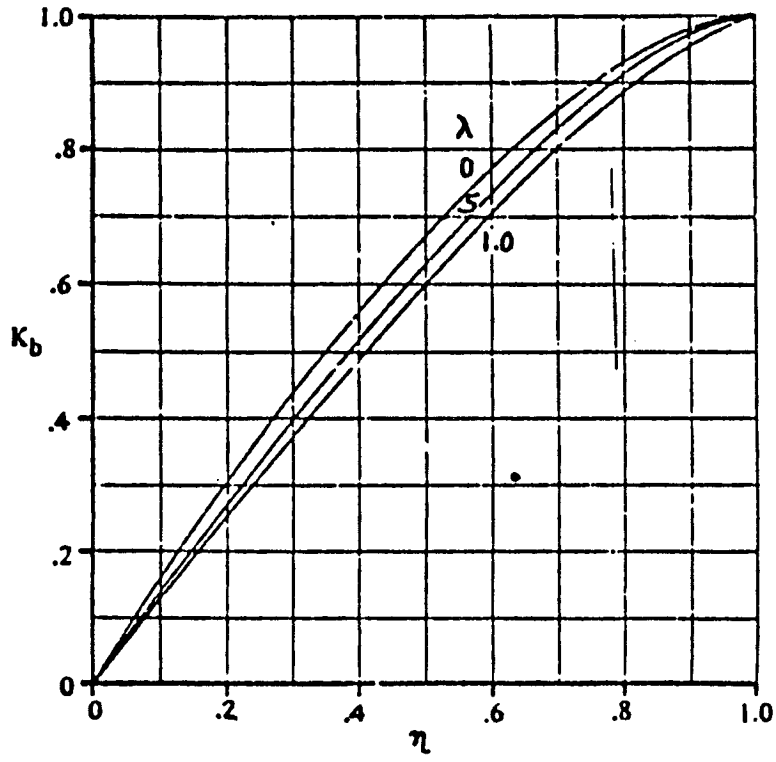

Figure 3.21 Effect of taper ratio and flap span on K_b.

To compute the roll and yawing moments due to rudder deflection, use the geometry illustrated in Fig. 3.22. Here, l_v and z_v are the lever arms of the vertical tail aerodynamic center with respect to the aircraft c.g.

The coefficient of rolling moment due to rudder deflection $C_{l\delta r}$ is a function of the side force coefficient $C_{y\delta r}$ as follows:

$$C_{l\delta r} = \{(z_v \cos \alpha - l_v \sin \alpha) / b\}\, C_{y\delta r} \tag{3.16}$$

Similarly, the yawing moment coefficient due to rudder deflection $C_{n\delta r}$ (the rudder control power coefficient) is

$$C_{n\delta r} = -C_{y\delta r}\, (l_v \cos \alpha + z_v \sin \alpha) / b \tag{3.17}$$

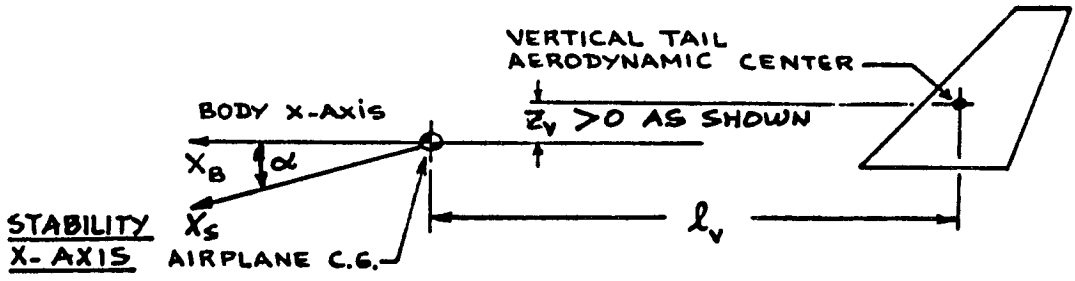

Figure 3.22 Geometry for locating vertical tail

3.2.3.3 *Elevator, stabilizer, canard and canardovator derivatives.* These are the control derivatives that affect longitudinal control. The method for computing these terms are similar to the aileron and rudder terms in that they use the same approach as used to determine flap effectiveness on a wing section.

a. Stabilizer. Deflection of the stabilizer from the trim point causes contributions to drag, lift and pitching moment; the associated coefficients are C_{Dih}, C_{Lih}, and C_{mih}, respectively. They are computed as follows:

The drag increment coefficient is

$$C_{Dih} = 2(\, C_{Lh} / \pi A_h\, e_h)\, (C_{L\alpha h})\, \eta_h \tag{3.18}$$

where

C_{Lh} = lift coefficient of the horizontal tail;

A_h = horizontal tail aspect ratio;

e_h = 0.5 for fuselage mounted tails

= 0.75 for T-tails;

$C_{L\alpha h}$ = the same formula as Eq. (3.14) applied to the horizontal tail

η_h = ratio of horizontal tail dynamic pressure to wing dynamic pressure

$$= [1 - \{\cos^2 (\pi z_h / 2 z_w)\}\{2.42 (C_{Dow})^{0.5}\} / (x_h/c + 0.30)] \quad (3.19)$$

and

$z_h = x_h \tan(\gamma_h + \varepsilon_{cl} - \alpha_w)$

$\varepsilon_{cl} = 1.62 C_{Lw} / \pi A$

$z_w = 0.68\ c\ \{C_{Dow} (x_h / c + 0.15)\}^{0.5}$

C_{Dow} = wing zero-lift drag coefficient

The lift increment coefficient is

$$C_{Lih} = \eta_h (S_h / S) C_{L\alpha h} \quad (3.20)$$

The pitching moment coefficient is

$$C_{mih} = - (x_{ach} - x_{cg}) (S_h / S) \eta_h C_{L\alpha h} \quad (3.21)$$

with the lever arm term $(x_{ach} - x_{cg})$ defined in Fig. 3.23.

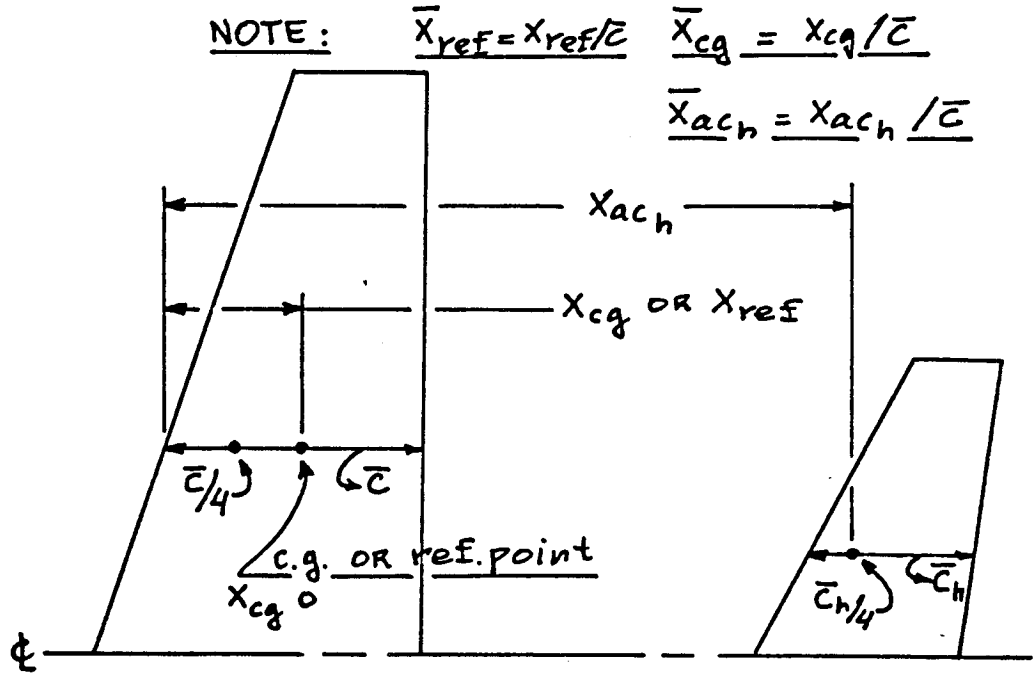

Figure 3. 23 Definition of geometric parameters for volume coefficient

b. Elevator Control Derivatives. These terms are computed as functions of the terms just presented for the stabilizer. That is,

$$C_{D\delta e} = \alpha_{\delta e} C_{Dih} \tag{3.22}$$

$$D_{L\delta e} = \alpha_{\delta e} C_{Lih} \tag{3.23}$$

$$C_{m\delta e} = \alpha_{\delta e} C_{mih} \tag{3.24}$$

$$\alpha_{\delta e} = K_b (C_{l\delta} / C_{l\delta\, theory})\, C_{l\delta\, theory}\, (k'/C_{L\alpha h})\, (a_{\delta cL} / a_{\delta cl}) \tag{3.25}$$

In Eq. (3.25),

K_b is the elevator span factor from Figs. 3.20 - 3.21;

$(C_{l\delta} / C_{l\delta\, theory})$ comes from Fig. 3.6 modified for the elevator;

$C_{l\delta\, theory}$ is derived from Fig. 3.7;

k' is derived from Fig. 3.19;

$C_{L\alpha h}$ is the lift curve slope for the horizontal tail; and

$(a_{\delta cL} / a_{\delta cl})$ is the three-dimensional elevator effectiveness factor from Fig. 3.24..

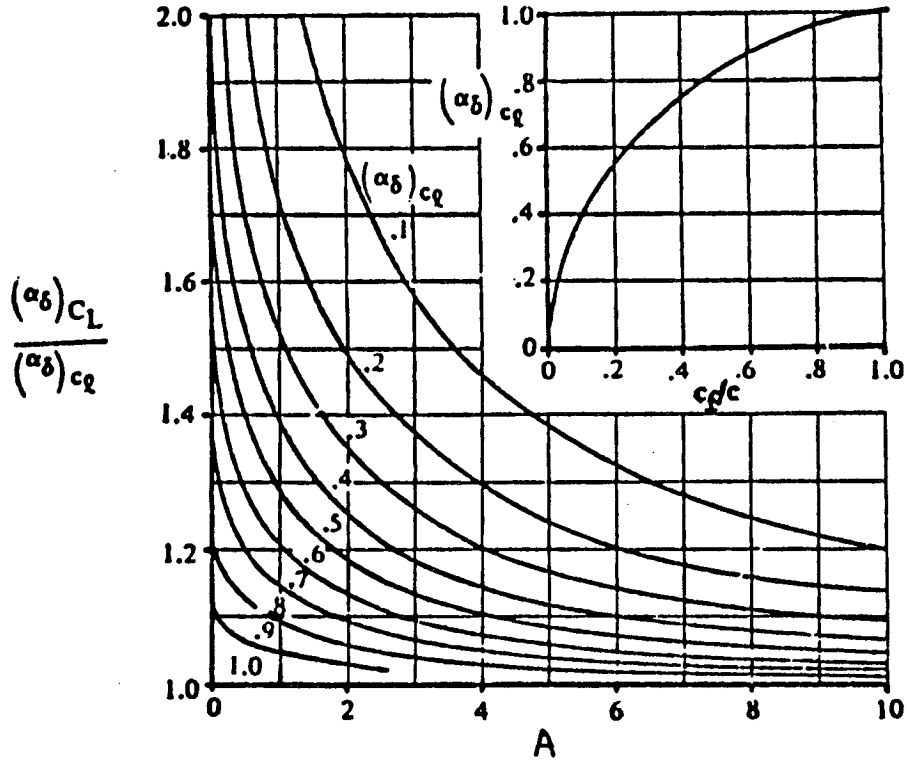

Figure 3.24 Effect of aspect ratio and flap-chord ratio on the 3D flap effectiveness

c. Canard Control Derivatives. These terms are similar to those for the stabilizer. The drag increment coefficient due to canard deflection is

$$C_{Dic} = 2(C_{Lc} / \pi A_c e_c)\, (C_{L\alpha c})\, \eta_c \tag{3.26}$$

Here,

C_{Lc} = lift coefficient of the canard;

A_c = canard aspect ratio;

e_c = 0.5

$C_{L\alpha c}$ = the same formula as Eq. (3.14) applied to the canard

η_c = 1

The lift increment due to canard deflection is

$$C_{Lic} = \eta_c \, (S_c/S) \, C_{L\alpha c} \tag{3.27}$$

The pitching moment due to canard deflection is

$$C_{mic} = - \, C_{L\alpha c} \, \eta_c \, (x_{acc} + x_{cg}) \, S_c/S \tag{3.28}$$

Here, the moment arm $(x_{acc} + x_{cg})$ is defined in Fig. 3.25.

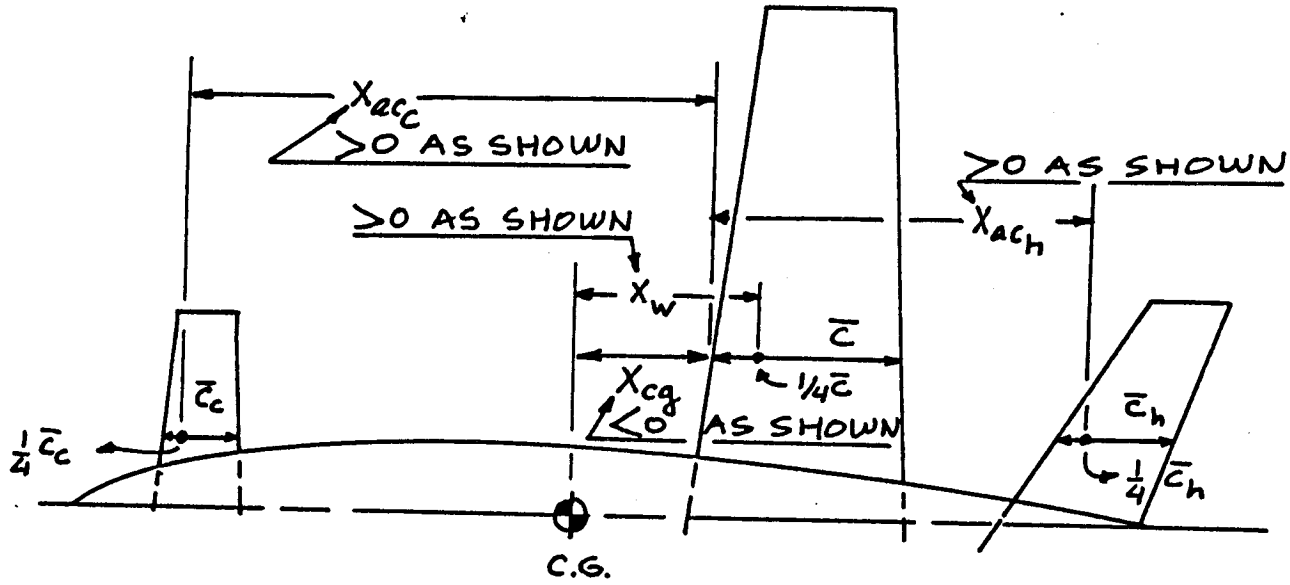

Figure 3.25 Definition of canard geometric parameters

d. Canardovator. The drag, lift and pitching moments coefficients due to deflection of the canardovator are analogous to that of the elevator Eqs. (3.22-3.25). That is,

$$C_{D\delta c} = a_{\delta c} \, C_{Dic} \tag{3.29}$$

$$C_{L\delta c} = a_{\delta c} \, C_{Lic} \tag{3.30}$$

$$C_{m\delta c} = a_{\delta c} \, C_{mic} \tag{3.31}$$

3.2.3.4 *Control derivative adjustment subject to constraints*. In the previous section, the equations used to compute the control derivatives have been defined. In most cases, these derivatives are non-linear functions of the geometry of the control surfaces, the wing or tail section they are a part of, the aerodynamic characteristics of those sections, and the moment arms of the surfaces relative to the aircraft c.g.

If the control derivatives are not large enough to meet the air worthiness constraints listed in Section 3.2.1 or the performance requirements discussed in Section 4, then the control surface geometry must be adjusted to increase the derivative magnitude. This can be done by increasing the chord and spanwise dimensions of the surface, moving the surface further out on the wing, or increasing the tail volume. Each of these adjustments would usually produce a weight and or drag penalty, so it is desirable to adjust the surface effectiveness only the amount required.

Because of the general non-linear character of the functions used to compute the control derivatives, it will be necessary to set up some type of iterative process to change the control surface geometry to just meet the control derivative magnitude requirements. The changes that are taken must be subject to the geometry constraints mentioned in Section 3.1.3. A series of sizing step computations should be determined with the resulting effects transmitted to the computations of the aircraft weights and inertias.

3.3 Conclusion

This section outlined procedures that can be used to perform a preliminary design of a variety of aerodynamic control surfaces. It also presented formulae to compute the control derivatives required to derive and analyze the aircraft dynamics and to design flight control systems.

4 Inner Loop Control Design

The main driver for the design of a stability and control module for ACSYNT is the requirement that it shall provide a "hands-off" or "black box" method to compute feedback gains for a flight control system. This is a very difficult requirement to meet—even for a conceptual aircraft—because of the wide variety of aircraft a designer can produce using ACSYNT. In addition, the dynamical properties of a single aircraft can change significantly over its flight envelope. For example, in the ten case studies done as a part of this work, six had unstable longitudinal dynamics and one had nonminimum phase dynamics. For the lateral/directional dynamics, one aircraft has a roll inertia that changes by a factor of three because of different fuel loadings for the flight conditions that were analyzed.

Furthermore, fielded flight control systems are very diverse.[9] The answers to the questions of what state variables must be measured, how to generate the required moments and forces, and how the measurements are used to form actuator commands vary with aircraft, mission, and designer experience. In practice, flight control design is an iterative, man-in-the-loop process that uses several mathematical techniques. Qualitative judgments are made at every point of the process.

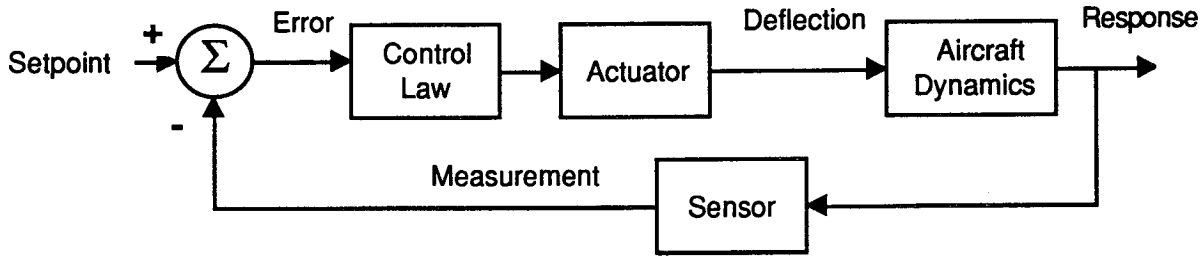

Figure 4.1: Control system elements

A flight control system comprises four fundamental kinds of elements: aircraft dynamics, actuators, sensors, and feedback control laws (Figure 4.1). For the purpose of conceptual design, we consider an actuator to be an aircraft control surface or vectored thrust, and the hydraulic or electric servoactuator that moves it. We consider the sensor to be a measurement of the aircraft state variables. The following subsections discuss each of these elements in turn.

4.1 Aircraft Dynamics

The aircraft dynamics used for the control design algorithm are derived by linearizing nonlinear equations of motion that include forces and moments due to aerodynamics, propulsion and gravity. The linearization is performed at a constant flight condition, *i.e.*, at a constant velocity and angular rate. The result is a set of linear, differential equations with the stability and control derivatives as coefficients. Table 4.1 defines the standard nomenclature used in flight dynamics and Table 4.2 shows the significant stability and control derivatives in the nondimensional form that aerodynamicists seem to prefer.

Table 4.1: Dynamics and control nomenclature

	Velocities		Forces &	Distances
	Steady	Perturbed	Moments	& Angles
Forward	U	u	X	x
Side	V	v	Y	y
Vertical	W	w	Z	z
Roll	P	p	L	ϕ
Pitch	Q	q	M	θ
Yaw	R	r	N	ψ

The inner loop control design algorithm uses dimensional stability and control derivatives because the physical units are used for performance metrics and constraints and for analysis and simulation.

Table 4.2: The significant stability and control derivatives

Longitudinal		Lateral	
C_D	C_{L_q}	C_{y_β}	C_{n_p}
C_{D_u}	C_{L_δ}	$C_{y_{\dot\beta}}$	C_{n_δ}
C_{D_α}	C_m	C_{y_r}	C_{l_β}
C_{D_δ}	C_{m_u}	C_{y_p}	$C_{l_{\dot\beta}}$
C_L	C_{m_α}	C_{y_δ}	C_{l_r}
C_{L_u}	$C_{m_{\dot\alpha}}$	C_{n_β}	C_{l_p}
C_{L_α}	C_{m_q}	$C_{n_{\dot\beta}}$	C_{l_δ}
$C_{L_{\dot\alpha}}$	C_{m_δ}	C_{n_r}	

4.1.1 Decoupled Dynamics

Equations 4.1 and 4.2 are the longitudinal and the lateral/directional dynamics, respectively, in state-space form. Table 4.1 shows the definitions of the state variables; the δ terms are control effector deflections. We use the state-space form because many computational algorithms and computer tools use this form and because it facilitates computer simulation of the dynamics.

$$\frac{d}{dt}\begin{bmatrix} u \\ w \\ q \\ \theta \end{bmatrix} = \begin{bmatrix} X_u & X_w & 0 & -g\cos(\theta_0) \\ Z_u & Z_w & U_0+Z_q & -g\sin(\theta_0) \\ M_u & M_w & M_q & 0 \\ 0 & 0 & 1 & 0 \end{bmatrix} \begin{bmatrix} u \\ w \\ q \\ \theta \end{bmatrix} + \begin{bmatrix} X_{\delta_E} \\ Z_{\delta_E} \\ M_{\delta_E} \\ 0 \end{bmatrix} \delta_E \tag{4.1}$$

$$\frac{d}{dt}\begin{bmatrix} v \\ p \\ r \\ \varphi \\ \psi \end{bmatrix} = \begin{bmatrix} Y_v & Y_p & Y_r - U_0 & g\cos(\theta_0) & g\sin(\theta_0) \\ L'_v & L'_p & L'_r & 0 & 0 \\ N'_v & N'_p & N'_r & 0 & 0 \\ 0 & 1 & 0 & 0 & 0 \\ 0 & 0 & 1 & 0 & 0 \end{bmatrix} \begin{bmatrix} v \\ p \\ r \\ \varphi \\ \psi \end{bmatrix} + \begin{bmatrix} Y_{\delta_A} & Y_{\delta_R} \\ L'_{\delta_A} & L'_{\delta_R} \\ N'_{\delta_A} & N'_{\delta_R} \\ 0 & 0 \\ 0 & 0 \end{bmatrix} \begin{bmatrix} \delta_A \\ \delta_R \end{bmatrix} \tag{4.2}$$

The derivation of Equations 4.1 and 4.2 is documented in most standard flight dynamics and control references.[10, 11] The equations used to convert dimensionless stability and control derivatives to dimensioned stability and control derivatives are in Roskam[11] and in the Appendix.

4.1.2 Coupled Dynamics

Equations 4.1 and 4.2 are decoupled, *i.e.*, the state variables in one equation do not depend on the state vectors in the other equation. This is the usual case because most aircraft are bilaterally symmetric with respect to the vertical longitudinal plane and because most steady flight conditions put the relative wind vector in the same plane.

Cross coupling has two causes. First, inertial cross coupling occurs when cross products of inertias and differences between moments of inertia are significant and the angular rates are high. For example, consider the moment equations, Eq. 4.3. When a roll moment, L, is applied, a yaw moment, N, is produced by the roll-yaw coupling in the first and third equations of Eq. 4.3 and the nonzero cross product of inertia, J_{xz}. When I_x and I_z are significantly different as in modern fighter aircraft, a pitch moment, M, is also produced.

$$\begin{aligned} L &= \dot{P}I_x - \dot{R}J_{xz} + QR(I_z - I_y) - PQJ_{xz} \\ M &= \dot{Q}I_y + PR(I_x - I_z) + (P^2 - R^2)J_{xz} \\ N &= \dot{R}I_z - \dot{P}J_{xz} + PQ(I_y - I_x) + QRJ_{xz} \end{aligned} \tag{4.3}$$

Blakelock[12] shows how to do a simplified analysis of inertial cross coupling for a constant roll rate. He first assumes that the steady velocities P and U are constants to eliminate the roll moment and forward force equations. This yields differential equations relating pitch rate, yaw rate, side velocity and vertical velocity:

$$\begin{aligned} \dot{q} + P_0 r\frac{(I_x - I_z)}{I_y} &= M_w w + M_{\dot{w}}\dot{w} + M_q q + M_{\delta_E}\delta_E \\ \dot{r} + P_0 q\frac{(I_y - I_x)}{I_z} &= N_v v + N_r r + N_p P_0 + N_{\delta_A}\delta_A + N_{\delta_R}\delta_R \\ \dot{v} + U_0 r - w P_0 &= Y_v v + Y_r r + Y_p P_0 + Y_{\delta_A}\delta_A + Y_{\delta_R}\delta_R \\ \dot{w} + v P_0 - U_0 r &= Z_w w + Z_{\dot{w}}\dot{w} + Z_q q + Z_{\delta_E}\delta_E \end{aligned} \tag{4.4}$$

Blakelock further simplifies the equations by ignoring the control surface terms and by assuming the aerodynamic side and vertical forces are zero. The latter assumptions are very limiting;

Eqs. 4.4 can easily be put into state-space form and the analysis performed on that result. Note that all three control surface deflections appear in Eq. 4.4, thus making the feedback control problem more complex. Blakelock concludes with two examples. The first is an aircraft stable for all roll rates and the second is an aircraft unstable for a range of roll rates.

In addition to inertial cross coupling, aerodynamic cross coupling occurs when the aircraft rotates around any axis except the velocity vector, *e.g.*, body axis roll at nonzero angles of attack. In the derivation of Eqs. 4.4, Blakelock assumed that the principle axes of the aircraft were aligned with the stability axes. For nonzero angles of attack, the aerodynamic moments are caused by the wind vector, but are expressed in the vehicle stability axes. The body axes are inclined to the stability axes by the steady-state angle of attack. Hence, the moments can depend on roll, pitch and yaw angle, *e.g.*, sideslip becomes angle of attack and angle of attack becomes sideslip at a 90° roll angle. In other words, terms depending on ϕ, θ, and ψ ought to be included in Equation 4-4.

The issue of cross coupling raises significant modeling and control questions. Blakelock's approach to inertial coupling during a steady roll is a reasonable approximation for conceptual design, provided the assumptions hold. Other maneuvers will require new derivations. In the case of aerodynamic coupling, the usual stability and control derivatives may not be applicable because they are derived at equilibrium flight conditions, either theoretically, or from wind tunnel or flight data. These flight conditions usually have the body axes fixed with respect to the relative wind. In either case, the control design methodology proposed in this report applies, given the correct data to form a linear, state-space model.

4.1.3 Dynamics of Case Studies Aircraft

Nine examples from Roskam[11] were used as case studies to determine the range of dynamical responses possible:

- Learjet Model 24 (cases 1 to 3)
  - Power approach at sea level
  - Cruise at 40,000 ft at maximum weight
  - Cruise at 40,000 ft at low weight
- Boeing 747 (cases 4 to 6)
  - Power approach at sea level
  - Cruise at 40,000 ft
  - Cruise at 20,000 ft
- McDonnell Douglas F-4C (cases 7 to 9)
  - Power approach at sea level
  - Subsonic cruise at 35,000 ft
  - Supersonic cruise at 55,000 ft

The data comprise the geometry and inertias, and the lateral and longitudinal dimensionless stability and control derivatives for three aircraft at three flight conditions. The data are listed in the Appendix. MATLAB scripts were used to convert to dimensioned stability and control derivatives and analyze the dynamics at each flight condition. Printouts showing the poles, natural frequencies and damping ratios for the longitudinal and lateral dynamics and plots

showing the frequency responses in each case are in the Appendix. The MATLAB computations checked with the computations for one flight condition for each aircraft that Roskam presented.

Table 4.3 summarizes the results of the dynamics analyses. Six of the longitudinal dynamics and two of the lateral dynamics cases were unstable. The unstable modes are indicated by negative numbers in the table. A negative ζ indicates an unstable second order mode; a negative τ or a negative ω indicates an unstable first order mode. The italicized entries in case 8 denote a phugoid mode that splits into stable and unstable first order modes at that flight condition.

Table 4.3: Dynamical parameters for the 9 case studies from Roskam.[11]

	LONGITUDINAL DYNAMICS				LATERAL DYNAMICS			
	Phugoid		Short Period		Dutch Roll		Spiral	Roll Sub.
	ω	ζ	ω	ζ	ω	ζ	τ^{-1}	τ^{-1}
CASE	rad/s		rad/s		rad/s		rad/s	rad/s
1	0.239	–0.0589	1.60	0.567	1.03	–0.0542	0.745	0.0296
2	0.0906	0.0584	2.82	0.352	1.68	0.0347	0.502	0.00119
3	0.101	0.0854	2.95	0.400	2.27	0.0117	2.27	0.00201
4	0.170	–0.132	0.773	0.617	0.752	0.0973	1.15	0.0431
5	0.0343	0.173	1.32	0.355	1.02	0.108	0.508	–0.00536
6	0.0682	–0.0272	1.24	0.468	1.05	0.119	0.940	0.0171
7	0.168	–0.135	0.778	0.600	1.81	0.175	1.11	0.0152
8	*–0.0354*	*0.0448*	2.85	0.222	2.40	0.0482	1.34	0.0131
9	0.0268	–0.0740	4.86	0.039	2.46	0.0562	0.782	0.00286

The F-4C at supersonic cruise has unstable or nonminimum phase *zeros* in the dynamics; Subsection 4.4.3 discusses the implications of this property for feedback control. The fastest mode in all the case studies is the 4.9 rad/s F-4C short period mode at supersonic cruise; the slowest mode is the 0.0012 rad/s Learjet roll subsidence mode at maximum weight cruise.

4.2 Actuators

Hydraulic solenoids or electric motors move the control surfaces of modern aircraft. Each of these actuators has dynamics that can affect control system performance. Furthermore, these actuators are constrained to move the surfaces only within rate and deflection limits. The control surface limits are set to ensure that maximum deflection is within the stall limits of that surface. Typical acceptability criteria are that aileron deflections are less than 25°. Single hinge rudder deflection is typically less than 25°, while double hinge rudder deflection is less than 30°.

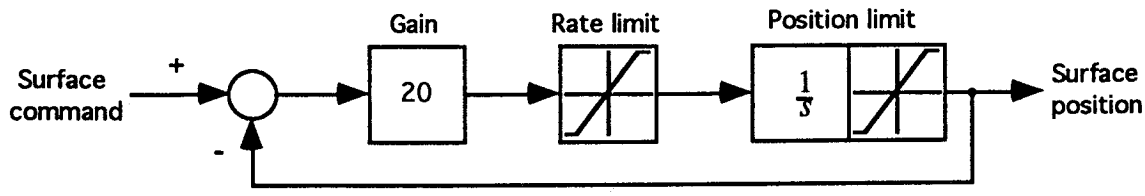

Figure 4.2 Control surface actuator model

Figure 4.2 shows a model of the control actuator used to study flight control system design for a generic fighter aircraft at NASA Dryden.[14] In this model, the actuator dynamics model is a first order lag with rate limits and maximum deflection limits. Here, the first order lag is modeled as an integrator in the forward loop and a gain of 20 producing a 0.05 sec time constant.

Mathematical models of actuator dynamics can be quite complex. Figure 4.3[14] shows the actuator model for a stabilizer with both symmetric and differential movement. Also, Bosworth[13] reports X-29A actuators that have 4th order dynamics.

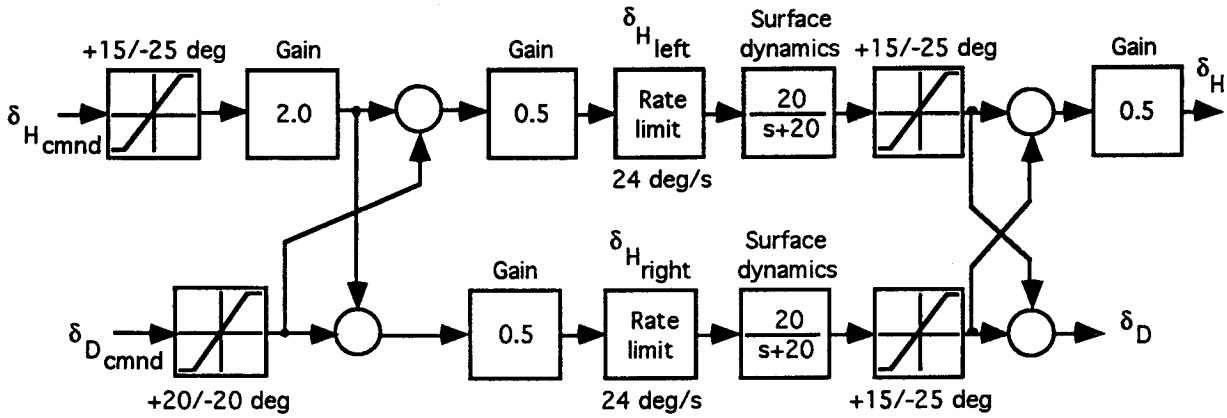

Figure 4.3 Actuator model for the stabilizer

The important question for conceptual design is how much faster or slower is the actuator dynamics than the aircraft dynamics. If the actuator response is faster than the aircraft response, the actuator dynamics can be ignored because it will have only a small effect on aircraft performance. For performance evaluation by simulation the complexity also depends on the kinds of control surfaces used, as in Figure 4.3. Consequently, the code for modeling the actuator system must be flexible so that more complex models can be added later as the need arises.

Table 4.4 presents actuator data from Johnston[9] , Bosworth[13], and Brumbaugh.[14] Johnston presents an uneven accumulation of block diagrams of flight control systems for some recent aircraft. The figures are derived from a variety of sources and present data ranging from names of hardware items to transfer functions. The slowest actuator is the C-5A aileron with a 0.250 s time constant. This converts to a 4.0 rad/s bandwidth which is slower than the F-4C phugoid mode, but about three times faster than any of the 747 modes. Most of the actuator bandwidths reported by Johnston and Bosworth are between 10 and 20 rad/s.

Table 4.4 Example actuator model parameters

Aircraft Type	Time Constant s	Rate Limit deg/s	Deflection Limits Aileron ± deg	Elevator ± deg	Rudder ± deg
Gen. Fighter	0.05	24.	20.	30	+15/-25
F-4	0.10				
F-105	0.07		10	7.5	2.2
X-29		30.	17.5	30.	30
B-52	0.027				
C-5A	0.25				
KC-135	0.05				
B747		37.	20.	25	+17/-23

Table 4.5 summarizes the extreme values of airframe and actuator dynamics found in these references. It shows that the case studies have dynamics at least 20 percent slower than the slowest actuators we found.

Table 4.5: Extreme values of airframe and actuator dynamics

Aircraft Class	Fastest Airframe Dynamics rad/s	Slowest Actuator Dynamics rad/s
Fighter	4.86	6.0
Transport	1.24	4.0
Sources	Roskam Bosworth	Johnston Bosworth

Consequently, the performance results for the case studies reported in this document were derived under the assumption that the dynamics of the actuators was sufficiently faster than the dynamics of the airframe that it could be ignored.

The overall actuator lag should be included as a design variable because actuator speed influences cost, weight, and power; the control design methodology we propose can easily accommodate different actuator models by including additional actuator state variables to the aircraft dynamics. For flight control system (FCS) conceptual design, the simple actuator model depicted in Figure 4.2 is probably adequate. The linear first order lag model can be used in the gain computations.

Rate and deflection limits on effectors are also important because they, along with position and area, determine the effectiveness (authority) of the control surfaces. The effect of rate and deflection limits on performance usually is determined during simulation analysis rather than the

design analysis. If the control law requires rates or deflections greater than the limits to achieve a specified performance, or to maintain stability, the control effector sizing must be changed. This is one of the simplest ways to feed effects on dynamical performance back to the aircraft design.

4.3 Sensors

The sensors that measure aircraft state variables have dynamics, generate noise, show biases and bias drift, and suffer from scale factor errors and drift. These characteristics of sensors are major concerns during the detailed design and analysis of flight control systems. Equation 4.5 shows a general measurement model, in which b and b_d are the bias and bias drift, K_{sf} is the scale factor, f and f_d are the scale factor error and drift, ν is the noise and the rational polynomial is the transfer function of the sensor dynamics.

$$x_{measured} = K_{sf}(1+f+f_d)x_{true}\frac{1+n_1 s+\cdots+n_M s^M}{1+d_1 s+\cdots+d_N s^N}+b+b_d+\nu \qquad (4.5)$$

The dynamics may cause a lag between the measurement and the aircraft state variable measured. Also, very fast (or very slow) changes in the state variables may not be measurable. Noise is a random variation added to the state variable measured. This can be reduced by adding a filter, and, consequently, more dynamics, to the signal path. Bias is a constant offset from the measured state variable and the associated drift is a slow change in the bias. A feedback control system will follow the bias because it assumes that the sensor is correct. The scale factor error changes the gain of the sensor, and the associated drift is a slow change in this error.

All of these characteristics, while important during detailed control system design, can be ignored when designing inner loop control systems for aircraft conceptual designs. First, most sensors and noise filters have a wider bandwidth, *i.e.*, are faster, than aircraft dynamics. Second, noise can and is typically filtered; an excessively noisy sensor will not be used, or it will be augmented with other sensors. A good estimate of a state variable from several sensors can be obtained using methods such as Kalman filtering. Next, the effect on a feedback system of bias is so predictable that modeling the bias for a design concept is unnecessary. Bias drifts depend on the instrument, the environment and on age. The effect of bias can be reduced by implementing a bias estimator in an extended Kalman filter. Finally, the scale factor error is usually a fraction of a percent. The effect on the loop gain is negligible. The results for the case studies presented in this report were obtained by assuming the flight sensors are perfect.

4.4 The FCS Design Algorithm

The inner loop control design concept developed and demonstrated as a part of this work uses the linear-quadratic (LQ) control design methodology to compute the feedback gains. The gains from this technique depend on the aircraft dynamics and design parameters that can be set by the designer or loaded from defaults. After the initial design choices are made, the software then iteratively modifies the design parameters based on the control system performance to converge toward performance specifications and satisfy constraints that, again, are set by the designer or loaded from defaults. If the control design does not converge, possible remedies are fed back to the aircraft design.

The LQ approach is used for three reasons.

- It is a "hands-off" gain computation.
- Stability is guaranteed.
- Performance is traceable to the design parameters.

It is a "hands-off" method for computing feedback gains once the control design parameters are set. Default sets can be provided to start the control design process. The stability of the closed loop system is guaranteed when the dynamics is "controllable" and "observable." Controllability and observability are mathematical conditions that are easy to verify. The stability ensures that performance metrics can be evaluated at each design iteration to provide a basis to change the control design parameters for the next iteration. The effect of changes in design parameters is clearly traceable to closed loop performance in the time domain. This means that the control design process will converge.

The theoretical foundations of the linear-quadratic method are well documented in standard references such and Kwakernaak[15], and Boyd.[16] The next subsection gives a brief outline of the relevant points.

4.4.1 The Linear-quadratic Method

The objective is to find a feedback controller that minimizes the integral of a quadratic cost function that penalizes large or long-term deviations in the state variables and the control effort. Mathematically, the problem is to minimize the cost functional

$$J[u]=\int_0^\infty x^{\mathrm{T}}Qx+u^{\mathrm{T}}Ru\,dt \tag{4.6}$$

subject to the constraints

$$\begin{aligned}\dot{x}&=Ax+Bu\\ y&=Cx+Du\end{aligned} \tag{4.7}$$

The aircraft dynamics, Eqs. 4.1 and 4.2, are already in the form of Eqs. 4.7. The matrix A depends on the stability derivatives and the flight conditions; the matrix B depends on the control derivatives. The vectors x, u, and y are the state variables, control variables, and output variables, respectively. If the state variables are the outputs of interest, the C matrix is the identity matrix and the D matrix is the zero matrix. If other outputs such a angle of attack, vertical acceleration, sideslip angle, and lateral acceleration, the C and D matrices are made up of stability and control derivatives, and instrument scale factors.

Designers pick the elements of the weighting matrices Q and R to achieve the relative deviations of the state variables and the control effort that they want; this is an iterative process that uses the computations necessary to solve the optimization problem defined by Eqs. 4.6 and 4.7, and a simulation of the resulting feedback control system. In actuality, the exact value of the integral in Eq. 4.6 is irrelevant; what are important are the time responses of the simulation and the closed loop frequencies and damping ratios.

The optimization problem is solved by using Eq. 4.8 to compute a gain matrix, K_r, that depends on the solution, S, of the algebraic matrix Riccati equation, Eq. 4.9.

$$K_r = -R^{-1}B^T S \tag{4.8}$$

$$0 = SA + A^T S - SBR^{-1}B^T S + Q \tag{4.9}$$

This yields a linear, full-state feedback law of the form

$$u = K_r x \tag{4.10}$$

For example, in the case of pitch control of the longitudinal dynamics, Equation 4.10 becomes

$$\delta_E = k_1 u + k_2 w + k_3 q + k_4 \theta + k_5 \int \theta \tag{4.11}$$

where the last term in Equation 4.11 is an integral feedback term added to reduce steady-state error and where δ_E is the elevator deflection.

Figure 4.4 is a SIMULAB block diagram of an inner loop control architecture implementing this kind of feedback law. The Mux block combines 4 scalar setpoints into a 4-vector; the vector of measurements of state variables from the Aircraft block is subracted from the setpoint vector to form an error vector. The DeMux block splits the vector into 4 scalars that are multiplied by their appropriate gains. The pitch error is integrated and multiplied by its gain. The results of the multiplications are summed to form the elevator command for the Aircraft block.

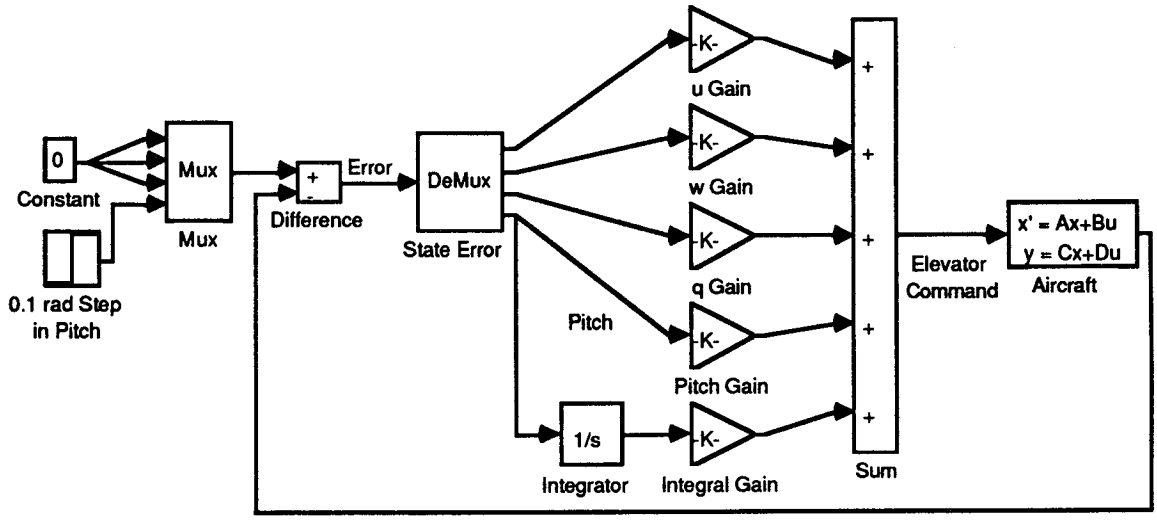

Figure 4.4: Inner loop control architecture implementing a linear, full-state feedback law

The solution of problems such as the optimization problem of Equations 4.6 and 4.7 and the algebraic matrix Riccati equation, Eq. 4.9, is possible using standard, commercially-available software tools such as MATLAB and MATRIX$_X$. Software that performs the same functions may be available in NASA's COSMIC library.

4.4.2 Enumeration of the Steps in the Algorithm

0. The inputs from ACSYNT modules are flight conditions, stability derivatives, control derivatives, actuator dynamics and mass properties. The input from the designer is the selection of a default set of control system performance metrics to optimize or constrain and the constraints or, optionally, overrides to some or all of the default set.
1. The ACSYNT inputs are used to compute the aircraft longitudinal and lateral dynamics in state-space form. An analysis is performed to report the stability, eigenvalues, natural frequencies, damping ratios, time constants, and numerator zeros of the dynamics.

   The designer inputs are used to initialize the control design parameters (the elements of the Q and R matrices in Eq. 4.6) and start the control design process.

   For example, the default longitudinal pitch controller has a pitch integral state to reduce steady-state error. Consequently, Q is a 5 by 5 matrix, and R is a scalar because the elevator is the only control. The gains are computed by using weightings (elements of the Q matrix) of 1 on the pitch rate, pitch angle and pitch integral, *i.e.*,

$$Q = \begin{bmatrix} 0 & 0 & 0 & 0 & 0 \\ 0 & 0 & 0 & 0 & 0 \\ 0 & 0 & 1 & 0 & 0 \\ 0 & 0 & 0 & 1 & 0 \\ 0 & 0 & 0 & 0 & 1 \end{bmatrix} \tag{4.12}$$

   and a weighting (design parameter) on the elevator deflection of

$$R = Z_{\delta_E}^2 + M_{\delta_E}^2 \tag{4.13}$$

   This particular set of design parameters have proven to be a reliable starting point for control design iterations for the nine case studies from Roskam[11] reported here and for an example from McRuer.[10]
2. Gains are computed using LQ methods and the designated or default performance metrics are evaluated using a fast simulation. Seven metrics are important for inner loop flight control design:
   - percent overshoot
   - rise time
   - percent steady-state error
   - peak control surface deflection
   - peak vertical and lateral acceleration
   - closed loop natural frequencies
   - closed loop damping ratios

   Figure 4.5 shows the standard definitions for the first three metrics on results for one of the study cases. These results use the default longitudinal pitch controller design parameters described earlier. The response is to a step change in pitch of 5.7° at 10 s, the standard test for the longitudinal case studies.

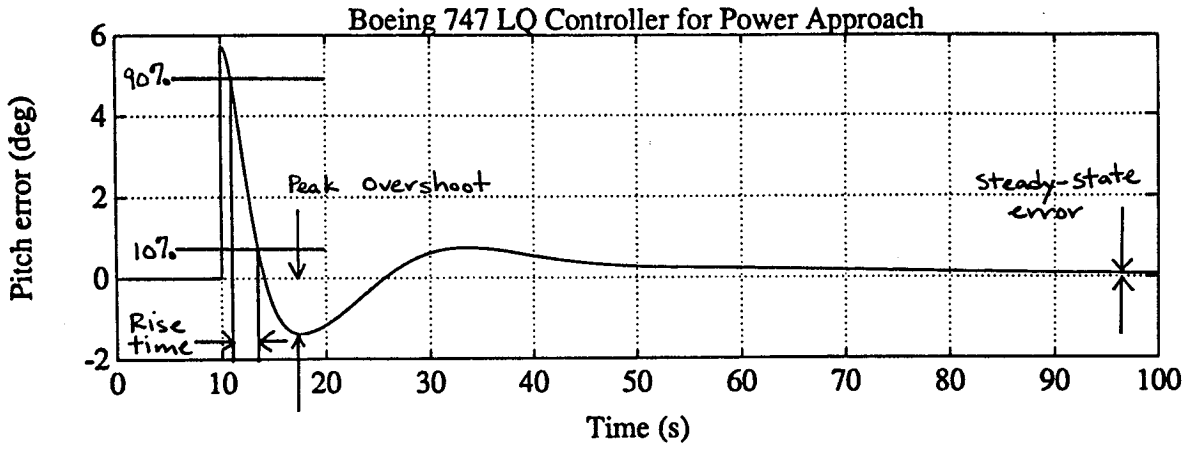

Figure 4.5: Standard definitions for overshoot, rise time and steady-state error.

3. If a constraint is violated or if an optimum is not yet achieved, a perturbation procedure is used to determine which design parameters cause the most change in the affected metrics. The procedure is to perturb each weight twice (*e.g.*, multiply and divide by 100) and compare the sensitivity. The program picks the greatest sensitivity to satisfy constraints first, and to improve the performance second.
4. The program meets or exceeds the required change by taking a large step in the design weights and backing off a little. After the new weights are computed, the optimization process continues with step 2. The iteration history is stored and reported to the designer.

4.4.3 Discussion of Case Studies

Controllers were designed using the LQ approach for the nine case studies from Roskam[11] described in Subsection 4.1 and for one example from McRuer[10]. The performance of the pitch controllers designed using the initial design parameters is summarized in Figure 4.6 and detailed results are presented in the Appendix.

Figure 4.6 shows bar graphs for the pitch overshoot, rise time, peak vertical acceleration, and peak elevator deflection metrics. Each graph plots the performance of pitch controllers for eight of the longitudinal case studies. The feedback gains for each of the controllers were computed using the initial design parameters in Eqs. 4.12 and 4.13. The cases are numbered as in Subsection 4.1. The results show that the initial design parameters are a reasonable choice to start a design iteration because the resulting controllers are stable and their performance is reasonable for a wide range of aircraft and flight conditions.

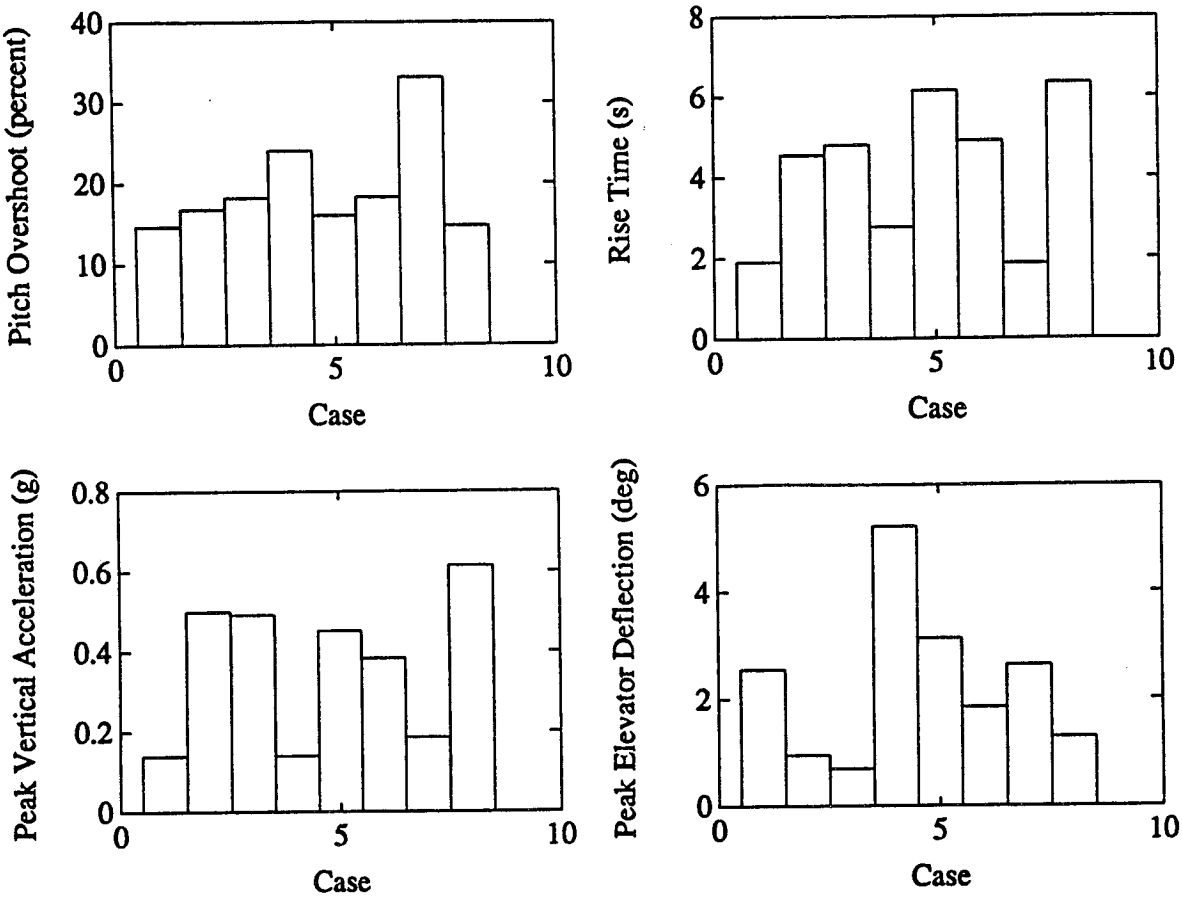

Figure 4.6: Results of the longitudinal pitch control case studies with the initial choice of design parameters

The convergence of the method was tested by determining the sensitivity of the controller performance to changes in the design parameters—the elements of the Q and R matrices. Figure 4.7 shows the effect on four performance metrics of changing only the pitch angle weight. The aircraft is the F-89 example from McRuer.[10] Both the pitch overshoot and the rise time decrease as the penalty on pitch angle increases. To achieve this decrease, both the peak vertical acceleration and the peak elevator deflection must increase. If there were constraints on vertical acceleration or elevator deflection, graphs such as Figure 4.7 can show the achievable minimum overshoot and rise time. If the minima were not acceptable, either the constraints must be changed, or the aircraft must be changed. The graphs indicate how much to change the constraints and how much to increase the control surface effectiveness.

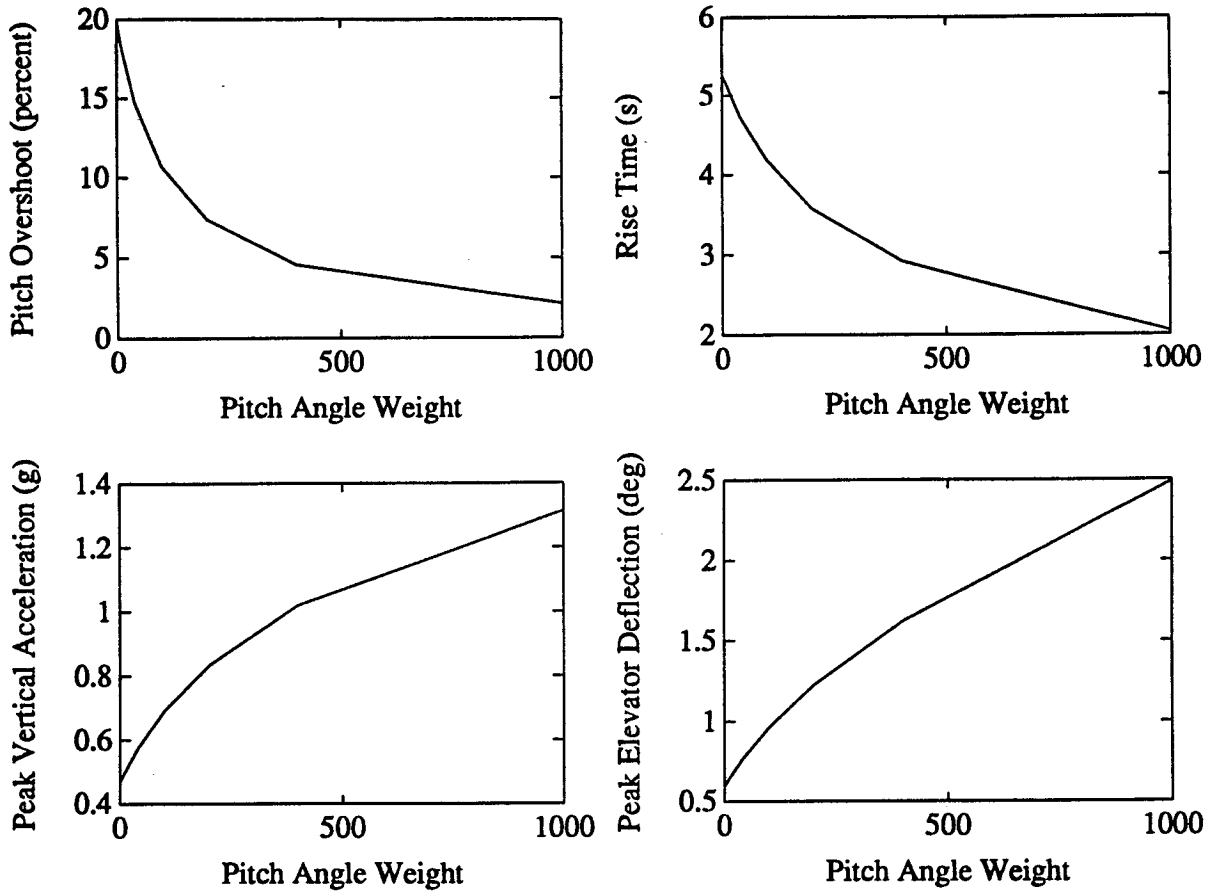

Figure 4.7: Pitch control performance convergence as functions of pitch angle weight

Figure 4.6 shows the results for eight of the case studies from Roskam. Case 9, the F-4 at supersonic cruise, is not shown because the controller performance for the *initial* design parameters was sufficiently worse than the first eight cases that the performance metric values for case 9 would have been off scale. The dynamics of the F-4 at this flight condition are called nonminimum phase dynamics because at least one zero of the transfer function has a positive real part. The existence of such a zero limits the magnitude of the feedback gains. This is a limit common to all control design methods, including classical, modern and linear-quadratic approaches. The LQ method still yields a stable controller; however, the performance is difficult to improve without modifying the method.

The classical solution to such a problem is to add a compensation filter that has poles and zeros with negative real parts to the control loop. The limit on the magnitude of the feedback gains can be increased by choosing suitable filter poles and zeros. The LQ approach can be modified by adding the compensation filter to the aircraft dynamics in much the same way that the pitch integral state was added to obtain the controllers for the case studies.

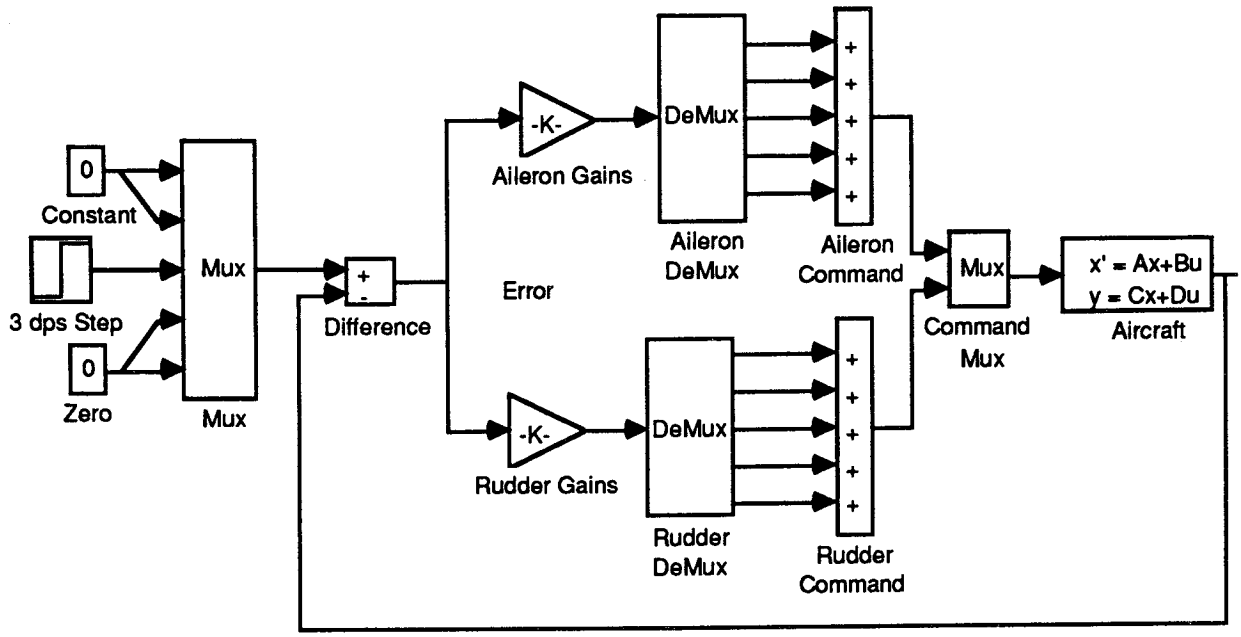

Figure 4.8 Lateral/directional inner loop flight control system for the Learjet Model 24

Figure 4.8 shows a SIMULAB block diagram of an inner loop flight control system implementing an LQ feedback law for the lateral/directional dynamics of the Learjet Model 24. The Mux block combines 5 scalar setpoints into a 5-vector; the vector of measurements of state variables from the Aircraft block is subracted from the setpoint vector to form an error vector. Each element of the error vector is multiplied by two feedback gains—one for the aileron, and one for the rudder—to form two 5-vectors. The DeMux blocks split the 5-vectors into two sets of 5 scalars each. Each set of scalars is summed; one sum forms the aileron deflection command and the other sum forms the rudder deflection command. Both scalar commands are combined into a 2-vector by a Mux block and sent to the Aircraft block.

Figure 4.9 shows the performance results for a Learjet Model 24 turn. The objective is to perform a 3 deg/s turn with a zero sideslip angle. Figure 4.8 shows a 3 deg/s step in the yaw rate setpoint. This occurs at 5 s in Figure 4.9. The yaw rate shows a 0.5° steady-state error and the sideslip angle is 2.5°. Roskam[6] says that a sideslip angle of less that 5° is "acceptable." The design parameters chosen give a reasonable compromise between sideslip and steady-state yaw rate error. Adding integral control would decrease the steady-state errors to much smaller values.

To achieve these results, only the lateral velocity and the yaw rate state variables had nonzero elements in the Q matrix, and all elements of the R matrix were nonzero. Specifically,

$$R = B^T B = \begin{bmatrix} Y_{\delta_A}{}^2 + L'_{\delta_A}{}^2 + N'_{\delta_A}{}^2 & Y_{\delta_A} Y_{\delta_R} + L'_{\delta_A} L'_{\delta_R} + N'_{\delta_A} N'_{\delta_R} \\ Y_{\delta_A} Y_{\delta_R} + L'_{\delta_A} L'_{\delta_R} + N'_{\delta_A} N'_{\delta_R} & 10\left(Y_{\delta_R}{}^2 + L'_{\delta_R}{}^2 + N'_{\delta_R}{}^2\right) \end{bmatrix} \tag{4.14}$$

and

$$Q=\begin{bmatrix} 0.1 & 0 & 0 & 0 & 0 \\ 0 & 0 & 0 & 0 & 0 \\ 0 & 0 & 10^5 & 0 & 0 \\ 0 & 0 & 0 & 0 & 0 \\ 0 & 0 & 0 & 0 & 0 \end{bmatrix} \tag{4.15}$$

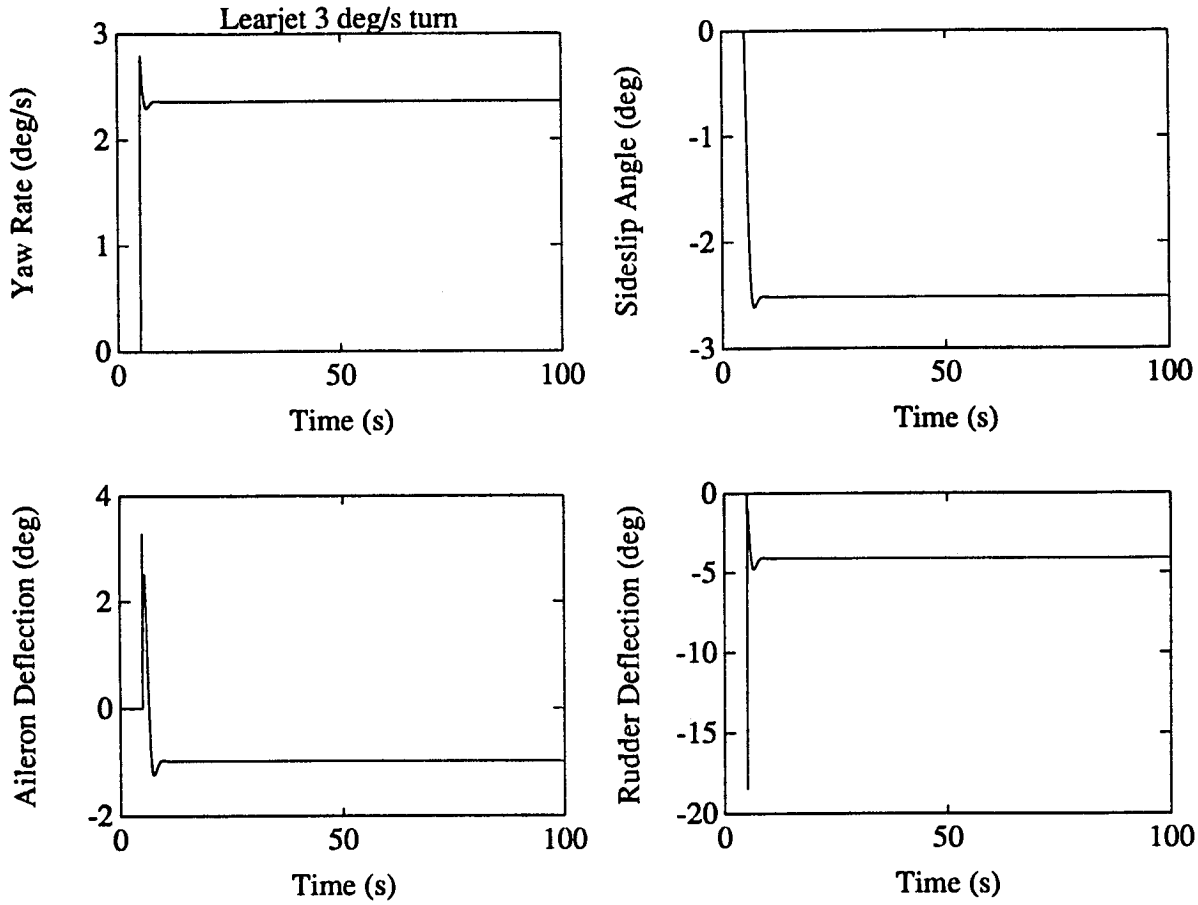

Figure 4.9 3 deg/s turn performance results for the Learjet Model 24 at flight condition 3.

Detailed results of the longitudinal and lateral/directional case studies are in the Appendix. This includes open loop frequency responses, Simulab block diagrams, Matlab scripts, and time responses of state variables, control surface deflections, and performance metrics.

4.5 Conclusion

This section discussed how aircraft data such as flight conditions, stability and control derivatives, and mass properties are used to compute equations describing the aircraft dynamics. Longitudinal, lateral/directional, and coupled dynamics were covered. The section also presented a method for computing inner loop flight control system feedback gains and an algorithm for improving the control system performance. Finally, the results of applying this methodology on several case studies were discussed.

5 Summary and Recommendations

5.1 Summary

The effort summarized in this report has specified the overall process to include the inner loop flight control system design module in aircraft conceptual design using the ACSYNT program. It has specified the methodology to design the inner loop FCS and to compute associated closed loop response and dynamic performance of the controlled aircraft. It has also pointed out how shortcomings of control performance are accounted for by modifying other components of the aircraft—particularly the geometry of the control surfaces.

5.1.1 FCS Design Requirements

Section 2 of this report presented the interface requirements for adding an inner loop flight control system design module to the ACSYNT program. Both user interface and program module interface requirements were discussed.

The user interface will use default control design parameters, classified by type of aircraft, to promote rapid design iterations and to allow aircraft designers to focus on improving total aircraft performance. A capability for overriding any default value can be used to determine how sensitive the aircraft design is to flight control design parameters.

Flight control design requires a mathematical model of the aircraft dynamics. ACSYNT software modules must provide the mass properties, stability and control derivatives, and the flight conditions used to compute such models. The control design module must provide ways to influence the aircraft design. Two methods for implementing this are discussed. Control effector deflections, evaluated performance metrics, the feedback gains, and the closed loop dynamics are output quantities that will be of use in either method.

5.1.2 Control Effector Design

Section 3 of this report outlined the process whereby the ACSYNT program could compute the geometries of the control surfaces and the resulting control derivatives. The control derivatives are necessary inputs to the FCS design process discussed in Section 4. The control surface geometry is necessary input to computation of the control derivatives. Also, this geometry has to have certain flexibility in layout to enable the aircraft to meet air worthiness and flight control performance specifications.

First, considerations of geometric constraints of the wing and tail on aileron, rudder, and elevator design were discussed. The historic trends in ratios of control surface to wing or tail surface areas, chord and span dimension fractions are presented for fighter, business jet, and commercial transport aircraft. This is followed by an outline of the logical procedure that can be followed in ACSYNT to design the control surface geometries.

Next, the process required to compute the control derivatives, as based on the DATCOM method, are summarized for roll, pitch, and yaw actuation. It is important to understand this process so that the method used first to design control surface geometries is set up to produce the required inputs for the control derivative computations. The air worthiness constraints that must be met in pitch, roll, and yaw control moments are given as minimums to be met by the control derivative values. This is followed by a summary of the DATCOM process to generate control

derivatives due to (a) aileron or elevon, (b) rudder, and (c) stabilizer, elevator, canard or canardovator deflections. Both subsonic and supersonic computation steps are given.

5.1.3 Inner Loop Flight Control Design

Section 4 of this report discussed the aircraft dynamics as the primary ingredient in the control design process, feedback gain computation using linear-quadratic methods, a design algorithm incorporating an LQ method, and the results of a wide variety of case studies.

The dynamics required is a composite of the airframe dynamics at the flight condition of interest, actuator dynamics and sensor dynamics. The section presented a summary of actuator time constants found in the open literature, a discussion of the bounds on the dynamics of these actuators and on the dynamics of the aircraft used in the case studies and conclusions on the relevance of these bounds to concept design. These results lead to the conclusion that simple first order dynamical models for actuators will suffice for aircraft conceptual design. This section also gave a justification for assuming that the flight sensors are ideal for the purpose of conceptual design.

Next, control gain computations using linear-quadratic methods were described. These methods provide a "hands-off" or "black box" approach to the qualitative, man-in-the-loop decisions that often have to be made during flight control design. The design parameters in the LQ method—the elements of the Q and R penalty matrices—can be related easily to time domain performance metrics. A design algorithm that uses this relationship was outlined. Finally, this section presented the results of some case studies that indicate that the algorithm will be effective.

5.2 Recommendations for Further Work

5.2.1 Immediate Tasks

The next efforts that are required to implement an FCS design module within ACSYNT are the following three tasks:

1. Prototype the LQ design process for generating the closed inner loop FCS design. This task would use a commercial software program MATLAB for control system synthesis off-line and external to ACSYNT. The goal is to create a semi-automatic "black box" procedure based on the previous work. The design process would be perfected before it is permanently added internal to ACSYNT as a later task. This task would include the following steps:
   a. Develop and document the input scripts and templates for designing inner loop longitudinal and lateral FCS. These make use of the desired closed loop performance metrics to drive the design iteration. This assumes that ACSYNT will be modified to produce the necessary input variables and parameters to drive the FCS design process.
   b. Use example stability and control derivatives, inertias, control actuator dynamics, and FCS performance metrics for transport, business jet and fighter aircraft types to test the input scripts. Use the FCS design output to test the closed loop performance of the aircraft. Develop the design iteration process to produce the desired control performance.

c. Develop the logic to direct the FCS design process to account for different aircraft dynamics properties, mission requirements, maneuvers, and user-specified output choices. Include the method of specifying need to change the control authority (control surface area, moment arms, etc.), if the closed loop design does not produce adequate performance.

d. Specify the logic and code for ACSYNT modification to compute the control laws and gains to replace the MATLAB tool and the prototyping process used in steps a-c above. This would consider use of public domain software modules, such as those available from COSMIC, as appropriate.

2. Develop the algorithms for computing the control surface geometry, the control actuator models, and the interface with the ACSYNT process for computing stability and control derivatives. Include output logic to produce the necessary parameters for input to the FCS design process developed in Task 1. These algorithms would be documented in data flow diagram, hierarchical diagram, and pseudocode form ready for ACSYNT coding.
3. Develop the algorithms for implementing the FCS design based on the requirements specified in Task 1.d. These algorithms would be documented in data flow diagram, hierarchical diagram, and pseudocode form. Where practical, specific modules available to duplicate the LQ FCS design process would be developed or delivered in C/C++ code form.

5.2.2 Intermediate Tasks

After the above tasks are complete, there are additional tasks that are required to complete the FCS design implementation. These include the following:

1. Complete the design of a flight control system performance metric module (PMM) to test the output of the FCS design against some desired aircraft dynamic performance standards. This would require providing the facility to integrate aircraft equations of motion, including action of the FCS, in response to selected aircraft guidance functions. The output of this module would be used to verify the FCS works as predicted by the design process, to judge the aircraft performance relative to given criteria, and to determine if design changes are needed for performance improvement.
2. Develop the technique within the PMM for designing optimal trajectories to conduct individual mission maneuvers using the ACSYNT-designed aircraft with the FCS.
3. Add feedback from the PMM to regulate aircraft design changes to meet performance requirements.
4. Specify requirements for taking the ACSYNT design including the FCS and PMM output to a cockpit simulator for man-in-the-loop testing of the conceptual design.
5. Expand the ACSYNT reference manual to describe the methodology to include FCS effects and performance criteria in the aircraft conceptual design process.

References

1 Raymer, Daniel P., 1989, *Aircraft Design: A Conceptual Approach*, American Institute of Aeronautics and Astronautics, Inc., Washington, D.C., ISBN 0-930403-51-7.

2 Hill, G.C., 1992, "Improving Designer Productivity," NASA TM-103929.

3 Moore, M., and Samuels, J., 1990, "ACSYNT–Aircraft Synthesis Program," NASA Ames Research Center, Advanced Aircraft Group, Systems Analysis Branch.

4 Gwartney, J.D., Hunter, C.G. , and Sorensen, J.A., 1992, "Comparison of Design and Analysis Methods Employed by ACSYNT and TASP," Report No. 92121-01, Seagull Technology, Incorporated, 1310 Hollenbeck Ave., Sunnyvale, CA 94087.

5 Roskam, J., 1989, *Airplane Design, Part II: Preliminary Configuration Design and Integration of the Propulsion System*, Roskam Aviation and Engineering Corporation, Ottawa, Kansas, USA.

6 Roskam, J., 1988, *Airplane Design, Part VII: Determination of Stability, Control and Performance Characteristics: FAR and Military Requirements*, Roskam Aviation and Engineering Corporation, Ottawa, Kansas, USA.

7 Roskam, J., 1987, *Airplane Design, Part VI: Preliminary Calculation of Aerodynamic, Thrust and Power Characteristics*, Roskam Aviation and Engineering Corporation, Ottawa, Kansas, USA.

8 Hoak, D.E., *et al.*, 1978, "USAF Stability and Control Datcom," Flight Control Division, Air Force Flight Dynamics Laboratory, WPAFB, Ohio, 45433-0000, revised.

9 Johnston, D.E., 1975, "Flight Control Systems Properties and Problems, Volume II—Block Diagram Compendium," NASA CR-2501, February 1975, Contract NAS 4-1881.

10 McRuer, D., Ashekenas, I., and Graham, D., 1973, *Aircraft Dynamics and Automatic Control*, Princeton University Press, Princeton, N.J., ISBN 0-691-08083-6.

11 Roskam., J., 1979, *Airplane Flight Dynamics and Automatic Flight Controls*, Part I, Roskam Aviation and Engineering Corporation, Ottawa, Kansas, USA.

12 Blakelock, John H., 1991, *Automatic Control of Aircraft and Missiles*, second edition, John Wiley and Sons, New York, ISBN 0-471-50651-6.

13 Bosworth, J.T., 1992, "Linearized Aerodynamic and Control Law Models of the X-29A Airplane and Comparison with Flight Data," NASA TM-4356.

14 Brumbaugh, Randal W., 1991, "An Aircraft Model for the AIAA Controls Design Challenge," AIAA Paper No. 91-2631, AIAA Guidance, Navigation and Control Conference, 12 August 1991, New Orleans, Louisiana. Also, NASA Contractor Report 186019, Contract NAS 2-12722.

[15] Kwakernaak, H., and Sivan, R., 1972, *Linear Optimal Control Systems*, John Wiley and Sons, Inc.

[16] Boyd, S.P., and Barratt, C.H., 1991, *Linear Control Design: Limits of Performance*, Prentice-Hall, Englewood Cliffs, NJ, ISBN 0-13-538687-X.

Appendix

This Appendix contains the data, MATLAB scripts, and the results of the nine case studies performed as a part of this work. The data and some flight dynamics equations are presented in the form of photocopies from Roskam.[1] This is done to establish a uniform nomenclature for the subsequent computations. The following are the contents of the Appendix.

1. Flight dynamics equations
2. Conversions from dimensionless to dimensioned stability and control derivatives
3. Dynamical parameter computation and frequency response scripts
4. Boeing 747
5. McDonnell Douglas F-4C
6. Learjet Model 24
7. Linear-quadratic control results

Some of the explanatory text in Sections 3, 4 , and 5 is repeated to make those sections more independent.

A.1 Flight Dynamics Equations

Table 6.4 Development of the Longitudinal Small Perturbation Equations of Motion in Dimensional Derivatives and Matrix Format

$$\dot{u} = - g\Theta\cos\Theta_1 + X_u u + X_{T_u} u + X_\alpha \alpha + X_{\delta_E} \delta_E \qquad a)$$

$$\dot{w} - U_1 q = - g\Theta\sin\Theta_1 + Z_u u + Z_\alpha \alpha + Z_{\dot{\alpha}} \dot{\alpha} + Z_q q + Z_{\delta_E} \delta_E \qquad b) \qquad (6.72)$$

$$\dot{q} = M_u u + M_{T_u} u + M_\alpha \alpha + M_{T_\alpha} \alpha + M_{\dot{\alpha}} \dot{\alpha} + M_q q + M_{\delta_E} \delta_E \qquad c)$$

Equations (6.72) after taking the Laplace Transform:

$$\begin{array}{llll} (s - X_u - X_{T_u})\, u(s) & -X_\alpha \alpha(s) & + g\cos\Theta_1 \theta(s) & = X_{\delta_E} \delta_E(s) \\ - Z_u u(s) & \{s(U_1 - Z_{\dot{\alpha}}) - Z_\alpha\}\alpha(s) & \{-(Z_q + U_1)s + g\sin\theta_1\}\theta(s) & = Z_{\delta_E} \delta_E(s) \\ - (M_u + M_{T_u}) u(s) & - \{M_{\dot{\alpha}} s + M_\alpha + M_{T_\alpha}\}\alpha(s) & (s^2 - M_q s)\theta(s) & = M_{\delta_E} \delta_E(s) \end{array} \qquad (6.73)$$

Equations (6.73) in Matrix Format :

$$\begin{bmatrix} (s - X_u - X_{T_u}) & - X_\alpha & g\cos\Theta_1 \\ - Z_u & \{s(U_1 - Z_{\dot{\alpha}}) - Z_\alpha\} & \{-(Z_q + U_1)s + g\sin\Theta_1\} \\ - (M_u + M_{T_u}) & -\{M_{\dot{\alpha}} s + M_\alpha + M_{T_\alpha}\} & (s^2 - M_q s) \end{bmatrix} \begin{Bmatrix} \frac{u(s)}{\delta_E(s)} \\ \frac{\alpha(s)}{\delta_E(s)} \\ \frac{\theta(s)}{\delta_E(s)} \end{Bmatrix} = \begin{Bmatrix} X_{\delta_E} \\ Z_{\delta_E} \\ M_{\delta_E} \end{Bmatrix} \qquad (6.74)$$

Table 6.9 Development of the Lateral-Directional Small Perturbation Equations of Motion in Dimensional Derivatives and Matrix Format

$$\dot{v} + U_1 r = g\phi\cos\Theta_1 + Y_\beta\beta + Y_p p + Y_r r + Y_{\delta_A}\delta_A + Y_{\delta_R}\delta_R \qquad \text{a)}$$

$$\dot{p} - A_1\dot{r} = L_\beta\beta + L_p p + L_r r + L_{\delta_A}\delta_A + L_{\delta_R}\delta_R \qquad A_1 = \frac{I_{xz}}{I_{xx}} \qquad \text{b)} \qquad (6.141)$$

$$\dot{r} - B_1\dot{p} = N_\beta\beta + N_{T_\beta}\beta + N_p p + N_r r + N_{\delta_A}\delta_A + N_{\delta_R}\delta_R \qquad B_1 = \frac{I_{xz}}{I_{zz}} \qquad \text{c)}$$

Equations (6.91) after taking the Laplace Transform:

$$\begin{aligned}
&(sU_1 - Y_\beta)\beta(s) && -(sY_p + g\cos\Theta_1)\phi(s) && + s(U_1 - Y_r)\psi(s) && = && Y_\delta\delta(s) \\
&-L_\beta\beta(s) && + (s^2 - L_p s)\phi(s) && - (s^2A_1 + sL_r)\psi(s) && = && L_\delta\delta(s) \qquad (6.142) \\
&-(N_\beta + N_{T_\beta})\beta(s) && - (s^2B_1 + N_p s)\phi(s) && + (s^2 - sN_r)\psi(s) && = && N_\delta\delta(s)
\end{aligned}$$

Equations (6.92) in Matrix Format:

$$\begin{bmatrix} (sU_1 - Y_\beta) & -(sY_p + g\cos\Theta_1) & s(U_1 - Y_r) \\ -L_\beta & s^2 - L_p s & -(s^2A_1 + sL_r) \\ -N_\beta - N_{T_\beta} & -(s^2B_1 + N_p s) & (s^2 - sN_r) \end{bmatrix} \begin{Bmatrix} \frac{\beta(s)}{\delta(s)} \\ \frac{\phi(s)}{\delta(s)} \\ \frac{\psi(s)}{\delta(s)} \end{Bmatrix} = \begin{Bmatrix} Y_\delta \\ L_\delta \\ N_\delta \end{Bmatrix} \qquad (6.143)$$

Note: $\delta=\delta_A$ for aileron response calculations

$\delta=\delta_R$ for rudder response calculations

A.2 Conversions from Dimensionless to Dimensioned Stability and Control Derivatives

Table 6.3 Longitudinal Dimensional Stability Derivatives

$$X_u = \frac{-\bar{q}_1 S(C_{D_u} + 2C_{D_1})}{mU_1} \quad (\text{sec}^{-1})$$

$$X_{T_u} = \frac{\bar{q}_1 S(C_{T_{x_u}} + 2C_{T_{x_1}})}{mU_1} \quad (\text{sec}^{-1})$$

$$X_\alpha = \frac{-\bar{q}_1 S(C_{D_\alpha} - C_{L_1})}{m} \quad (\text{ft sec}^{-2})$$

$$X_{\delta_E} = \frac{-\bar{q}_1 S C_{D_{\delta_E}}}{m} \quad (\text{ft sec}^{-2} \text{ or } \text{ft sec}^{-2}\text{deg}^{-1})$$

$$Z_u = -\frac{\bar{q}_1 S(C_{L_u} + 2C_{L_1})}{mU_1} \quad (\text{sec}^{-1})$$

$$Z_\alpha = -\frac{\bar{q}_1 S(C_{L_\alpha} + C_{D_1})}{m} \quad (\text{ft sec}^{-2})$$

$$Z_{\dot{\alpha}} = -\frac{\bar{q}_1 S C_{L_{\dot{\alpha}}} \bar{c}}{2mU_1} \quad (\text{ft sec}^{-1})$$

$$Z_q = -\frac{\bar{q}_1 S C_{L_q} \bar{c}}{2mU_1} \quad (\text{ft sec}^{-1})$$

$$Z_{\delta_E} = -\frac{\bar{q}_1 S C_{L_{\delta_E}}}{m} \quad (\text{ft sec}^{-2} \text{ or } \text{ft sec}^{-2}\text{deg}^{-1})$$

$$M_u = \frac{\bar{q}_1 S\bar{c}(C_{m_u} + 2C_{m_1})}{I_{yy}U_1} \quad (\text{ft}^{-1}\ \text{sec}^{-1})$$

$$M_{T_u} = \frac{\bar{q}_1 S\bar{c}(C_{m_{T_u}} + 2C_{m_{T_1}})}{I_{yy}U_1} \quad (\text{ft}^{-1}\ \text{sec}^{-1})$$

$$M_\alpha = \frac{\bar{q}_1 S\bar{c} C_{m_\alpha}}{I_{yy}} \quad (\text{sec}^{-2})$$

$$M_{T_\alpha} = \frac{\bar{q}_1 S\bar{c} C_{m_{T_\alpha}}}{I_{yy}} \quad (\text{sec}^{-2})$$

$$M_{\dot{\alpha}} = \frac{\bar{q}_1 S\bar{c}^2 C_{m_{\dot{\alpha}}}}{2I_{yy}U_1} \quad (\text{sec}^{-1})$$

$$M_q = \frac{\bar{q}_1 S\bar{c}^2 C_{m_q}}{2I_{yy}U_1} \quad (\text{sec}^{-1})$$

$$M_{\delta_E} = \frac{\bar{q}_1 S\bar{c} C_{m_{\delta_E}}}{I_{yy}} \quad (\text{sec}^{-2} \text{ or } \text{sec}^{-2}\text{deg}^{-1})$$

Table 6.8 Lateral-Directional Dimensional Stability Derivatives

$$Y_\beta = \frac{\bar{q}_1 S C_{y_\beta}}{m} \quad (\text{ft sec}^{-2})$$

$$Y_p = \frac{\bar{q}_1 S b C_{y_p}}{2mU_1} \quad (\text{ft sec}^{-1})$$

$$Y_r = \frac{\bar{q}_1 S b C_{y_r}}{2mU_1} \quad (\text{ft sec}^{-1})$$

$$Y_{\delta_A} = \frac{\bar{q}_1 S C_{y_{\delta_A}}}{m} \quad (\text{ft sec}^{-2} \text{ or } \text{ft sec}^{-2}\ \text{deg}^{-1})$$

$$Y_{\delta_R} = \frac{\bar{q}_1 S C_{y_{\delta_R}}}{m} \quad (\text{ft sec}^{-2} \text{ or } \text{ft sec}^{-2}\ \text{deg}^{-1})$$

$$L_\beta = \frac{\bar{q}_1 S b C_{\ell_\beta}}{I_{xx}} \quad (\text{sec}^{-2})$$

$$L_p = \frac{\bar{q}_1 S b^2 C_{\ell_p}}{2I_{xx}U_1} \quad (\text{sec}^{-1})$$

$$L_r = \frac{\bar{q}_1 S b^2 C_{\ell_r}}{2I_{xx}U_1} \quad (\text{sec}^{-1})$$

$$L_{\delta_A} = \frac{\bar{q}_1 S b C_{\ell_{\delta_A}}}{I_{xx}} \quad (\text{sec}^{-2} \text{ or } \text{sec}^{-2}\ \text{deg}^{-1})$$

$$L_{\delta_R} = \frac{\bar{q}_1 S b C_{\ell_{\delta_R}}}{I_{xx}} \quad (\text{sec}^{-2} \text{ or } \text{sec}^{-2}\ \text{deg}^{-1})$$

$$N_\beta = \frac{\bar{q}_1 S b C_{n_\beta}}{I_{zz}} \quad (\text{sec}^{-2})$$

$$N_{T_\beta} = \frac{\bar{q}_1 S b C_{n_{T_\beta}}}{I_{zz}} \quad (\text{sec}^{-2})$$

$$N_p = \frac{\bar{q}_1 S b^2 C_{n_p}}{2I_{zz}U_1} \quad (\text{sec}^{-1})$$

$$N_r = \frac{\bar{q}_1 S b^2 C_{n_r}}{2I_{zz}U_1} \quad (\text{sec}^{-1})$$

$$N_{\delta_A} = \frac{\bar{q}_1 S b C_{n_{\delta_A}}}{I_{zz}} \quad (\text{sec}^{-2} \text{ or } \text{sec}^{-2}\ \text{deg}^{-1})$$

$$N_{\delta_R} = \frac{\bar{q}_1 S b C_{n_{\delta_R}}}{I_{zz}} \quad (\text{sec}^{-2} \text{ or } \text{sec}^{-2}\ \text{deg}^{-1})$$

A.3 Dynamical Parameter Computation and Frequency Response Scripts

The contents of this subsection of the Appendix are MATLAB scripts to compute eigenvalues, natural frequencies, damping ratios and frequency responses of aircraft for

longitudinal dynamics

lateral/directional dynamics

The variables used in these scripts are created by the scripts listed in Subsections A.4, A.5, and A.6. The eigenvalues of the dynamics are also called the roots of the characteristic polynomial or the poles of the system transfer function. When the eigenvalues are real, rather than complex or imaginary, the scripts return a damping ratio of –1 if the eigenvalue is greater than zero and +1 if the eigenvalue is less than zero, and a natural frequency that is the absolute value of the eigenvalue.

The numerical print outs and the graphs of the frequency responses for each aircraft are in Subsections A.4, A.5, and A.6.

```
OPEN LOOP ANALYSIS OF AIRCRAFT LONGITUDINAL DYNAMICS

%Print eigenvalues ("ev flight conditions 1, 2, and 3"),
%natural frequencies ("Wn flight conditions 1, 2, and 3"),
%and damping ratios ("Z flight conditions 1, 2, and 3").

evfc1=eig(Afc1)
[Wnfc1,Zfc1]=damp(Afc1);
evfc2=eig(Afc2)
[Wnfc2,Zfc2]=damp(Afc2);
evfc3=eig(Afc3)
[Wnfc3,Zfc3]=damp(Afc3);
temp='NATURAL FREQUENCIES';
temp
[Wnfc1 Wnfc2 Wnfc3]
temp='DAMPING RATIOS';
temp
[Zfc1 Zfc2 Zfc3]

%Compute and plot aircraft longitudinal frequency response.
%The input matrix, Bfc?, and the direct term matrix, Dfc?, have
%minus signs so that the phase angles can be compared
%directly to MA&G.

om=logspace(-4,2,512);
iu=1;

[mgfc1,phfc1] = BODE(Afc1,-Bfc1,Cfc1,-Dfc1,iu,om);
[mgfc2,phfc2] = BODE(Afc2,-Bfc2,Cfc2,-Dfc2,iu,om);
[mgfc3,phfc3] = BODE(Afc3,-Bfc3,Cfc3,-Dfc3,iu,om);
clg;subplot(211);
for io=1:4,
loglog(om,[mgfc1(:,io),mgfc2(:,io),mgfc3(:,io)]);
xlabel('Frequency (rad/s)');
ylabel('Magnitude');
if io==1, title('Longitudinal Aircraft Frequency Response: Elevator to
Pitch Angle'),
else if io==2, title('Longitudinal Aircraft Frequency Response: Elevator
to Angle of Attack'),
else if io==3, title('Longitudinal Aircraft Frequency Response: Elevator
to Forward Speed'),
else title('Longitudinal Aircraft Frequency Response: Elevator to
Vertical Acceleration'),
end;end;end;
semilogx(om,[phfc1(:,io),phfc2(:,io),phfc3(:,io)]);
xlabel('Frequency (rad/s)');
ylabel('Phase (deg)');
pause;
end;
```

```
OPEN LOOP ANALYSIS OF AIRCRAFT LATERAL DYNAMICS

%Print eigenvalues ("ev flight conditions 1, 2, and 3"),
%natural frequencies ("Wn flight conditions 1, 2, and 3"),
%and damping ratios ("Z flight conditions 1, 2, and 3").

evfc1=eig(Afc1)
[Wnfc1,Zfc1]=damp(Afc1);
evfc2=eig(Afc2)
[Wnfc2,Zfc2]=damp(Afc2);
evfc3=eig(Afc3)
[Wnfc3,Zfc3]=damp(Afc3);
temp='NATURAL FREQUENCIES';
temp
[Wnfc1 Wnfc2 Wnfc3]
temp='DAMPING RATIOS';
temp
[Zfc1 Zfc2 Zfc3]

%Compute and plot aircraft longitudinal frequency response.

format short e
om=logspace(-4,2,512);

for iu=1:2,
[mgfc1,phfc1] = BODE(Afc1,Bfc1,Cfc1,Dfc1,iu,om);
[mgfc2,phfc2] = BODE(Afc2,Bfc2,Cfc2,Dfc2,iu,om);
[mgfc3,phfc3] = BODE(Afc3,Bfc3,Cfc3,Dfc3,iu,om);
clg;subplot(211);
for io=1:4,
loglog(om,[mgfc1(:,io),mgfc2(:,io),mgfc3(:,io)]);
xlabel('Frequency (rad/s)');
ylabel('Magnitude');
if io==1,
  if iu==1,
  title('Lateral Aircraft Frequency Response: Aileron to Sideslip'),
  else,
  title('Lateral Aircraft Frequency Response: Rudder to Sideslip'),
  end;
else if io==2,
  if iu==1,
  title('Lateral Aircraft Frequency Response: Aileron to Roll Angle'),
  else,
  title('Lateral Aircraft Frequency Response: Rudder to Roll Angle'),
  end;
else if io==3,
  if iu==1,
  title('Lateral Aircraft Frequency Response: Aileron to Yaw Angle'),
  else,
  title('Lateral Aircraft Frequency Response: Rudder to Yaw Angle'),
  end;
else,
  if iu==1,
  title('Lateral Aircraft Frequency Response: Aileron to Lateral
Acceleration'),
  else,
  title('Lateral Aircraft Frequency Response: Rudder to Lateral
Acceleration'),
```

```
  end;
end;end;end;
semilogx(om,[phfc1(:,io),phfc2(:,io),phfc3(:,io)]);
xlabel('Frequency (rad/s)');
ylabel('Phase (deg)');
pause;
end;end;
```

A.4 Boeing 747

The contents of this section of the Appendix are:

Stability and control data

MATLAB script to form longitudinal dynamics

MATLAB eigenvalue, natural frequency and damping print out from script for longitudinal dynamics

Frequency responses of longitudinal dynamics

MATLAB script to form lateral dynamics

MATLAB eigenvalue, natural frequency and damping print out from script for lateral dynamics

Frequency responses of lateral dynamics

The stability and control data are photocopies from Roskam.[1] The data were entered into MATLAB scripts to form the state-space differential equations for the longitudinal and lateral dynamics. Two additional scripts, one for longitudinal dynamics and one for lateral dynamics, were written to compute eigenvalues, natural frequencies, damping ratios, and frequency responses for the dynamics. These scripts are listed in Section A.3.

The conversions from dimensionless to dimensioned stability and control derivatives were done three at a time by first making each parameter, stability derivative and control derivative a 3-vector—one element for each flight condition. The conversion computations are then performed using vector arithmetic. The state-space matrices were formed from the appropriate elements of each vector.

$$\begin{aligned} E\dot{x} &= \tilde{A}x + \tilde{B}u \\ y &= Cx + Du \end{aligned} \tag{A-1}$$

Equation A-1 is an intermediate form for the state-space equation that was formed because some stability derivatives depend on the derivatives of the state variables in the case of the longitudinal dynamics and because of the roll/yaw coupling in moment equations in the case of the lateral dynamics. The final form is obtained by multiplying the first equation of the pair by the inverse of E.

The frequency response graphs show three traces—one for each of the three flight conditions. The line styles for the Boeing 747 cases denote the following:

Solid:	power approach at sea level
Dashes:	cruise at 40,000 ft
Points:	cruise at 20,000 ft

C6 DATA FOR AIRPLANE F

Figure C6 shows a three-view for Airplane F. This airplane is representative of large wide-body jet-transport airplanes. Stability and control derivatives for this airplane are presented in Table C6.

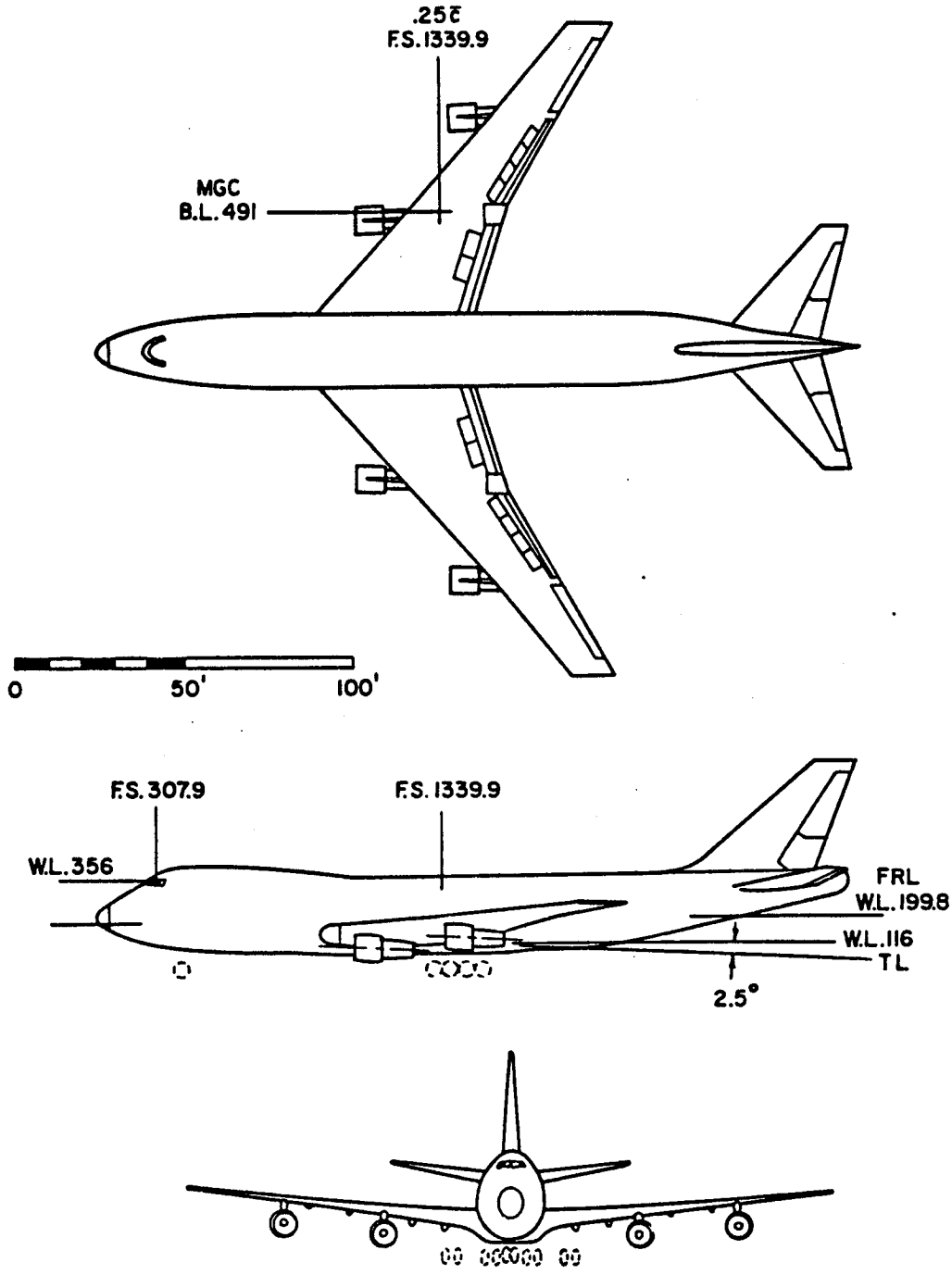

Figure C6 Three-View of Airplane F

Table C6 Stability and Control Deirvatives for Airplane F

Flight Condition	1	2	3
	Power Approach	Cruise (High)	Cruise (Low)
Altitude (ft)	Sealevel	40,000	20,000
Air Density (slugs/ft^3)	.002389	.000588	.001268
Speed (fps)	221	871	673
Center of Gravity ($\bar{x}_{cg}$)	.25	.25	.25
Initial Attitude (deg)	8.5	2.4	2.5
Geometry and Inertias			
Wing Area (ft^2)	5,500	5,500	5,500
Wing Span (ft)	196	196	196
Wing Mean Geometric Chord (ft)	27.3	27.3	27.3
Weight (lbs)	564,000	636,636	636,636
I_{xx_B} (slug ft^2)	13.7×10^6	18.2×10^6	18.2×10^6
I_{yy_B} (slug ft^2)	30.5×10^6	33.1×10^6	33.1×10^6
I_{zz_B} (slug ft^2)	43.1×10^6	49.7×10^6	49.7×10^6
I_{xz_B} (slug ft^2)	$.83 \times 10^6$	$.97 \times 10^6$	$.97 \times 10^6$
Steady State Coefficients			
C_{L_1}	1.76	.52	.40
C_{D_1}	.263	.045	.025
$C_{T_{X_1}}$	.263	.045	.025
C_{m_1}	0	0	0
$C_{m_{T_1}}$	0	0	0

Table C6 Stability and Control Derivatives for Airplane F (Cont.)

Longitudinal Derivatives	1	2	3
C_{m_u}	.071	-.09	+.013
C_{m_α}	-1.45 ✓	-1.60	-1.00
$C_{m_{\dot{\alpha}}}$	-3.3 ✓	-9.0	-4.0
C_{m_q}	-21.4 ✓	-25.5	-20.5
$C_{m_{T_u}}$	0	0	0
$C_{m_{T_\alpha}}$	0	0	0
C_{L_u}	-.22	-.23	+.13
C_{L_α}	5.67 ✓	5.5	4.4
$C_{L_{\dot{\alpha}}}$	−6.7 ?	8.0	7.0
C_{L_q}	5.65 ✓	7.8	6.6
C_{D_α}	1.13 ✓	.50	.20
C_{D_u}	0	.22	0
$C_{T_{X_u}}$	0	0	0
$C_{L_{\delta_E}}$	.36 ✓	.30	.32
$C_{D_{\delta_E}}$	0	0	0
$C_{m_{\delta_E}}$	-1.40 ✓	-1.20	-1.30

$C_{L_{\dot{\alpha}}}$ sign reversed in Heffley & Jewell

Table C6 Stability and Control Derivatives for Airplane F (Cont.)

Lateral-Directional Derivatives	1	2	3
C_{ℓ_β}	-.281	-.095	-.160
C_{ℓ_p}	-.502	-.320	-.340
C_{ℓ_r}	.195	.200	.130
$C_{\ell_{\delta_A}}$	.053	.014	.013
$C_{\ell_{\delta_R}}$	0	.005	.008
C_{n_β}	.184	.210	.160
C_{n_p}	-.222	+.020	-.026
C_{n_r}	-.36	-.33	-.28
$C_{n_{\delta_A}}$	+.0083	-.0028	+.0018
$C_{n_{\delta_R}}$	-.113	-.095	-.100
C_{y_β}	-1.08	-.90	-.90
C_{y_p}	0	0	0
C_{y_r}	0	0	0
$C_{y_{\delta_A}}$	0	0	0
$C_{y_{\delta_R}}$	.179	.060	.120

```
%LONGITUDINAL DYNAMICS
%Boeing 747, sea level--power approach       <--fc1
%            40,000 ft--high altitude cruise <--fc2
%            20,000 ft--low altitude cruise  <--fc3
%Roskam, J., 1979,
%Airplane Flight Dynamics and Automatic Flight Controls,
%Part I, pp. 616-642

format short e

%Enter flight condition, geometry, mass and MOI parameters.

g=32.2;                                 %gravity (ft/s^2)
theta0=[8.5 2.4 2.5]*pi/180;            %equilibrium pitch angle (deg)
rho=[.002389 .000588 .001268];          %density (slug/ft^3)
Uo=[221 871 673];                       %equilibrium speed (ft/s)
mass=[564000 636636 636636]/g;          %weight (lbs)
Ixx=[13.7e6 18.2e6 18.2e6];             %roll inertia (slug ft^2)
Iyy=[30.5e6 33.1e6 33.1e6];             %pitch inertia (slug ft^2)
Izz=[43.1e6 49.7e6 49.7e6];             %yaw inertia (slug ft^2)
Ixz=[.83e6 .97e6 .97e6];                %cross product of inertia (slug ft^2)
S=[5500 5500 5500];                     %wing area (ft^2)
b=[196 196 196];                        %wing span (ft)
cbar=[27.3 27.3 27.3];                  %mean geometric chord (ft)

%Enter steady-state coefficients.

CL1=[1.76 .52 .40];
CD1=[.263 .045 .025];
CTx1=[.263 .045 .025];
Cm1=[0 0 0];
CmT1=[0 0 0];

%Enter dimensionless stability and control derivatives.

Cmu=[.071 -.09 +.013];
Cma=[-1.45 -1.60 -1.00];
Cmad=[-3.3 -9.0 -4.0];
Cmq=[-21.4 -25.5 -20.5];
CmTu=[0 0 0];
CmTa=[0 0 0];
CLu=[-.22 -.23 +.13];
CLa=[+5.67 +5.5 +4.4];
CLad=[6.7 8.0 7.0];
CLq=[5.65 7.8 6.6];
CDa=[1.13 .50 .20];
CDu=[0 .22 0];
CTxu=[0 0 0];
CLde=[.36 .30 .32];
CDde=[0 0 0];
Cmde=[-1.40 -1.20 -1.30];

CDad=[0 0 0];  %No numbers in Roskam
CDq=[0 0 0];   %No numbers in Roskam

%Compute dimensioned stability and control derivatives

qbar=0.5*rho.*Uo.^2;
```

```
Xu =-qbar.*S.*(CDu+2*CD1)./(mass.*Uo);
XTu= qbar.*S.*(CTxu+2*CTx1)./(mass.*Uo);
Xa =-qbar.*S.*(CDa-CL1)./mass;
Xde=-qbar.*S.*CDde./mass;
Zu =-qbar.*S.*(CLu+2*CL1)./(mass.*Uo);
Za =-qbar.*S.*(CLa+CD1)./mass;
Zad=-qbar.*S.*CLad.*cbar./(2*mass.*Uo);
Zq =-qbar.*S.*CLq.*cbar./(2*mass.*Uo);
Zde=-qbar.*S.*CLde./mass;
Mu = qbar.*S.*cbar.*(Cmu+2*Cm1)./(Iyy.*Uo);
MTu= qbar.*S.*cbar.*(CmTu+2*CmT1)./(Iyy.*Uo);
Ma = qbar.*S.*cbar.*Cma./Iyy;
MTa= qbar.*S.*cbar.*CmTa./Iyy;
Mad= qbar.*S.*(cbar.^2).*Cmad./(2*Iyy.*Uo);
Mq = qbar.*S.*(cbar.^2).*Cmq./(2*Iyy.*Uo);
Mde= qbar.*S.*cbar.*Cmde./Iyy;

%Compute dynamics for flight condition 1 in state-space form.

Afc1=[
      Xu(1)+XTu(1) Xa(1)/Uo(1)                 0
-g*cos(theta0(1))
      Zu(1)        Za(1)/Uo(1)                 Uo(1)+Zq(1)
-g*sin(theta0(1))
      Mu(1)+MTu(1) Ma(1)/Uo(1)+MTa(1)/Uo(1) Mq(1)          0
      0            0                          1            0
     ];

Bfc1=[Xde(1);Zde(1);Mde(1);0];

Efc1=[
      1 0                0 0
      0 1-Zad(1)/Uo(1)   0 0
      0  -Mad(1)/Uo(1)   1 0
      0 0                0 1];

Afc1=Efc1\Afc1;
Bfc1=Efc1\Bfc1;

%Compute pitch angle
%        angle of attack
%        forward speed
%        vertical acceleration
%output matrix and direct input matrix.

Cfc1=[
      0   0        0    1
      0   1/Uo(1)  0    0
      1   0        0    0
      Afc1(2,:)-[0 0 Uo(1) 0]
     ];
Dfc1=0*Cfc1*Bfc1;
Dfc1(4,1)=Bfc1(2,1);

%Compute dynamics for flight condition 2 in state-space form.

Afc2=[
```

```
      Xu(2)+XTu(2)  Xa(2)/Uo(2)                0
-g*cos(theta0(2))
      Zu(2)         Za(2)/Uo(2)                Uo(2)+Zq(2)
-g*sin(theta0(2))
      Mu(2)+MTu(2)  Ma(2)/Uo(2)+MTa(2)/Uo(2)  Mq(2)          0
      0             0                          1             0
     ];

Bfc2=[Xde(2);Zde(2);Mde(2);0];

Efc2=[
      1 0               0 0
      0 1-Zad(2)/Uo(2)  0 0
      0  -Mad(2)/Uo(2)  1 0
      0 0               0 1
     ];

Afc2=Efc2\Afc2;
Bfc2=Efc2\Bfc2;

%Compute pitch angle
%         angle of attack
%         forward speed
%         vertical acceleration
%output matrix and direct input matrix.

Cfc2=[
     0   0         0    1
     0   1/Uo(2)   0    0
     1   0         0    0
     Afc2(2,:)-[0 0 Uo(2) 0]
    ];
Dfc2=0*Cfc2*Bfc2;
Dfc2(4,1)=Bfc2(2,1);

%Compute dynamics for flight condition 3 in state-space form.

Afc3=[
      Xu(3)+XTu(3)  Xa(3)/Uo(3)                0
-g*cos(theta0(3))
      Zu(3)         Za(3)/Uo(3)                Uo(3)+Zq(3)
-g*sin(theta0(3))
      Mu(3)+MTu(3)  Ma(3)/Uo(3)+MTa(3)/Uo(3)  Mq(3)          0
      0             0                          1             0
     ];

Bfc3=[Xde(3);Zde(3);Mde(3);0];

Efc3=[
      1 0               0 0
      0 1-Zad(3)/Uo(3)  0 0
      0  -Mad(3)/Uo(3)  1 0
      0 0               0 1
     ];

Afc3=Efc3\Afc3;
Bfc3=Efc3\Bfc3;
```

```
%Compute pitch angle
%         angle of attack
%         forward speed
%         vertical acceleration
%output matrix and direct input matrix.

Cfc3=[
     0   0         0    1
     0   1/Uo(3)   0    0
     1   0         0    0
     Afc3(2,:)-[0 0 Uo(3) 0]
    ];
Dfc3=0*Cfc3*Bfc3;
Dfc3(4,1)=Bfc3(2,1);
```

```
%LONGITUDINAL DYNAMICS RESULTS
%Boeing 747, sea level--power approach       <--fc1
%            40,000 ft--high altitude cruise <--fc2
%            20,000 ft--low altitude cruise  <--fc3
%Roskam, J., 1979,
%Airplane Flight Dynamics and Automatic Flight Controls,
%Part I, pp. 616-642

EIGENVALUES

evfc1 =
 -4.7750e-01+  6.0834e-01i
 -4.7750e-01-  6.0834e-01i
  2.2462e-02+  1.6854e-01i
  2.2462e-02-  1.6854e-01i


evfc2 =
 -4.6988e-01+  1.2370e+00i
 -4.6988e-01-  1.2370e+00i
 -5.9712e-03+  3.3808e-02i
 -5.9712e-03-  3.3808e-02i


evfc3 =
 -5.8206e-01+  1.0971e+00i
 -5.8206e-01-  1.0971e+00i
  1.8563e-03+  6.8193e-02i
  1.8563e-03-  6.8193e-02i

NATURAL FREQUENCIES
   7.7336e-01   1.3232e+00   1.2420e+00
   7.7336e-01   1.3232e+00   1.2420e+00
   1.7003e-01   3.4331e-02   6.8218e-02
   1.7003e-01   3.4331e-02   6.8218e-02

DAMPING RATIOS
   6.1744e-01   3.5510e-01   4.6866e-01
   6.1744e-01   3.5510e-01   4.6866e-01
  -1.3210e-01   1.7393e-01  -2.7211e-02
  -1.3210e-01   1.7393e-01  -2.7211e-02
```

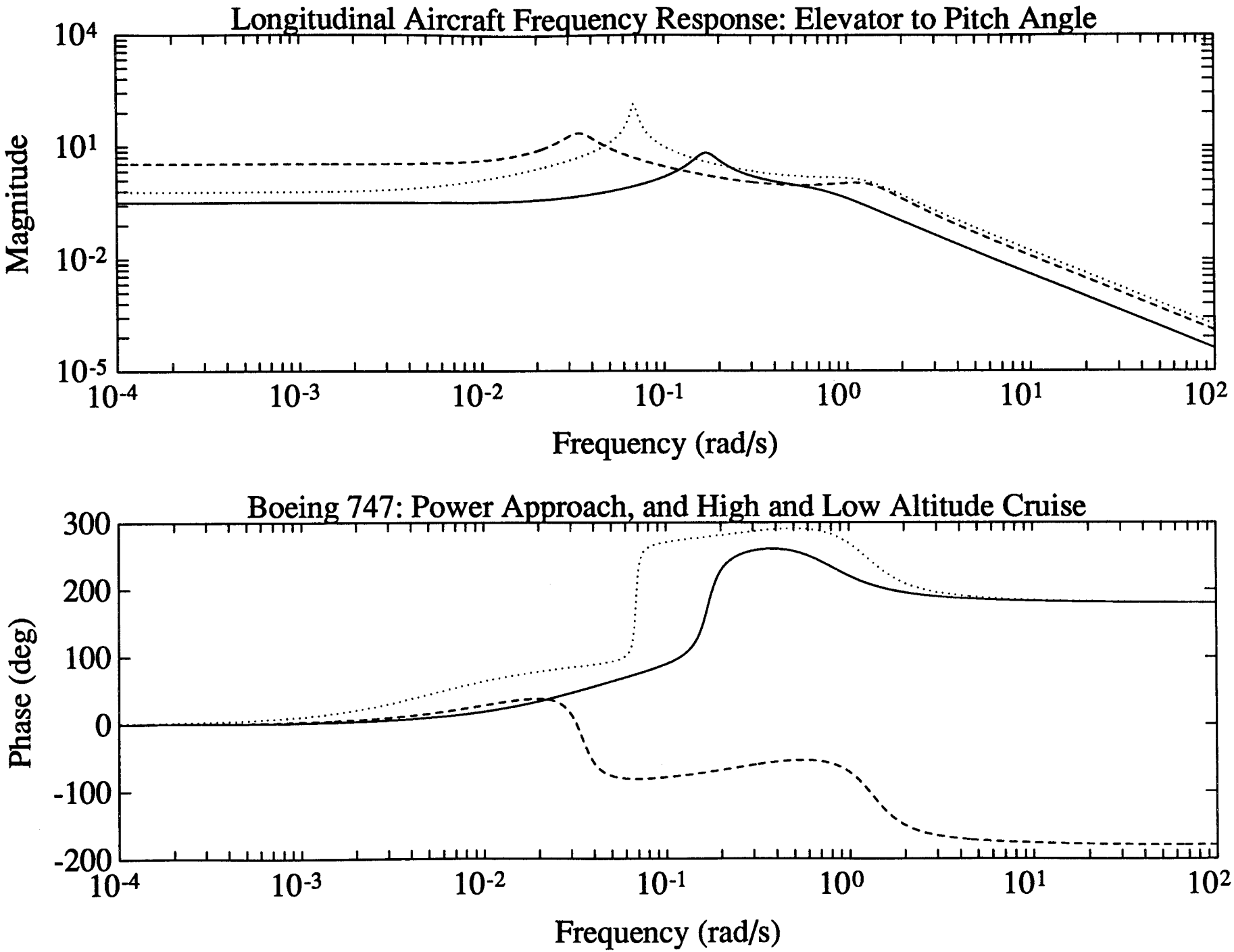
Longitudinal Aircraft Frequency Response: Elevator to Pitch Angle
Magnitude
10^4
10^1
10^-2
10^-5
10^-4
10^-3
10^-2
10^-1
10^0
10^1
10^2
Frequency (rad/s)
Boeing 747: Power Approach, and High and Low Altitude Cruise
Phase (deg)
300
200
100
0
-100
-200
10^-4
10^-3
10^-2
10^-1
10^0
10^1
10^2
Frequency (rad/s)

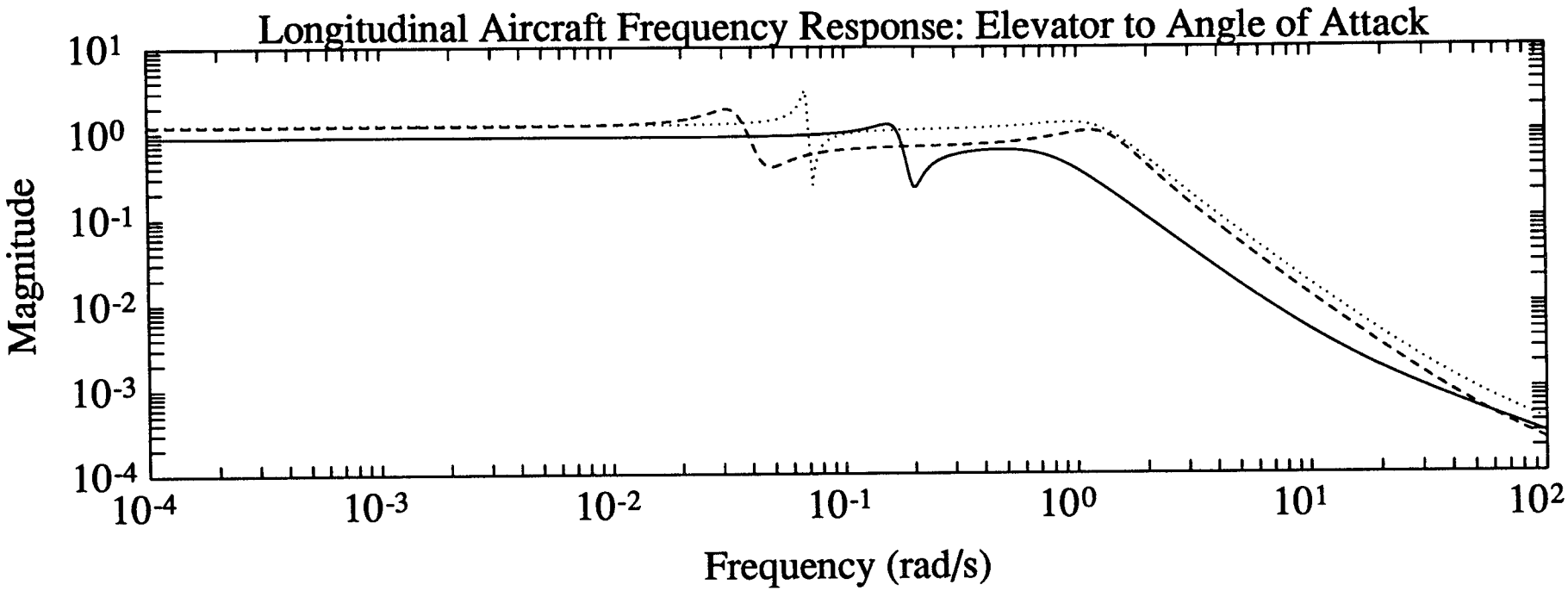
Longitudinal Aircraft Frequency Response: Elevator to Angle of Attack
Magnitude
10^{1}
10^{0}
10^{-1}
10^{-2}
10^{-3}
10^{-4}
10^{-4}
10^{-3}
10^{-2}
10^{-1}
10^{0}
10^{1}
10^{2}
Frequency (rad/s)

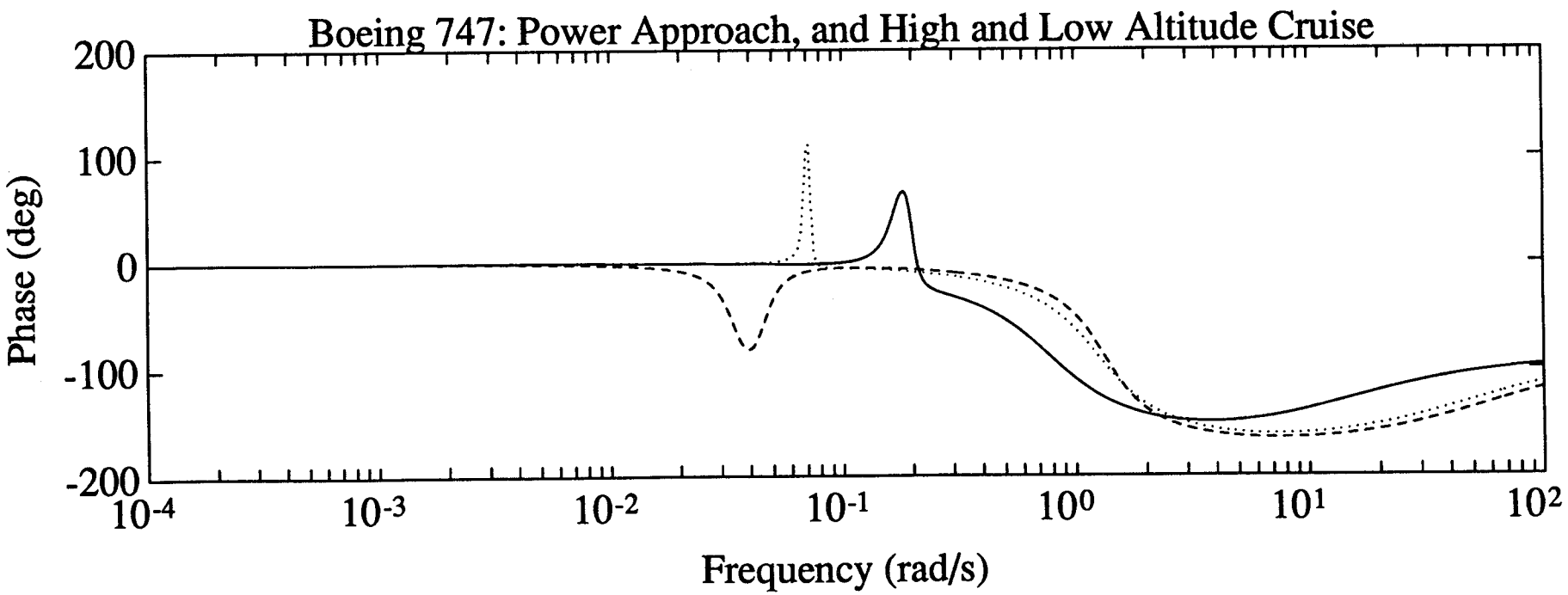
Boeing 747: Power Approach, and High and Low Altitude Cruise
Phase (deg)
200
100
0
-100
-200
10^{-4}
10^{-3}
10^{-2}
10^{-1}
10^{0}
10^{1}
10^{2}
Frequency (rad/s)

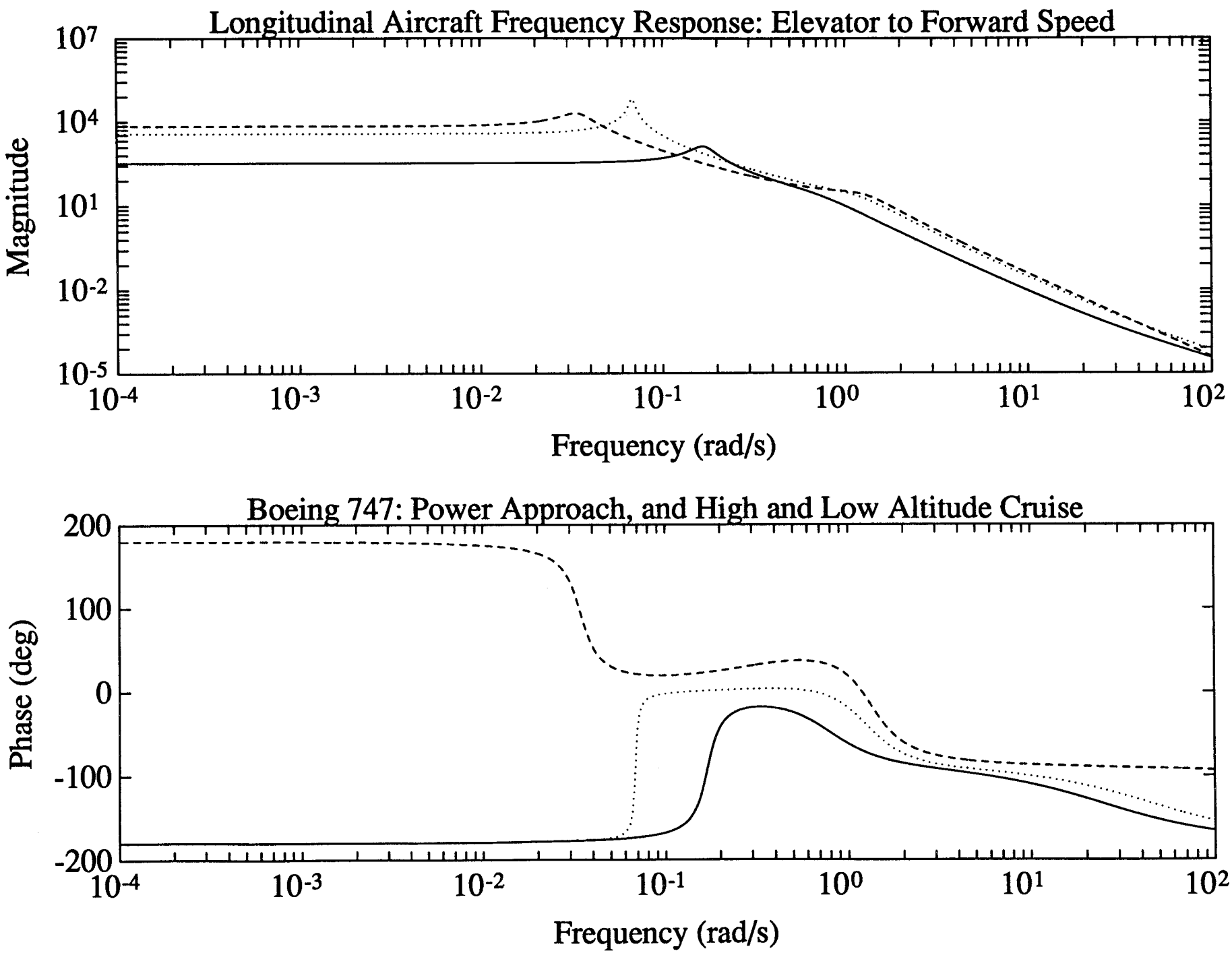
Longitudinal Aircraft Frequency Response: Elevator to Forward Speed
Magnitude
10^7
10^4
10^1
10^-2
10^-5
10^-4
10^-3
10^-2
10^-1
10^0
10^1
10^2
Frequency (rad/s)
Boeing 747: Power Approach, and High and Low Altitude Cruise
Phase (deg)
200
100
0
-100
-200
10^-4
10^-3
10^-2
10^-1
10^0
10^1
10^2
Frequency (rad/s)

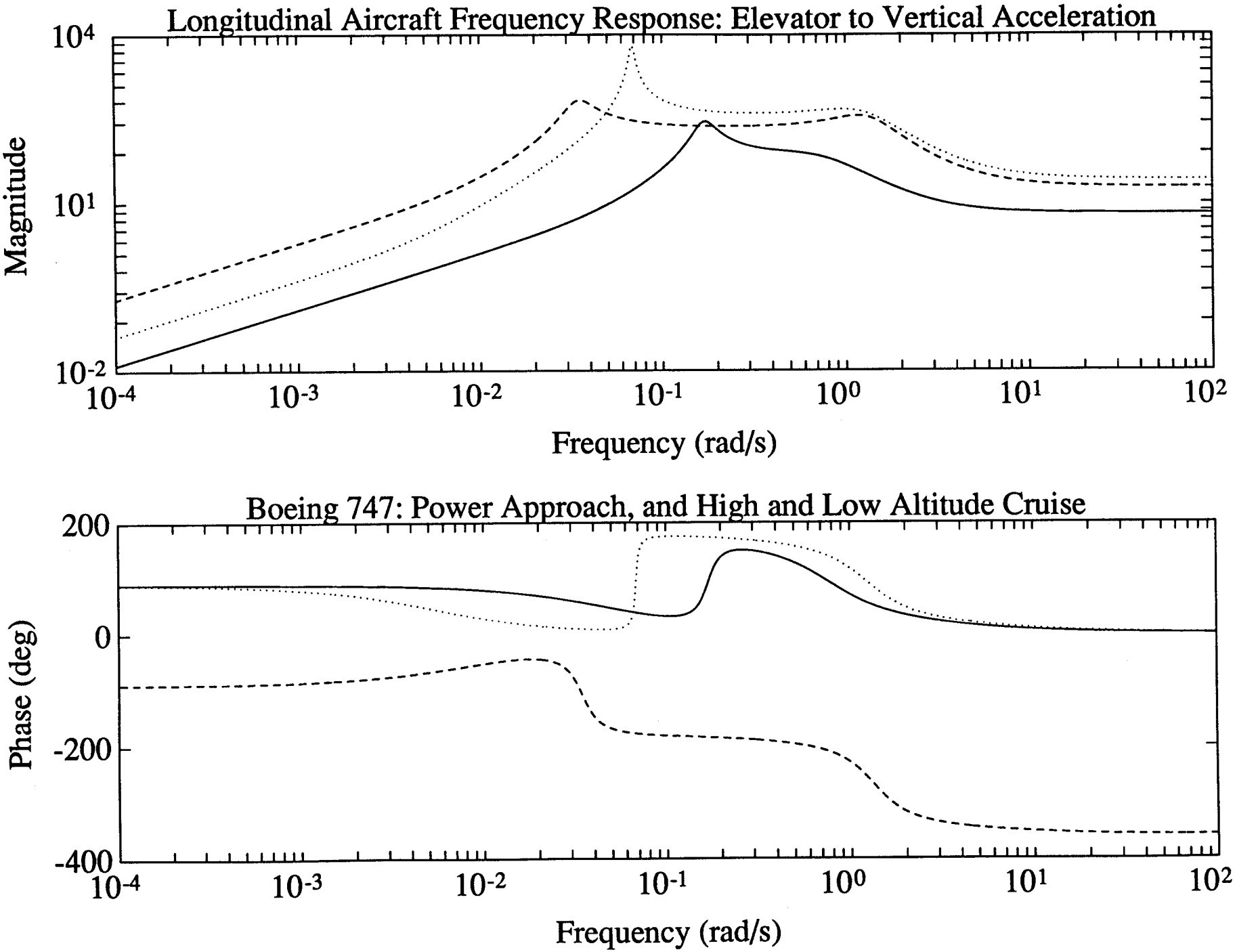
Longitudinal Aircraft Frequency Response: Elevator to Vertical Acceleration
Magnitude
10^4
10^1
10^-2
10^-4
10^-3
10^-2
10^-1
10^0
10^1
10^2
Frequency (rad/s)
Boeing 747: Power Approach, and High and Low Altitude Cruise
Phase (deg)
200
0
-200
-400
10^-4
10^-3
10^-2
10^-1
10^0
10^1
10^2
Frequency (rad/s)

```
%LATERAL DYNAMICS
%Boeing 747, sea level--power approach        <--fc1
%            40,000 ft--high altitude cruise  <--fc2
%            20,000 ft--low altitude cruise   <--fc3
%Roskam, J., 1979,
%Airplane Flight Dynamics and Automatic Flight Controls,
%Part I, pp. 616-642

format short e

%Enter flight condition, geometry, mass and MOI parameters.

g=32.2;                                 %gravity (ft/s^2)
theta0=[8.5 2.4 2.5]*pi/180;            %equilibrium pitch angle (deg)
rho=[.002389 .000588 .001268];          %density (slug/ft^3)
Uo=[221 871 673];                       %equilibrium speed (ft/s)
mass=[564000 636636 636636]/g;          %weight (lbs)
Ixx=[13.7e6 18.2e6 18.2e6];             %roll inertia (slug ft^2)
Izz=[43.1e6 49.7e6 49.7e6];             %yaw inertia (slug ft^2)
Ixz=[.83e6 .97e6 .97e6];                %cross product of inertia (slug ft^2)
S=[5500 5500 5500];                     %wing area (ft^2)
b=[196 196 196];                        %wing span (ft)
cbar=[27.3 27.3 27.3];                  %mean geometric chord (ft)

%Transform relevant inertias from body frame to stability frame.

for ifc=1:3,
  ang=theta0(ifc);
  Tba2sa=[
          cos(ang)^2     sin(ang)^2    -sin(2*ang)
          sin(ang)^2     cos(ang)^2     sin(2*ang)
          sin(2*ang)/2 -sin(2*ang)/2   cos(2*ang)
         ];
  Isa=Tba2sa*[Ixx(ifc);Izz(ifc);Ixz(ifc)];
  Ixx(ifc)=Isa(1);
  Izz(ifc)=Isa(2);
  Ixz(ifc)=Isa(3);
end;

%Enter steady-state coefficients.

CL1=[1.76 .52 .40];
CD1=[.263 .045 .025];
CTx1=[.263 .045 .025];
Cm1=[0 0 0];
CmT1=[0 0 0];

%Enter dimensionless stability and control derivatives.

Clb=[-.281 -.095 -.160];
Clp=[-.502 -.320 -.340];
Clr=[.195 .200 .130];
Clda=[.053 .014 .013];
Cldr=[0 .005 .008];

Cnb=[.184 .210 .160];
Cnp=[-.222 .020 -.026];
Cnr=[-.36 -.33 -.28];
```

```
Cnda=[.0083 -.0028 .0018];
Cndr=[-.113 -.095 -.100];

Cyb=[-1.08 -.90 -.90];
Cyp=[0 0 0];
Cyr=[0 0 0];
Cyda=[0 0 0];
Cydr=[.179 .060 .120];

CnTb=[0 0 0];  %No numbers in Roskam

%Compute dimensioned stability and control derivatives

qbar=0.5*rho.*Uo.^2;
Yb = qbar.*S.*Cyb./mass;
Yp = qbar.*S.*b.*Cyp./(2*mass.*Uo);
Yr = qbar.*S.*b.*Cyr./(2*mass.*Uo);
Yda= qbar.*S.*Cyda./mass;
Ydr= qbar.*S.*Cydr./mass;

Lb = qbar.*S.*b.*Clb./Ixx;
Lp = qbar.*S.*(b.^2).*Clp./(2*Ixx.*Uo);
Lr = qbar.*S.*(b.^2).*Clr./(2*Ixx.*Uo);
Lda= qbar.*S.*b.*Clda./Ixx;
Ldr= qbar.*S.*b.*Cldr./Ixx;

Nb = qbar.*S.*b.*Cnb./Izz;
NTb= qbar.*S.*b.*CnTb./Izz;
Np = qbar.*S.*(b.^2).*Cnp./(2*Izz.*Uo);
Nr = qbar.*S.*(b.^2).*Cnr./(2*Izz.*Uo);
Nda= qbar.*S.*b.*Cnda./Izz;
Ndr= qbar.*S.*b.*Cndr./Izz;

%Compute dynamics for flight condition 1 in state-space form.

Afc1=[
      Yb(1)/Uo(1)           Yp(1) Yr(1)-Uo(1) g*cos(theta0(1))
g*sin(theta0(1))
      Lb(1)/Uo(1)           Lp(1) Lr(1)       0                 0
      (Nb(1)+NTb(1))/Uo(1) Np(1) Nr(1)       0                 0
      0                     1     0           0                 0
      0                     0     1           0                 0
     ];

Bfc1=[
      Yda(1) Ydr(1)
      Lda(1) Ldr(1)
      Nda(1) Ndr(1)
      0*ones(2,2)
     ];

Efc1=[
      1  0              0              0 0
      0  1             -Ixz(1)/Ixx(1) 0 0
      0 -Ixz(1)/Izz(1)  1              0 0
      0  0              0              1 0
      0  0              0              0 1
     ];
```

```
Afc1=Efc1\Afc1;
Bfc1=Efc1\Bfc1;

%Compute sideslip angle
%        roll angle
%        yaw angle
%        lateral acceleration
%output matrix and direct input matrix.

Cfc1=[
      1/Uo(1)  0  0  0  0
      0        0  0  1  0
      0        0  0  0  1
      Afc1(1,:)+[0 0 Uo(1) -g 0]
     ];
Dfc1=0*Cfc1*Bfc1;
Dfc1(4,:)=Bfc1(1,:);

%Compute dynamics for flight condition 2 in state-space form.

Afc2=[
      Yb(2)/Uo(2)           Yp(2) Yr(2)-Uo(2) g*cos(theta0(2))
g*sin(theta0(2))
      Lb(2)/Uo(2)           Lp(2) Lr(2)       0                0
      (Nb(2)+NTb(2))/Uo(2) Np(2) Nr(2)       0                0
      0                     1     0           0                0
      0                     0     1           0                0
     ];

Bfc2=[
      Yda(2) Ydr(2)
      Lda(2) Ldr(2)
      Nda(2) Ndr(2)
      0*ones(2,2)
     ];

Efc2=[
      1  0              0              0 0
      0  1             -Ixz(2)/Ixx(2) 0 0
      0 -Ixz(2)/Izz(2)  1              0 0
      0  0              0              1 0
      0  0              0              0 1
     ];

Afc2=Efc2\Afc2;
Bfc2=Efc2\Bfc2;

%Compute sideslip angle
%        roll angle
%        yaw angle
%        lateral acceleration
%output matrix and direct input matrix.

Cfc2=[
      1/Uo(2)  0  0  0  0
      0        0  0  1  0
      0        0  0  0  1
```


C-2.

```
      Afc2(1,:)+[0 0 Uo(2) -g 0]
     ];
Dfc2=0*Cfc2*Bfc2;
Dfc2(4,:)=Bfc2(1,:);

%Compute dynamics for flight condition 3 in state-space form.

Afc3=[
      Yb(3)/Uo(3)           Yp(3) Yr(3)-Uo(3) g*cos(theta0(3))
g*sin(theta0(3))
      Lb(3)/Uo(3)           Lp(3) Lr(3)       0                 0
      (Nb(3)+NTb(3))/Uo(3) Np(3) Nr(3)       0                 0
      0                     1     0           0                 0
      0                     0     1           0                 0
     ];

Bfc3=[
      Yda(3) Ydr(3)
      Lda(3) Ldr(3)
      Nda(3) Ndr(3)
      0*ones(2,2)
     ];

Efc3=[
      1  0              0              0 0
      0  1             -Ixz(3)/Ixx(3) 0 0
      0 -Ixz(3)/Izz(3) 1              0 0
      0  0              0              1 0
      0  0              0              0 1
     ];

Afc3=Efc3\Afc3;
Bfc3=Efc3\Bfc3;

%Compute sideslip angle
%        roll angle
%        yaw angle
%        lateral acceleration
%output matrix and direct input matrix.

Cfc3=[
      1/Uo(3)  0  0  0  0
      0        0  0  1  0
      0        0  0  0  1
      Afc3(1,:)+[0 0 Uo(3) -g 0]
     ];
Dfc3=0*Cfc3*Bfc3;
Dfc3(4,:)=Bfc3(1,:);
```

```
%LATERAL DYNAMICS RESULTS
%Boeing 747, sea level--power approach        <--fc1
%            40,000 ft--high altitude cruise  <--fc2
%            20,000 ft--low altitude cruise   <--fc3
%Roskam, J., 1979,
%Airplane Flight Dynamics and Automatic Flight Controls,
%Part I, pp. 616-642

EIGENVALUES

evfc1 =
            0
 -1.1493e+00
 -7.3124e-02+  7.4809e-01i
 -7.3124e-02-  7.4809e-01i
 -4.3081e-02

evfc2 =
            0
 -5.0778e-01
  5.3563e-03
 -1.0998e-01+  1.0144e+00i
 -1.0998e-01-  1.0144e+00i

evfc3 =
            0
 -9.3977e-01
 -1.7097e-02
 -1.2491e-01+  1.0437e+00i
 -1.2491e-01-  1.0437e+00i

NATURAL FREQUENCIES
             0             0             0
   1.1493e+00    5.0778e-01    9.3977e-01
   7.5165e-01    5.3563e-03    1.7097e-02
   7.5165e-01    1.0204e+00    1.0511e+00
   4.3081e-02    1.0204e+00    1.0511e+00

DAMPING RATIOS
           NaN           NaN           NaN
   1.0000e+00    1.0000e+00    1.0000e+00
   9.7284e-02   -1.0000e+00    1.0000e+00
   9.7284e-02    1.0778e-01    1.1883e-01
   1.0000e+00    1.0778e-01    1.1883e-01
```

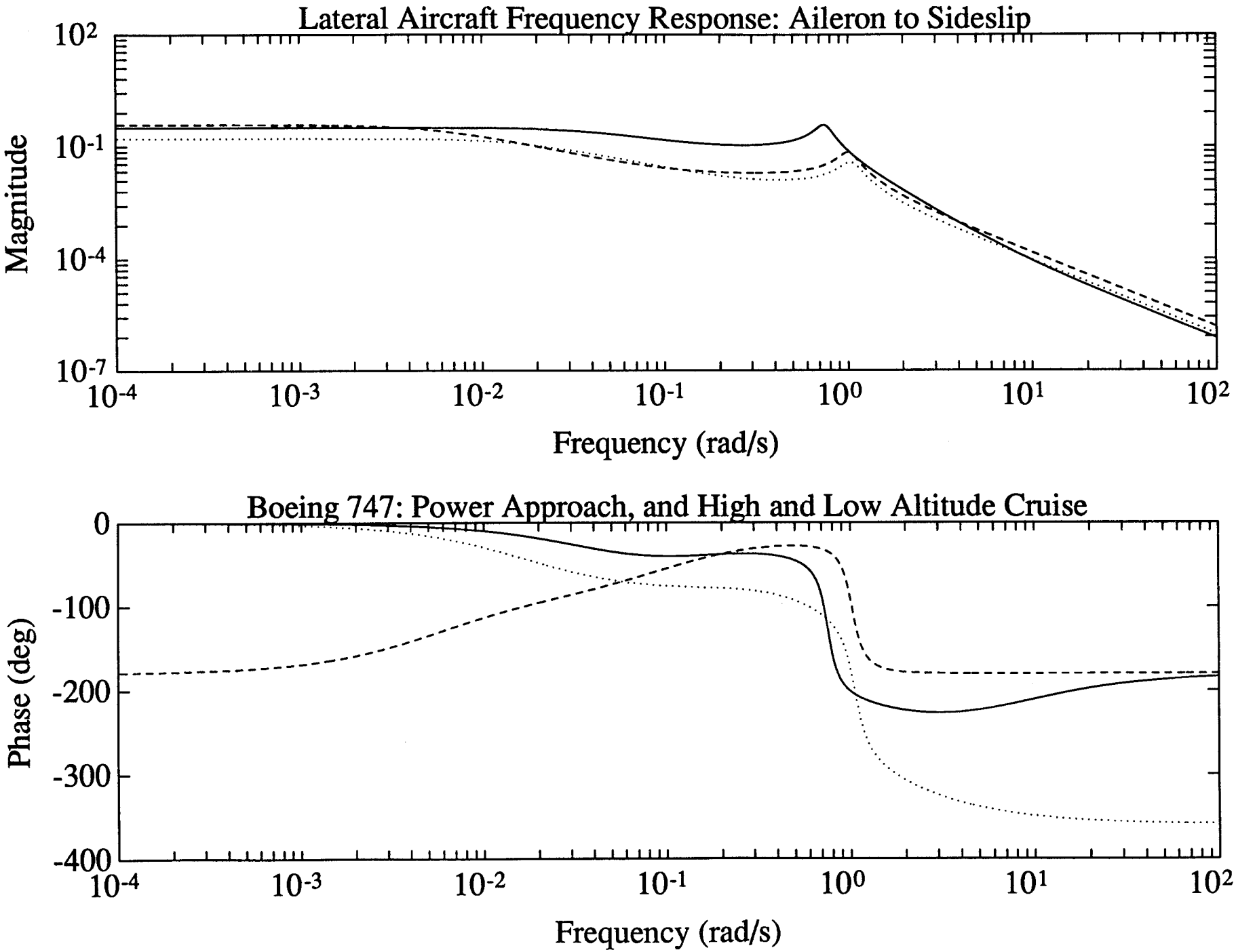
Lateral Aircraft Frequency Response: Aileron to Sideslip
Magnitude
10^2
10^-1
10^-4
10^-7
10^-4
10^-3
10^-2
10^-1
10^0
10^1
10^2
Frequency (rad/s)
Boeing 747: Power Approach, and High and Low Altitude Cruise
Phase (deg)
0
-100
-200
-300
-400
10^-4
10^-3
10^-2
10^-1
10^0
10^1
10^2
Frequency (rad/s)

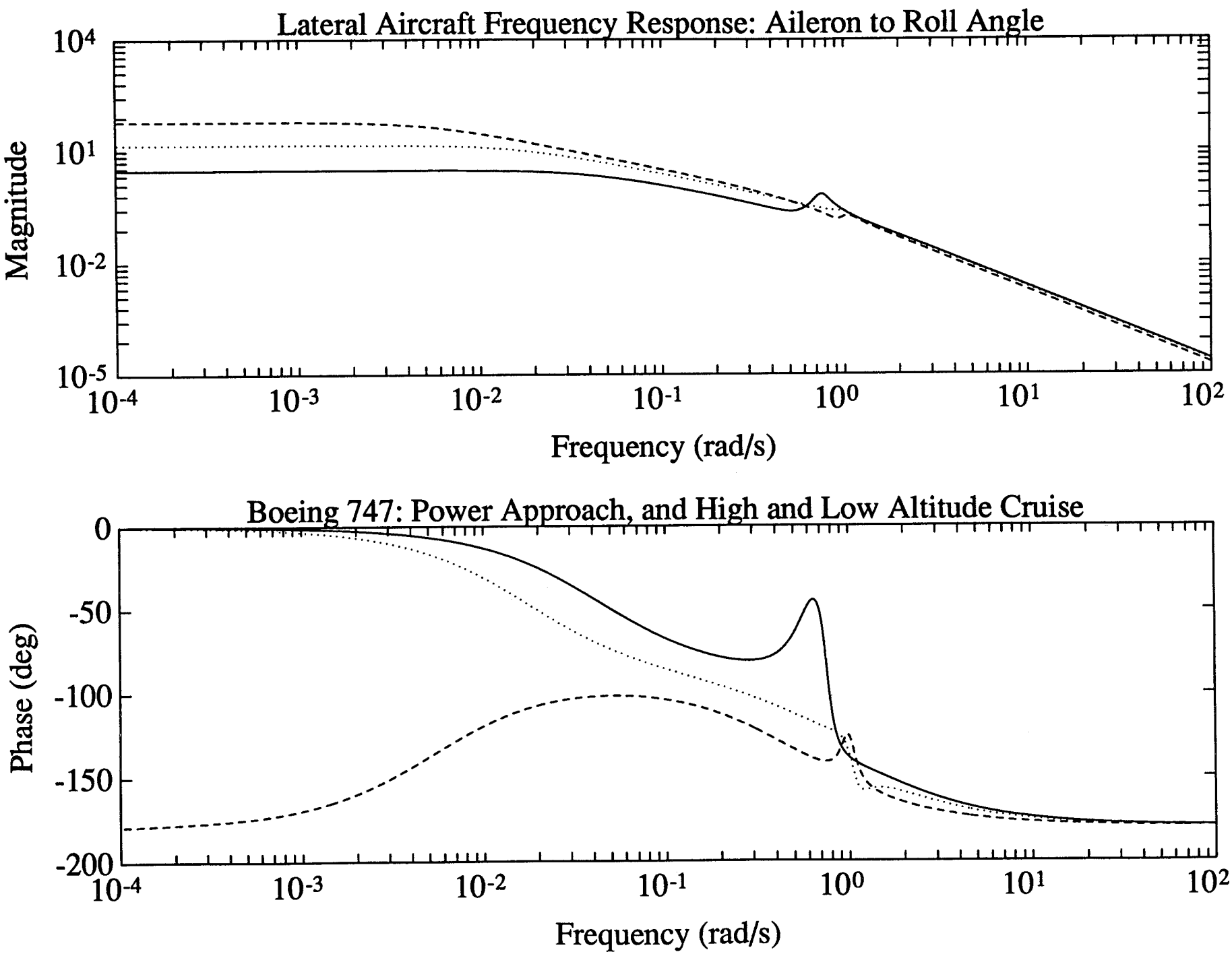
Lateral Aircraft Frequency Response: Aileron to Roll Angle
Magnitude
10^4
10^1
10^-2
10^-5
10^-4
10^-3
10^-2
10^-1
10^0
10^1
10^2
Frequency (rad/s)
Boeing 747: Power Approach, and High and Low Altitude Cruise
Phase (deg)
0
-50
-100
-150
-200
10^-4
10^-3
10^-2
10^-1
10^0
10^1
10^2
Frequency (rad/s)

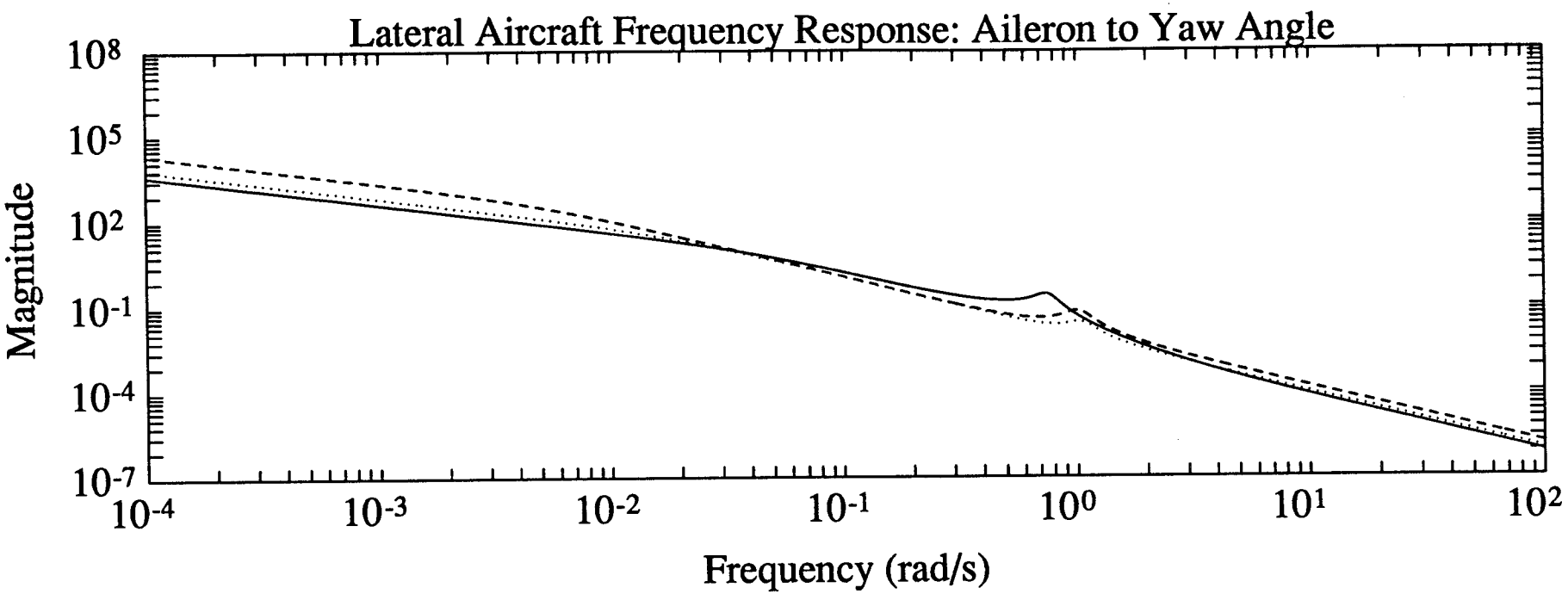
Lateral Aircraft Frequency Response: Aileron to Yaw Angle
Magnitude
10^8
10^5
10^2
10^-1
10^-4
10^-7
10^-4
10^-3
10^-2
10^-1
10^0
10^1
10^2
Frequency (rad/s)

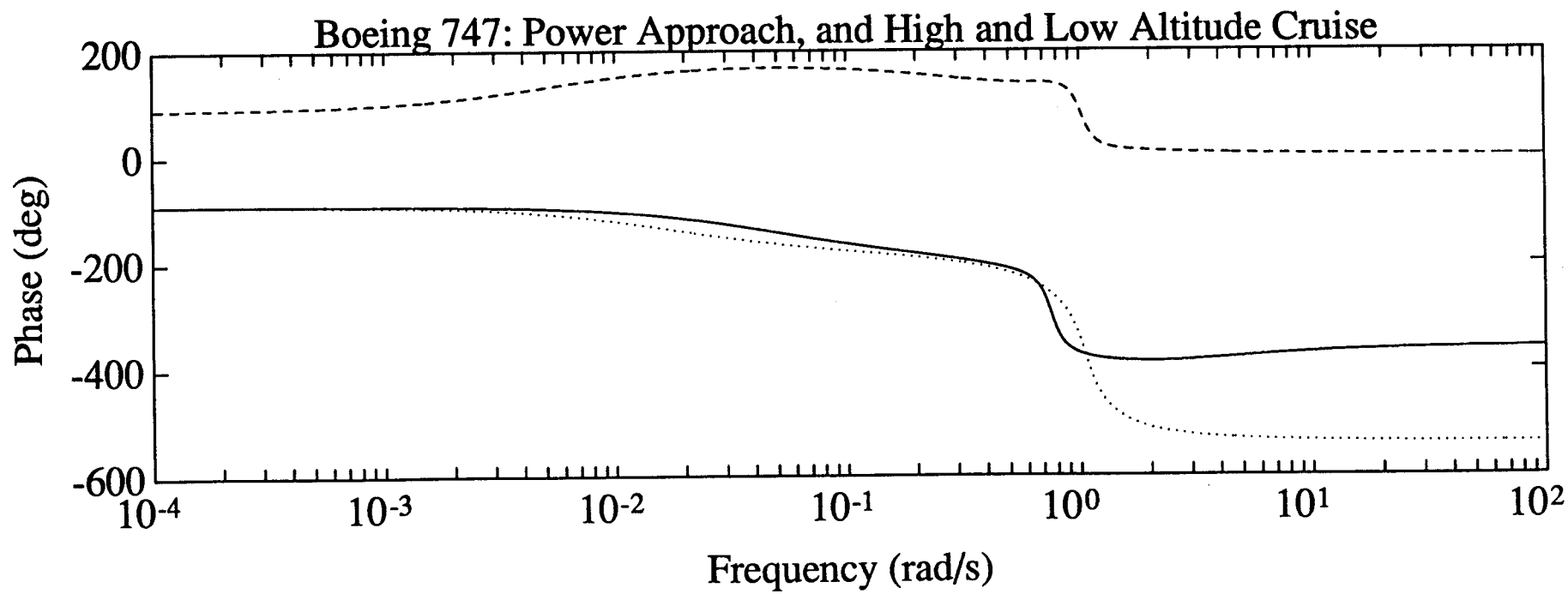
Boeing 747: Power Approach, and High and Low Altitude Cruise
Phase (deg)
200
0
-200
-400
-600
10^-4
10^-3
10^-2
10^-1
10^0
10^1
10^2
Frequency (rad/s)

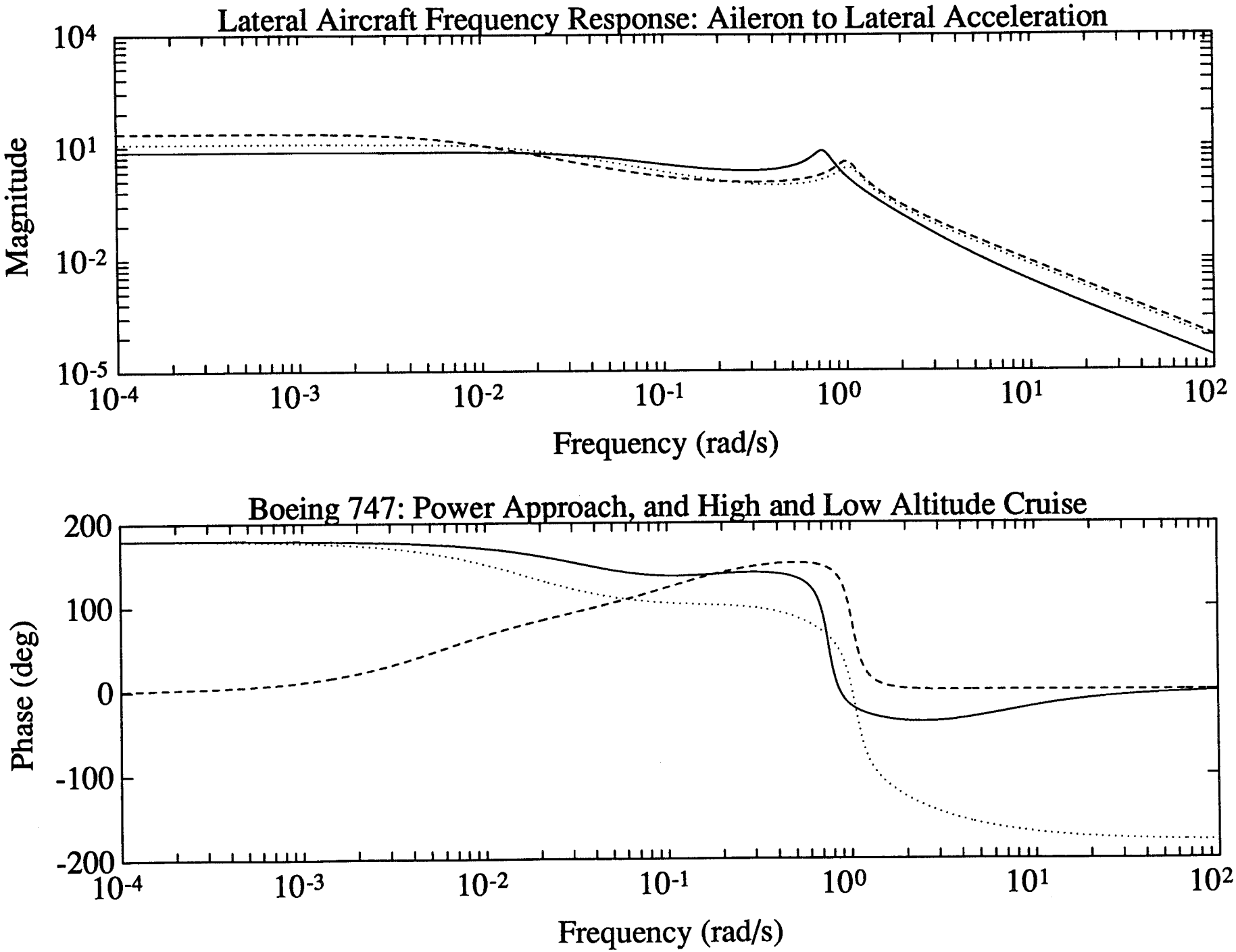
Lateral Aircraft Frequency Response: Aileron to Lateral Acceleration
Magnitude
10^4
10^1
10^-2
10^-5
10^-4
10^-3
10^-2
10^-1
10^0
10^1
10^2
Frequency (rad/s)
Boeing 747: Power Approach, and High and Low Altitude Cruise
Phase (deg)
200
100
0
-100
-200
10^-4
10^-3
10^-2
10^-1
10^0
10^1
10^2
Frequency (rad/s)

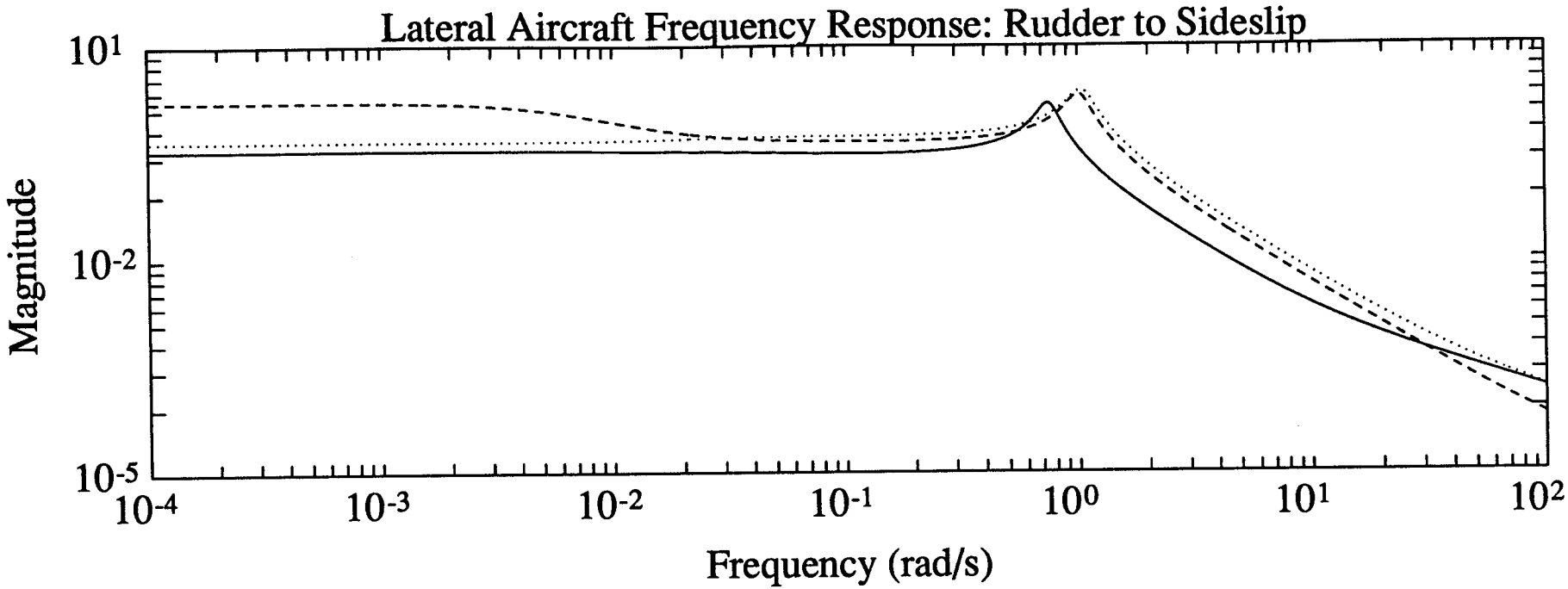
Lateral Aircraft Frequency Response: Rudder to Sideslip
Magnitude
10^1
10^-2
10^-5
10^-4
10^-3
10^-2
10^-1
10^0
10^1
10^2
Frequency (rad/s)

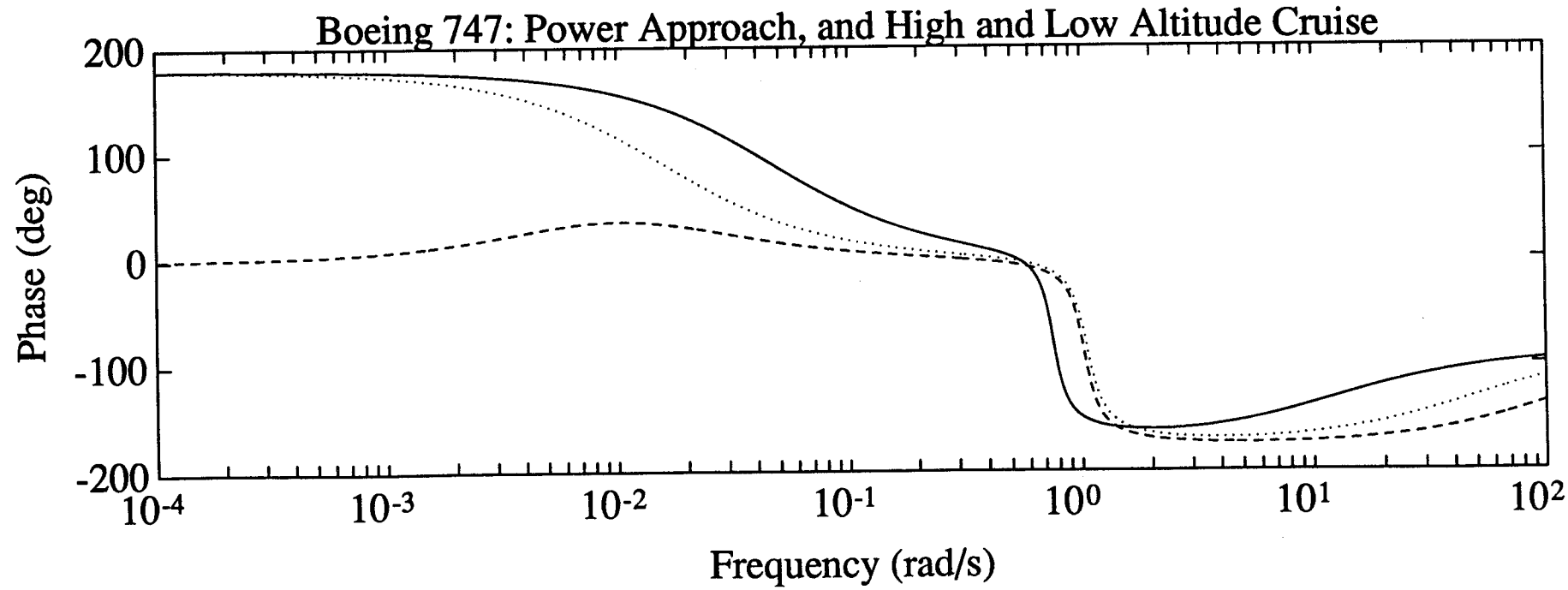
Boeing 747: Power Approach, and High and Low Altitude Cruise
Phase (deg)
200
100
0
-100
-200
10^-4
10^-3
10^-2
10^-1
10^0
10^1
10^2
Frequency (rad/s)

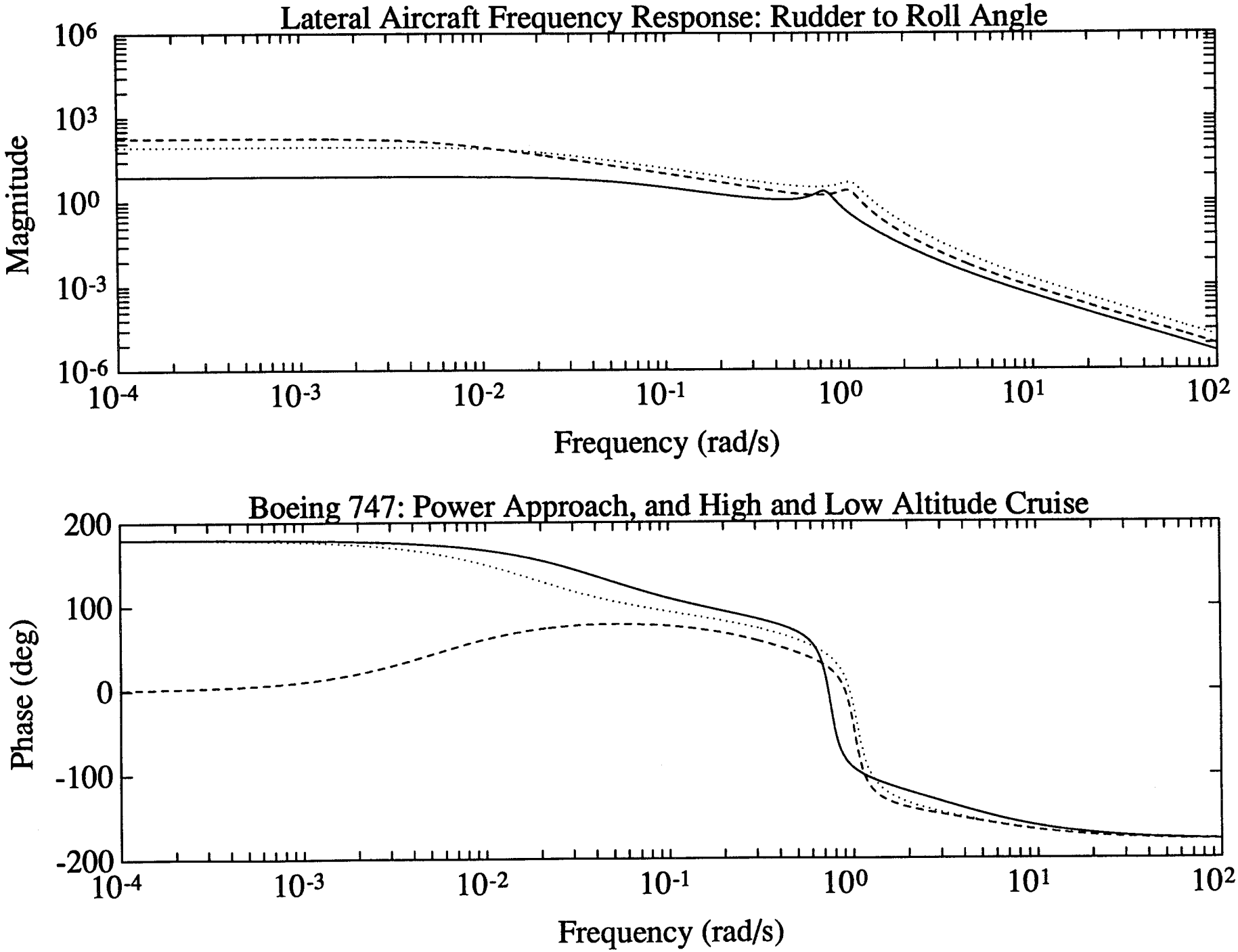
Lateral Aircraft Frequency Response: Rudder to Roll Angle
Magnitude
10^6
10^3
10^0
10^-3
10^-6
10^-4
10^-3
10^-2
10^-1
10^0
10^1
10^2
Frequency (rad/s)
Boeing 747: Power Approach, and High and Low Altitude Cruise
Phase (deg)
200
100
0
-100
-200
10^-4
10^-3
10^-2
10^-1
10^0
10^1
10^2
Frequency (rad/s)

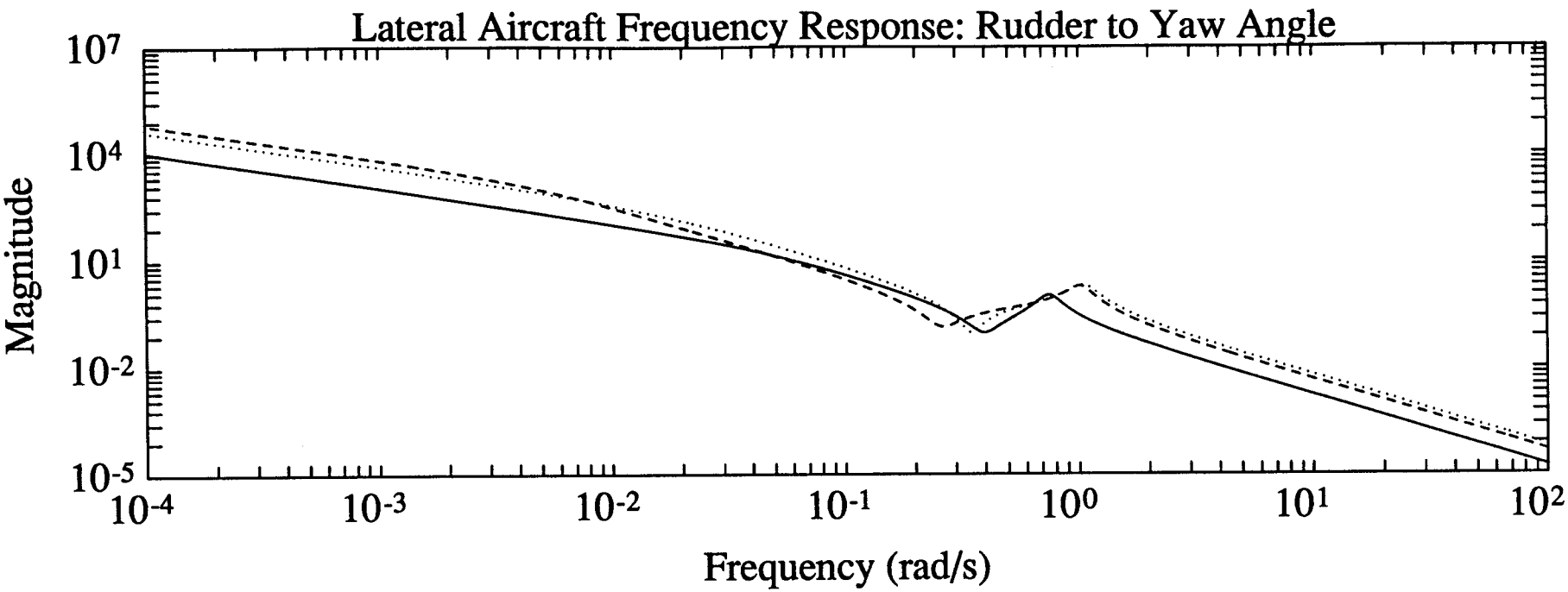
Lateral Aircraft Frequency Response: Rudder to Yaw Angle
Magnitude
10^7
10^4
10^1
10^-2
10^-5
10^-4
10^-3
10^-2
10^-1
10^0
10^1
10^2
Frequency (rad/s)

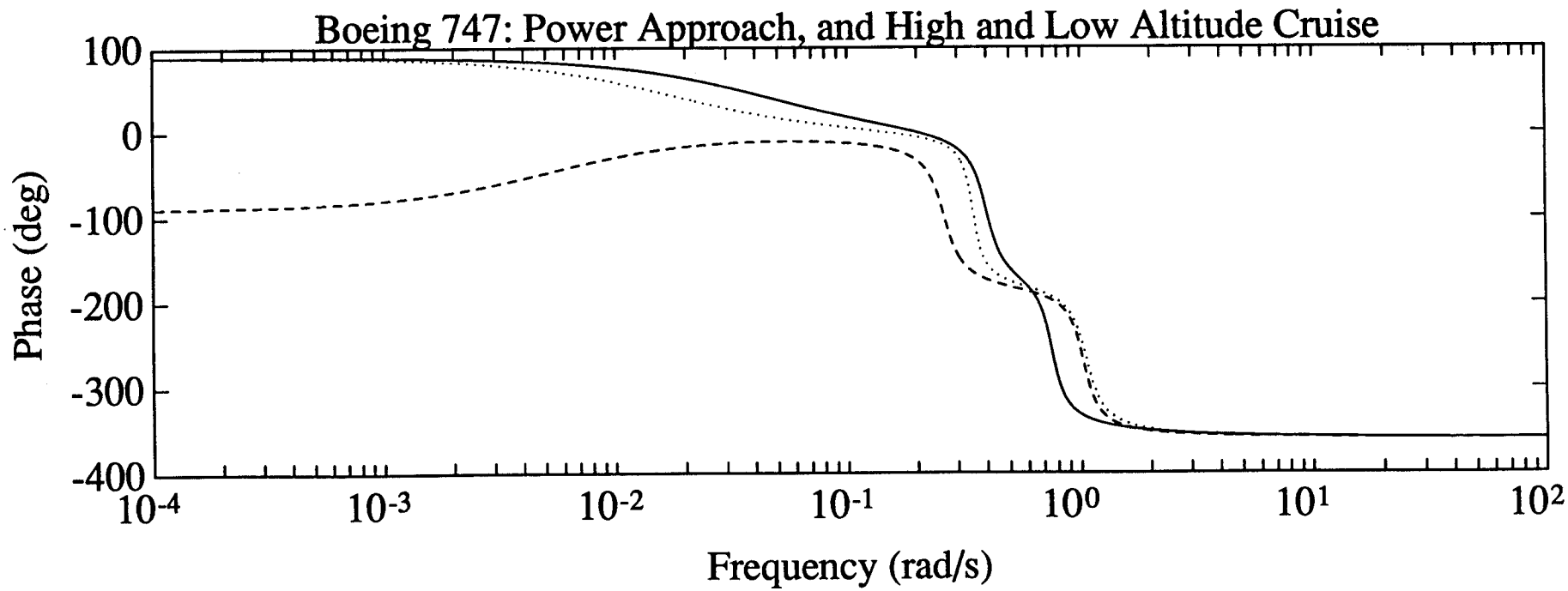
Boeing 747: Power Approach, and High and Low Altitude Cruise
Phase (deg)
100
0
-100
-200
-300
-400
10^-4
10^-3
10^-2
10^-1
10^0
10^1
10^2
Frequency (rad/s)

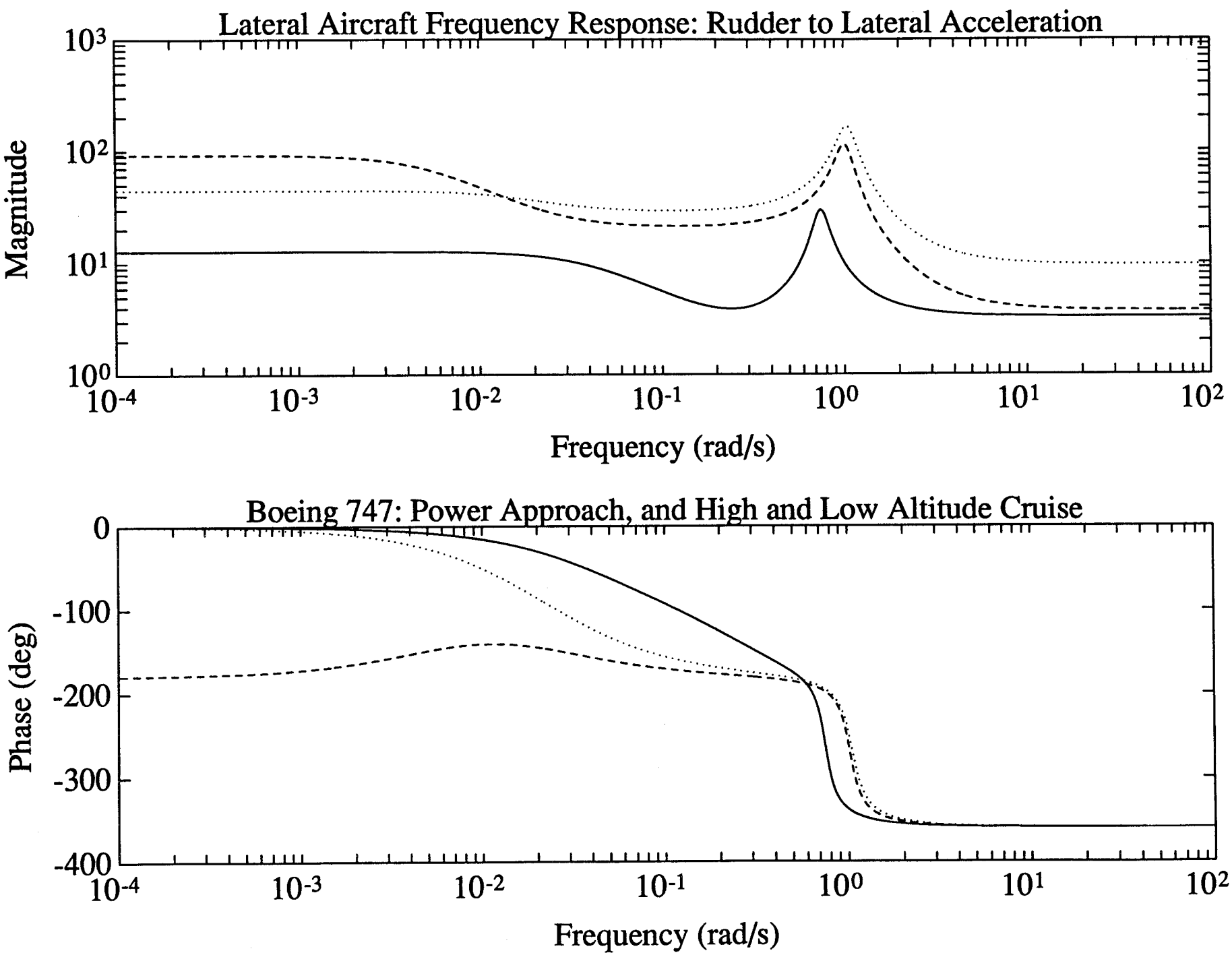
Lateral Aircraft Frequency Response: Rudder to Lateral Acceleration
Magnitude
10^3
10^2
10^1
10^0
10^{-4}
10^{-3}
10^{-2}
10^{-1}
10^0
10^1
10^2
Frequency (rad/s)
Boeing 747: Power Approach, and High and Low Altitude Cruise
Phase (deg)
0
-100
-200
-300
-400
10^{-4}
10^{-3}
10^{-2}
10^{-1}
10^0
10^1
10^2
Frequency (rad/s)

A.5 McDonnell Douglas F-4C

The contents of this section of the Appendix are:

- Stability and control data
- MATLAB script to form longitudinal dynamics
- MATLAB eigenvalue, natural frequency and damping print out from script for longitudinal dynamics
- Frequency responses of longitudinal dynamics
- MATLAB script to form lateral dynamics
- MATLAB eigenvalue, natural frequency and damping print out from script for lateral dynamics
- Frequency responses of lateral dynamics

The stability and control data are photocopies from Roskam.[1] The data were entered into MATLAB scripts to form the state-space differential equations for the longitudinal and lateral dynamics. Two additional scripts, one for longitudinal dynamics and one for lateral dynamics, were written to compute eigenvalues, natural frequencies, damping ratios, and frequency responses for the dynamics. These scripts are listed in Section A.3.

The conversions from dimensionless to dimensioned stability and control derivatives were done three at a time by first making each parameter, stability derivative and control derivative a 3-vector—one element for each flight condition. The conversion computations are then performed using vector arithmetic. The state-space matrices were formed from the appropriate elements of each vector.

$$\begin{aligned} E\dot{x} &= \tilde{A}x + \tilde{B}u \\ y &= Cx + Du \end{aligned} \tag{A-1}$$

Equation A-1 is an intermediate form for the state-space equation that was formed because some stability derivatives depend on the derivatives of the state variables in the case of the longitudinal dynamics and because of the roll/yaw coupling in moment equations in the case of the lateral dynamics. The final form is obtained by multiplying the first equation of the pair by the inverse of E.

The frequency response graphs show three traces—one for each of the three flight conditions. The line styles for the F-4C cases denote the following:

Solid:	power approach at sea level
Dashes:	subsonic cruise at 35,000 ft
Points:	supersonic cruise at 55,000 ft

C5 DATA FOR AIRPLANE E

Figure C5 presents a three-view for Airplane E. This airplane is representative of a supersonic fighter-bomber airplane. Stability and control derivatives for this airplane are given in Table C5.

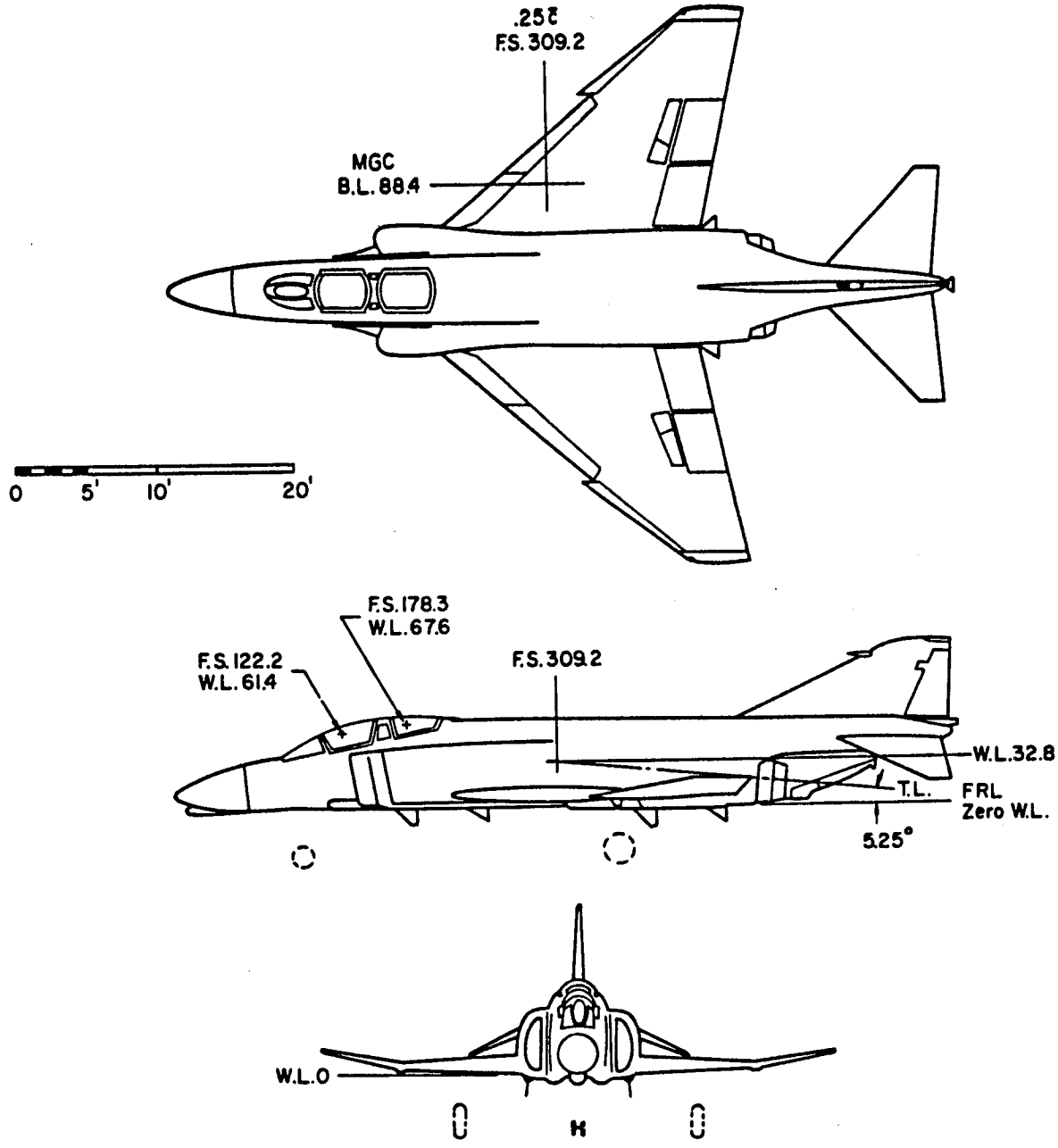

Figure C5 Three-View of Airplane E

Table C5 Stability and Control Derivatives for Airplane E

Flight Condition	1	2	3
	Power Approach	Subsonic Cruise	Supersonic Cruise
Altitude (ft)	Sealevel	35,000	55,000
Air Density (slugs/ft^3)	.002378	.000739	.000287
Speed (fps)	230	876	1742
Center of Gravity ($\bar{x}_{cg}$)	.29	.29	.29
Initial Attitude (deg)	11.7	2.6	3.3
Geometry and Inertias			
Wing Area (ft^2)	530	530	530
Wing Span (ft)	38.7	38.7	38.7
Wing Mean Geometric Chord (ft)	16.0	16.0	16.0
Weight (lbs)	33,200	39,000	39,000
I_{xx_B} (slug ft^2)	23,700	25,000	25,000
I_{yy_B} (slug ft^2)	117,500	122,200	122,200
I_{zz_B} (slug ft^2)	133,700	139,800	139,800
I_{xz_B} (slug ft^2)	1,600	2,200	2,200
Steady State Coefficients			
C_{L_1}	1.0	.26	.17
C_{D_1}	.2	.03	.048
$C_{T_{X_1}}$	.2	.03	.048
C_{m_1}	0	0	0
$C_{m_{T_1}}$	0	0	0

Table C5 Stability and Control Derivatives for Airplane E (Cont.)

Longitudinal Derivatives	1	2	3
C_{m_u}	0	-.117	+.054
C_{m_α}	-.098	-.40	-.78
$C_{m_{\dot{\alpha}}}$	-.95	-1.3	-.25
C_{m_q}	-2.0	-2.7	-2.0
$C_{m_{T_u}}$	0	0	0
$C_{m_{T_\alpha}}$	0	0	0
C_{L_u}	0	+.27	-.18
C_{L_α}	2.8	3.75	2.8
$C_{L_{\dot{\alpha}}}$	0	0	0
C_{L_q}	0	0	0
C_{D_α}	.555	.3	.4
C_{D_u}	0	+.027	-.054
$C_{T_{X_u}}$	0	0	0
$C_{L_{i_H}}$	.24	.40	.25
$C_{D_{i_H}}$	-.14	-.10	-.15
$C_{m_{i_H}}$	-.322	-.58	-.38

(Note: longitudinal control through stabilizer only)

Table C5 Stability and Control Derivatives for Airplane E (Cont.)

Lateral-Directional Derivatives	1	2	3
C_{ℓ_β}	-.156	-.080	-.025
C_{ℓ_p}	-.272	-.240	-.200
C_{ℓ_r}	.205	.070	.040
$C_{\ell_{\delta_A}}$	.057	.042	.015
$C_{\ell_{\delta_R}}$	.0009	.0060	.0030
C_{n_β}	.199	.125	.090
C_{n_p}	.013	-.036	0
C_{n_r}	-.320	-.270	-.260
$C_{n_{\delta_A}}$	+.0041	-.0010	-.0009
$C_{n_{\delta_R}}$	-.072	-.066	-.025
C_{y_β}	-.655	-.68	-.70
C_{y_p}	0	0	0
C_{y_r}	0	0	0
$C_{y_{\delta_A}}$	-.0355	-.016	-.010
$C_{y_{\delta_R}}$	.124	.095	.050

```
%LONGITUDINAL DYNAMICS
%McDonnell Douglas F-4C, power approach     <--fc1
%                        subsonic cruise    <--fc2
%                        Supersonic cruise  <--fc3

format short e

%Enter flight condition, geometry, mass and MOI parameters.

g=32.2;                                 %gravity (ft/s^2)
theta0=[11.7 2.6 3.3]*pi/180;           %equilibrium pitch angle (deg)
rho=[.002378 .000739 .000287];          %density (slug/ft^3)
Uo=[230 876 1742];                      %equilibrium speed (ft/s)
mass=[33200 39000 39000]/g;             %weight (lbs)
Ixx=[23700 25000 25000];                %roll inertia (slug ft^2)
Iyy=[117500 122200 122200];             %pitch inertia (slug ft^2)
Izz=[133700 139800 139800];             %yaw inertia (slug ft^2)
Ixz=[1600 2200 2200];                   %cross product of inertia (slug ft^2)
S=[530 530 530];                        %wing area (ft^2)
b=[38.7 38.7 38.7];                     %wing span (ft)
cbar=[16 16 16];                        %mean geometric chord (ft)

%Enter steady-state coefficients.

CL1=[1.0 .26 .17];
CD1=[.2 .03 .048];
CTx1=[.2 .03 .048];
Cm1=[0 0 0];
CmT1=[0 0 0];

%Enter dimensionless stability and control derivatives.

Cmu=[0 -.117 +.054];
Cma=[-.098 -.40 -.78];
Cmad=[-.95 -1.3 -.25];
Cmq=[-2.0 -2.7 -2.0];
CmTu=[0 0 0];
CmTa=[0 0 0];
CLu=[0 +.27 -.18];
CLa=[+2.8 +3.75 +2.8];
CLad=[0 0 0];
CLq=[0 0 0];
CDa=[+.555 +.3 +.4];
CDu=[0 +.027 -.054];
CTxu=[0 0 0];
CLde=[+.24 +.40 +.25];
CDde=[-.14 -.10 -.15];
Cmde=[-.322 -.58 -.38];

CDad=[0 0 0];  %No numbers in Roskam
CDq=[0 0 0];   %No numbers in Roskam


%Compute dimensioned stability and control derivatives

qbar=0.5*rho.*Uo.^2;
Xu =-qbar.*S.*(CDu+2*CD1)./(mass.*Uo);
XTu= qbar.*S.*(CTxu+2*CTx1)./(mass.*Uo);
```

```
Xa =-qbar.*S.*(CDa-CL1)./mass;
Xde=-qbar.*S.*CDde./mass;
Zu =-qbar.*S.*(CLu+2*CL1)./(mass.*Uo);
Za =-qbar.*S.*(CLa+CD1)./mass;
Zad=-qbar.*S.*CLad.*cbar./(2*mass.*Uo);
Zq =-qbar.*S.*CLq.*cbar./(2*mass.*Uo);
Zde=-qbar.*S.*CLde./mass;
Mu = qbar.*S.*cbar.*(Cmu+2*Cm1)./(Iyy.*Uo);
MTu= qbar.*S.*cbar.*(CmTu+2*CmT1)./(Iyy.*Uo);
Ma = qbar.*S.*cbar.*Cma./Iyy;
MTa= qbar.*S.*cbar.*CmTa./Iyy;
Mad= qbar.*S.*(cbar.^2).*Cmad./(2*Iyy.*Uo);
Mq = qbar.*S.*(cbar.^2).*Cmq./(2*Iyy.*Uo);
Mde= qbar.*S.*cbar.*Cmde./Iyy;

%Compute dynamics for flight condition 1 in state-space form.

Afc1=[
      Xu(1)+XTu(1) Xa(1)/Uo(1)                 0
-g*cos(theta0(1))
      Zu(1)        Za(1)/Uo(1)                 Uo(1)+Zq(1)
-g*sin(theta0(1))
      Mu(1)+MTu(1) Ma(1)/Uo(1)+MTa(1)/Uo(1) Mq(1)          0
      0            0                          1            0
     ];

Bfc1=[Xde(1);Zde(1);Mde(1);0];

Efc1=[
      1 0               0 0
      0 1-Zad(1)/Uo(1)  0 0
      0  -Mad(1)/Uo(1)  1 0
      0 0               0 1];

Afc1=Efc1\Afc1;
Bfc1=Efc1\Bfc1;

%Compute pitch angle
%         angle of attack
%         forward speed
%         vertical acceleration
%output matrix and direct input matrix.

Cfc1=[
      0   0        0    1
      0   1/Uo(1)  0    0
      1   0        0    0
      Afc1(2,:)-[0 0 Uo(1) 0]
     ];
Dfc1=0*Cfc1*Bfc1;
Dfc1(4,1)=Bfc1(2,1);

%Compute dynamics for flight condition 2 in state-space form.

Afc2=[
      Xu(2)+XTu(2) Xa(2)/Uo(2)                 0
-g*cos(theta0(2))
```

```
      Zu(2)          Za(2)/Uo(2)                 Uo(2)+Zq(2)
-g*sin(theta0(2))
      Mu(2)+MTu(2)  Ma(2)/Uo(2)+MTa(2)/Uo(2)  Mq(2)          0
      0             0                           1             0
     ];

Bfc2=[Xde(2);Zde(2);Mde(2);0];

Efc2=[
      1 0               0 0
      0 1-Zad(2)/Uo(2)  0 0
      0  -Mad(2)/Uo(2)  1 0
      0 0               0 1
     ];

Afc2=Efc2\Afc2;
Bfc2=Efc2\Bfc2;

%Compute pitch angle
%         angle of attack
%         forward speed
%         vertical acceleration
%output matrix and direct input matrix.

Cfc2=[
     0   0         0    1
     0   1/Uo(2)   0    0
     1   0         0    0
     Afc2(2,:)-[0 0 Uo(2) 0]
    ];
Dfc2=0*Cfc2*Bfc2;
Dfc2(4,1)=Bfc2(2,1);

%Compute dynamics for flight condition 3 in state-space form.

Afc3=[
      Xu(3)+XTu(3) Xa(3)/Uo(3)                 0
-g*cos(theta0(3))
      Zu(3)        Za(3)/Uo(3)                 Uo(3)+Zq(3)
-g*sin(theta0(3))
      Mu(3)+MTu(3) Ma(3)/Uo(3)+MTa(3)/Uo(3)  Mq(3)          0
      0            0                           1             0
     ];

Bfc3=[Xde(3);Zde(3);Mde(3);0];

Efc3=[
      1 0               0 0
      0 1-Zad(3)/Uo(3)  0 0
      0  -Mad(3)/Uo(3)  1 0
      0 0               0 1
     ];

Afc3=Efc3\Afc3;
Bfc3=Efc3\Bfc3;

%Compute pitch angle
%         angle of attack
```

```
%         forward speed
%         vertical acceleration
%output matrix and direct input matrix.

Cfc3=[
     0   0         0    1
     0   1/Uo(3)   0    0
     1   0         0    0
     Afc3(2,:)-[0 0 Uo(3) 0]
    ];
Dfc3=0*Cfc3*Bfc3;
Dfc3(4,1)=Bfc3(2,1);
```

```
%LONGITUDINAL DYNAMICS RESULTS
%McDonnell Douglas F-4C, sea level-power approach     <--fc1
%                        35,000 ft-subsonic cruise    <--fc2
%                        55,000 ft-supersonic cruise <--fc3
%Roskam, J., 1979,
%Airplane Flight Dynamics and Automatic Flight Controls,
%Part I, pp. 616-642

EIGENVALUES

evfc1 =
 -4.6662e-01+  6.2290e-01i
 -4.6662e-01-  6.2290e-01i
  2.2873e-02+  1.6668e-01i
  2.2873e-02-  1.6668e-01i

evfc2 =
 -6.3372e-01+  2.7832e+00i
 -6.3372e-01-  2.7832e+00i
  4.4867e-02
 -3.5424e-02


evfc3 =
 -3.1093e-01+  4.8536e+00i
 -3.1093e-01-  4.8536e+00i
  1.9914e-03+  2.6812e-02i
  1.9914e-03-  2.6812e-02i

NATURAL FREQUENCIES
   7.7830e-01   2.8544e+00   4.8636e+00
   7.7830e-01   2.8544e+00   4.8636e+00
   1.6824e-01   4.4867e-02   2.6886e-02
   1.6824e-01   3.5424e-02   2.6886e-02

DAMPING RATIOS
   5.9954e-01   2.2201e-01   6.3930e-02
   5.9954e-01   2.2201e-01   6.3930e-02
  -1.3595e-01  -1.0000e+00  -7.4070e-02
  -1.3595e-01   1.0000e+00  -7.4070e-02
```

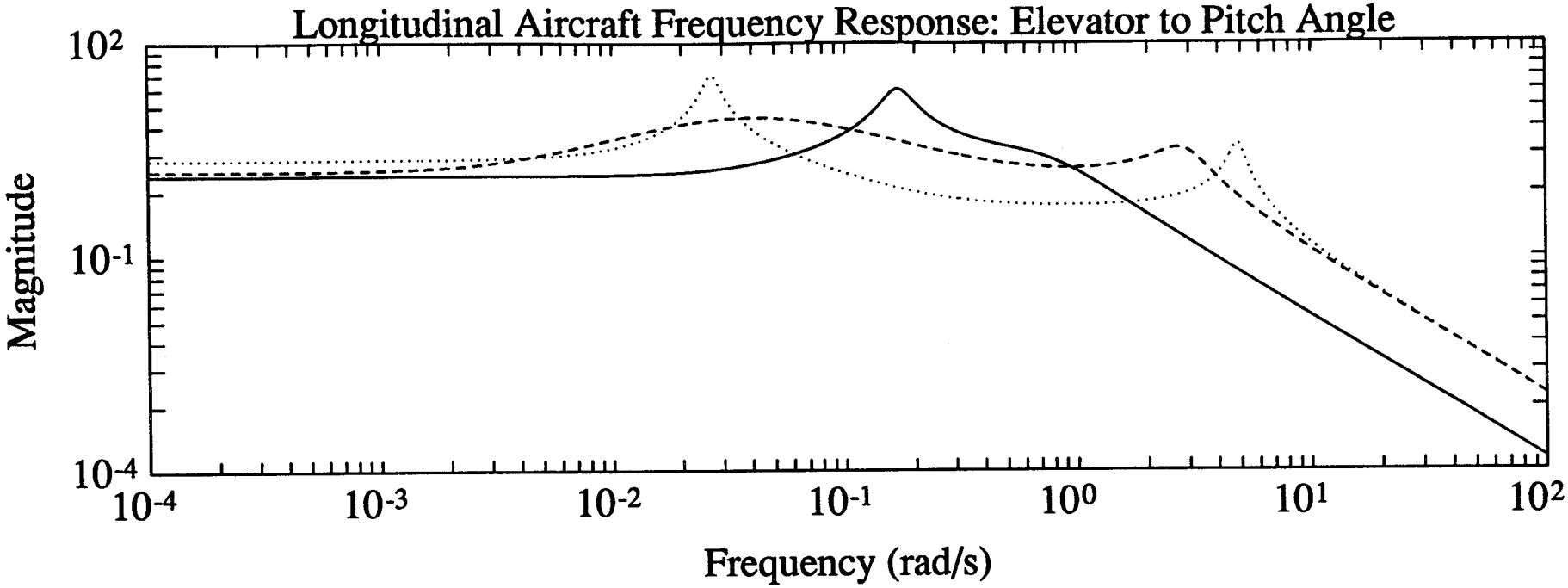
Longitudinal Aircraft Frequency Response: Elevator to Pitch Angle
Magnitude
10^{2}
10^{-1}
10^{-4}
10^{-4}
10^{-3}
10^{-2}
10^{-1}
10^{0}
10^{1}
10^{2}
Frequency (rad/s)

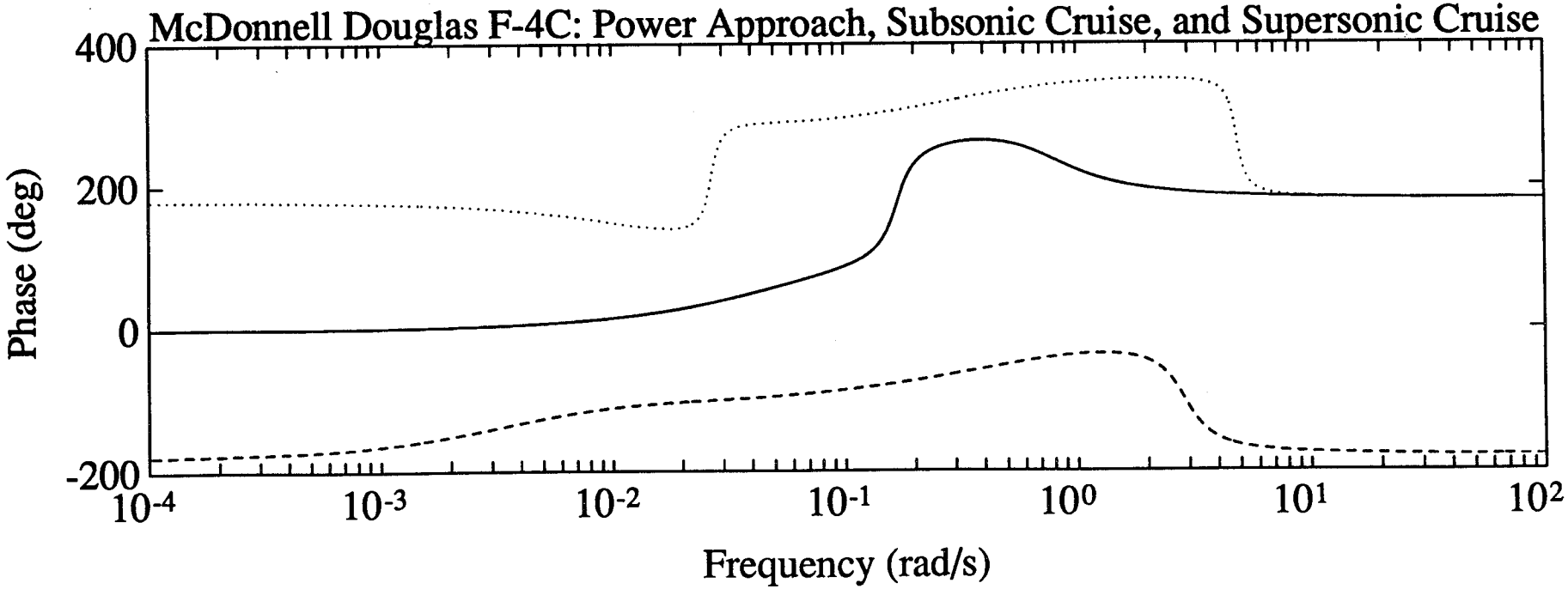
McDonnell Douglas F-4C: Power Approach, Subsonic Cruise, and Supersonic Cruise
Phase (deg)
400
200
0
-200
10^{-4}
10^{-3}
10^{-2}
10^{-1}
10^{0}
10^{1}
10^{2}
Frequency (rad/s)

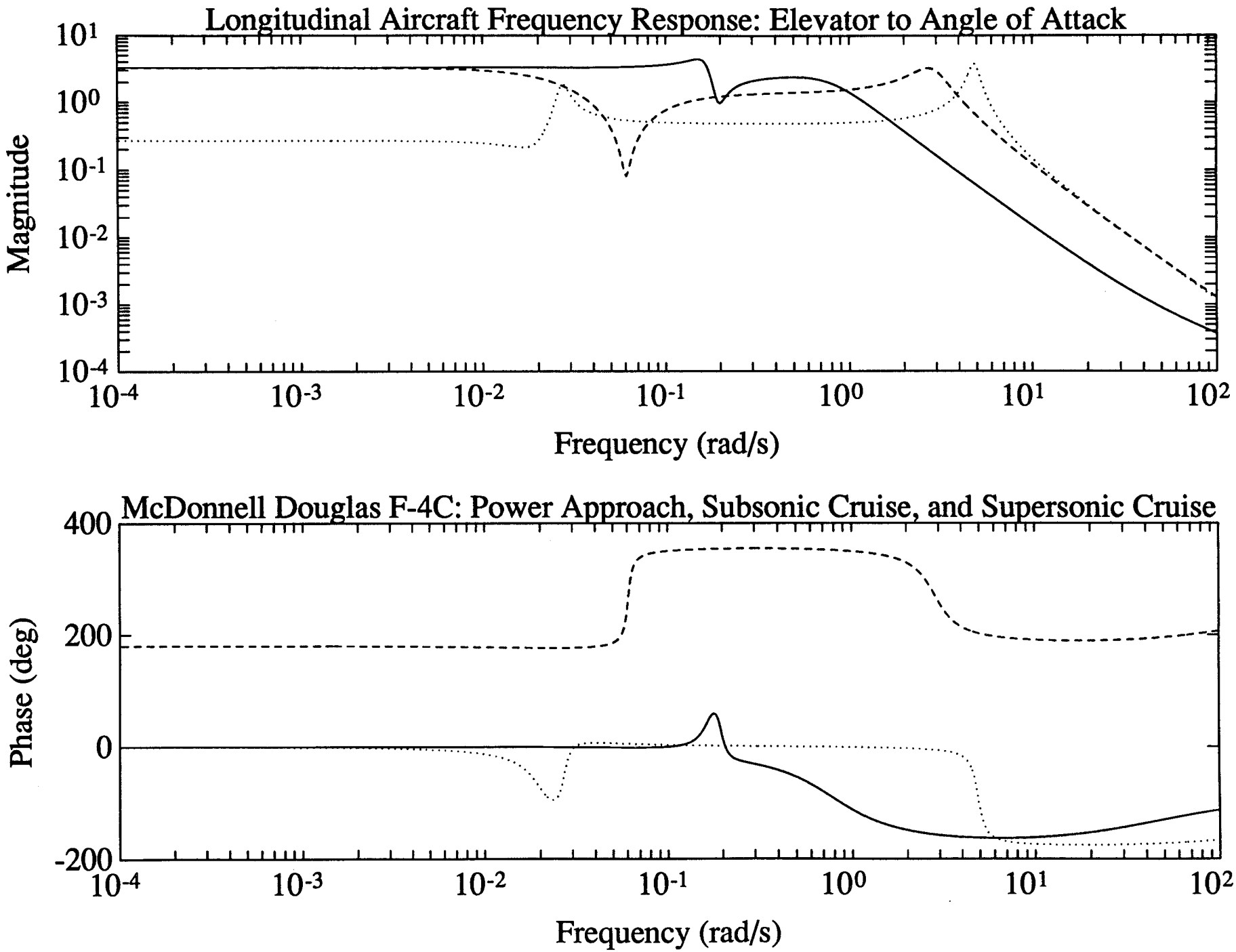
Longitudinal Aircraft Frequency Response: Elevator to Angle of Attack
Magnitude
10^1
10^0
10^-1
10^-2
10^-3
10^-4
10^-4
10^-3
10^-2
10^-1
10^0
10^1
10^2
Frequency (rad/s)
McDonnell Douglas F-4C: Power Approach, Subsonic Cruise, and Supersonic Cruise
Phase (deg)
400
200
0
-200
10^-4
10^-3
10^-2
10^-1
10^0
10^1
10^2
Frequency (rad/s)

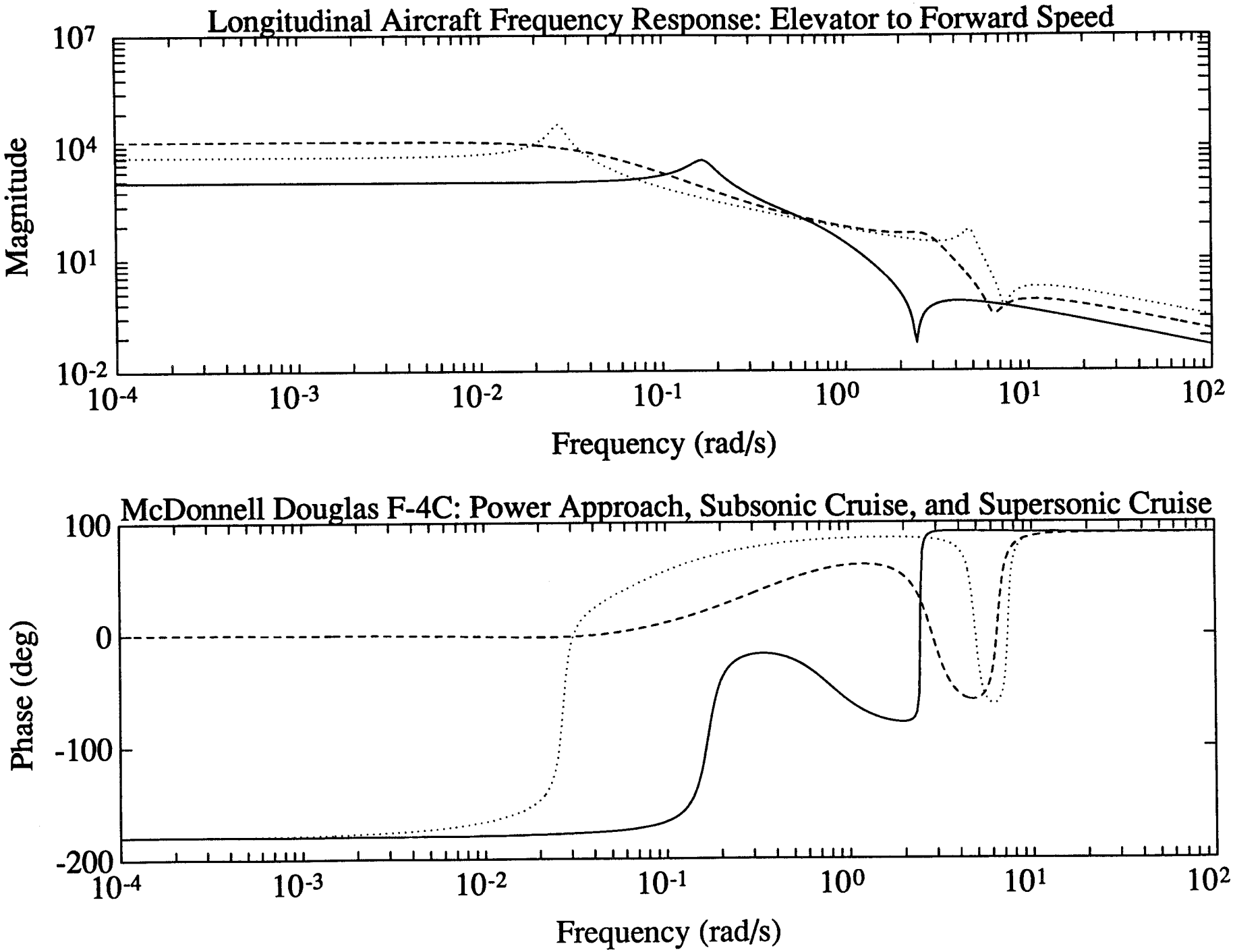
Longitudinal Aircraft Frequency Response: Elevator to Forward Speed
Magnitude
10^7
10^4
10^1
10^-2
10^-4
10^-3
10^-2
10^-1
10^0
10^1
10^2
Frequency (rad/s)
McDonnell Douglas F-4C: Power Approach, Subsonic Cruise, and Supersonic Cruise
Phase (deg)
100
0
-100
-200
10^-4
10^-3
10^-2
10^-1
10^0
10^1
10^2
Frequency (rad/s)

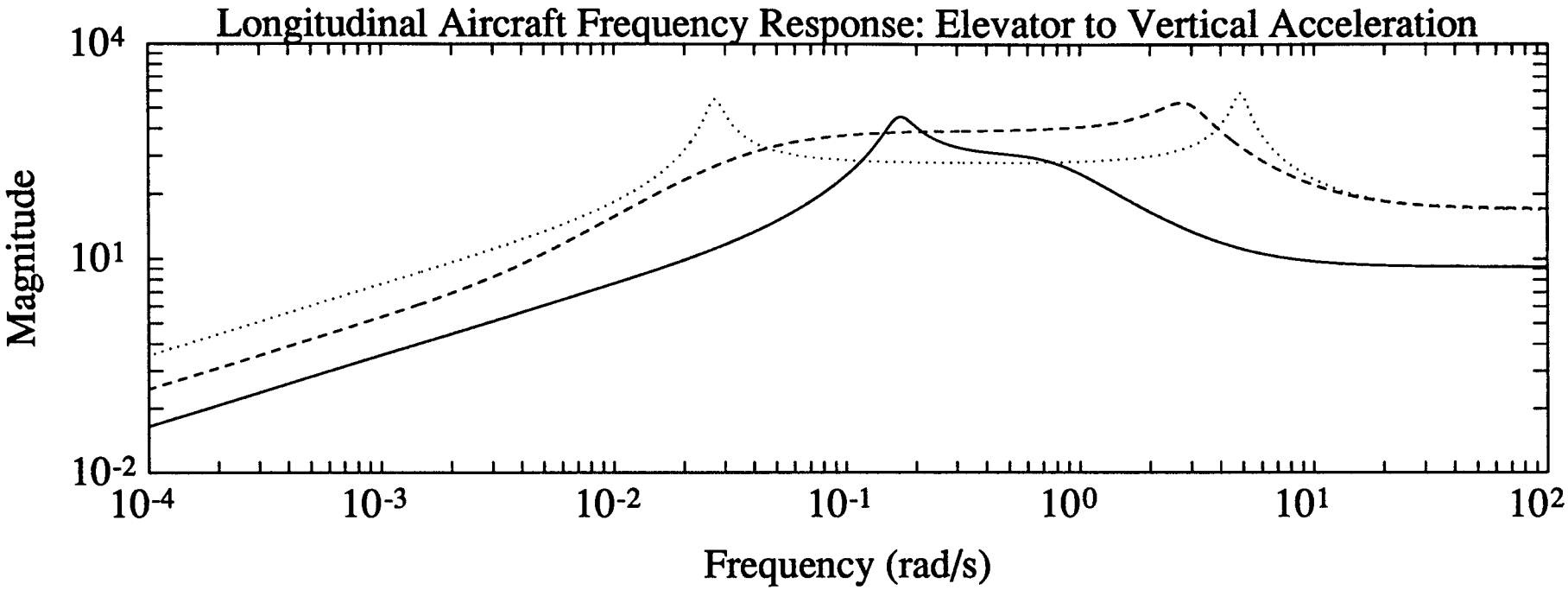
Longitudinal Aircraft Frequency Response: Elevator to Vertical Acceleration
Magnitude
10^4
10^1
10^-2
10^-4
10^-3
10^-2
10^-1
10^0
10^1
10^2
Frequency (rad/s)

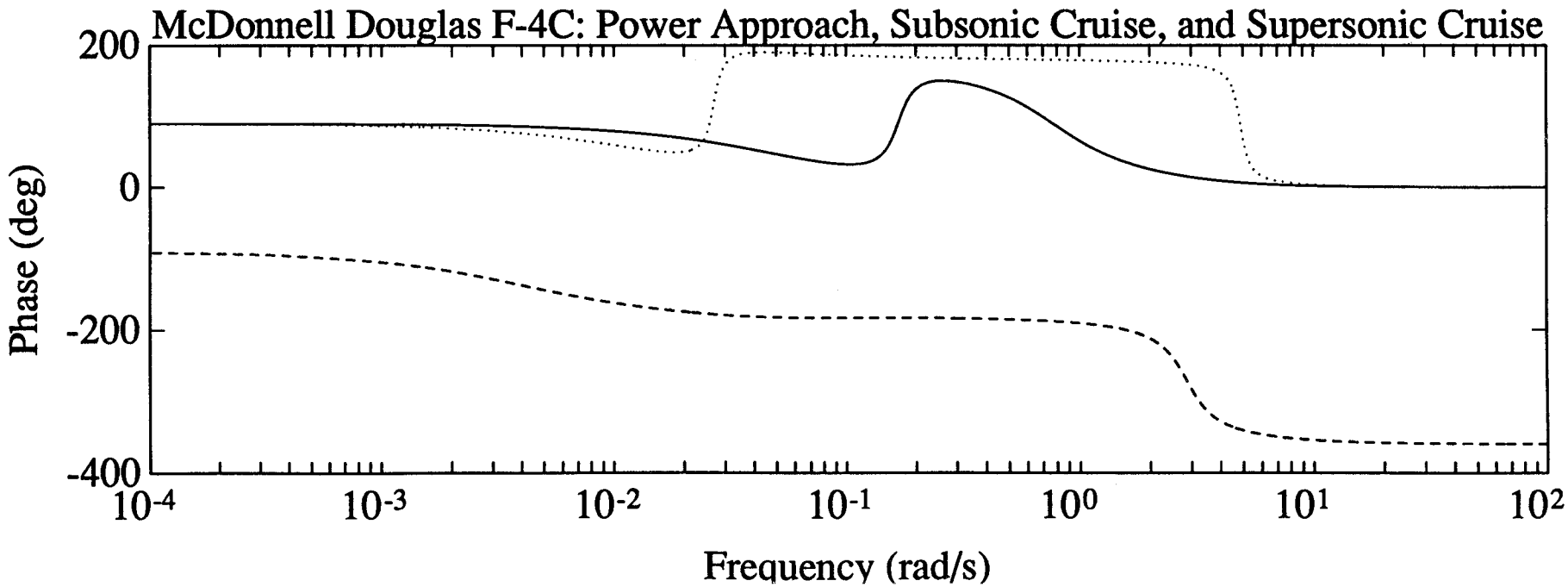
McDonnell Douglas F-4C: Power Approach, Subsonic Cruise, and Supersonic Cruise
Phase (deg)
200
0
-200
-400
10^-4
10^-3
10^-2
10^-1
10^0
10^1
10^2
Frequency (rad/s)

```
%LATERAL DYNAMICS
%McDonnell Douglas F-4C, power approach     <--fc1
%                        subsonic cruise    <--fc2
%                        Supersonic cruise  <--fc3
%Roskam, J., 1979,
%Airplane Flight Dynamics and Automatic Flight Controls,
%Part I, pp. 616-642

format short e

%Enter flight condition, geometry, mass and MOI parameters.

g=32.2;                                 %gravity (ft/s^2)
theta0=[11.7 2.6 3.3]*pi/180;           %equilibrium pitch angle (deg)
rho=[.002378 .000739 .000287];          %density (slug/ft^3)
Uo=[230 876 1742];                      %equilibrium speed (ft/s)
mass=[33200 39000 39000]/g;             %weight (lbs)
Ixx=[23700 25000 25000];                %roll inertia (slug ft^2)
Izz=[133700 139800 139800];             %yaw inertia (slug ft^2)
Ixz=[1600 2200 2200];                   %cross product of inertia (slug ft^2)
S=[530 530 530];                        %wing area (ft^2)
b=[38.7 38.7 38.7];                     %wing span (ft)
cbar=[16 16 16];                        %mean geometric chord (ft)

%Transform relevant inertias from body axis to stability axis.

for ifc=1:3,
  ang=theta0(ifc);
  Tba2sa=[
          cos(ang)^2     sin(ang)^2    -sin(2*ang)
          sin(ang)^2     cos(ang)^2     sin(2*ang)
          sin(2*ang)/2 -sin(2*ang)/2   cos(2*ang)
         ];
  Isa=Tba2sa*[Ixx(ifc);Izz(ifc);Ixz(ifc)];
  Ixx(ifc)=Isa(1);
  Izz(ifc)=Isa(2);
  Ixz(ifc)=Isa(3);
end;

%Enter steady-state coefficients.

CL1=[1.0 .26 .17];
CD1=[.2 .03 .048];
CTx1=[.2 .03 .048];
Cm1=[0 0 0];
CmT1=[0 0 0];

%Enter dimensionless stability and control derivatives.

Clb=[-.156 -.080 -.025];
Clp=[-.272 -.240 -.200];
Clr=[.205 .070 .040];
Clda=[.057 .042 .015];
Cldr=[.0009 .0060 .0030];

Cnb=[.199 .125 .090];
Cnp=[.013 -.036 0];
Cnr=[-.320 -.270 -.260];
```

```
Cnda=[.0041 -.0010 -.0009];
Cndr=[-.072 -.066 -.025];

Cyb=[-.655 -.68 -.70];
Cyp=[0 0 0];
Cyr=[0 0 0];
Cyda=[-.0355 -.016 -.010];
Cydr=[.124 .095 .050];

CnTb=[0 0 0];  %No numbers in Roskam

%Compute dimensioned stability and control derivatives

qbar=0.5*rho.*Uo.^2;
Yb = qbar.*S.*Cyb./mass;
Yp = qbar.*S.*b.*Cyp./(2*mass.*Uo);
Yr = qbar.*S.*b.*Cyr./(2*mass.*Uo);
Yda= qbar.*S.*Cyda./mass;
Ydr= qbar.*S.*Cydr./mass;

Lb = qbar.*S.*b.*Clb./Ixx;
Lp = qbar.*S.*(b.^2).*Clp./(2*Ixx.*Uo);
Lr = qbar.*S.*(b.^2).*Clr./(2*Ixx.*Uo);
Lda= qbar.*S.*b.*Clda./Ixx;
Ldr= qbar.*S.*b.*Cldr./Ixx;

Nb = qbar.*S.*b.*Cnb./Izz;
NTb= qbar.*S.*b.*CnTb./Izz;
Np = qbar.*S.*(b.^2).*Cnp./(2*Izz.*Uo);
Nr = qbar.*S.*(b.^2).*Cnr./(2*Izz.*Uo);
Nda= qbar.*S.*b.*Cnda./Izz;
Ndr= qbar.*S.*b.*Cndr./Izz;

%Compute dynamics for flight condition 1 in state-space form.

Afc1=[
      Yb(1)/Uo(1)           Yp(1) Yr(1)-Uo(1) g*cos(theta0(1))
g*sin(theta0(1))
      Lb(1)/Uo(1)           Lp(1) Lr(1)       0                0
      (Nb(1)+NTb(1))/Uo(1) Np(1) Nr(1)       0                0
      0                     1     0           0                0
      0                     0     1           0                0
     ];

Bfc1=[
      Yda(1) Ydr(1)
      Lda(1) Ldr(1)
      Nda(1) Ndr(1)
      0*ones(2,2)
     ];

Efc1=[
      1  0             0               0 0
      0  1            -Ixz(1)/Ixx(1)   0 0
      0 -Ixz(1)/Izz(1) 1               0 0
      0  0             0               1 0
      0  0             0               0 1
     ];
```

```
Afc1=Efc1\Afc1;
Bfc1=Efc1\Bfc1;

%Compute sideslip angle
%        roll angle
%        yaw angle
%        lateral acceleration
%output matrix and direct input matrix.

Cfc1=[
      1/Uo(1)  0  0  0  0
      0        0  0  1  0
      0        0  0  0  1
      Afc1(1,:)+[0 0 Uo(1) -g 0]
     ];
Dfc1=0*Cfc1*Bfc1;
Dfc1(4,:)=Bfc1(1,:);

%Compute dynamics for flight condition 2 in state-space form.

Afc2=[
      Yb(2)/Uo(2)           Yp(2) Yr(2)-Uo(2) g*cos(theta0(2))
g*sin(theta0(2))
      Lb(2)/Uo(2)           Lp(2) Lr(2)       0                0
      (Nb(2)+NTb(2))/Uo(2) Np(2) Nr(2)       0                0
      0                     1     0           0                0
      0                     0     1           0                0
     ];

Bfc2=[
      Yda(2) Ydr(2)
      Lda(2) Ldr(2)
      Nda(2) Ndr(2)
      0*ones(2,2)
     ];

Efc2=[
      1  0              0              0 0
      0  1             -Ixz(2)/Ixx(2) 0 0
      0 -Ixz(2)/Izz(2)  1              0 0
      0  0              0              1 0
      0  0              0              0 1
     ];

Afc2=Efc2\Afc2;
Bfc2=Efc2\Bfc2;

%Compute sideslip angle
%        roll angle
%        yaw angle
%        lateral acceleration
%output matrix and direct input matrix.

Cfc2=[
      1/Uo(2)  0  0  0  0
      0        0  0  1  0
      0        0  0  0  1
```

```
      Afc2(1,:)+[0 0 Uo(2) -g 0]
     ];
Dfc2=0*Cfc2*Bfc2;
Dfc2(4,:)=Bfc2(1,:);

%Compute dynamics for flight condition 3 in state-space form.

Afc3=[
      Yb(3)/Uo(3)           Yp(3) Yr(3)-Uo(3) g*cos(theta0(3))
g*sin(theta0(3))
      Lb(3)/Uo(3)           Lp(3) Lr(3)       0                 0
      (Nb(3)+NTb(3))/Uo(3) Np(3) Nr(3)       0                 0
      0                     1     0           0                 0
      0                     0     1           0                 0
     ];

Bfc3=[
      Yda(3) Ydr(3)
      Lda(3) Ldr(3)
      Nda(3) Ndr(3)
      0*ones(2,2)
     ];

Efc3=[
      1  0              0              0 0
      0  1             -Ixz(3)/Ixx(3) 0 0
      0 -Ixz(3)/Izz(3) 1              0 0
      0  0              0              1 0
      0  0              0              0 1
     ];

Afc3=Efc3\Afc3;
Bfc3=Efc3\Bfc3;

%Compute sideslip angle
%        roll angle
%        yaw angle
%        lateral acceleration
%output matrix and direct input matrix.

Cfc3=[
      1/Uo(3)  0  0  0  0
      0        0  0  1  0
      0        0  0  0  1
      Afc3(1,:)+[0 0 Uo(3) -g 0]
     ];
Dfc3=0*Cfc3*Bfc3;
Dfc3(4,:)=Bfc3(1,:);
```

```
%LATERAL DYNAMICS RESULTS
%McDonnell Douglas F-4C, power approach      <--fc1 (solid)
%                        subsonic cruise     <--fc2 (dashed)
%                        Supersonic cruise   <--fc3 (dotted)
%Roskam, J., 1979,
%Airplane Flight Dynamics and Automatic Flight Controls,
%Part I, pp. 616-642

EIGENVALUES

evfc1 =
            0
 -1.1098e+00
 -1.5240e-02
 -3.1618e-01+  1.7808e+00i
 -3.1618e-01-  1.7808e+00i

evfc2 =
            0
 -1.3391e+00
 -1.3123e-02
 -1.1565e-01+  2.3946e+00i
 -1.1565e-01-  2.3946e+00i

evfc3 =
            0
 -7.8175e-01
 -2.8623e-03
 -1.3838e-01+  2.4603e+00i
 -1.3838e-01-  2.4603e+00i

NATURAL FREQUENCIES
            0             0             0
   1.1098e+00    1.3391e+00    7.8175e-01
   1.5240e-02    1.3123e-02    2.8623e-03
   1.8086e+00    2.3974e+00    2.4642e+00
   1.8086e+00    2.3974e+00    2.4642e+00

DAMPING RATIOS
          NaN           NaN           NaN
   1.0000e+00    1.0000e+00    1.0000e+00
   1.0000e+00    1.0000e+00    1.0000e+00
   1.7482e-01    4.8239e-02    5.6158e-02
   1.7482e-01    4.8239e-02    5.6158e-02
```

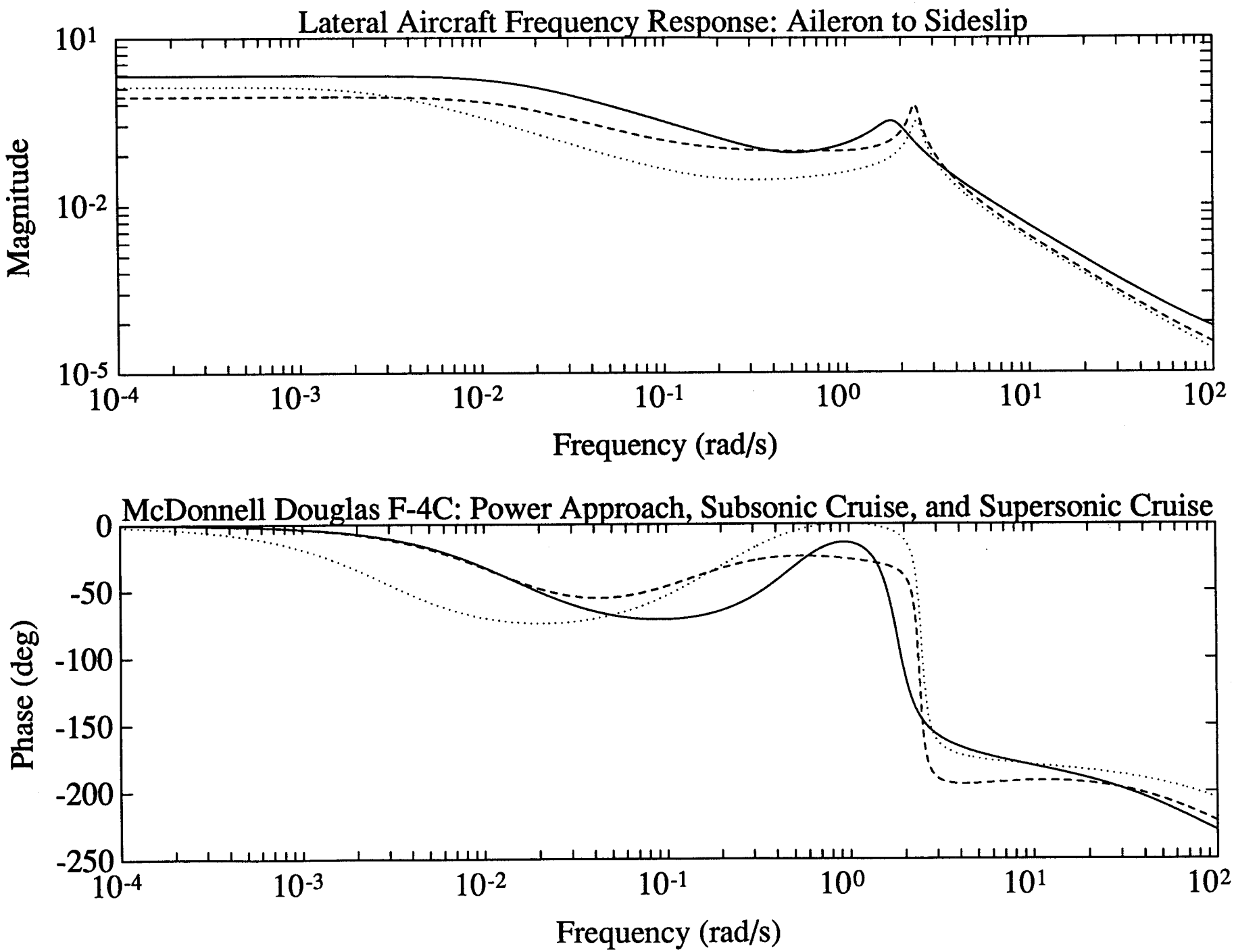
Lateral Aircraft Frequency Response: Aileron to Sideslip
Magnitude
10^1
10^-2
10^-5
10^-4
10^-3
10^-2
10^-1
10^0
10^1
10^2
Frequency (rad/s)
McDonnell Douglas F-4C: Power Approach, Subsonic Cruise, and Supersonic Cruise
Phase (deg)
0
-50
-100
-150
-200
-250
10^-4
10^-3
10^-2
10^-1
10^0
10^1
10^2
Frequency (rad/s)

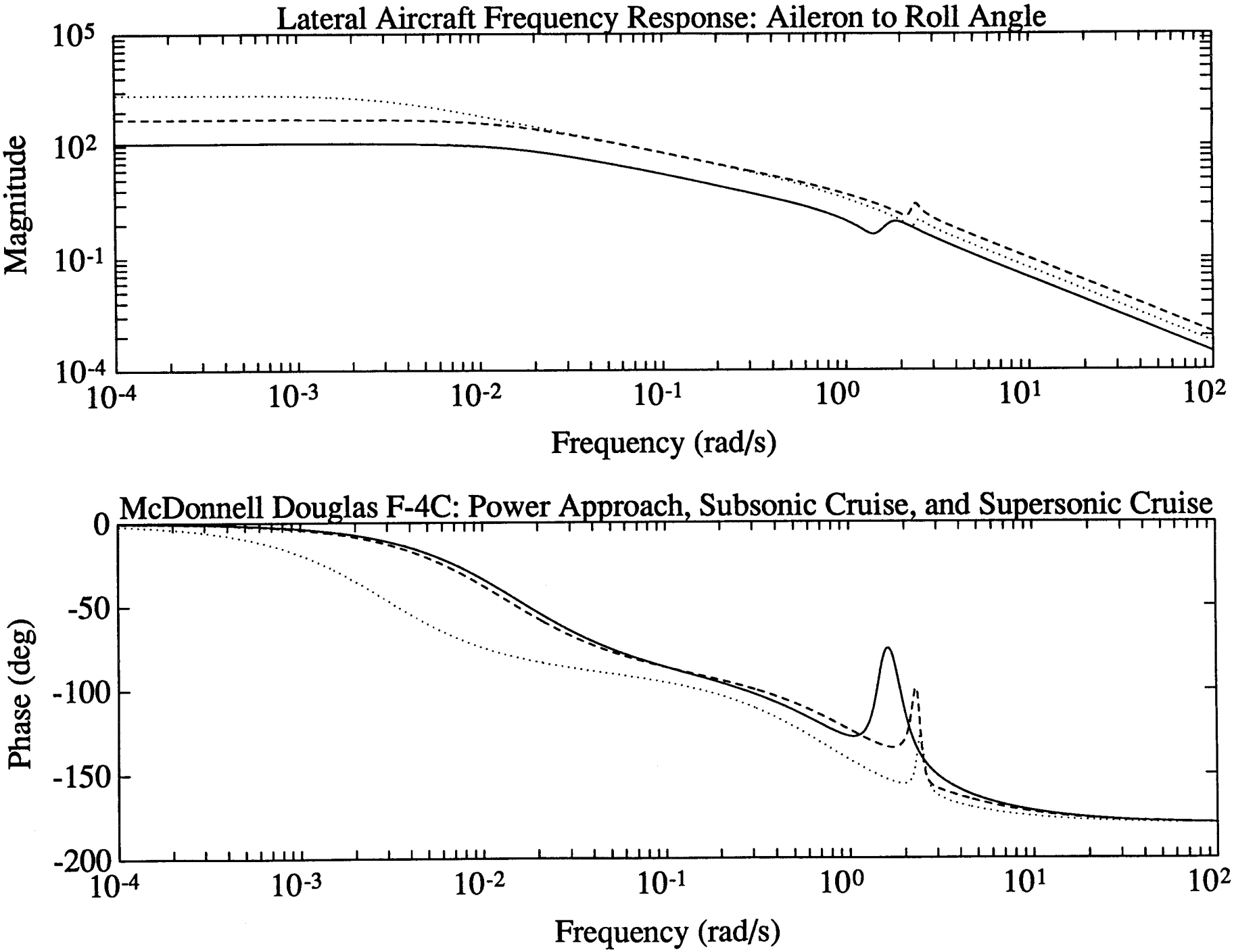
Lateral Aircraft Frequency Response: Aileron to Roll Angle
Magnitude
10^5
10^2
10^-1
10^-4
10^-4
10^-3
10^-2
10^-1
10^0
10^1
10^2
Frequency (rad/s)
McDonnell Douglas F-4C: Power Approach, Subsonic Cruise, and Supersonic Cruise
Phase (deg)
0
-50
-100
-150
-200
10^-4
10^-3
10^-2
10^-1
10^0
10^1
10^2
Frequency (rad/s)

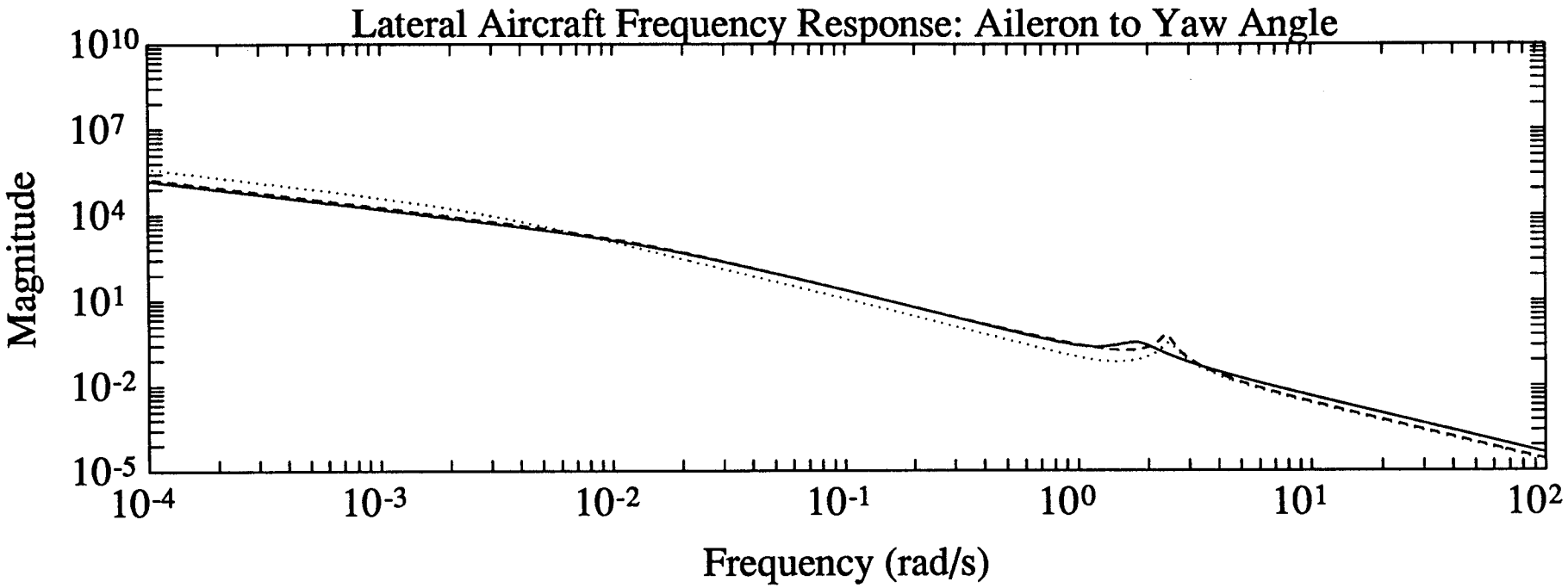
Lateral Aircraft Frequency Response: Aileron to Yaw Angle
Magnitude
10^10
10^7
10^4
10^1
10^-2
10^-5
10^-4
10^-3
10^-2
10^-1
10^0
10^1
10^2
Frequency (rad/s)

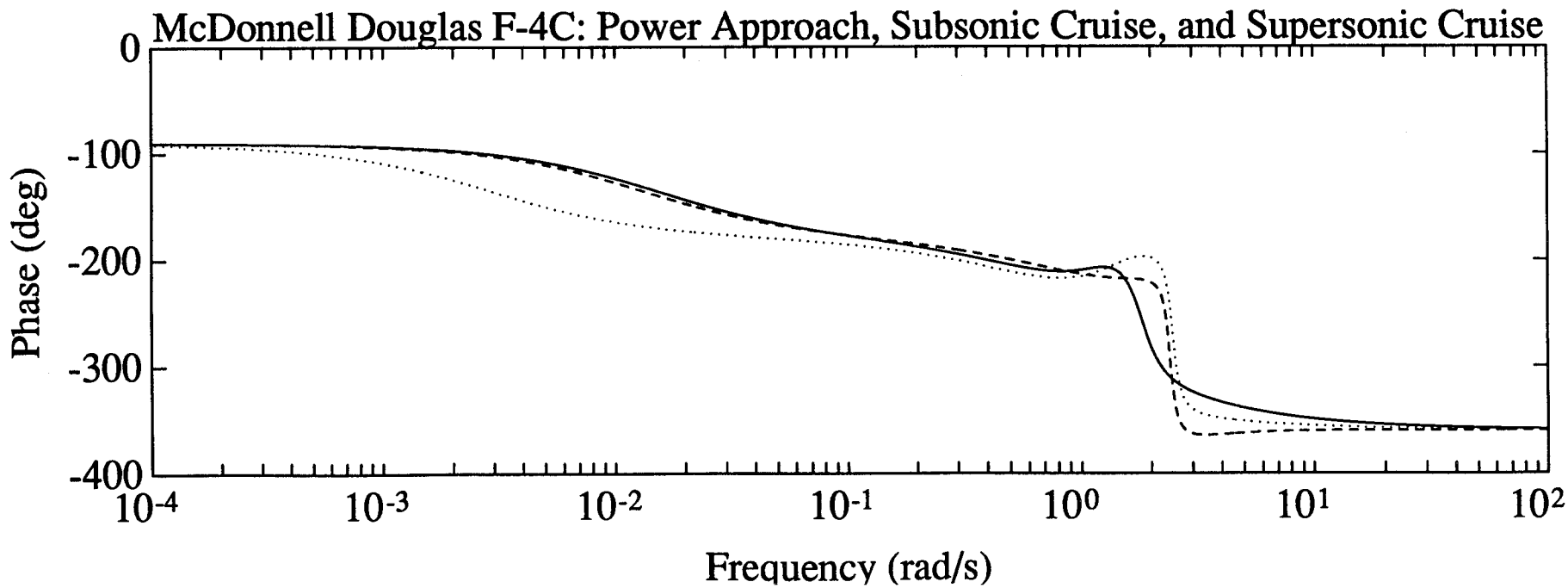
McDonnell Douglas F-4C: Power Approach, Subsonic Cruise, and Supersonic Cruise
Phase (deg)
0
-100
-200
-300
-400
10^-4
10^-3
10^-2
10^-1
10^0
10^1
10^2
Frequency (rad/s)

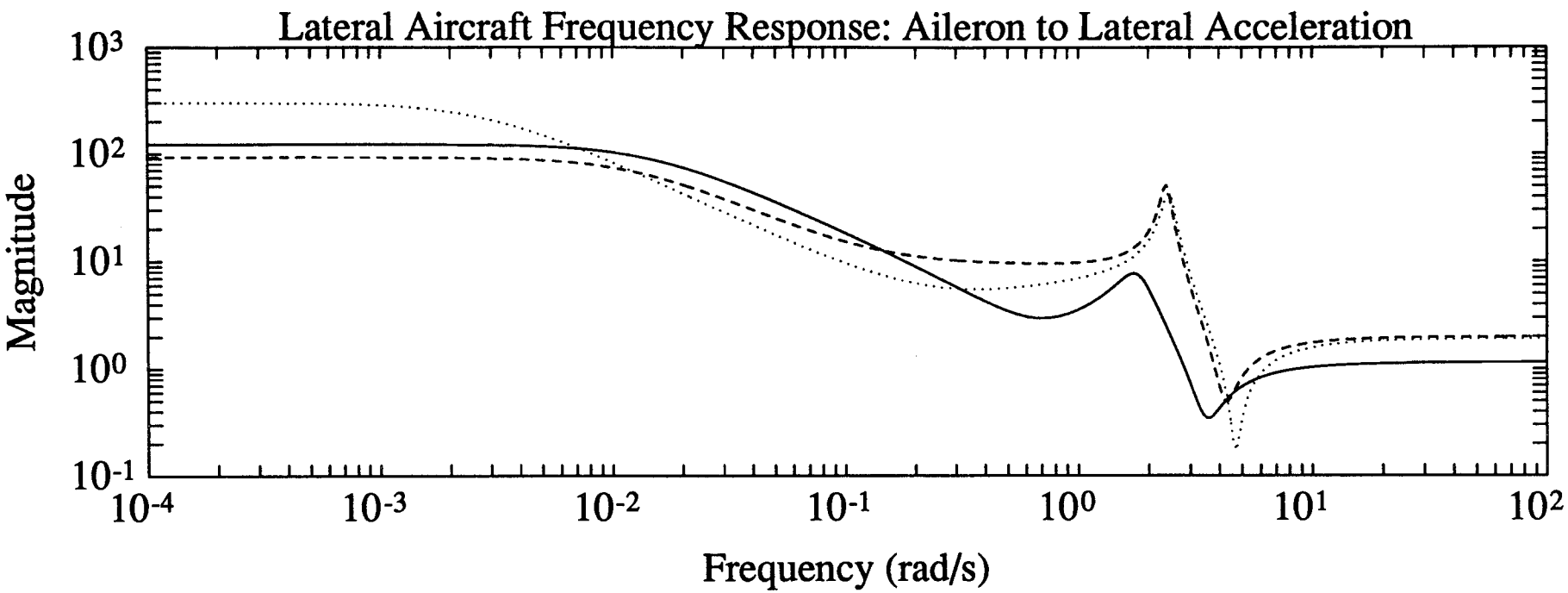
Lateral Aircraft Frequency Response: Aileron to Lateral Acceleration
Magnitude
10^3
10^2
10^1
10^0
10^-1
10^-4
10^-3
10^-2
10^-1
10^0
10^1
10^2
Frequency (rad/s)

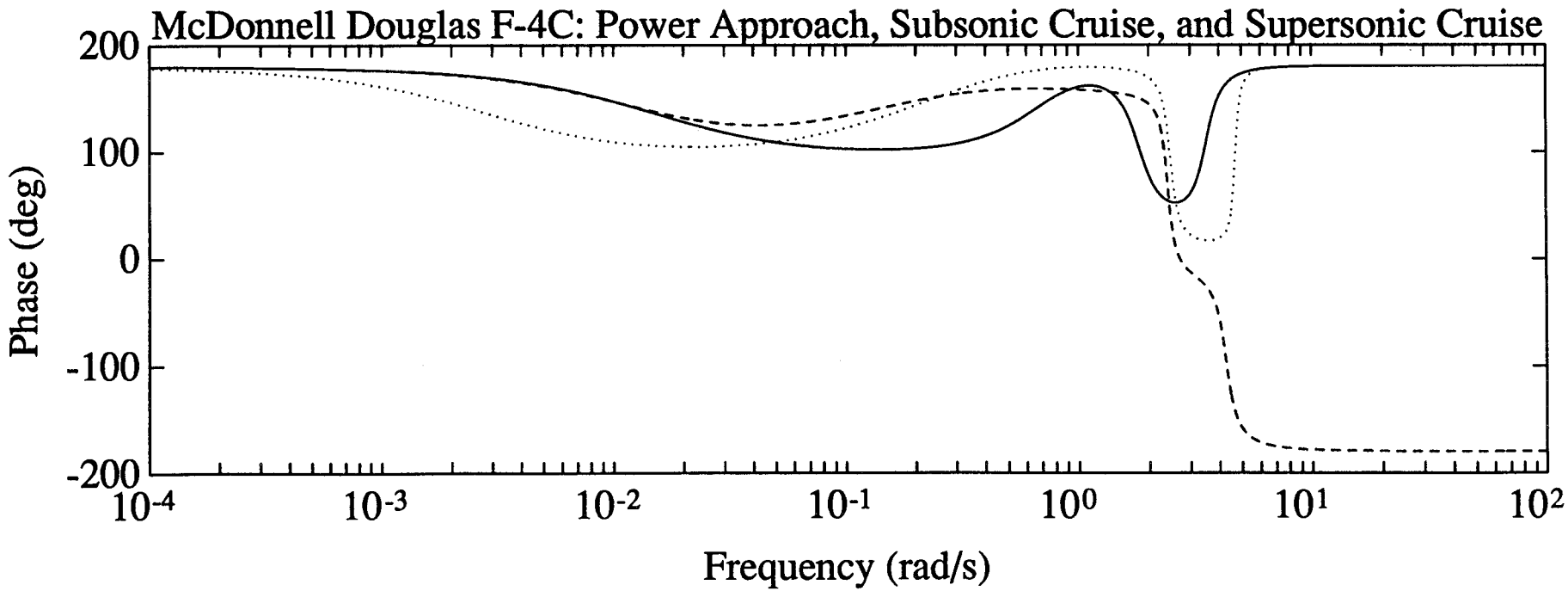
McDonnell Douglas F-4C: Power Approach, Subsonic Cruise, and Supersonic Cruise
Phase (deg)
200
100
0
-100
-200
10^-4
10^-3
10^-2
10^-1
10^0
10^1
10^2
Frequency (rad/s)

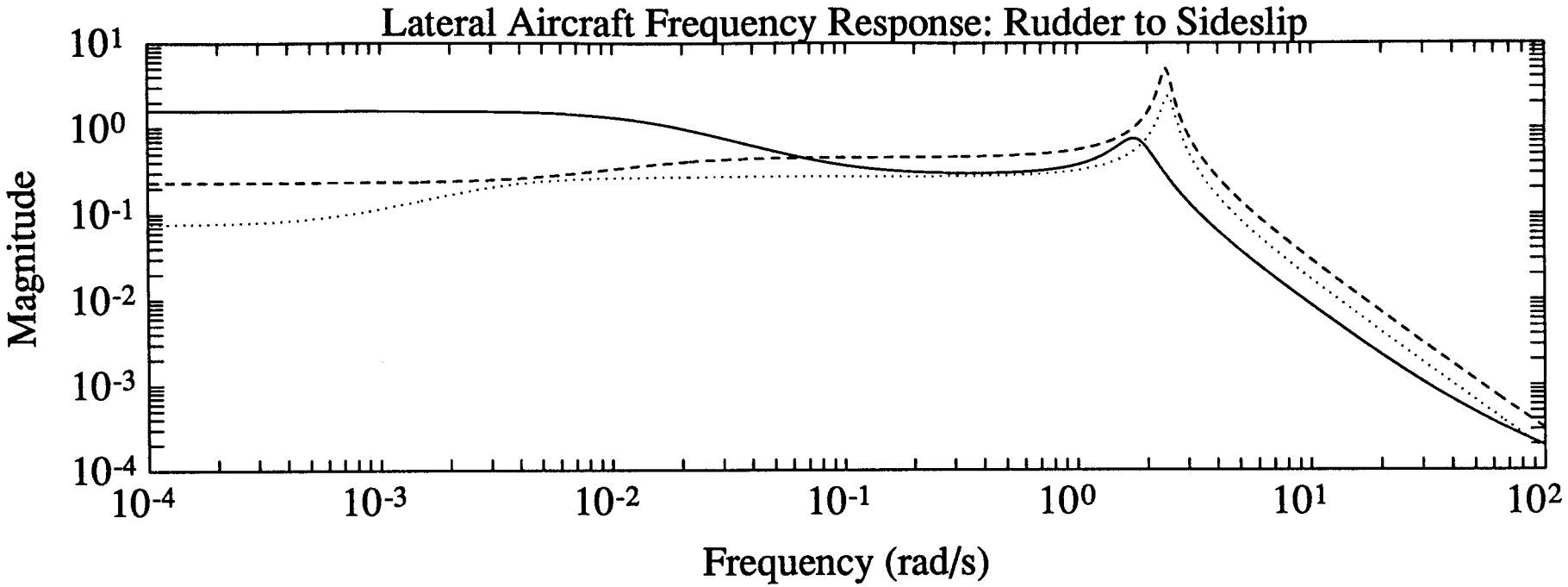
Lateral Aircraft Frequency Response: Rudder to Sideslip
Magnitude
10^{1}
10^{0}
10^{-1}
10^{-2}
10^{-3}
10^{-4}
10^{-4}
10^{-3}
10^{-2}
10^{-1}
10^{0}
10^{1}
10^{2}
Frequency (rad/s)

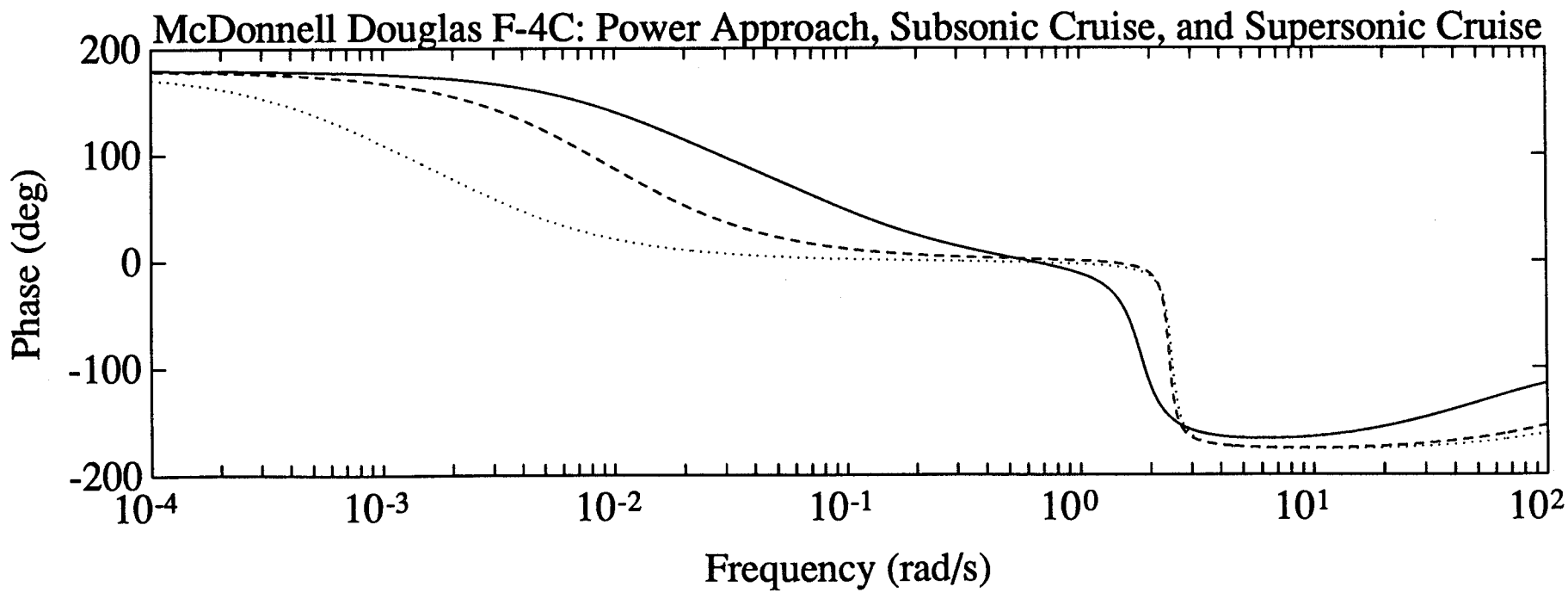
McDonnell Douglas F-4C: Power Approach, Subsonic Cruise, and Supersonic Cruise
Phase (deg)
200
100
0
-100
-200
10^{-4}
10^{-3}
10^{-2}
10^{-1}
10^{0}
10^{1}
10^{2}
Frequency (rad/s)

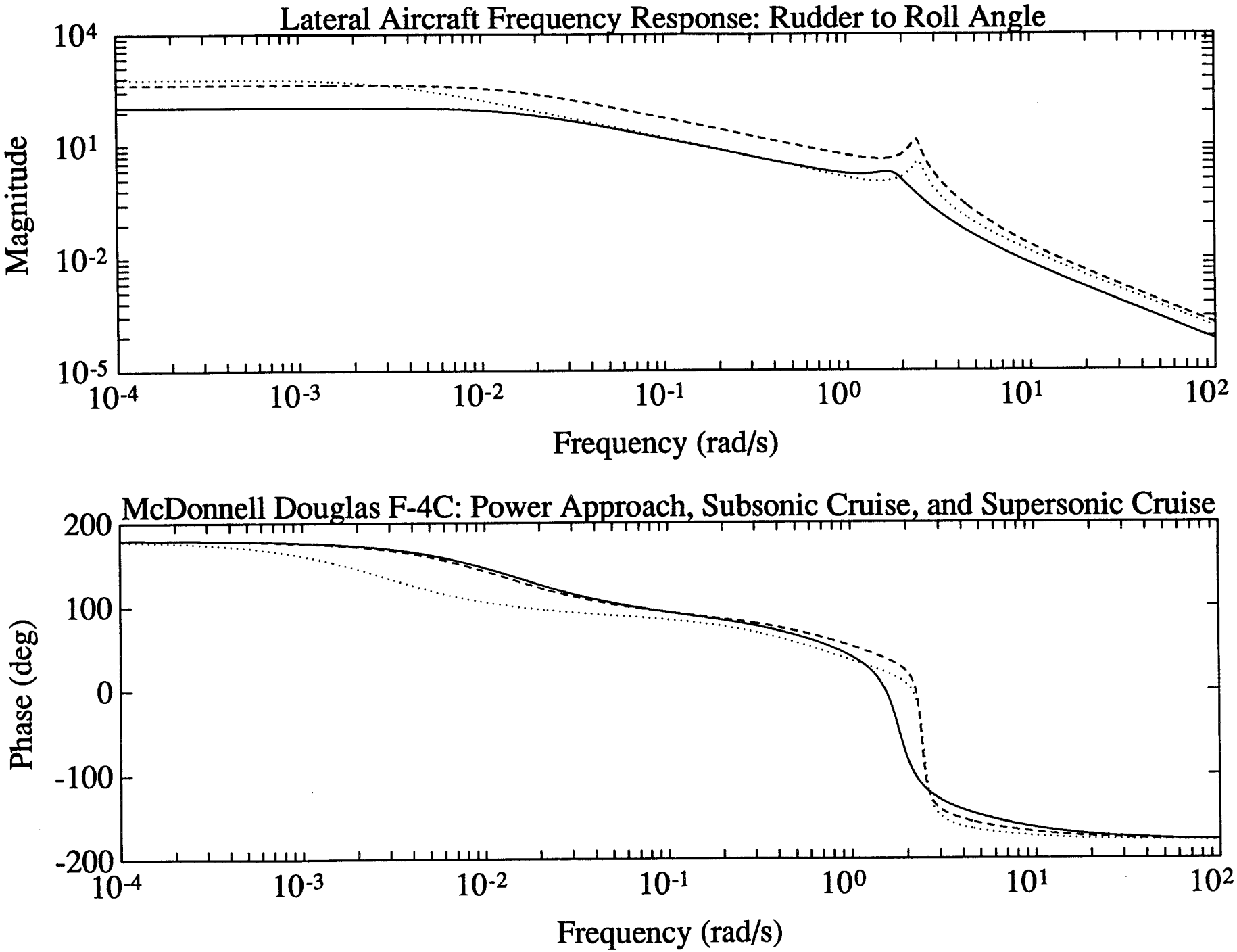
Lateral Aircraft Frequency Response: Rudder to Roll Angle
Magnitude
10^4
10^1
10^-2
10^-5
10^-4
10^-3
10^-2
10^-1
10^0
10^1
10^2
Frequency (rad/s)
McDonnell Douglas F-4C: Power Approach, Subsonic Cruise, and Supersonic Cruise
Phase (deg)
200
100
0
-100
-200
10^-4
10^-3
10^-2
10^-1
10^0
10^1
10^2
Frequency (rad/s)

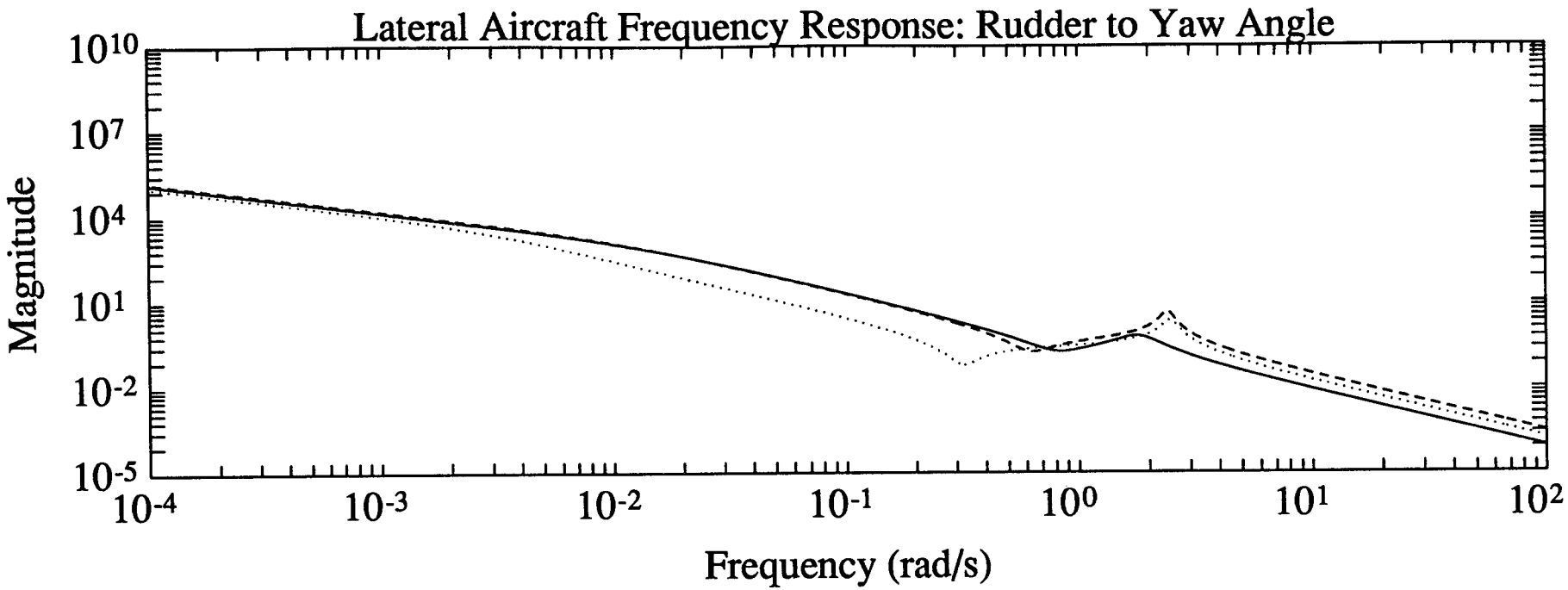
Lateral Aircraft Frequency Response: Rudder to Yaw Angle
Magnitude
10^10
10^7
10^4
10^1
10^-2
10^-5
10^-4
10^-3
10^-2
10^-1
10^0
10^1
10^2
Frequency (rad/s)

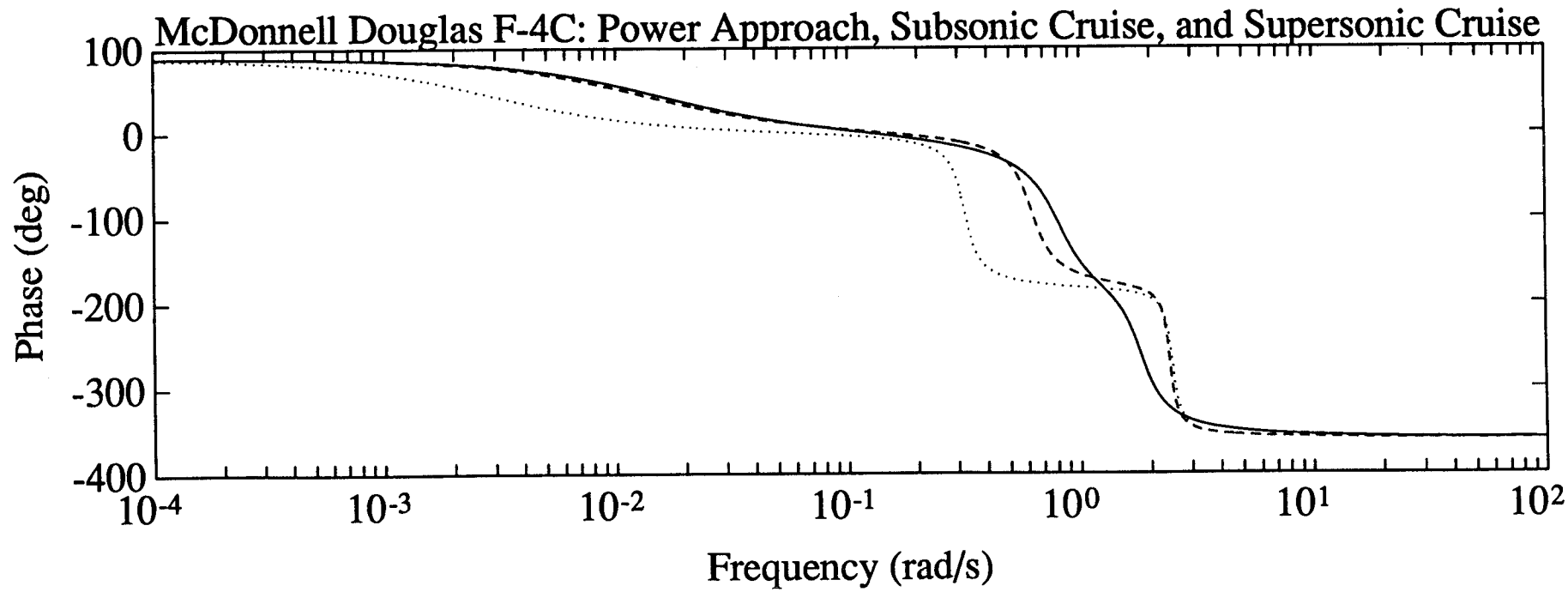
McDonnell Douglas F-4C: Power Approach, Subsonic Cruise, and Supersonic Cruise
Phase (deg)
100
0
-100
-200
-300
-400
10^-4
10^-3
10^-2
10^-1
10^0
10^1
10^2
Frequency (rad/s)

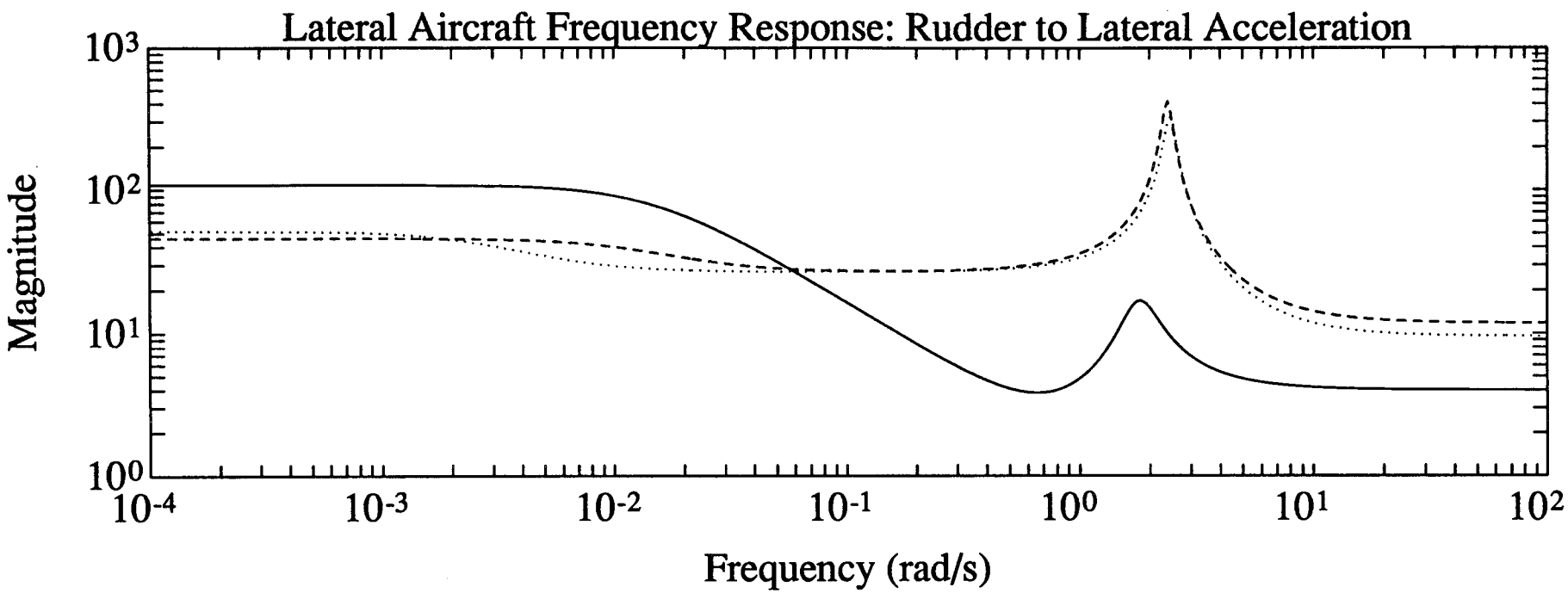
Lateral Aircraft Frequency Response: Rudder to Lateral Acceleration
Magnitude
10^3
10^2
10^1
10^0
10^{-4}
10^{-3}
10^{-2}
10^{-1}
10^0
10^1
10^2
Frequency (rad/s)

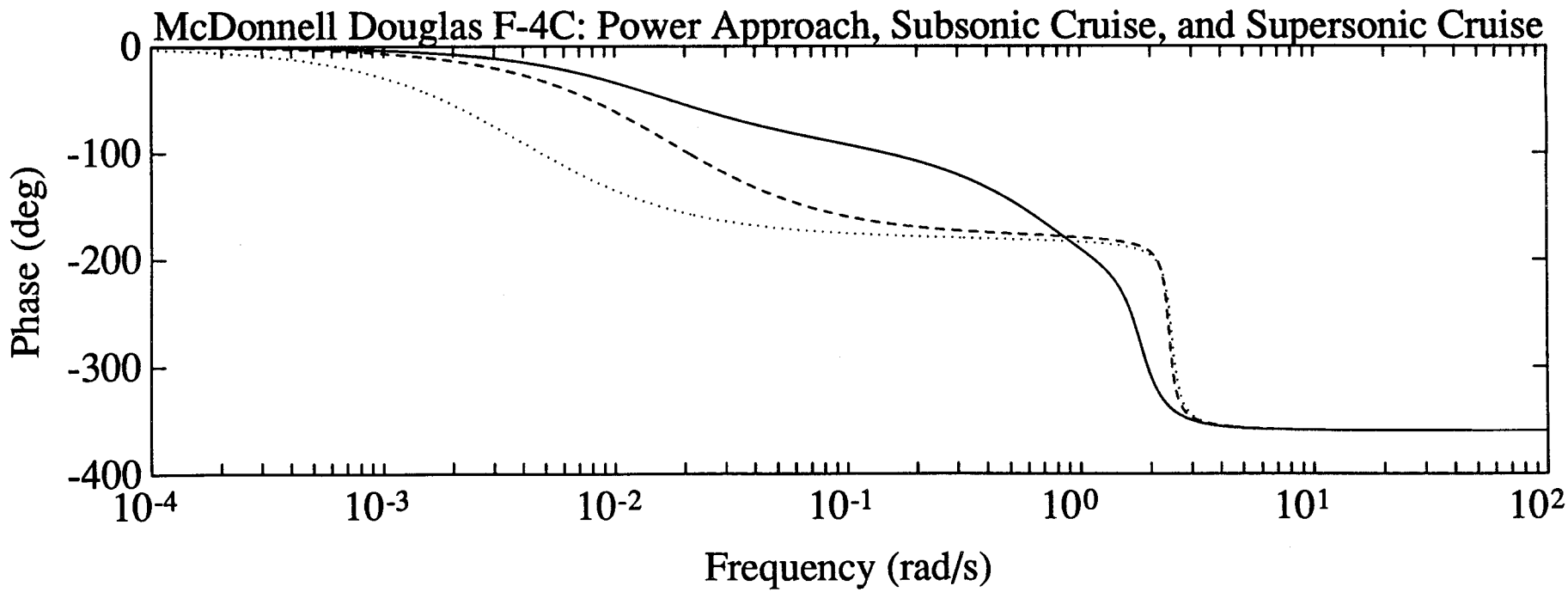
McDonnell Douglas F-4C: Power Approach, Subsonic Cruise, and Supersonic Cruise
Phase (deg)
0
-100
-200
-300
-400
10^{-4}
10^{-3}
10^{-2}
10^{-1}
10^0
10^1
10^2
Frequency (rad/s)

A.6 Learjet Model 24

The contents of this section of the Appendix are:

- Stability and control data
- MATLAB script to form longitudinal dynamics
- MATLAB eigenvalue, natural frequency and damping print out from script for longitudinal dynamics
- Frequency responses of longitudinal dynamics
- MATLAB script to form lateral dynamics
- MATLAB eigenvalue, natural frequency and damping print out from script for lateral dynamics
- Frequency responses of lateral dynamics

The stability and control data are photocopies from Roskam.[1] The data were entered into MATLAB scripts to form the state-space differential equations for the longitudinal and lateral dynamics. Two additional scripts, one for longitudinal dynamics and one for lateral dynamics, were written to compute eigenvalues, natural frequencies, damping ratios, and frequency responses for the dynamics. These scripts are listed in Section A.3.

The conversions from dimensionless to dimensioned stability and control derivatives were done three at a time by first making each parameter, stability derivative and control derivative a 3-vector—one element for each flight condition. The conversion computations are then performed using vector arithmetic. The state-space matrices were formed from the appropriate elements of each vector.

$$\begin{aligned} E\dot{x} &= \tilde{A}x + \tilde{B}u \\ y &= Cx + Du \end{aligned} \tag{A-1}$$

Equation A-1 is an intermediate form for the state-space equation that was formed because some stability derivatives depend on the derivatives of the state variables in the case of the longitudinal dynamics and because of the roll/yaw coupling in moment equations in the case of the lateral dynamics. The final form is obtained by multiplying the first equation of the pair by the inverse of E.

The frequency response graphs show three traces—one for each of the three flight conditions. The line styles for the Learjet Model 24 cases denote the following:

Solid:	power approach at sea level
Dashes:	Cruise at 40,000 ft at maximum weight
Points:	Cruise at 40,000 ft at low weight

C4 DATA FOR AIRPLANE D

A three-view for Airplane D is presented in Figure C4. This airplane is representative of a medium sized high performance business jet. Stability and control derivatives for Airplane D are presented in Table C4.

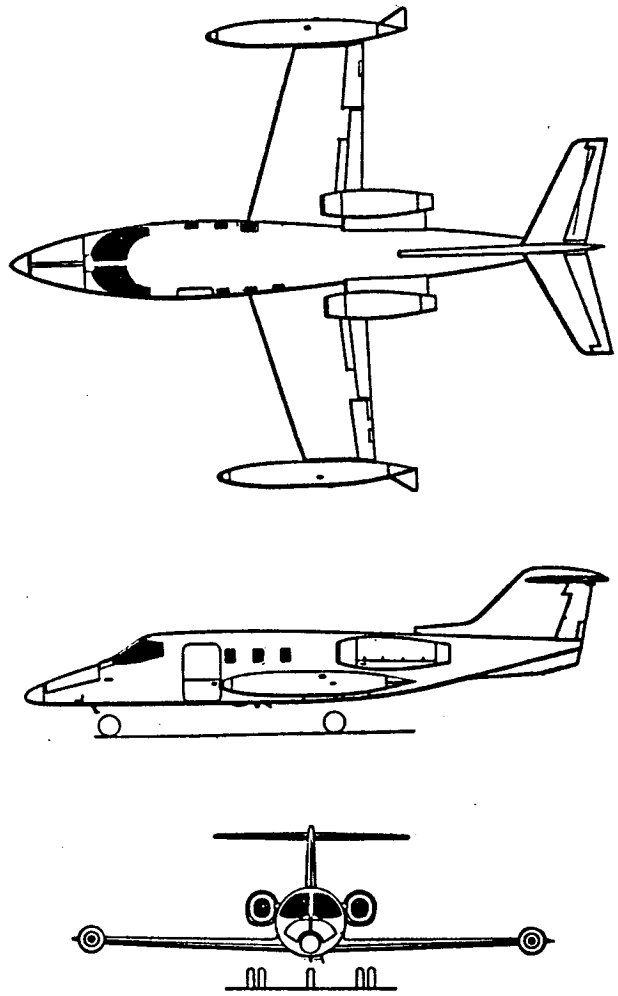

Figure C4 Three-View of Airplane D

Table C4 Stability and Control Derivatives for Airplane D

Flight Condition	1	2	3
	Power Approach	Cruise Max. Wht.	Cruise Low Wht.
Altitude (ft)	Sealevel	40,000	40,000
Air Density (slugs/ft^3)	.002378	.000588	.000588
Speed (fps)	170	677 (M = .7)	677 (M = .7)
Center of Gravity ($\bar{x}_{cg}$)	.32 (aft)	.32 (aft)	.32 (aft)
Initial Attitude (deg)	1.8	2.7	1.5
Geometry and Inertias			
Wing Area (ft^2)	230	230	230
Wing Span (ft)	34	34	34
Wing Mean Geometric Chord (ft)	7	7	7
Weight (lbs)	13,000	13,000	9,000
I_{xx_B} (slug ft^2)	28,000	28,000	6,000
I_{yy_B} (slug ft^2)	17,800	18,800	17,800
I_{zz_B} (slug ft^2)	47,000	47,000	25,000
I_{xz_B} (slug ft^2)	1,300	1,300	1,400
Steady State Coefficients			
C_{L_1}	1.64	.41	.28
C_{D_1}	.256	.0335	.0279
$C_{T_{X_1}}$	.256	.0335	.0279
C_{m_1}	0	0	0
$C_{m_{T_1}}$	0	0	0

Table C4 Stability and Control Derivatives for Airplane D (Cont.)

Longitudinal Derivatives	1	2	3
C_{m_u}	-.01	.05	.07
C_{m_α}	-.66	-.64	-.64
$C_{m_{\dot{\alpha}}}$	-5.0	-6.7	-6.7
C_{m_q}	-13.5	-15.5	-15.5
$C_{m_{T_u}}$	.006	-.003	-.003
$C_{m_{T_\alpha}}$	0	0	0
C_{L_u}	.04	.40	.28
C_{L_α}	5.04	5.84	5.84
$C_{L_{\dot{\alpha}}}$	1.6	2.2	2.2
C_{L_q}	4.1	4.7	4.7
C_{D_α}	1.06	.30	.22
C_{D_u}	0	.104	.104
$C_{T_{X_u}}$	0	0	0
$C_{L_{\delta_E}}$	.40	.46	.46
$C_{D_{\delta_E}}$	0	0	0
$C_{m_{\delta_E}}$	-.98	-1.24	-1.24

Table C4 Stability and Control Derivatives for Airplane D (Cont.)

Lateral-Directional Derivatives	1	2	3
C_{ℓ_β}	-.173	-.110	-.100
C_{ℓ_p}	-.39	-.45	-.45
C_{ℓ_r}	.45	.16	.14
$C_{\ell_{\delta_A}}$	.149	.178	.178
$C_{\ell_{\delta_R}}$	.014	.019	.021
C_{n_β}	.150	.127	.124
C_{n_p}	-.13	-.008	-.022
C_{n_r}	-.26	-.20	-.20
$C_{n_{\delta_A}}$	-.05	-.02	-.02
$C_{n_{\delta_R}}$	-.074	-.074	-.074
C_{y_β}	-.73	-.73	-.73
C_{y_p}	0	0	0
C_{y_r}	.4	.4	.4
$C_{y_{\delta_A}}$	0	0	0
$C_{y_{\delta_R}}$	.140	.140	.140

```
%LONGITUDINDAL DYNAMICS
%Learjet Model 24, sea level-power approach    <--fc1
%                  40,000 ft-max weight cruise <--fc2
%                  40,000 ft-low weight cruise <--fc3
%Roskam, J., 1979,
%Airplane Flight Dynamics and Automatic Flight Controls,
%Part I, pp. 616-642

format short e

%Enter flight condition, geometry, mass and MOI parameters.

g=32.2;                                 %gravity (ft/s^2)
theta0=[1.8 2.7 1.5]*pi/180;            %equilibrium pitch angle (deg)
rho=[.002378 .000588 .000588];          %density (slug/ft^3)
Uo=[170 677 677];                       %equilibrium speed (ft/s)
mass=[13000 13000 9000]/g;              %weight (lbs)
Ixx=[28000 28000 6000];                 %roll inertia (slug ft^2)
Iyy=[17800 18800 17800];                %pitch inertia (slug ft^2)
Izz=[47000 47000 25000];                %yaw inertia (slug ft^2)
Ixz=[1300 1300 1400];                   %cross product of inertia (slug ft^2)
S=[230 230 230];                        %wing area (ft^2)
b=[34 34 34];                           %wing span (ft)
cbar=[7 7 7];                           %mean geometric chord (ft)

%Enter steady-state coefficients.

CL1=[1.64 .41 .28];
CD1=[.256 .0335 .0279];
CTx1=[.256 .0335 .0279];
Cm1=[0 0 0];
CmT1=[0 0 0];

%Enter dimensionless stability and control derivatives.

Cmu=[-.01 .05 .07];
Cma=[-.66 -.64 -.64];
Cmad=[-5.0 -6.7 -6.7];
Cmq=[-13.5 -15.5 -15.5];
CmTu=[.006 -.003 -.003];
CmTa=[0 0 0];
CLu=[.04 .40 .28];
CLa=[5.04 5.84 5.84];
CLad=[1.6 2.2 2.2];
CLq=[4.1 4.7 4.7];
CDa=[1.06 .30 .22];
CDu=[0 .104 .104];
CTxu=[0 0 0];
CLde=[.40 .46 .46];
CDde=[0 0 0];
Cmde=[-.98 -1.24 -1.24];

CDad=[0 0 0];  %No numbers in Roskam
CDq=[0 0 0];   %No numbers in Roskam

%Compute dimensioned stability and control derivatives

qbar=0.5*rho.*Uo.^2;
```

```
Xu =-qbar.*S.*(CDu+2*CD1)./(mass.*Uo);
XTu= qbar.*S.*(CTxu+2*CTx1)./(mass.*Uo);
Xa =-qbar.*S.*(CDa-CL1)./mass;
Xde=-qbar.*S.*CDde./mass;
Zu =-qbar.*S.*(CLu+2*CL1)./(mass.*Uo);
Za =-qbar.*S.*(CLa+CD1)./mass;
Zad=-qbar.*S.*CLad.*cbar./(2*mass.*Uo);
Zq =-qbar.*S.*CLq.*cbar./(2*mass.*Uo);
Zde=-qbar.*S.*CLde./mass;
Mu = qbar.*S.*cbar.*(Cmu+2*Cm1)./(Iyy.*Uo);
MTu= qbar.*S.*cbar.*(CmTu+2*CmT1)./(Iyy.*Uo);
Ma = qbar.*S.*cbar.*Cma./Iyy;
MTa= qbar.*S.*cbar.*CmTa./Iyy;
Mad= qbar.*S.*(cbar.^2).*Cmad./(2*Iyy.*Uo);
Mq = qbar.*S.*(cbar.^2).*Cmq./(2*Iyy.*Uo);
Mde= qbar.*S.*cbar.*Cmde./Iyy;

%Compute dynamics for flight condition 1 in state-space form.

Afc1=[
      Xu(1)+XTu(1) Xa(1)/Uo(1)                 0
-g*cos(theta0(1))
      Zu(1)        Za(1)/Uo(1)                 Uo(1)+Zq(1)
-g*sin(theta0(1))
      Mu(1)+MTu(1) Ma(1)/Uo(1)+MTa(1)/Uo(1) Mq(1)          0
      0            0                          1            0
     ];

Bfc1=[Xde(1);Zde(1);Mde(1);0];

Efc1=[
      1 0               0 0
      0 1-Zad(1)/Uo(1)  0 0
      0  -Mad(1)/Uo(1)  1 0
      0 0               0 1];

Afc1=Efc1\Afc1;
Bfc1=Efc1\Bfc1;

%Compute pitch angle
%        angle of attack
%        forward speed
%        vertical acceleration
%output matrix and direct input matrix.

Cfc1=[
      0   0        0    1
      0   1/Uo(1)  0    0
      1   0        0    0
      Afc1(2,:)-[0 0 Uo(1) 0]
     ];
Dfc1=0*Cfc1*Bfc1;
Dfc1(4,1)=Bfc1(2,1);

%Compute dynamics for flight condition 2 in state-space form.

Afc2=[
```

```
      Xu(2)+XTu(2)  Xa(2)/Uo(2)                0
-g*cos(theta0(2))
      Zu(2)         Za(2)/Uo(2)                Uo(2)+Zq(2)
-g*sin(theta0(2))
      Mu(2)+MTu(2)  Ma(2)/Uo(2)+MTa(2)/Uo(2)  Mq(2)          0
      0             0                          1             0
     ];

Bfc2=[Xde(2);Zde(2);Mde(2);0];

Efc2=[
      1 0               0 0
      0 1-Zad(2)/Uo(2)  0 0
      0  -Mad(2)/Uo(2)  1 0
      0 0               0 1
     ];

Afc2=Efc2\Afc2;
Bfc2=Efc2\Bfc2;

%Compute pitch angle
%         angle of attack
%         forward speed
%         vertical acceleration
%output matrix and direct input matrix.

Cfc2=[
     0   0         0    1
     0   1/Uo(2)   0    0
     1   0         0    0
     Afc2(2,:)-[0 0 Uo(2) 0]
    ];
Dfc2=0*Cfc2*Bfc2;
Dfc2(4,1)=Bfc2(2,1);

%Compute dynamics for flight condition 3 in state-space form.

Afc3=[
      Xu(3)+XTu(3)  Xa(3)/Uo(3)                0
-g*cos(theta0(3))
      Zu(3)         Za(3)/Uo(3)                Uo(3)+Zq(3)
-g*sin(theta0(3))
      Mu(3)+MTu(3)  Ma(3)/Uo(3)+MTa(3)/Uo(3)  Mq(3)          0
      0             0                          1             0
     ];

Bfc3=[Xde(3);Zde(3);Mde(3);0];

Efc3=[
      1 0               0 0
      0 1-Zad(3)/Uo(3)  0 0
      0  -Mad(3)/Uo(3)  1 0
      0 0               0 1
     ];

Afc3=Efc3\Afc3;
Bfc3=Efc3\Bfc3;
```

```
%Compute pitch angle
%         angle of attack
%         forward speed
%         vertical acceleration
%output matrix and direct input matrix.

Cfc3=[
     0   0         0    1
     0   1/Uo(3)   0    0
     1   0         0    0
     Afc3(2,:)-[0 0 Uo(3) 0]
    ];
Dfc3=0*Cfc3*Bfc3;
Dfc3(4,1)=Bfc3(2,1);
```

```
%LONGITUDINAL DYNAMICS
%Learjet Model 24, sea level--power approach    <--fc1
%                  40,000 ft--max weight cruise <--fc2
%                  40,000 ft--low weight cruise <--fc3
%Roskam, J., 1979,
%Airplane Flight Dynamics and Automatic Flight Controls,
%Part I, pp. 616-642

EIGENVALUES

evfc1 =
 -9.0759e-01+  1.3200e+00i
 -9.0759e-01-  1.3200e+00i
  1.4080e-02+  2.3850e-01i
  1.4080e-02-  2.3850e-01i


evfc2 =
 -9.9457e-01+  2.6413e+00i
 -9.9457e-01-  2.6413e+00i
 -5.2956e-03+  9.0481e-02i
 -5.2956e-03-  9.0481e-02i


evfc3 =
 -1.1777e+00+  2.7009e+00i
 -1.1777e+00-  2.7009e+00i
 -8.6035e-03+  1.0032e-01i
 -8.6035e-03-  1.0032e-01i


NATURAL FREQUENCIES
   1.6019e+00   2.8223e+00   2.9465e+00
   1.6019e+00   2.8223e+00   2.9465e+00
   2.3891e-01   9.0636e-02   1.0069e-01
   2.3891e-01   9.0636e-02   1.0069e-01


DAMPING RATIOS
   5.6657e-01   3.5239e-01   3.9971e-01
   5.6657e-01   3.5239e-01   3.9971e-01
  -5.8933e-02   5.8427e-02   8.5446e-02
  -5.8933e-02   5.8427e-02   8.5446e-02
```

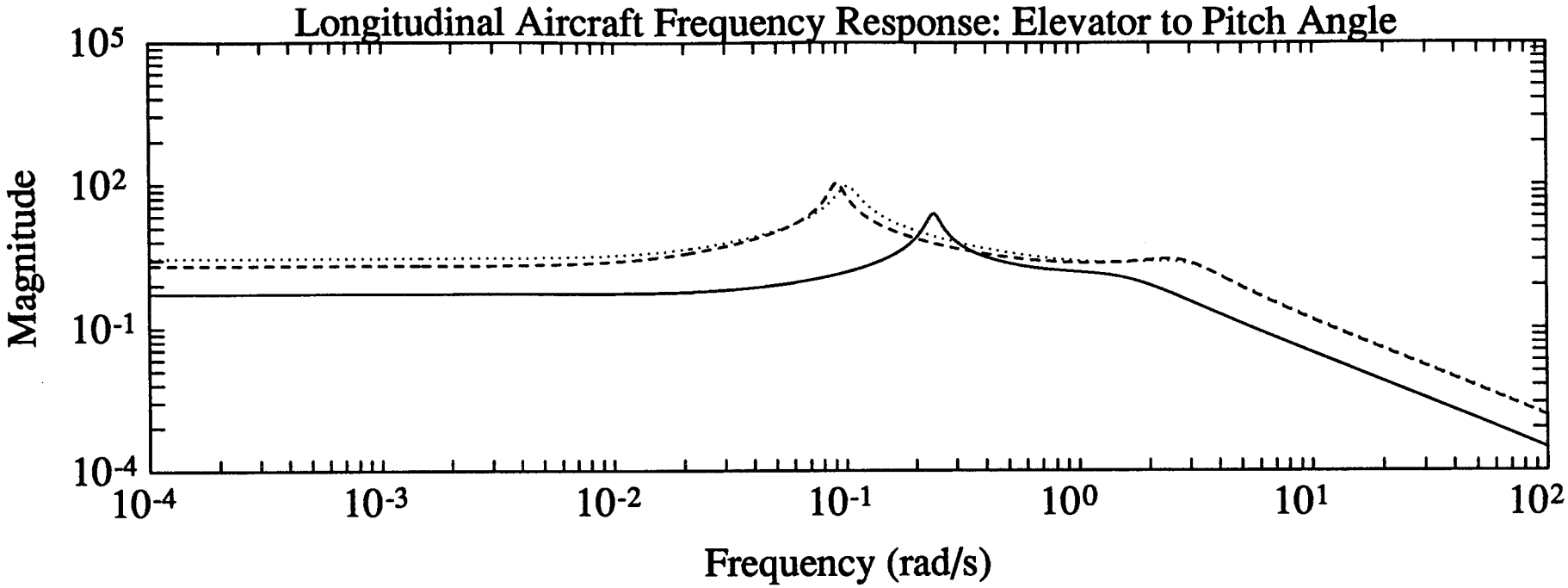
Longitudinal Aircraft Frequency Response: Elevator to Pitch Angle
Magnitude
10^5
10^2
10^-1
10^-4
10^-4
10^-3
10^-2
10^-1
10^0
10^1
10^2
Frequency (rad/s)

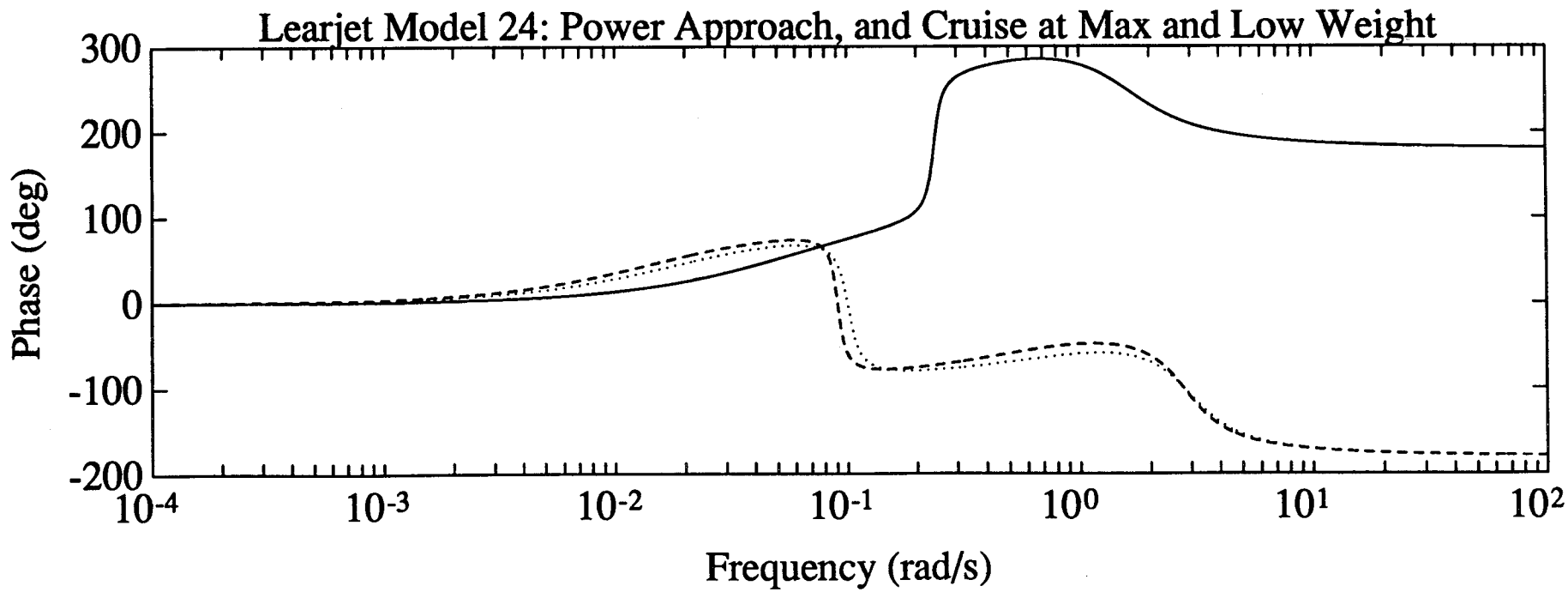
Learjet Model 24: Power Approach, and Cruise at Max and Low Weight
Phase (deg)
300
200
100
0
-100
-200
10^-4
10^-3
10^-2
10^-1
10^0
10^1
10^2
Frequency (rad/s)

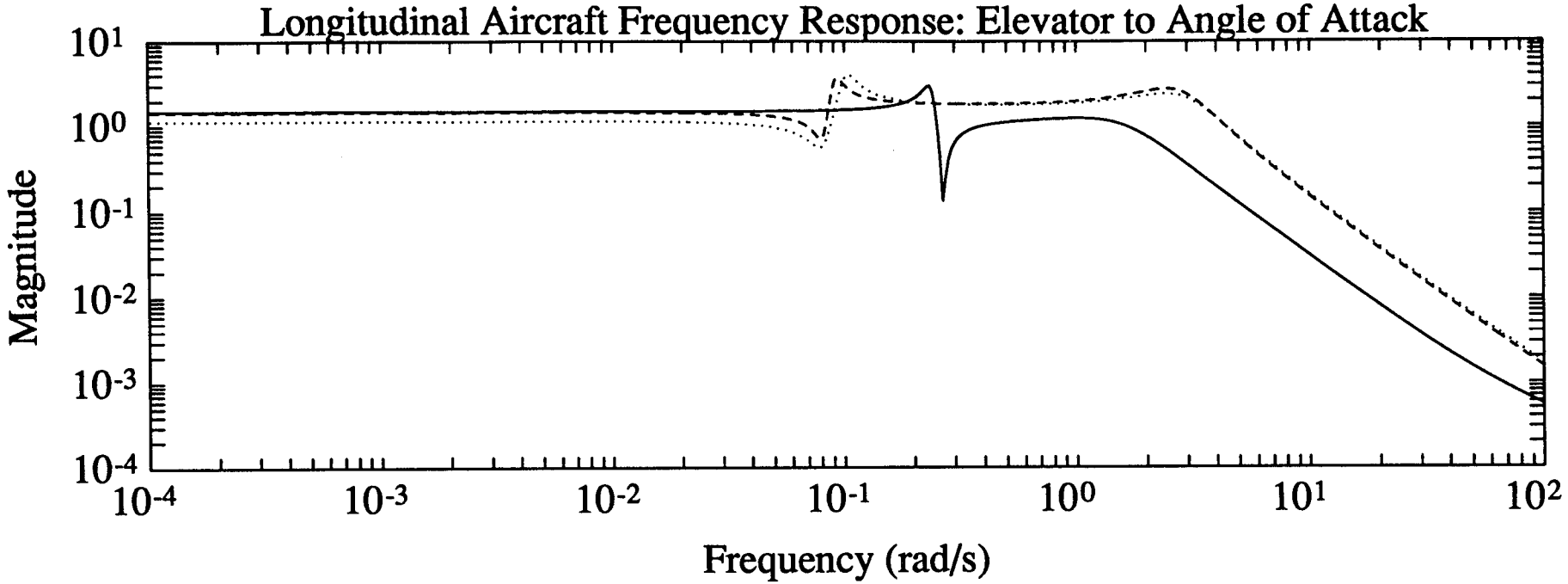
Longitudinal Aircraft Frequency Response: Elevator to Angle of Attack
Magnitude
10^{1}
10^{0}
10^{-1}
10^{-2}
10^{-3}
10^{-4}
10^{-4}
10^{-3}
10^{-2}
10^{-1}
10^{0}
10^{1}
10^{2}
Frequency (rad/s)

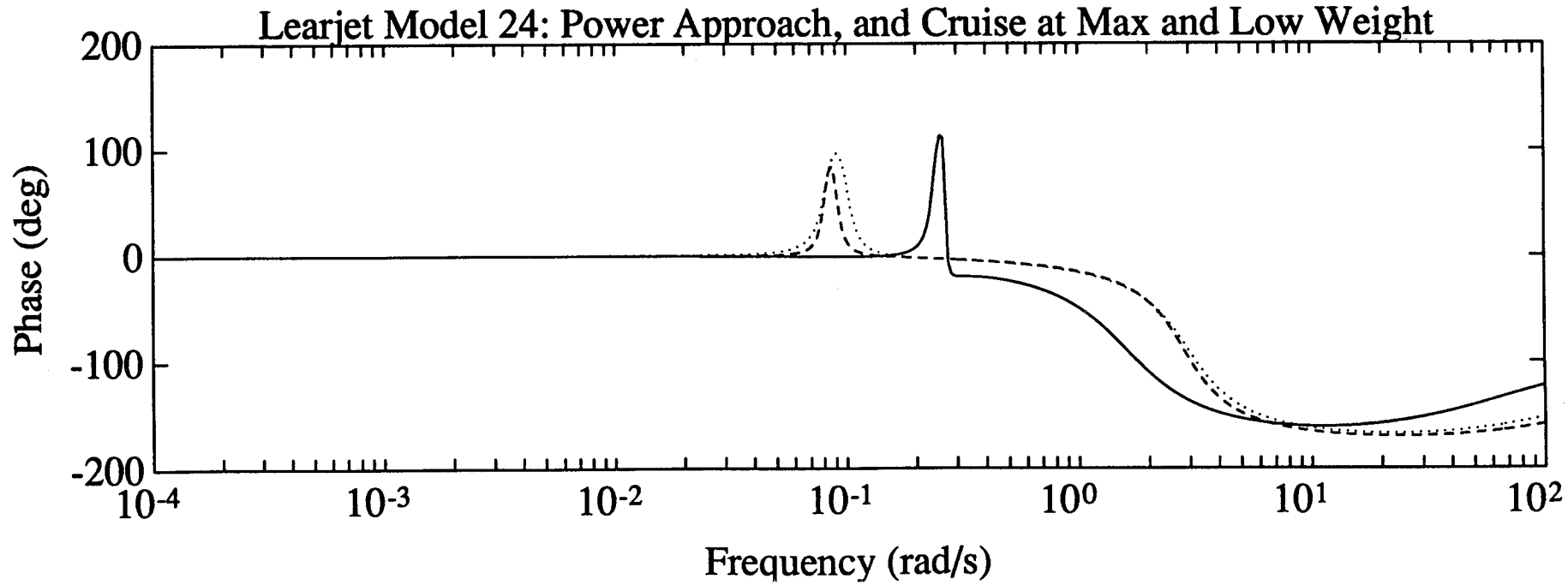
Learjet Model 24: Power Approach, and Cruise at Max and Low Weight
Phase (deg)
200
100
0
-100
-200
10^{-4}
10^{-3}
10^{-2}
10^{-1}
10^{0}
10^{1}
10^{2}
Frequency (rad/s)

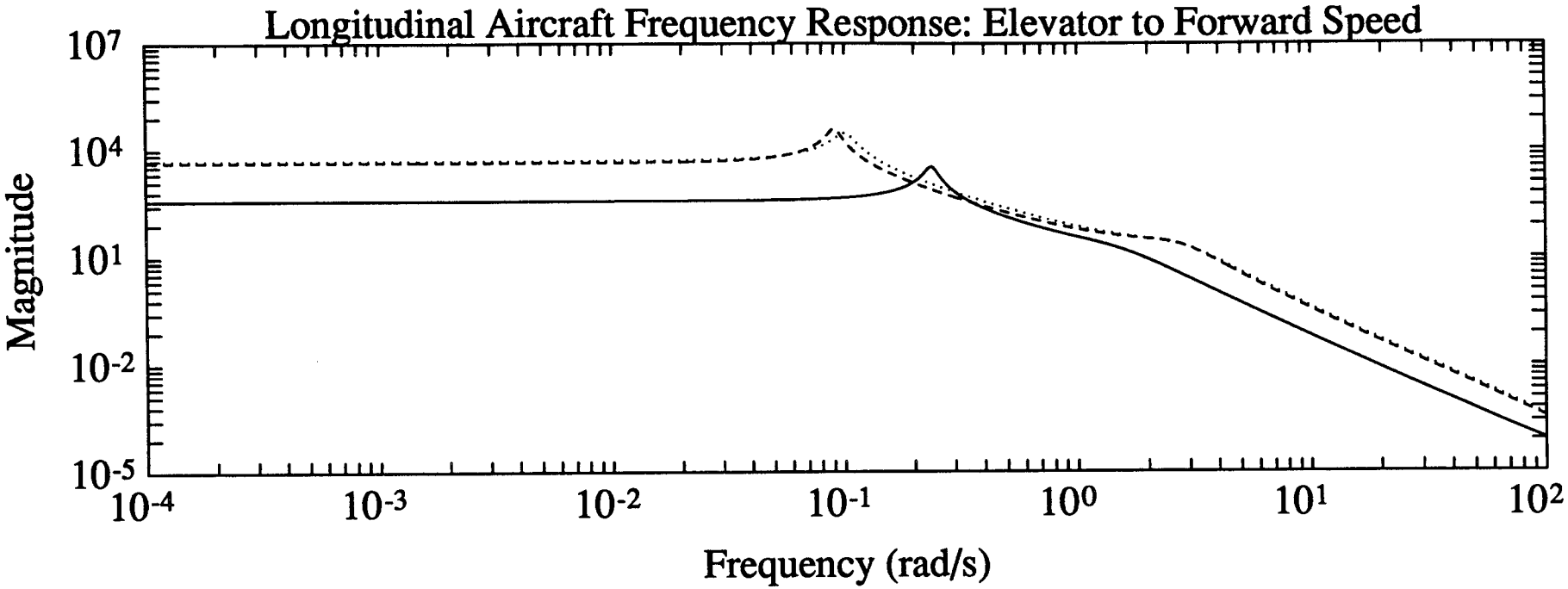
Longitudinal Aircraft Frequency Response: Elevator to Forward Speed
Magnitude
10^7
10^4
10^1
10^-2
10^-5
10^-4
10^-3
10^-2
10^-1
10^0
10^1
10^2
Frequency (rad/s)

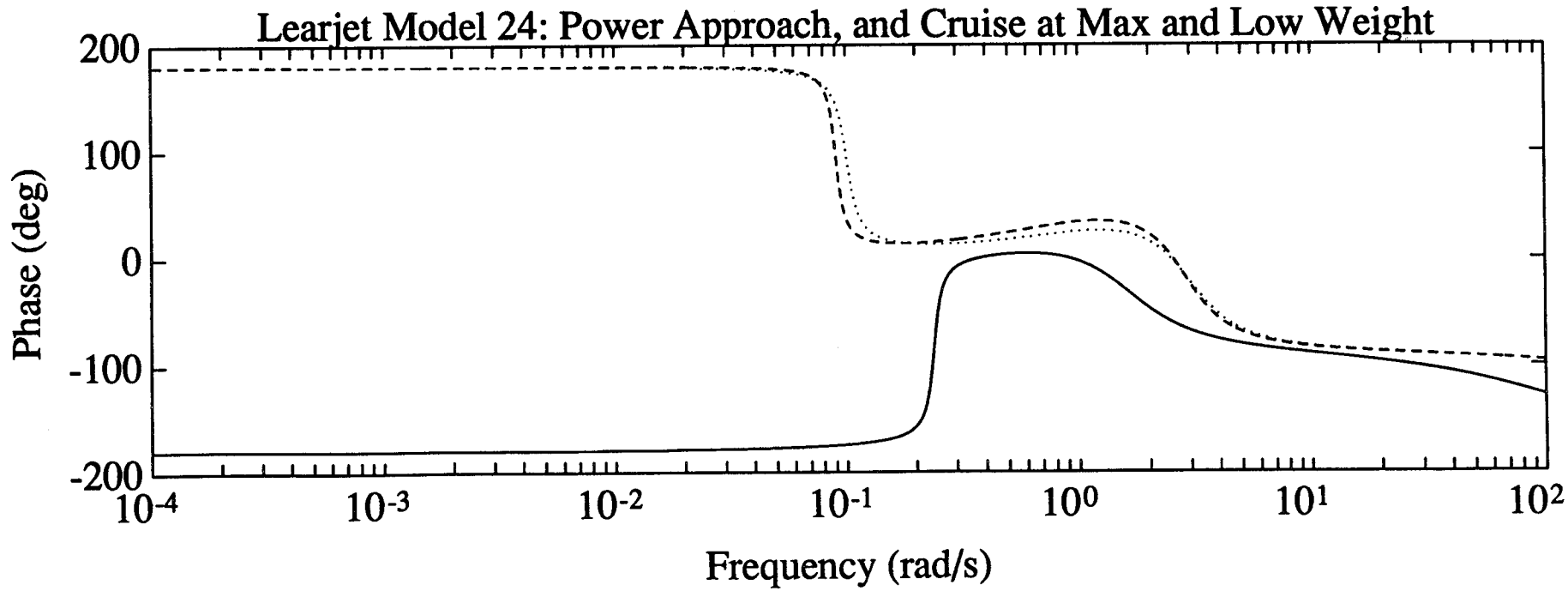
Learjet Model 24: Power Approach, and Cruise at Max and Low Weight
Phase (deg)
200
100
0
-100
-200
10^-4
10^-3
10^-2
10^-1
10^0
10^1
10^2
Frequency (rad/s)

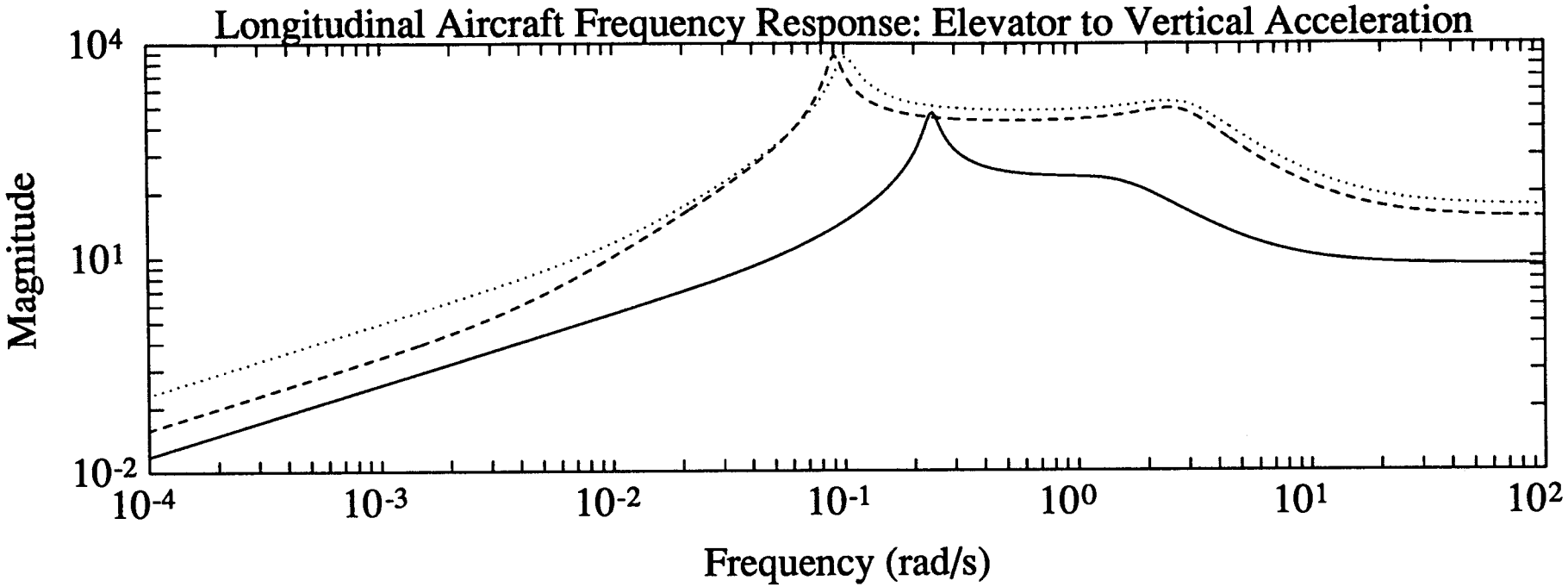
Longitudinal Aircraft Frequency Response: Elevator to Vertical Acceleration
Magnitude
10^4
10^1
10^-2
10^-4
10^-3
10^-2
10^-1
10^0
10^1
10^2
Frequency (rad/s)

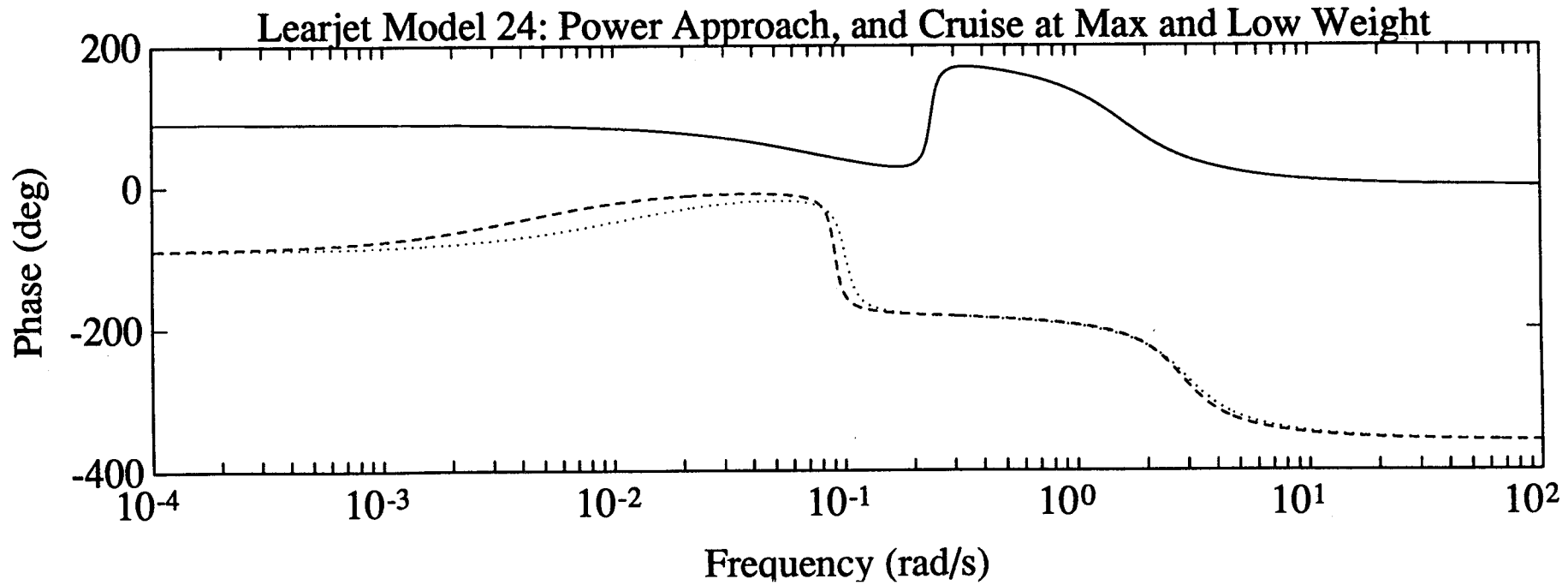
Learjet Model 24: Power Approach, and Cruise at Max and Low Weight
Phase (deg)
200
0
-200
-400
10^-4
10^-3
10^-2
10^-1
10^0
10^1
10^2
Frequency (rad/s)

```
%LATERAL DYNAMICS
%Learjet Model 24, sea level-power approach    <--fc1
%                  40,000 ft-max weight cruise <--fc2
%                  40,000 ft-low weight cruise <--fc3
%Roskam, J., 1979,
%Airplane Flight Dynamics and Automatic Flight Controls,
%Part I, pp. 616-642

format short e

%Enter flight condition, geometry, mass and MOI parameters.

g=32.2;                                 %gravity (ft/s^2)
theta0=[1.8 2.7 1.5]*pi/180;            %equilibrium pitch angle (deg)
rho=[.002378 .000588 .000588];          %density (slug/ft^3)
Uo=[170 677 677];                       %equilibrium speed (ft/s)
mass=[13000 13000 9000]/g;              %weight (lbs)
Ixx=[28000 28000 6000];                 %roll inertia (slug ft^2)
Izz=[47000 47000 25000];                %yaw inertia (slug ft^2)
Ixz=[1300 1300 1400];                   %cross product of inertia (slug ft^2)
S=[230 230 230];                        %wing area (ft^2)
b=[34 34 34];                           %wing span (ft)
cbar=[7 7 7];                           %mean geometric chord (ft)

%Transform relevant inertias from body axis to stability axis.

for ifc=1:3,
  ang=theta0(ifc);
  Tba2sa=[
          cos(ang)^2     sin(ang)^2    -sin(2*ang)
          sin(ang)^2     cos(ang)^2     sin(2*ang)
          sin(2*ang)/2 -sin(2*ang)/2   cos(2*ang)
         ];
  Isa=Tba2sa*[Ixx(ifc);Izz(ifc);Ixz(ifc)];
  Ixx(ifc)=Isa(1);
  Izz(ifc)=Isa(2);
  Ixz(ifc)=Isa(3);
end;

%Enter steady-state coefficients.

CL1=[1.64 .41 .28];
CD1=[.256 .0335 .0279];
CTx1=[.256 .0335 .0279];
Cm1=[0 0 0];
CmT1=[0 0 0];

%Enter dimensionless stability and control derivatives.

Clb=[-.173 -.110 -.100];
Clp=[-.39 -.45 -.45];
Clr=[.45 .16 .14];
Clda=[.149 .178 .178];
Cldr=[.014 .019 .021];

Cnb=[.150 .127 .124];
Cnp=[-.13 -.008 -.022];
Cnr=[-.26 -.20 -.20];
```

```
Cnda=[-.05 -.02 -.02];
Cndr=[-.074 -.074 -.074];

Cyb=[-.73 -.73 -.73];
Cyp=[0 0 0];
Cyr=[.4 .4 .4];
Cyda=[0 0 0];
Cydr=[.140 .140 .140];

CnTb=[0 0 0];  %No numbers in Roskam

%Compute dimensioned stability and control derivatives

qbar=0.5*rho.*Uo.^2;
Yb = qbar.*S.*Cyb./mass;
Yp = qbar.*S.*b.*Cyp./(2*mass.*Uo);
Yr = qbar.*S.*b.*Cyr./(2*mass.*Uo);
Yda= qbar.*S.*Cyda./mass;
Ydr= qbar.*S.*Cydr./mass;

Lb = qbar.*S.*b.*Clb./Ixx;
Lp = qbar.*S.*(b.^2).*Clp./(2*Ixx.*Uo);
Lr = qbar.*S.*(b.^2).*Clr./(2*Ixx.*Uo);
Lda= qbar.*S.*b.*Clda./Ixx;
Ldr= qbar.*S.*b.*Cldr./Ixx;

Nb = qbar.*S.*b.*Cnb./Izz;
NTb= qbar.*S.*b.*CnTb./Izz;
Np = qbar.*S.*(b.^2).*Cnp./(2*Izz.*Uo);
Nr = qbar.*S.*(b.^2).*Cnr./(2*Izz.*Uo);
Nda= qbar.*S.*b.*Cnda./Izz;
Ndr= qbar.*S.*b.*Cndr./Izz;

%Compute dynamics for flight condition 1 in state-space form.

Afc1=[
      Yb(1)/Uo(1)          Yp(1) Yr(1)-Uo(1) g*cos(theta0(1))
g*sin(theta0(1))
      Lb(1)/Uo(1)          Lp(1) Lr(1)       0                0
      (Nb(1)+NTb(1))/Uo(1) Np(1) Nr(1)       0                0
      0                    1     0           0                0
      0                    0     1           0                0
     ];

Bfc1=[
      Yda(1) Ydr(1)
      Lda(1) Ldr(1)
      Nda(1) Ndr(1)
      0*ones(2,2)
     ];

Efc1=[
      1  0              0              0 0
      0  1             -Ixz(1)/Ixx(1)  0 0
      0 -Ixz(1)/Izz(1)  1              0 0
      0  0              0              1 0
      0  0              0              0 1
     ];
```

```
Afc1=Efc1\Afc1;
Bfc1=Efc1\Bfc1;

%Compute sideslip angle
%        roll angle
%        yaw angle
%        lateral acceleration
%output matrix and direct input matrix.

Cfc1=[
      1/Uo(1)   0   0   0   0
      0         0   0   1   0
      0         0   0   0   1
      Afc1(1,:)+[0 0 Uo(1) -g 0]
     ];
Dfc1=0*Cfc1*Bfc1;
Dfc1(4,:)=Bfc1(1,:);

%Compute dynamics for flight condition 2 in state-space form.

Afc2=[
      Yb(2)/Uo(2)           Yp(2)  Yr(2)-Uo(2)  g*cos(theta0(2))
g*sin(theta0(2))
      Lb(2)/Uo(2)           Lp(2)  Lr(2)        0                  0
      (Nb(2)+NTb(2))/Uo(2)  Np(2)  Nr(2)        0                  0
      0                     1      0            0                  0
      0                     0      1            0                  0
     ];

Bfc2=[
      Yda(2)  Ydr(2)
      Lda(2)  Ldr(2)
      Nda(2)  Ndr(2)
      0*ones(2,2)
     ];

Efc2=[
      1   0              0               0 0
      0   1             -Ixz(2)/Ixx(2)   0 0
      0  -Ixz(2)/Izz(2)  1               0 0
      0   0              0               1 0
      0   0              0               0 1
     ];

Afc2=Efc2\Afc2;
Bfc2=Efc2\Bfc2;

%Compute sideslip angle
%        roll angle
%        yaw angle
%        lateral acceleration
%output matrix and direct input matrix.

Cfc2=[
      1/Uo(2)   0   0   0   0
      0         0   0   1   0
      0         0   0   0   1
```

```
      Afc2(1,:)+[0 0 Uo(2) -g 0]
     ];
Dfc2=0*Cfc2*Bfc2;
Dfc2(4,:)=Bfc2(1,:);

%Compute dynamics for flight condition 3 in state-space form.

Afc3=[
      Yb(3)/Uo(3)           Yp(3) Yr(3)-Uo(3) g*cos(theta0(3))
g*sin(theta0(3))
      Lb(3)/Uo(3)           Lp(3) Lr(3)       0                 0
      (Nb(3)+NTb(3))/Uo(3) Np(3) Nr(3)       0                 0
      0                     1     0           0                 0
      0                     0     1           0                 0
     ];

Bfc3=[
      Yda(3) Ydr(3)
      Lda(3) Ldr(3)
      Nda(3) Ndr(3)
      0*ones(2,2)
     ];

Efc3=[
      1  0              0              0 0
      0  1             -Ixz(3)/Ixx(3) 0 0
      0 -Ixz(3)/Izz(3) 1              0 0
      0  0              0              1 0
      0  0              0              0 1
     ];

Afc3=Efc3\Afc3;
Bfc3=Efc3\Bfc3;

%Compute sideslip angle
%        roll angle
%        yaw angle
%        lateral acceleration
%output matrix and direct input matrix.

Cfc3=[
      1/Uo(3)  0  0  0  0
      0        0  0  1  0
      0        0  0  0  1
      Afc3(1,:)+[0 0 Uo(3) -g 0]
     ];
Dfc3=0*Cfc3*Bfc3;
Dfc3(4,:)=Bfc3(1,:);
```

```
%LATERAL DYNAMICS
%Learjet Model 24, sea level-power approach     <--fc1
%                  40,000 ft-max weight cruise <--fc2
%                  40,000 ft-low weight cruise <--fc3
%Roskam, J., 1979,
%Airplane Flight Dynamics and Automatic Flight Controls,
%Part I, pp. 616-642

EIGENVALUES

evfc1 =
            0
  5.5832e-02+  1.0288e+00i
  5.5832e-02-  1.0288e+00i
 -7.4454e-01
  2.9636e-02

evfc2 =
            0
 -5.0232e-01
 -1.1878e-03
 -5.8493e-02+  1.6836e+00i
 -5.8493e-02-  1.6836e+00i

evfc3 =
            0
 -2.2733e+00
 -2.6623e-02+  2.2741e+00i
 -2.6623e-02-  2.2741e+00i
 -2.0106e-03

NATURAL FREQUENCIES
             0             0             0
   1.0303e+00   5.0232e-01   2.2733e+00
   1.0303e+00   1.1878e-03   2.2743e+00
   7.4454e-01   1.6846e+00   2.2743e+00
   2.9636e-02   1.6846e+00   2.0106e-03

DAMPING RATIOS
           NaN           NaN           NaN
  -5.4190e-02   1.0000e+00   1.0000e+00
  -5.4190e-02   1.0000e+00   1.1706e-02
   1.0000e+00   3.4722e-02   1.1706e-02
  -1.0000e+00   3.4722e-02   1.0000e+00
```

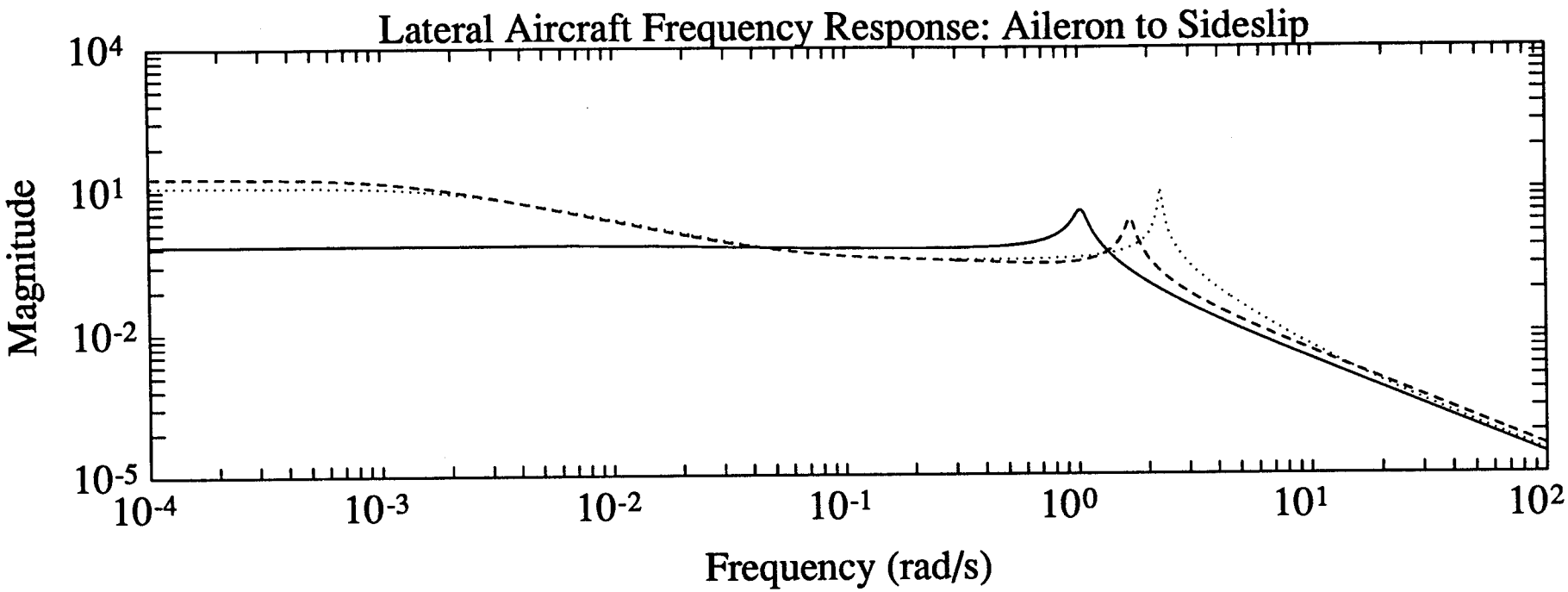
Lateral Aircraft Frequency Response: Aileron to Sideslip
Magnitude
10^4
10^1
10^-2
10^-5
10^-4
10^-3
10^-2
10^-1
10^0
10^1
10^2
Frequency (rad/s)

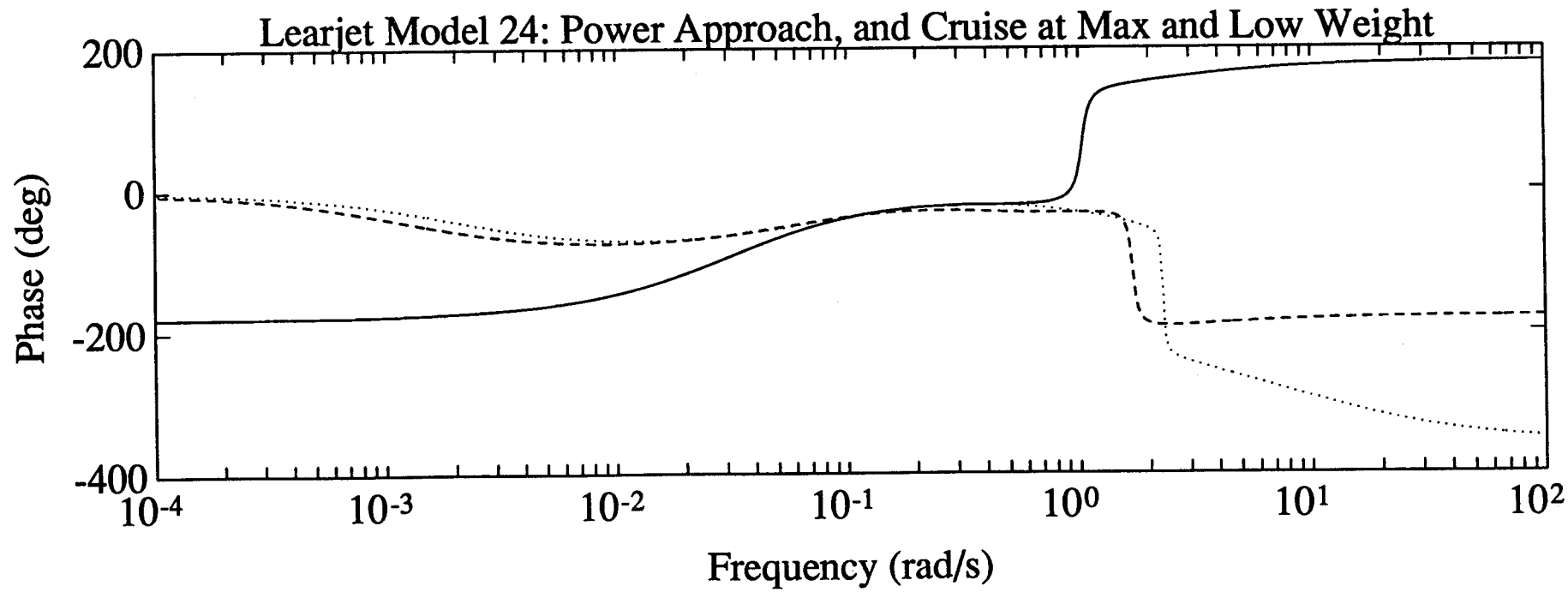
Learjet Model 24: Power Approach, and Cruise at Max and Low Weight
Phase (deg)
200
0
-200
-400
10^-4
10^-3
10^-2
10^-1
10^0
10^1
10^2
Frequency (rad/s)

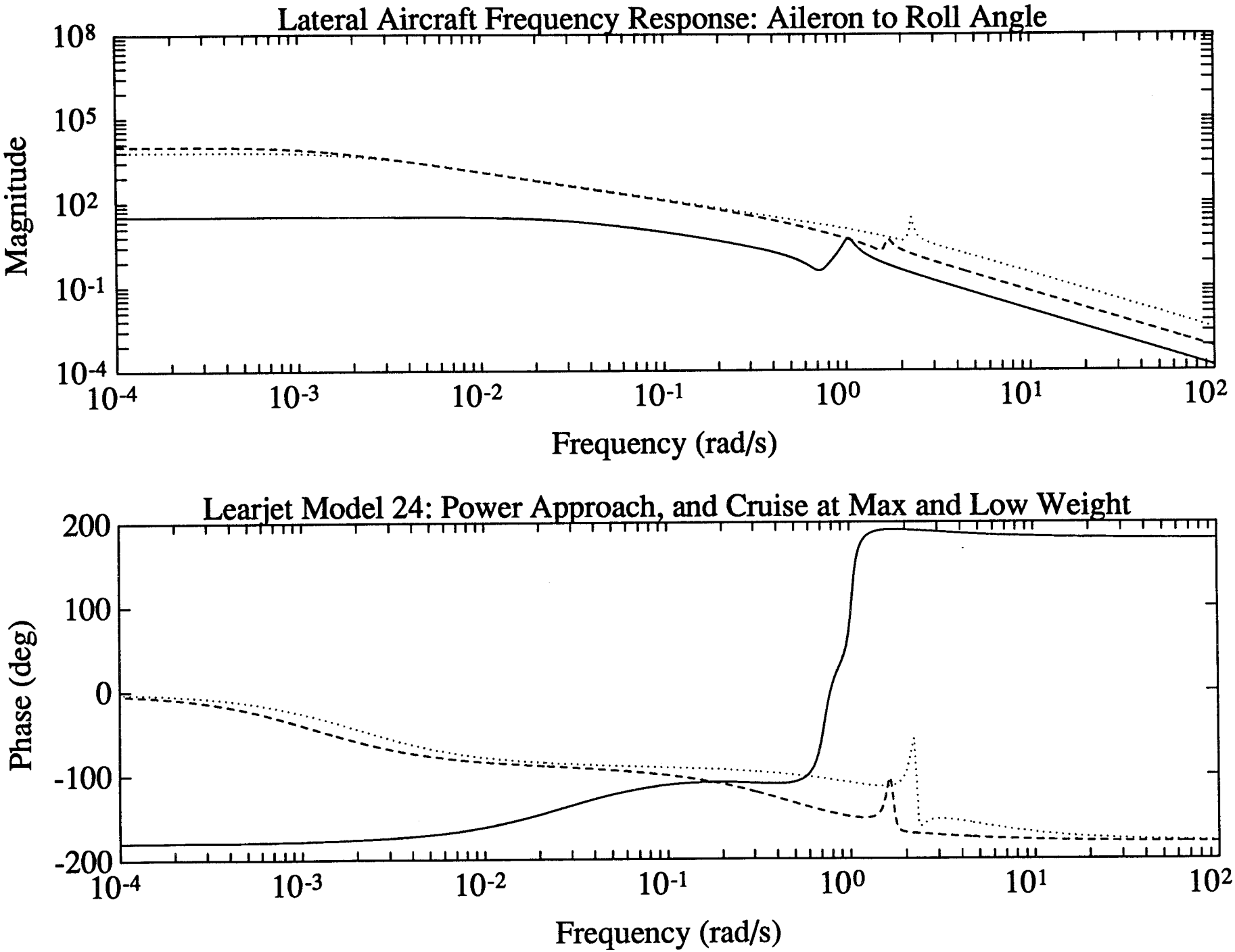
Lateral Aircraft Frequency Response: Aileron to Roll Angle
Magnitude
10^8
10^5
10^2
10^-1
10^-4
10^-4
10^-3
10^-2
10^-1
10^0
10^1
10^2
Frequency (rad/s)
Learjet Model 24: Power Approach, and Cruise at Max and Low Weight
Phase (deg)
200
100
0
-100
-200
10^-4
10^-3
10^-2
10^-1
10^0
10^1
10^2
Frequency (rad/s)

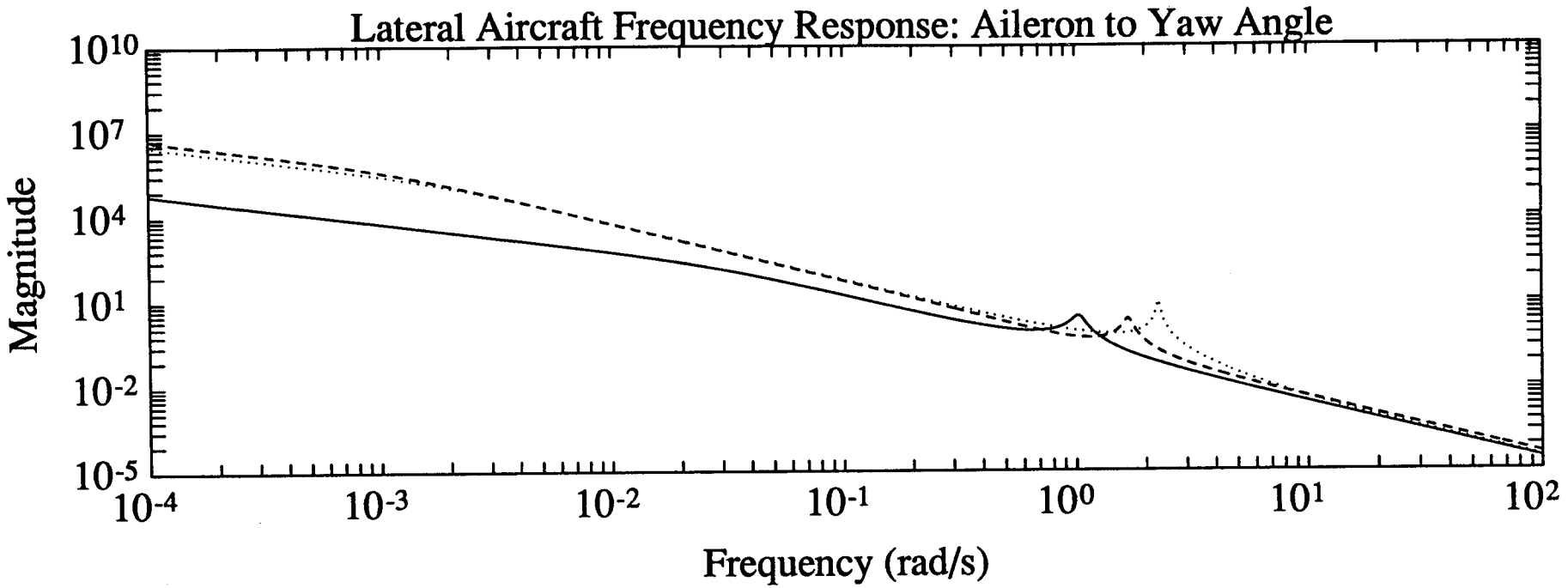
Lateral Aircraft Frequency Response: Aileron to Yaw Angle
Magnitude
10^10
10^7
10^4
10^1
10^-2
10^-5
10^-4
10^-3
10^-2
10^-1
10^0
10^1
10^2
Frequency (rad/s)

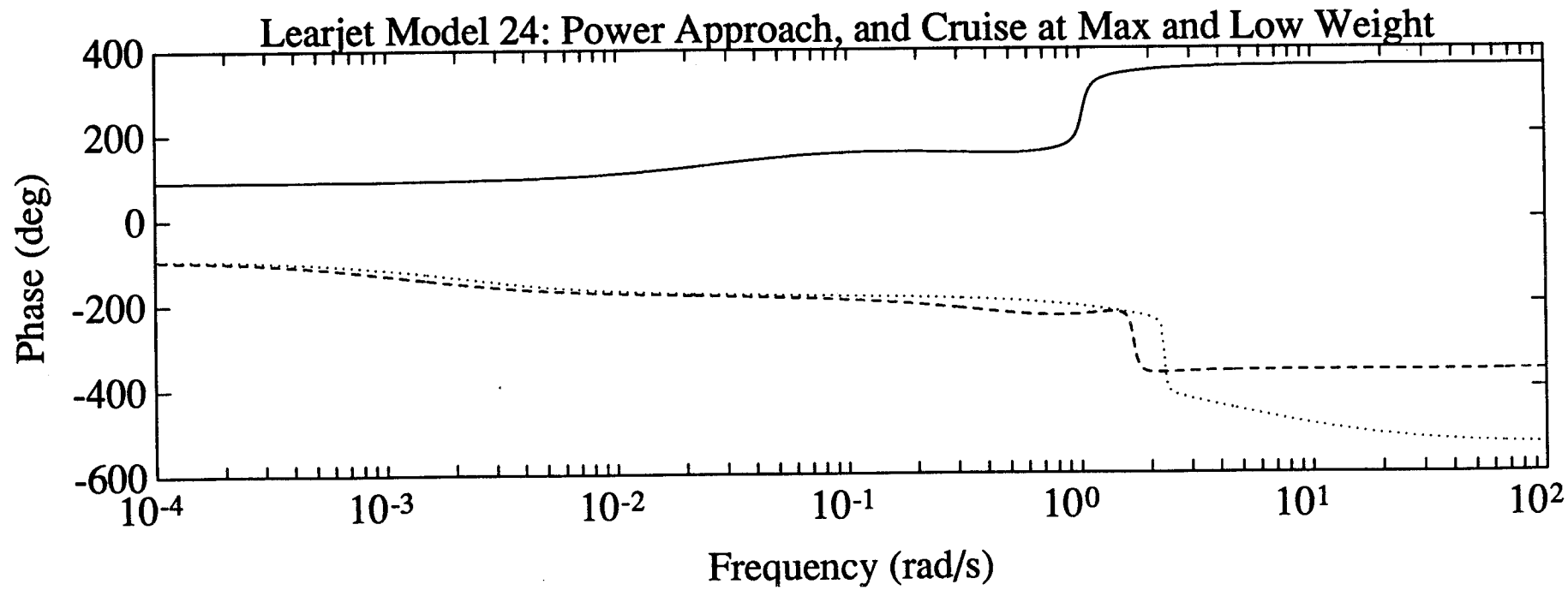
Learjet Model 24: Power Approach, and Cruise at Max and Low Weight
Phase (deg)
400
200
0
-200
-400
-600
10^-4
10^-3
10^-2
10^-1
10^0
10^1
10^2
Frequency (rad/s)

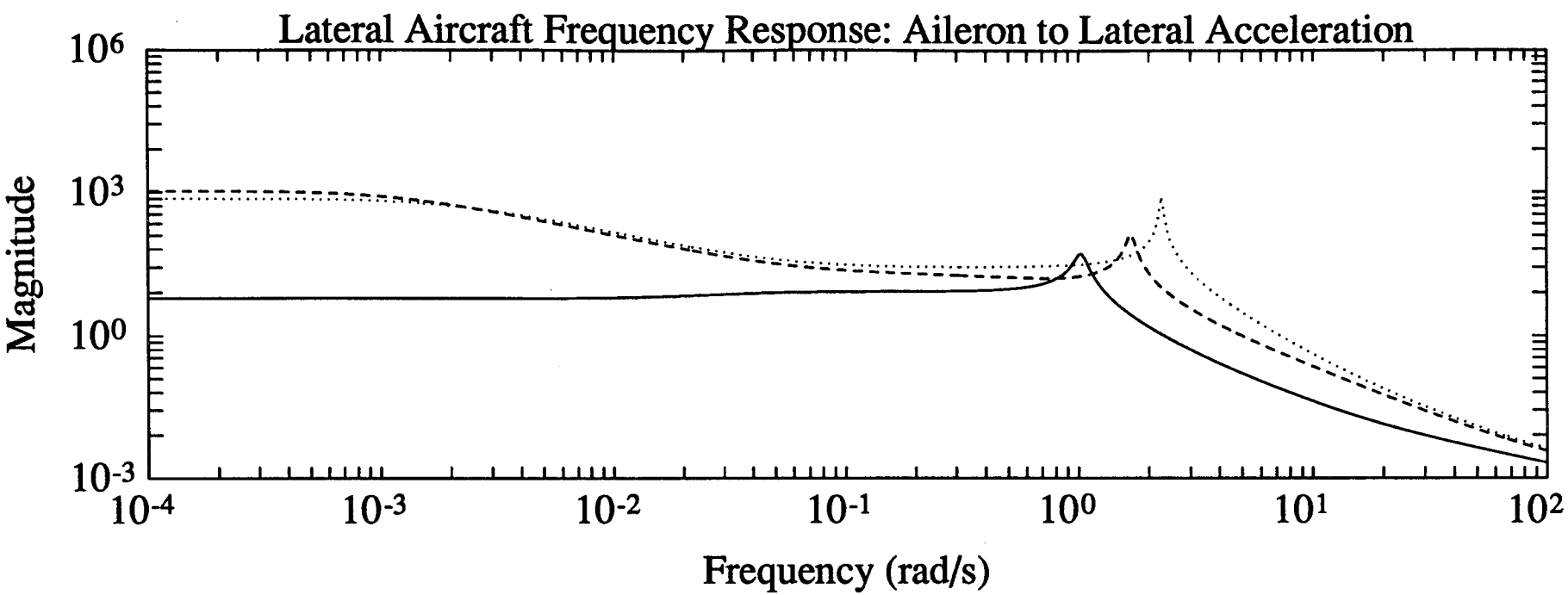
Lateral Aircraft Frequency Response: Aileron to Lateral Acceleration
Magnitude
10^6
10^3
10^0
10^-3
10^-4
10^-3
10^-2
10^-1
10^0
10^1
10^2
Frequency (rad/s)

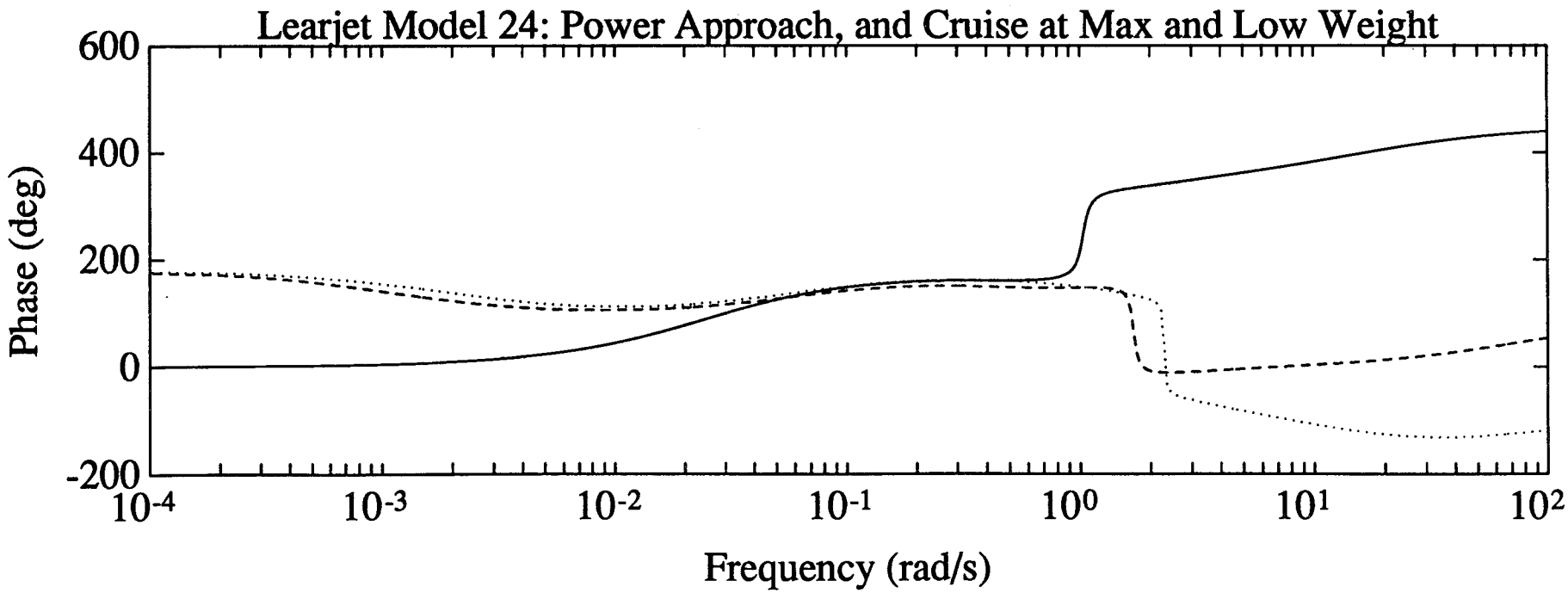
Learjet Model 24: Power Approach, and Cruise at Max and Low Weight
Phase (deg)
600
400
200
0
-200
10^-4
10^-3
10^-2
10^-1
10^0
10^1
10^2
Frequency (rad/s)

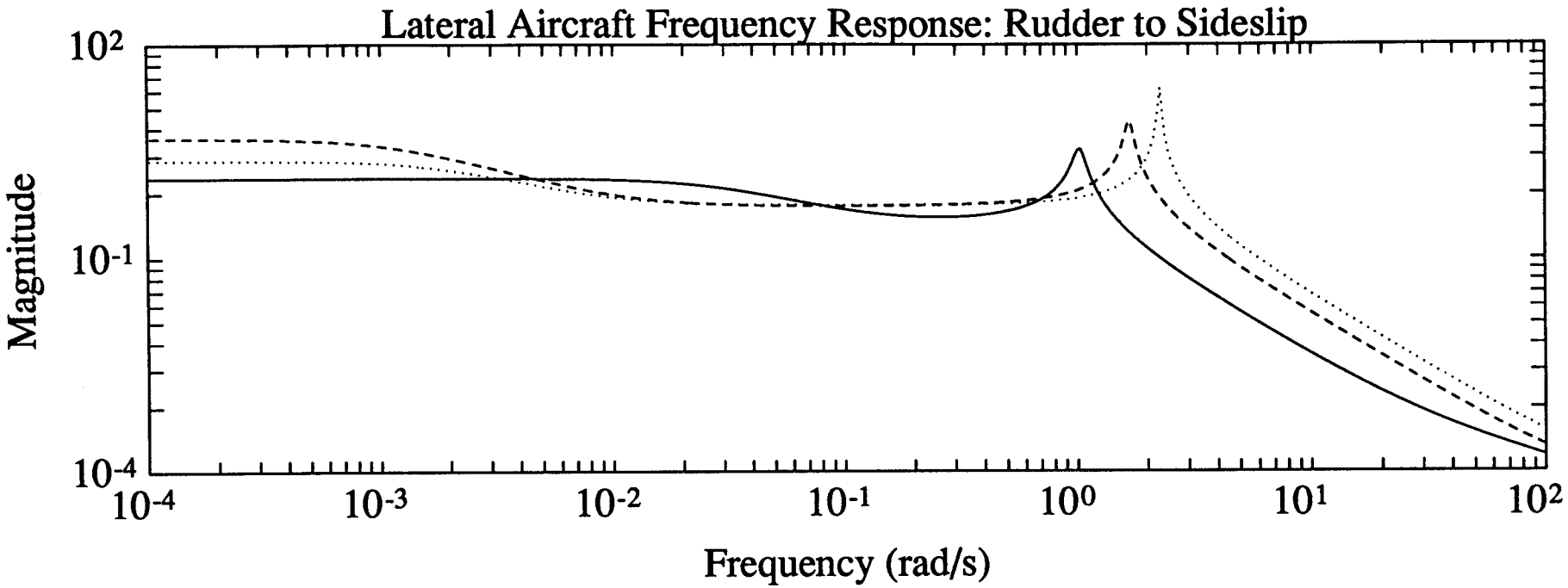
Lateral Aircraft Frequency Response: Rudder to Sideslip
Magnitude
10^{2}
10^{-1}
10^{-4}
10^{-4} 10^{-3} 10^{-2} 10^{-1} 10^{0} 10^{1} 10^{2}
Frequency (rad/s)

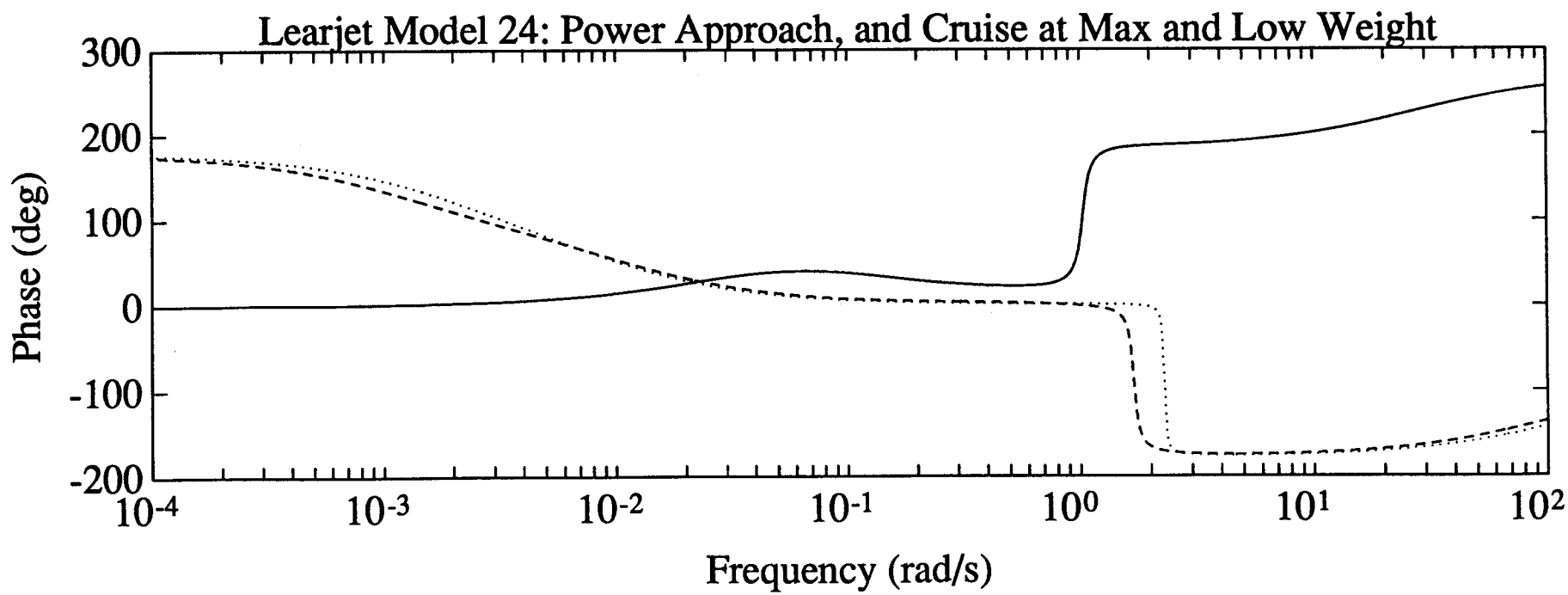
Learjet Model 24: Power Approach, and Cruise at Max and Low Weight
Phase (deg)
300
200
100
0
-100
-200
10^{-4} 10^{-3} 10^{-2} 10^{-1} 10^{0} 10^{1} 10^{2}
Frequency (rad/s)

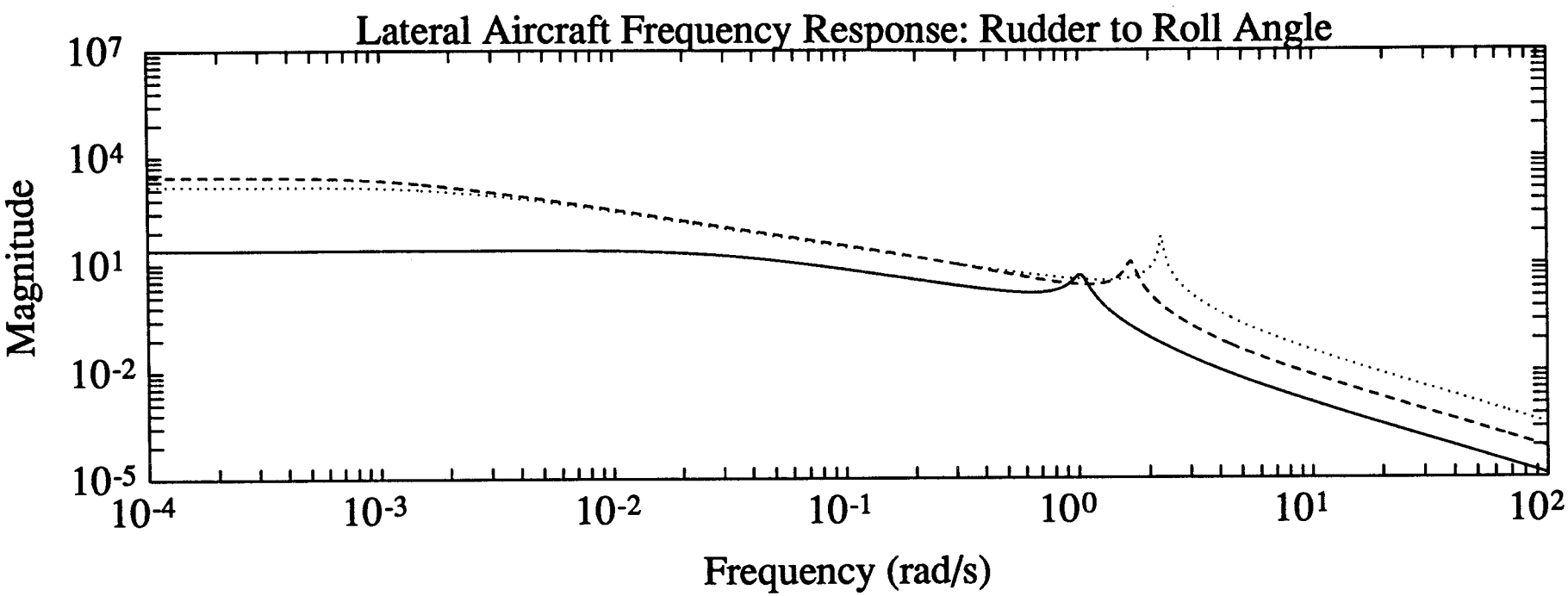
Lateral Aircraft Frequency Response: Rudder to Roll Angle
Magnitude
10^7
10^4
10^1
10^-2
10^-5
10^-4
10^-3
10^-2
10^-1
10^0
10^1
10^2
Frequency (rad/s)

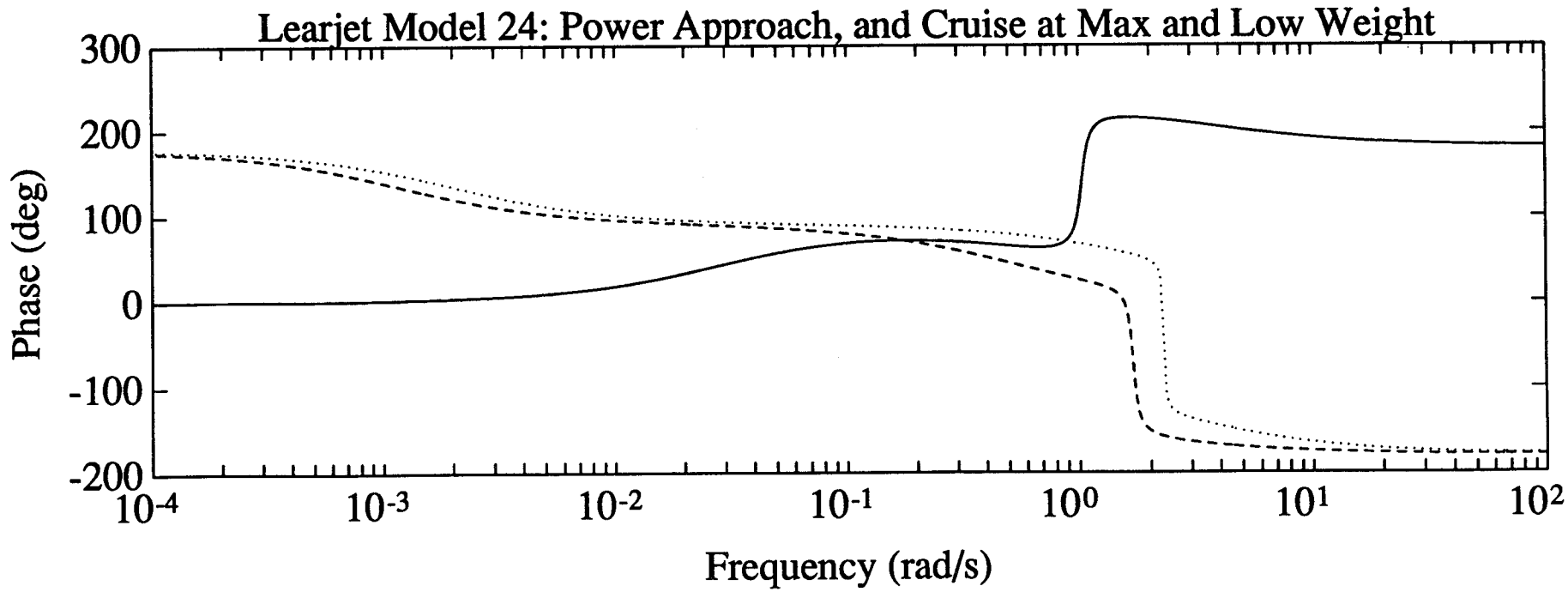
Learjet Model 24: Power Approach, and Cruise at Max and Low Weight
Phase (deg)
300
200
100
0
-100
-200
10^-4
10^-3
10^-2
10^-1
10^0
10^1
10^2
Frequency (rad/s)

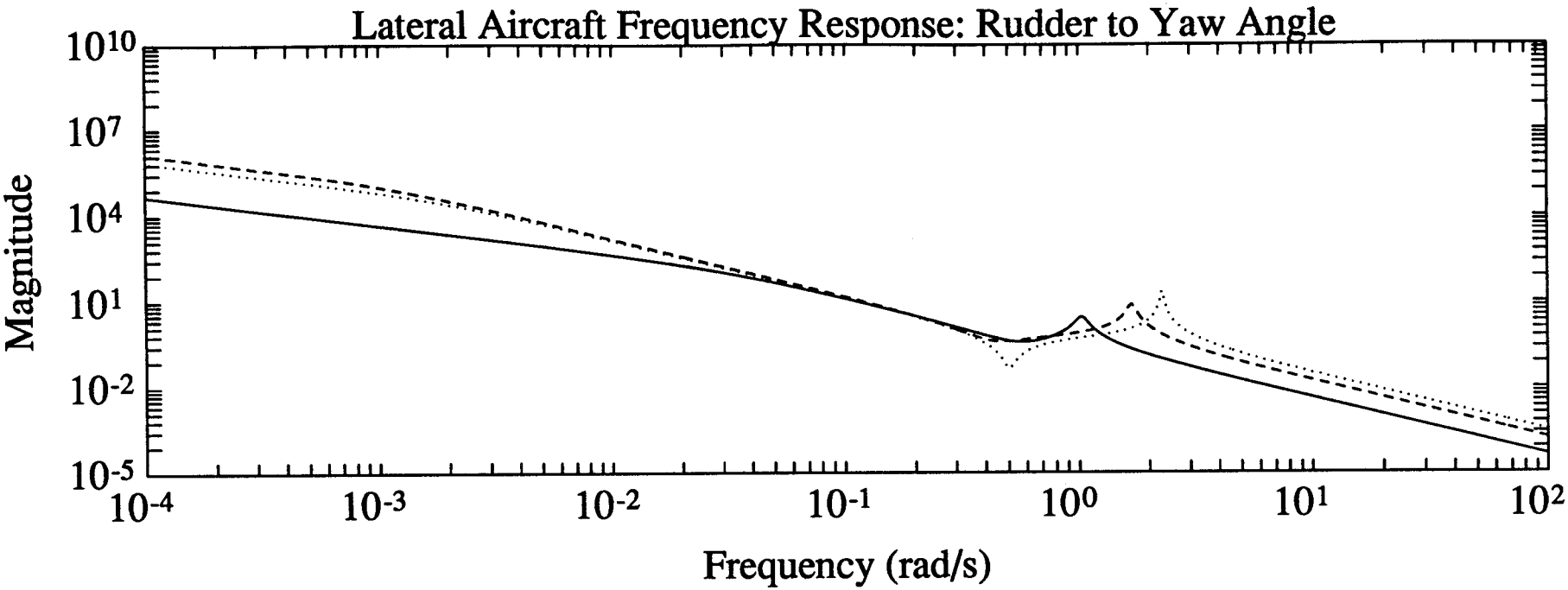
Lateral Aircraft Frequency Response: Rudder to Yaw Angle
Magnitude
10^{10}
10^{7}
10^{4}
10^{1}
10^{-2}
10^{-5}
10^{-4}
10^{-3}
10^{-2}
10^{-1}
10^{0}
10^{1}
10^{2}
Frequency (rad/s)

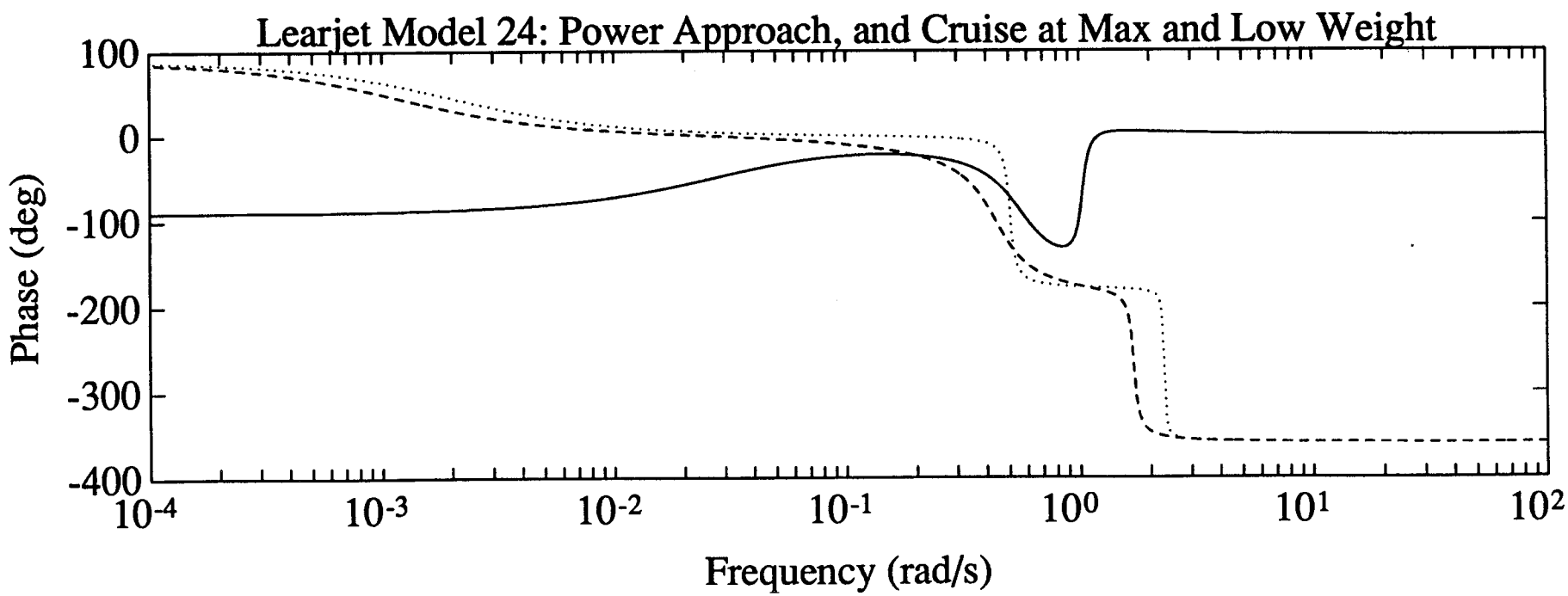
Learjet Model 24: Power Approach, and Cruise at Max and Low Weight
Phase (deg)
100
0
-100
-200
-300
-400
10^{-4}
10^{-3}
10^{-2}
10^{-1}
10^{0}
10^{1}
10^{2}
Frequency (rad/s)

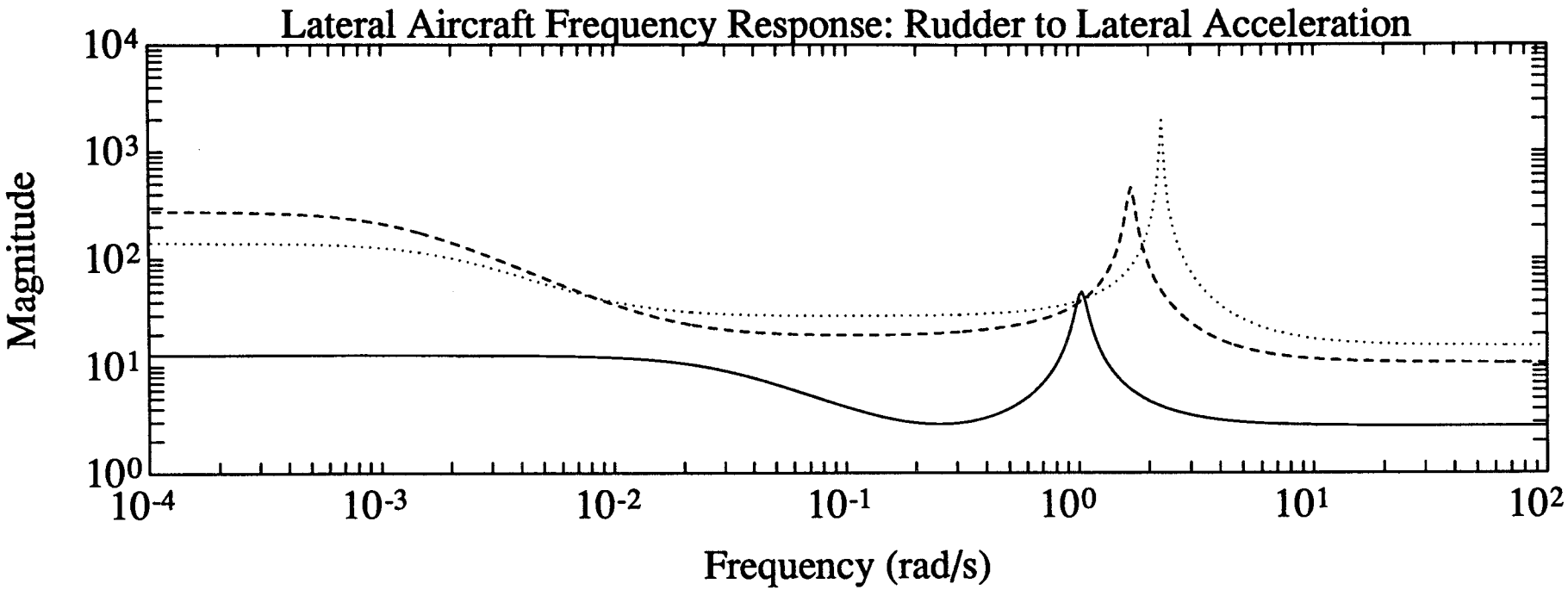
Lateral Aircraft Frequency Response: Rudder to Lateral Acceleration
Magnitude
10^4
10^3
10^2
10^1
10^0
10^{-4}
10^{-3}
10^{-2}
10^{-1}
10^0
10^1
10^2
Frequency (rad/s)

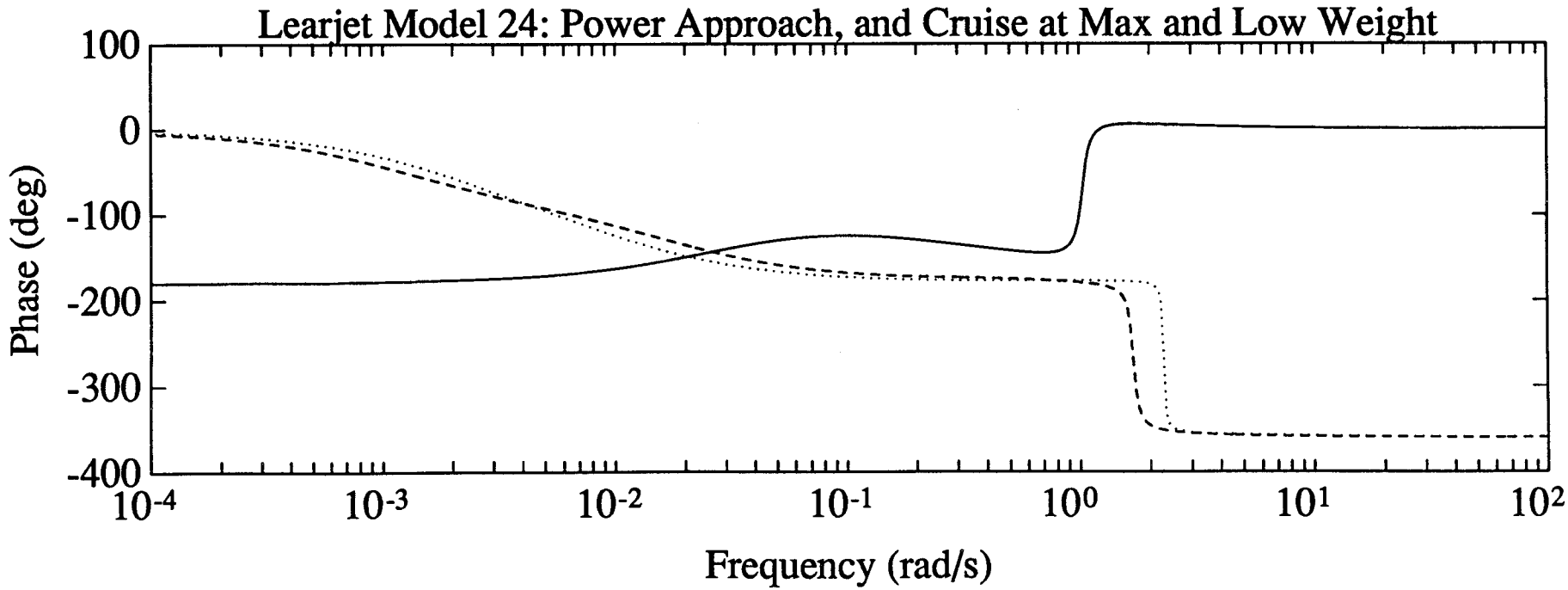
Learjet Model 24: Power Approach, and Cruise at Max and Low Weight
Phase (deg)
100
0
-100
-200
-300
-400
10^{-4}
10^{-3}
10^{-2}
10^{-1}
10^0
10^1
10^2
Frequency (rad/s)

A.7 Linear-quadratic Control Results

The contents of this subsection of the Appendix are:

- MATLAB script to compute linear quadratic controller for longitudinal pitch control
- Simulab block diagrams
  - Frequency domain analysis
  - Performance simulation
- Graphs of performance results
  - Boeing 747
  - McDonnell Douglas F-4C
  - Learjet Model 24
- MATLAB script to compute linear quadratic controller for lateral/directional control
- SIMULAB block diagrams
  - Frequency domain analysis
  - Performance simulation
- Graphs of performance results
  - Learjet Model 24, flight condition 3

Both the analyses and simulations use SIMULAB block diagrams. The block diagrams automatically use the dynamics parameters and the feedback gain that are computed in MATLAB. The open loop transfer function evaluation is performed by linearizing a SIMULAB block diagram with the appropriate feedback path cut. For these case studies, the path is either the elevator, the aileron, or the rudder.

```
%LINEAR QUADRATIC REGULATOR SOLUTION TO AIRCRAFT PITCH CONTROL

%Augment aircraft dynamics with an integral state
%for zero steady-state error.

format short e
Aaug=[Alo,0*ones(4,1);[0 0 0 1 0]]
Baug=[Blo;0]
Caug=[Clo(1,:) 0]
Daug=Dlo(1,:)
evaug=eig(Aaug)

%Compute feedback gains for the augmented aircraft dynamics using
%the steady-state solution for the linear, quadratic regulator.

%Weight only the pitch rate, pitch angle and pitch integral
%states so that the gains on the speed states are small. Use
%weighting in the workspace (a.k.a.) stack, if they exist.

if exist('Qaug')*exist('Raug')~=1,
  Qaug=diag([0 0 1 1 1])
  Raug=Baug'*Baug
end;

%Compute feedback gains for the augmented dynamics and the
%selected error and control weightings using the MATLAB function "lqr".

[Kr,S]=lqr(Aaug,Baug,Qaug,Raug);
Kr
evcl=eig(Aaug-Baug*Kr)

%Compute and plot open loop frequency response.
%Note that Col and Dol have minus signs so that "bode"
%evaluates GH rather than -GH (see block diagram).

[Aol,Bol,Col,Dol]=linmod('RegulatorOL');
[mgol,phol]=bode(Aol,Bol,-Col,-Dol,1,om);
clg;
subplot(211);
if exist('mgollast')*exist('mgol0')==1,
  loglog(om,[mgol,mgollast mgol0]);
elseif exist('mgollast')==1,
  loglog(om,[mgol,mgollast]);
else
  loglog(om,mgol);
end;
title('Open Loop Linear Quadratic Regulator Frequency Response');
xlabel('Frequency (rad/s)');ylabel('Magnitude');
if exist('phollast')*exist('phol0')==1,
  semilogx(om,[phol,phollast phol0]);
elseif exist('phollast')==1,
  semilogx(om,[phol,phollast]);
else
  semilogx(om,phol);
end;
xlabel('Frequency (rad/s)');ylabel('Phase (deg)');
```

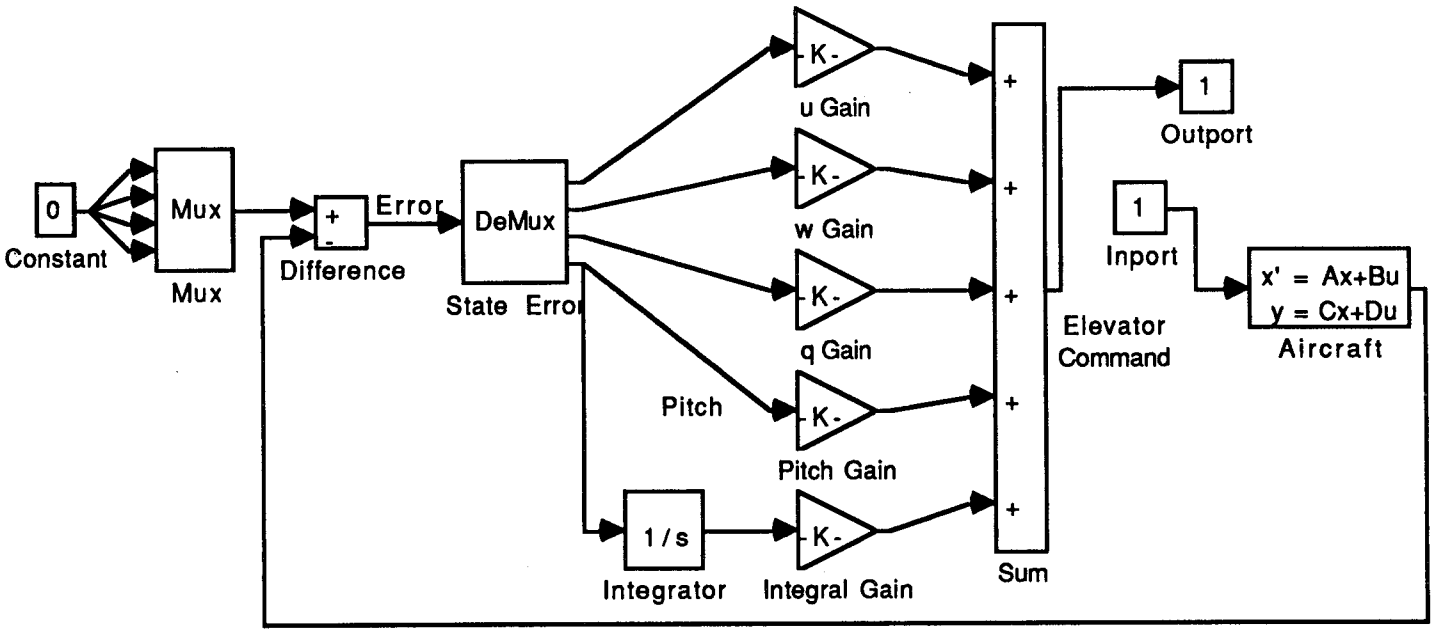

OPEN LOOP ANALYSIS OF A LINEAR-QUADRATIC REGULATOR FOR AIRCRAFT LONGITUDINAL DYNAMIC

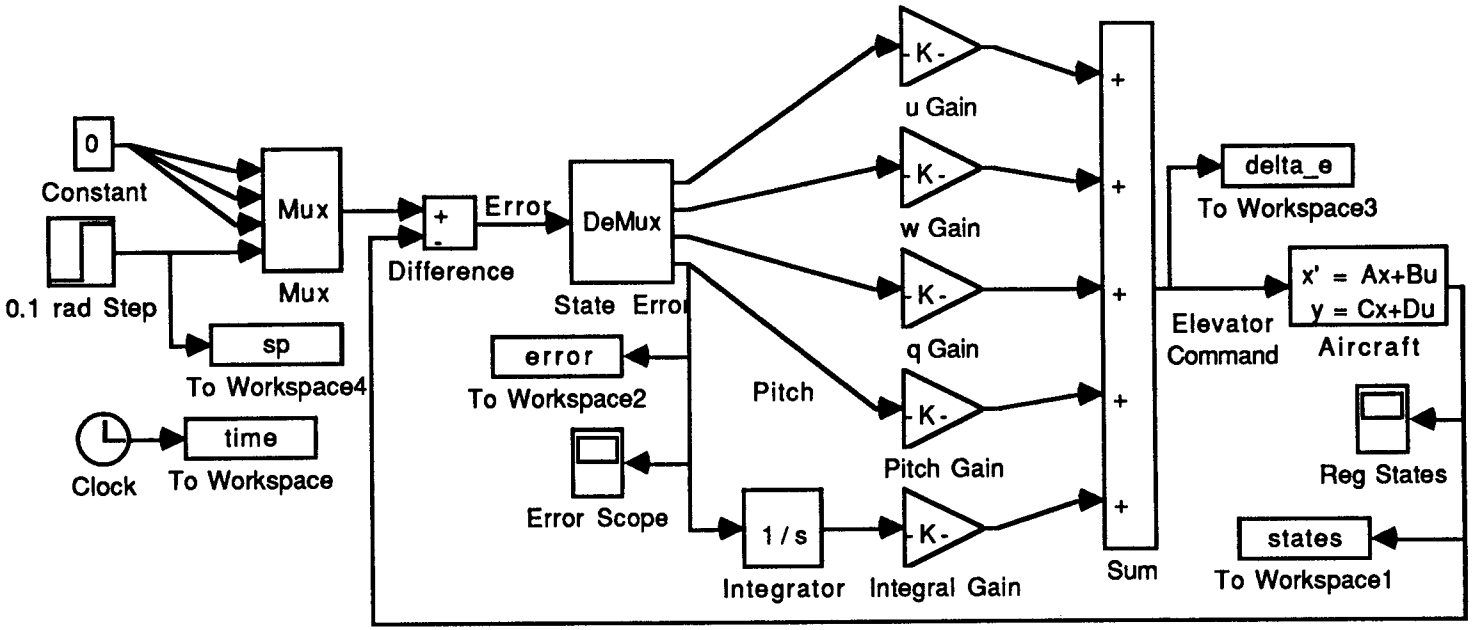

SIMULATION OF A LINEAR-QUADRATIC REGULATOR FOR AIRCRAFT LONGITUDINAL DYNAMIC

```
Linear quadratic controller
28 May 1993: Boeing 747 at 3 flight conditions

Ruu=    "s"              "d"              "p"
  4.0817e+01       3.4183e+02       6.3480e+02


diag(Qxx)=
    0       0       0
    0       0       0
    1       1       1
    1       1       1
    1       1       1


Kr=
 -1.1353e-03   1.9992e-03  -8.3901e-01  -9.1237e-01  -1.5652e-01

 -6.5992e-05   5.2964e-04  -1.4940e-01  -5.4586e-01  -5.4087e-02

 -1.6488e-04   3.5187e-04  -1.2544e-01  -3.2152e-01  -3.9690e-02


evcl1=
-4.7744e-01+  6.1289e-01i
-4.7744e-01-  6.1289e-01i
-2.7794e-02
-1.2530e-01+  1.9079e-01i
-1.2530e-01-  1.9079e-01i


evcl2=
-4.7196e-01+  1.2373e+00i
-4.7196e-01-  1.2373e+00i
-1.5814e-02
-8.1573e-02+  8.3750e-02i
-8.1573e-02-  8.3750e-02i


evcl3=
-5.8381e-01+  1.0976e+00i
-5.8381e-01-  1.0976e+00i
-5.2319e-03
-9.5320e-02+  1.1139e-01i
-9.5320e-02-  1.1139e-01i
```

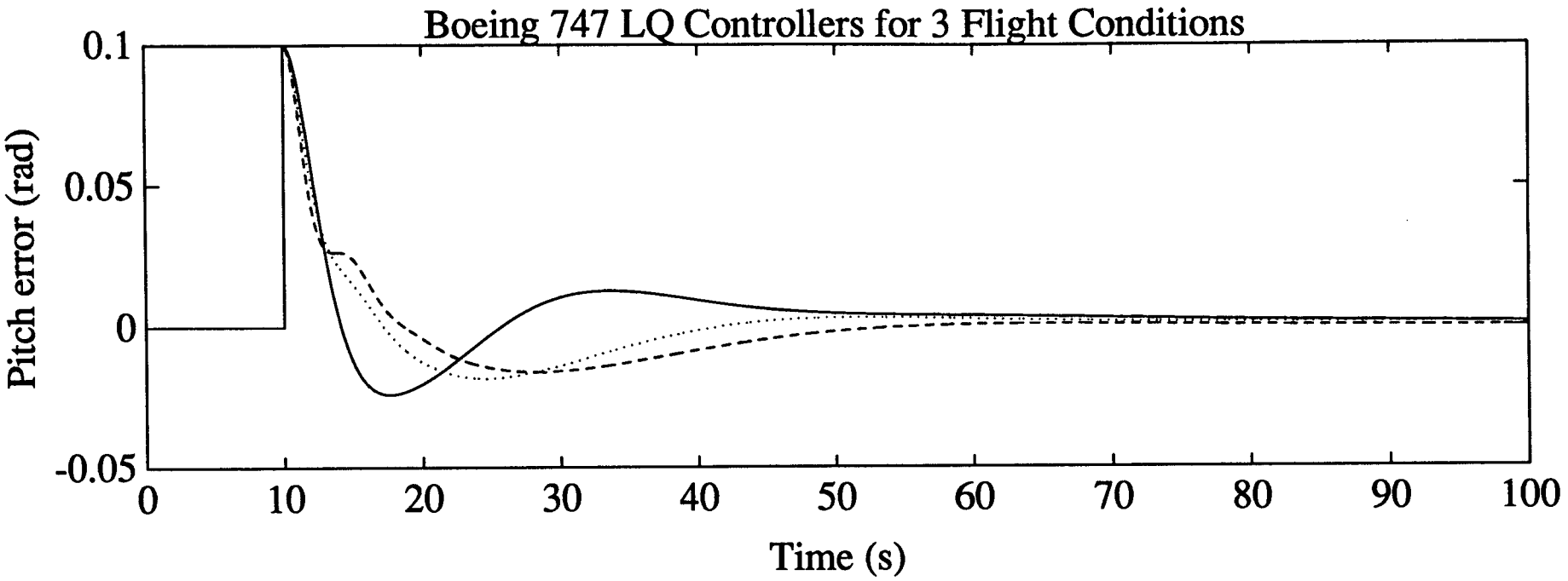
Boeing 747 LQ Controllers for 3 Flight Conditions
Pitch error (rad)
0.1
0.05
0
-0.05
0
10
20
30
40
50
60
70
80
90
100
Time (s)

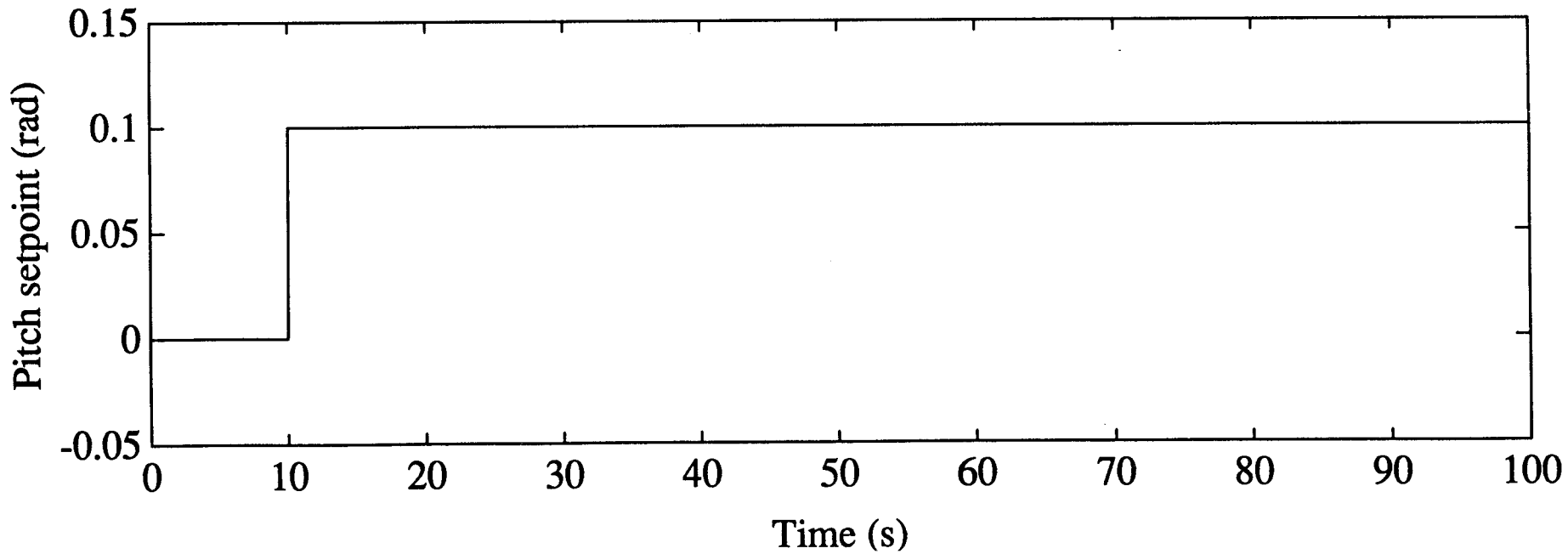
Pitch setpoint (rad)
0.15
0.1
0.05
0
-0.05
0
10
20
30
40
50
60
70
80
90
100
Time (s)

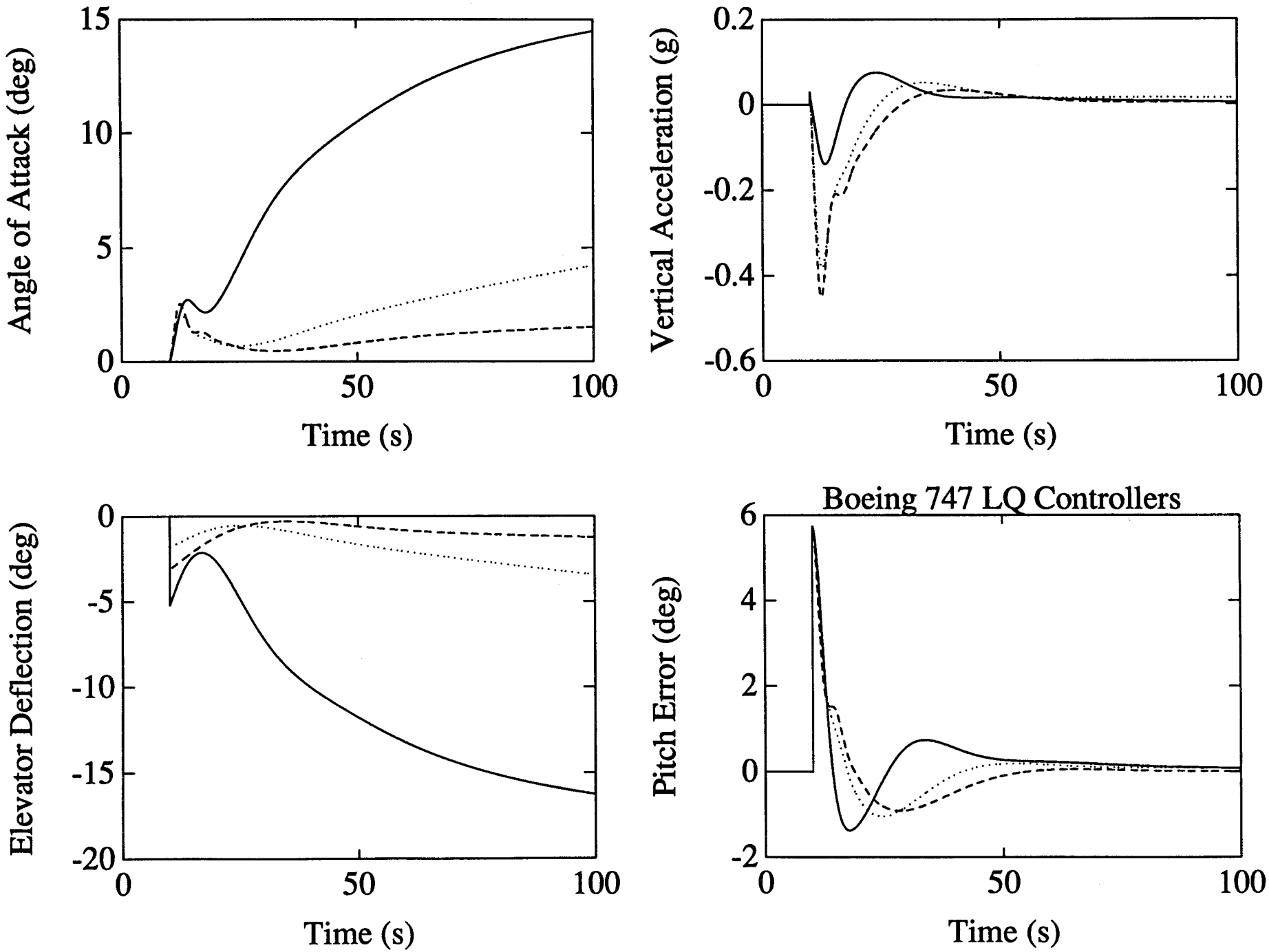
Angle of Attack (deg)
15
10
5
0
0
50
100
Time (s)
Vertical Acceleration (g)
0.2
0
-0.2
-0.4
-0.6
0
50
100
Time (s)
Elevator Deflection (deg)
0
-5
-10
-15
-20
0
50
100
Time (s)
Boeing 747 LQ Controllers
Pitch Error (deg)
6
4
2
0
-2
0
50
100
Time (s)

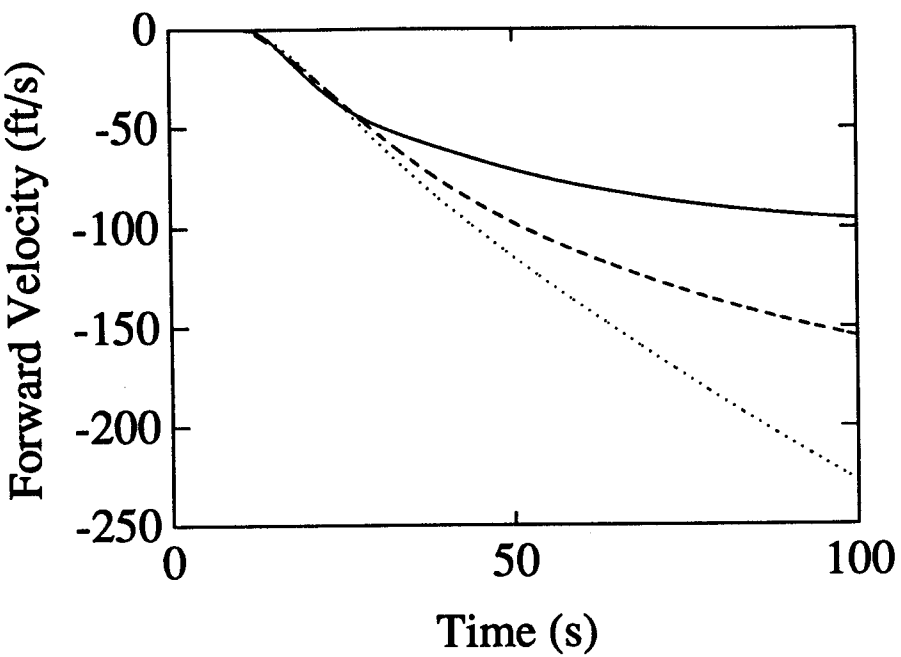
Forward Velocity (ft/s)
0
-50
-100
-150
-200
-250
0
50
100
Time (s)

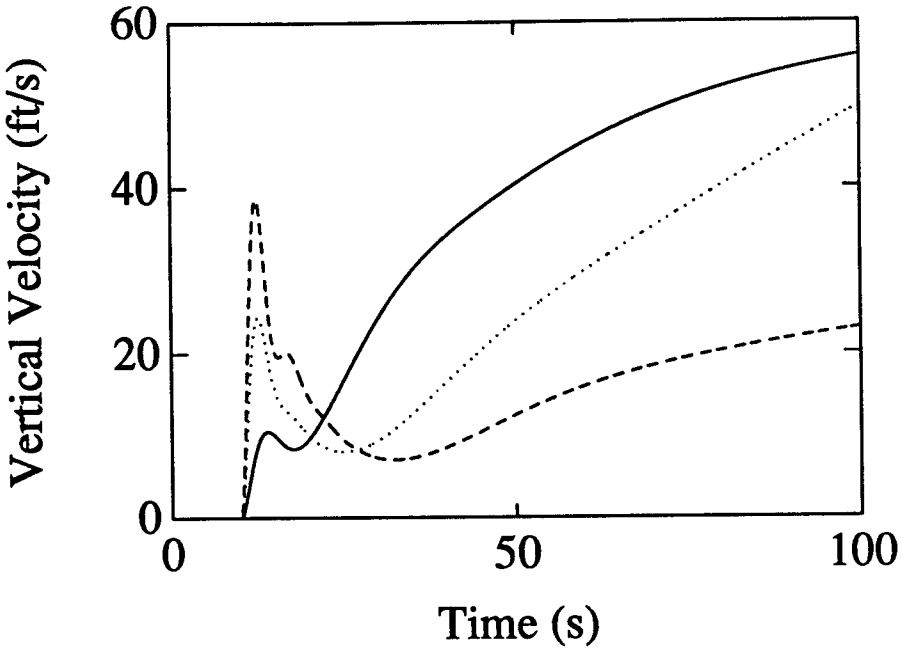
Vertical Velocity (ft/s)
60
40
20
0
0
50
100
Time (s)

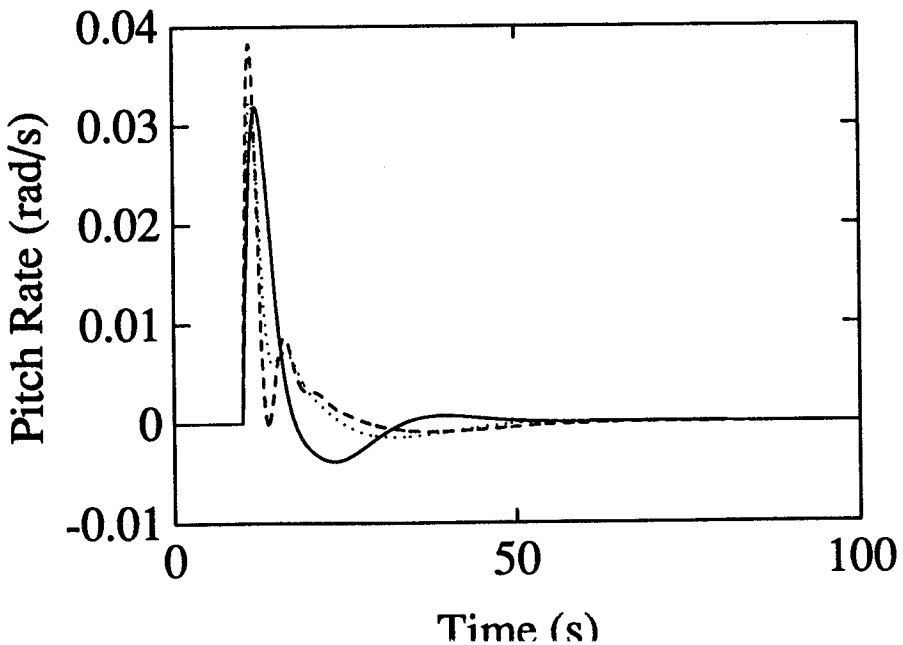
Pitch Rate (rad/s)
0.04
0.03
0.02
0.01
0
-0.01
0
50
100
Time (s)

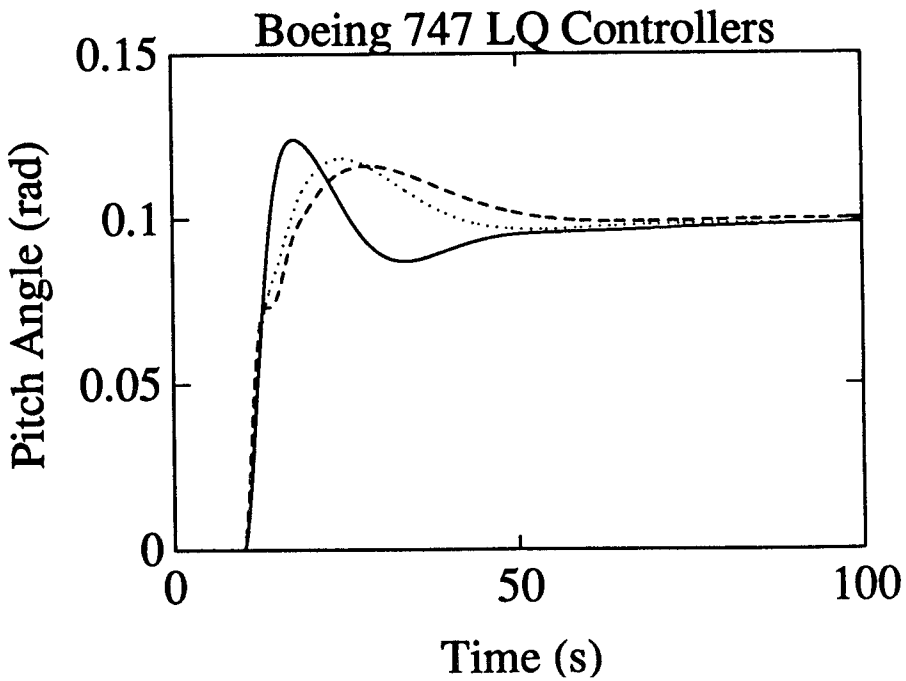
Boeing 747 LQ Controllers
Pitch Angle (rad)
0.15
0.1
0.05
0
0
50
100
Time (s)

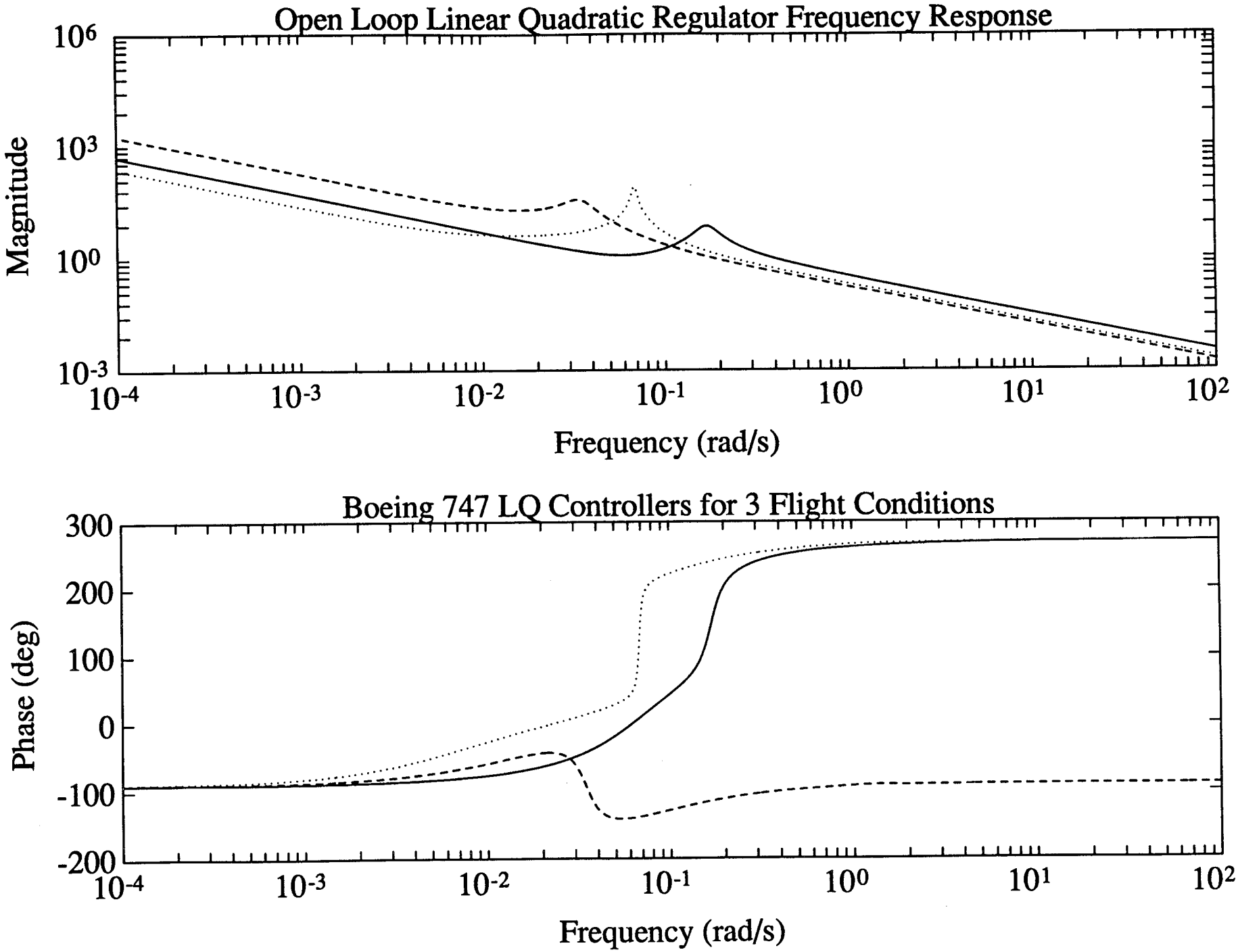
Open Loop Linear Quadratic Regulator Frequency Response
Magnitude
10^6
10^3
10^0
10^-3
10^-4
10^-3
10^-2
10^-1
10^0
10^1
10^2
Frequency (rad/s)
Boeing 747 LQ Controllers for 3 Flight Conditions
Phase (deg)
300
200
100
0
-100
-200
10^-4
10^-3
10^-2
10^-1
10^0
10^1
10^2
Frequency (rad/s)

```
Linear quadratic controller
28 May 1993: McDonnell Douglas F-4C at 3 flight conditions

Ruu=    "s"              "d"              "p"
  8.2823e+01       2.7471e+03       3.2182e+03


diag(Qxx)=
     0         0         0
     0         0         0
     1         1         1
     1         1         1
     1         1         1


Kr=
 -3.1177e-04   7.4538e-04  -3.9478e-01  -4.5979e-01  -1.0988e-01

  1.2293e-04   2.4100e-04  -1.9405e-02  -2.2510e-01  -1.9079e-02

  1.1595e-03   2.7233e-05  -6.5360e-03  -4.8405e-02   1.7628e-02


evcl1=
-3.2772e-01+  4.8526e+00i
-3.2772e-01-  4.8526e+00i
-2.8641e-02+  3.9603e-02i
-2.8641e-02-  3.9603e-02i
-1.2046e-02

evcl2=
-6.4453e-01+  2.7815e+00i
-6.4453e-01-  2.7815e+00i
-3.5108e-03
-8.8100e-02+  7.5306e-02i
-8.8100e-02-  7.5306e-02i

evlc3=
-4.7276e-01+  6.5055e-01i
-4.7276e-01-  6.5055e-01i
-4.1305e-02
-2.3426e-01+  2.0184e-01i
-2.3426e-01-  2.0184e-01i
```

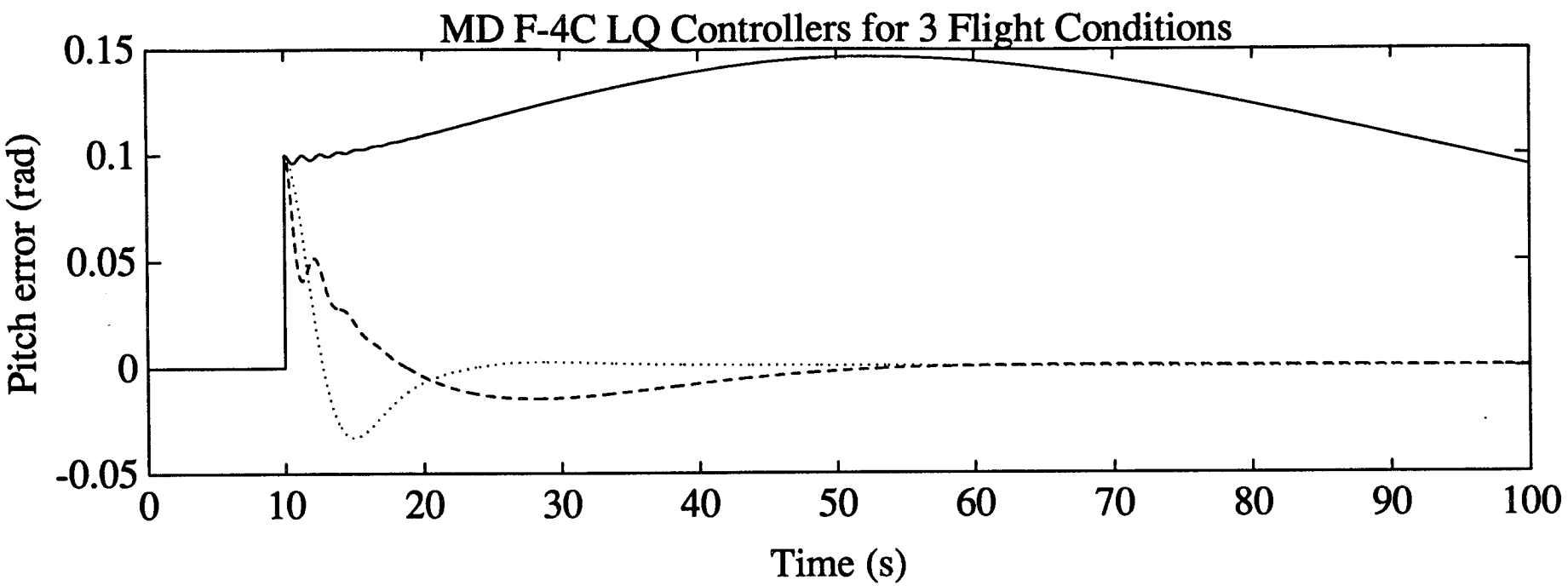
MD F-4C LQ Controllers for 3 Flight Conditions
Pitch error (rad)
0.15
0.1
0.05
0
-0.05
0
10
20
30
40
50
60
70
80
90
100
Time (s)

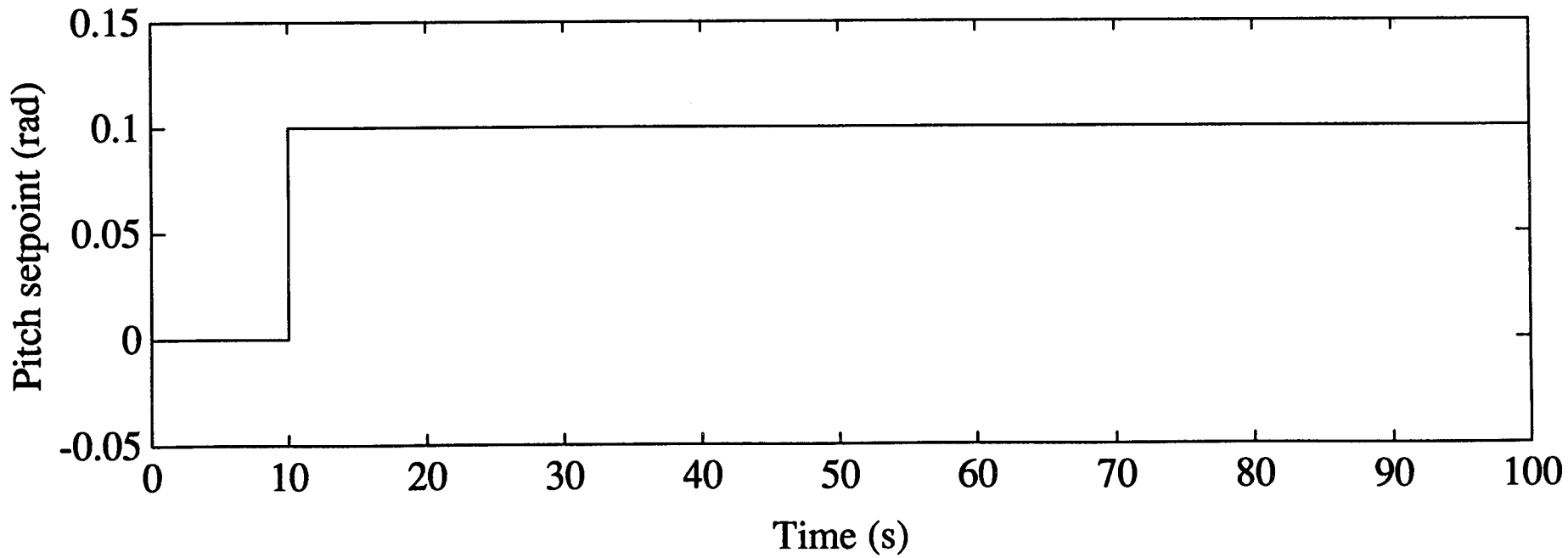
Pitch setpoint (rad)
0.15
0.1
0.05
0
-0.05
0
10
20
30
40
50
60
70
80
90
100
Time (s)

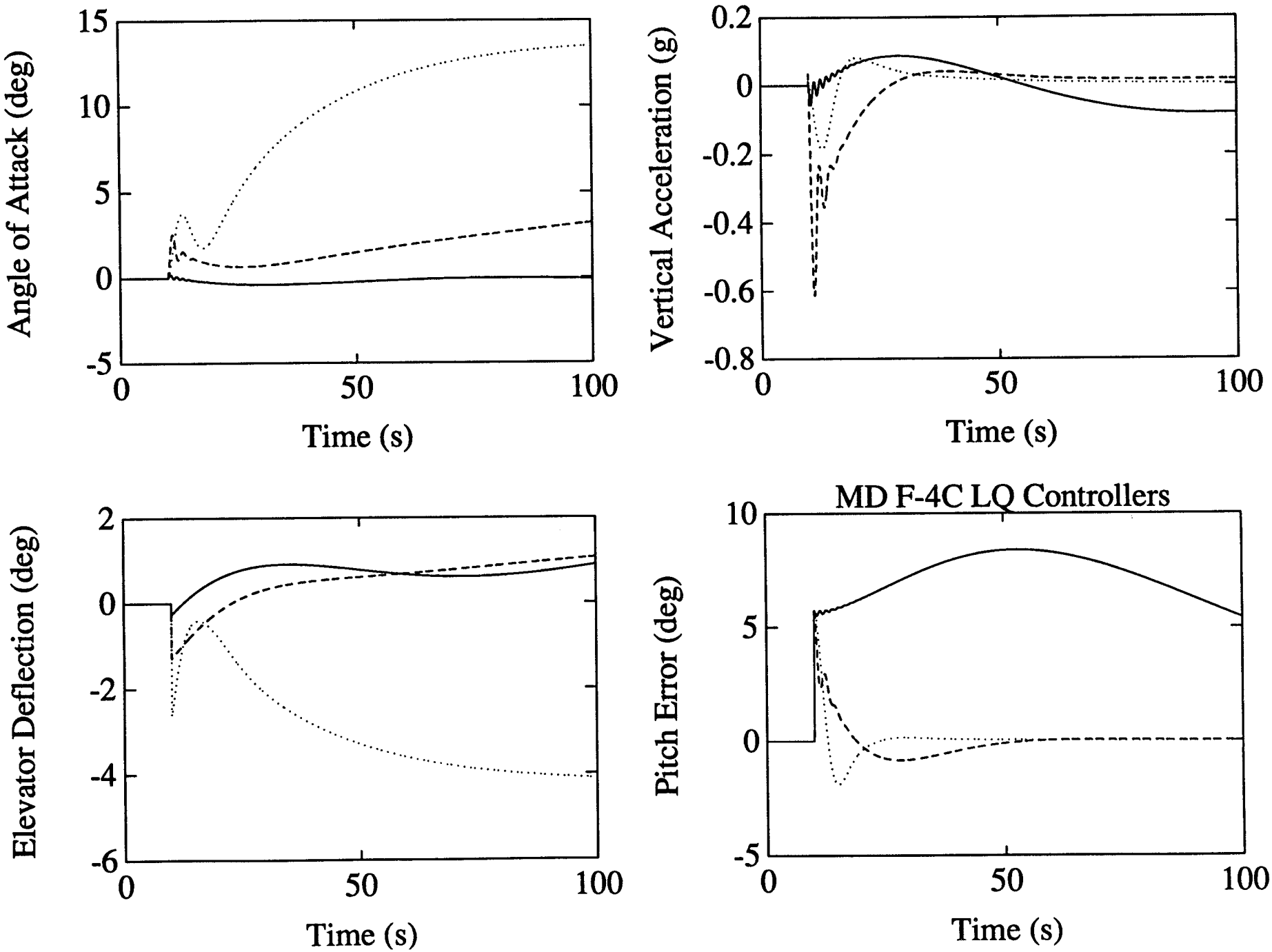
MD F-4C LQ Controllers
Angle of Attack (deg)
15
10
5
0
-5
0
50
100
Time (s)
Vertical Acceleration (g)
0.2
0
-0.2
-0.4
-0.6
-0.8
0
50
100
Time (s)
Elevator Deflection (deg)
2
0
-2
-4
-6
0
50
100
Time (s)
Pitch Error (deg)
10
5
0
-5
0
50
100
Time (s)

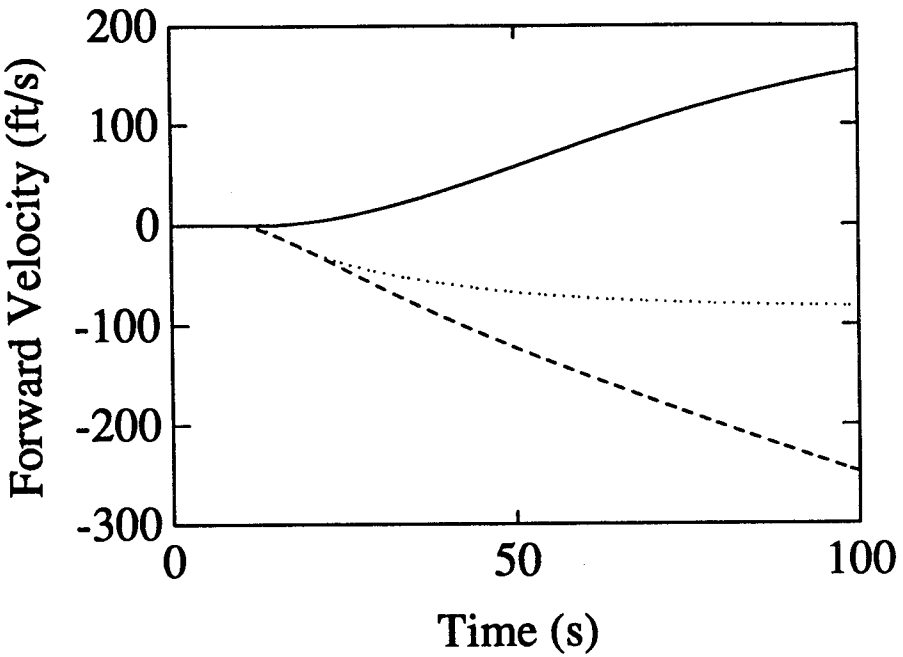
200
100
0
-100
-200
-300
0
50
100
Forward Velocity (ft/s)
Time (s)

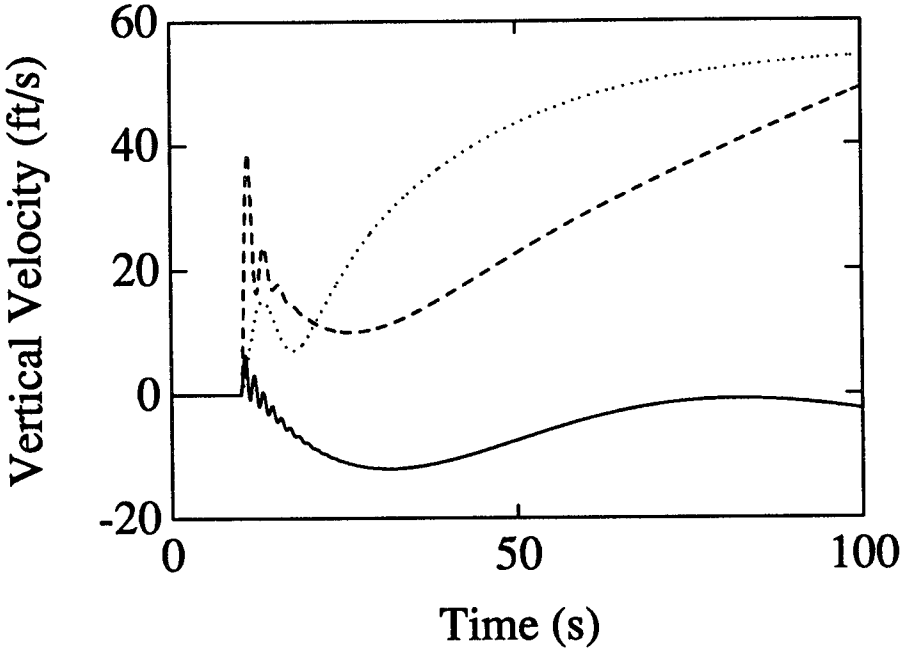
60
40
20
0
-20
0
50
100
Vertical Velocity (ft/s)
Time (s)

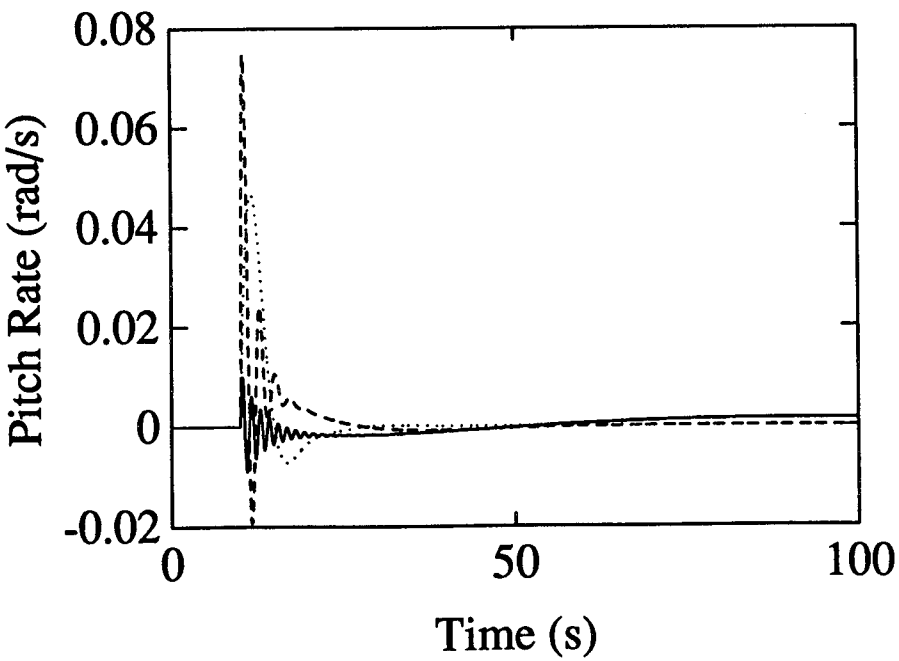
0.08
0.06
0.04
0.02
0
-0.02
0
50
100
Pitch Rate (rad/s)
Time (s)

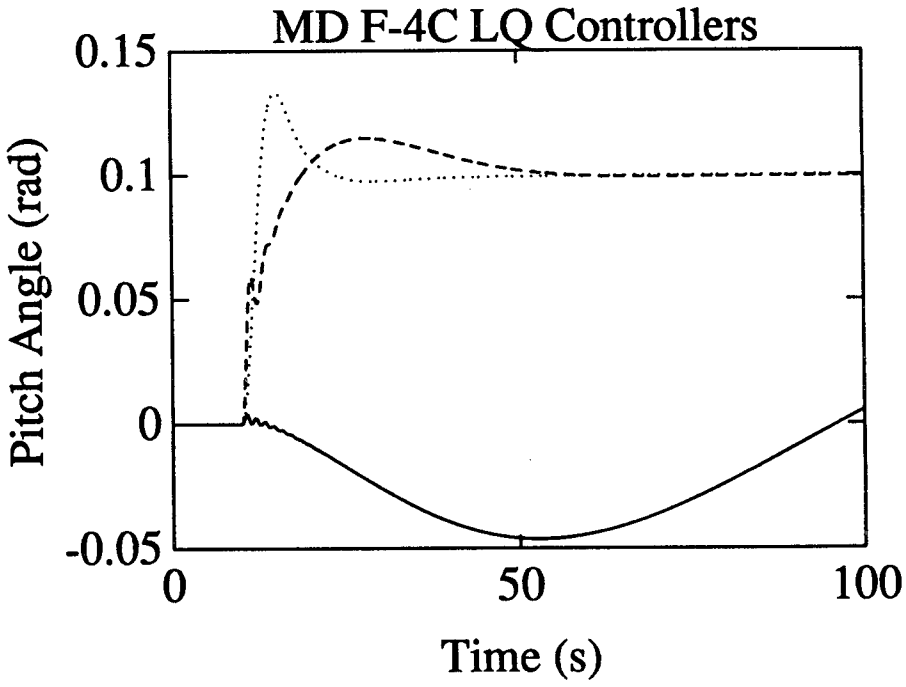
MD F-4C LQ Controllers
0.15
0.1
0.05
0
-0.05
0
50
100
Pitch Angle (rad)
Time (s)

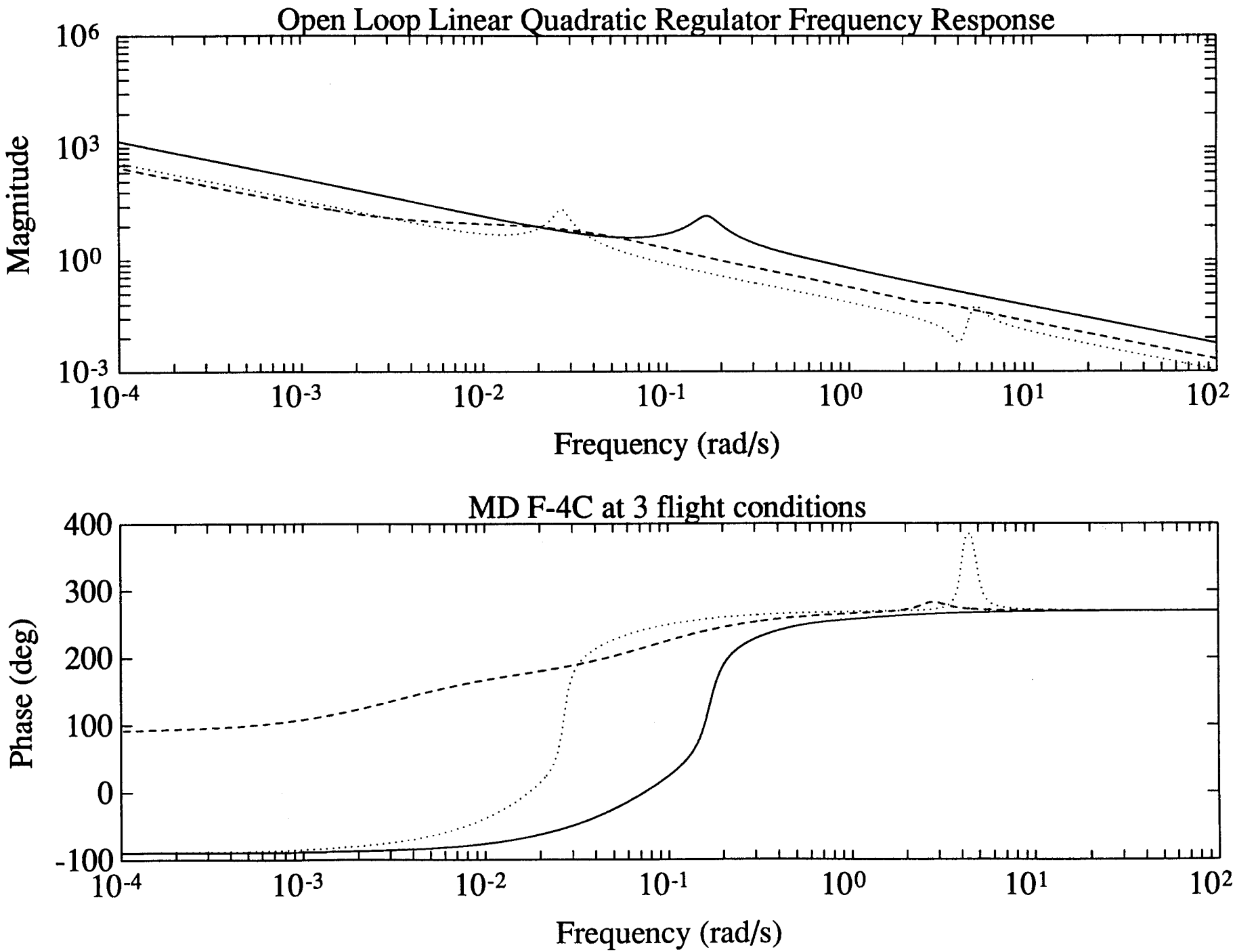
Open Loop Linear Quadratic Regulator Frequency Response
Magnitude
10^6
10^3
10^0
10^-3
10^-4
10^-3
10^-2
10^-1
10^0
10^1
10^2
Frequency (rad/s)
MD F-4C at 3 flight conditions
Phase (deg)
400
300
200
100
0
-100
10^-4
10^-3
10^-2
10^-1
10^0
10^1
10^2
Frequency (rad/s)

```
Linear quadratic controller
28 May 1993: Learjet Model 24 at 3 flight conditions

 Ruu=    "s"                "d"                "p"
   7.0040e+01         1.4479e+03         2.8194e+03


 diag(Qxx)
     0          0          0
     0          0          0
     1          1          1
     1          1          1
     1          1          1


 Kr=
  -8.9272e-04    1.5410e-03  -1.4820e-01  -4.4474e-01  -1.1949e-01

  -1.5093e-04    2.1149e-04  -1.9179e-02  -1.6567e-01  -2.6280e-02

  -1.4555e-04    1.4727e-04  -1.6057e-02  -1.2080e-01  -1.8833e-02


 evcl1=
 -9.3324e-01+  1.3187e+00i
 -9.3324e-01-  1.3187e+00i
 -3.7861e-02
 -1.5995e-01+  2.6089e-01i
 -1.5995e-01-  2.6089e-01i


 evcl2=
 -1.0154e+00+  2.6362e+00i
 -1.0154e+00-  2.6362e+00i
 -1.4053e-02
 -1.1070e-01+  1.3727e-01i
 -1.1070e-01-  1.3727e-01i


 evcl3=
 -1.1882e+00+  2.6982e+00i
 -1.1882e+00-  2.6982e+00i
 -1.7549e-02
 -1.0674e-01+  1.4303e-01i
 -1.0674e-01-  1.4303e-01i
```

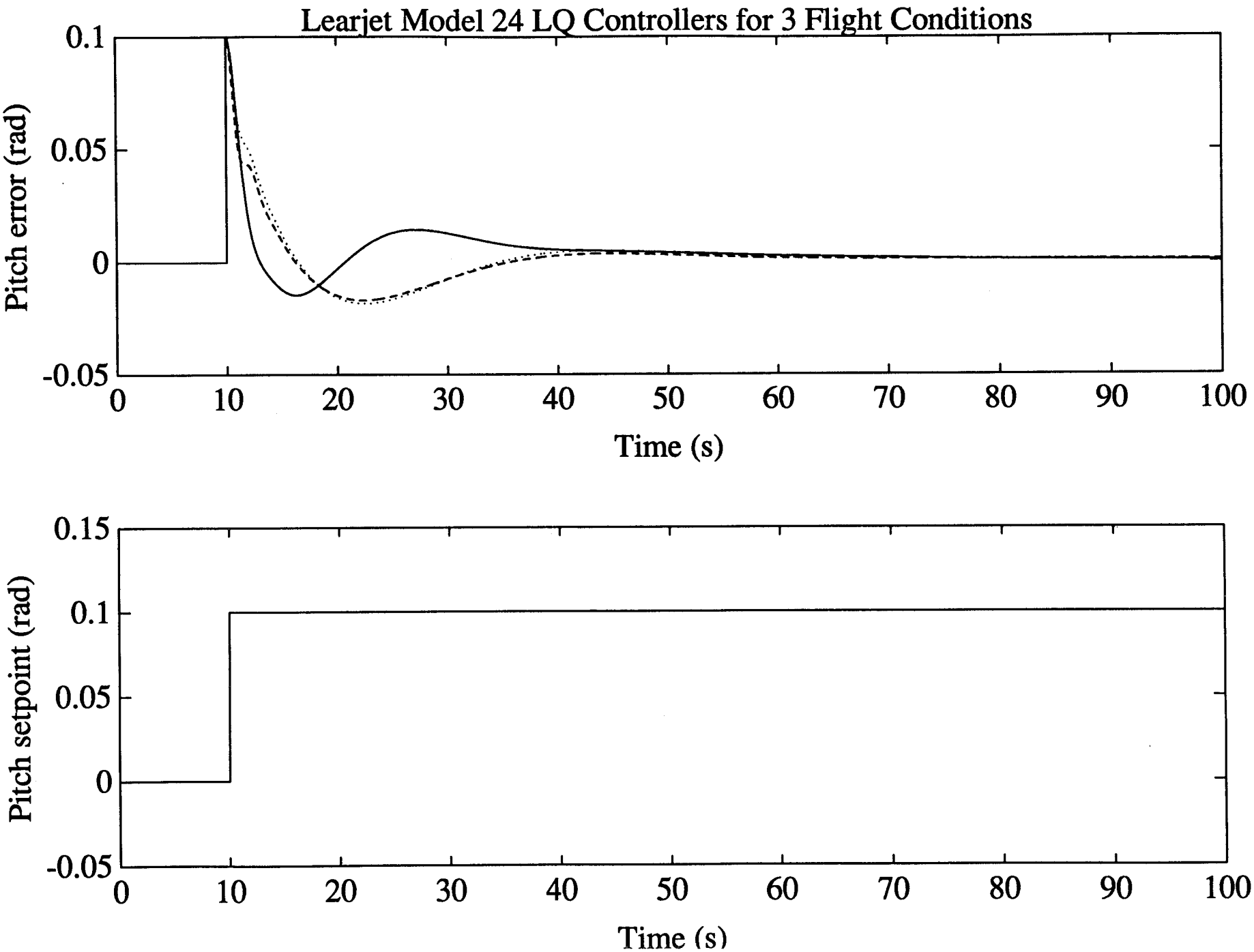
Learjet Model 24 LQ Controllers for 3 Flight Conditions
Pitch error (rad)
0.1
0.05
0
-0.05
0
10
20
30
40
50
60
70
80
90
100
Time (s)
Pitch setpoint (rad)
0.15
0.1
0.05
0
-0.05
0
10
20
30
40
50
60
70
80
90
100
Time (s)

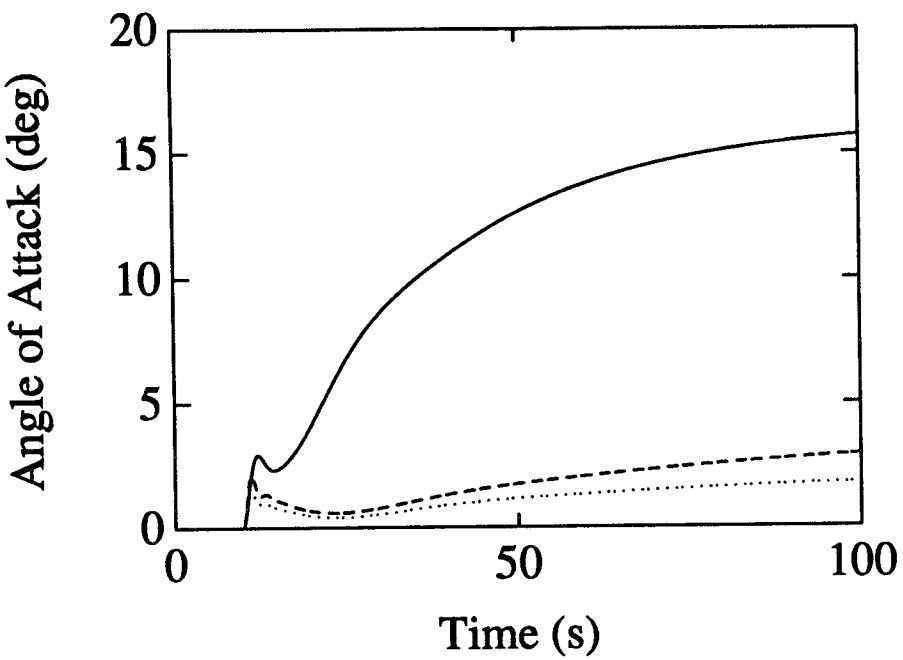
Angle of Attack (deg)
20
15
10
5
0
0
50
100
Time (s)

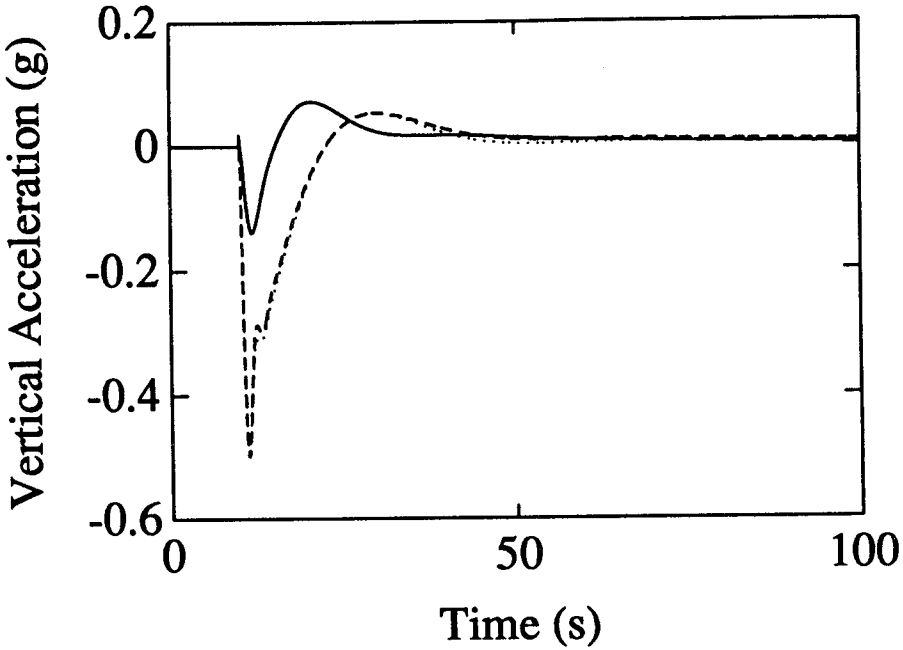
Vertical Acceleration (g)
0.2
0
-0.2
-0.4
-0.6
0
50
100
Time (s)

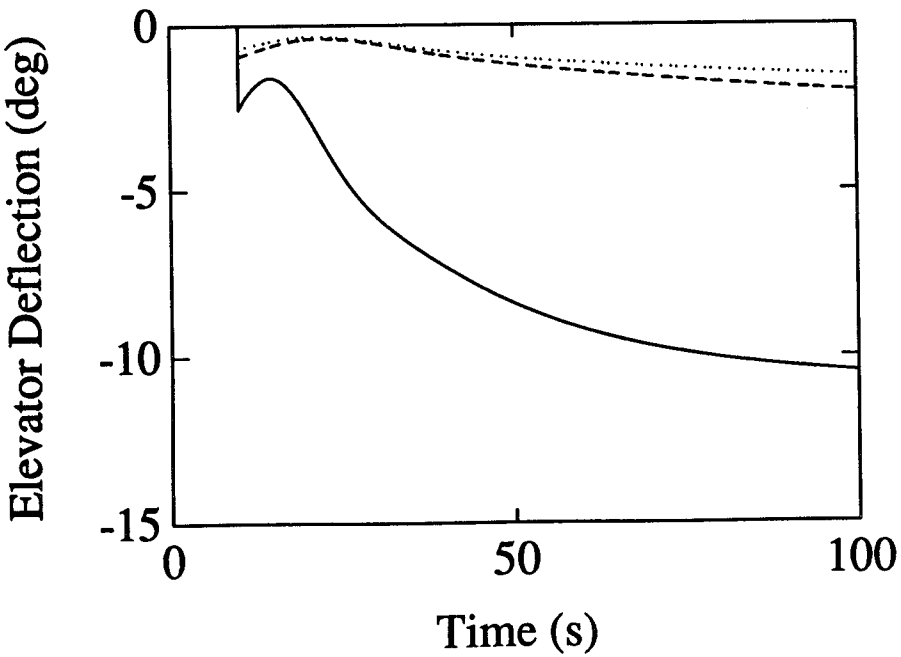
Elevator Deflection (deg)
0
-5
-10
-15
0
50
100
Time (s)

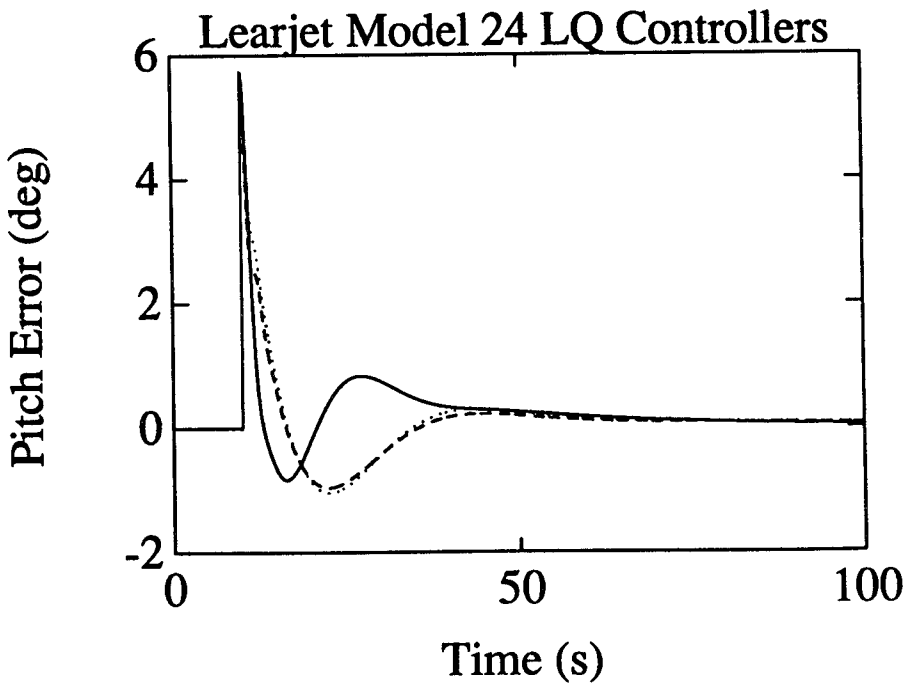
Learjet Model 24 LQ Controllers
Pitch Error (deg)
6
4
2
0
-2
0
50
100
Time (s)

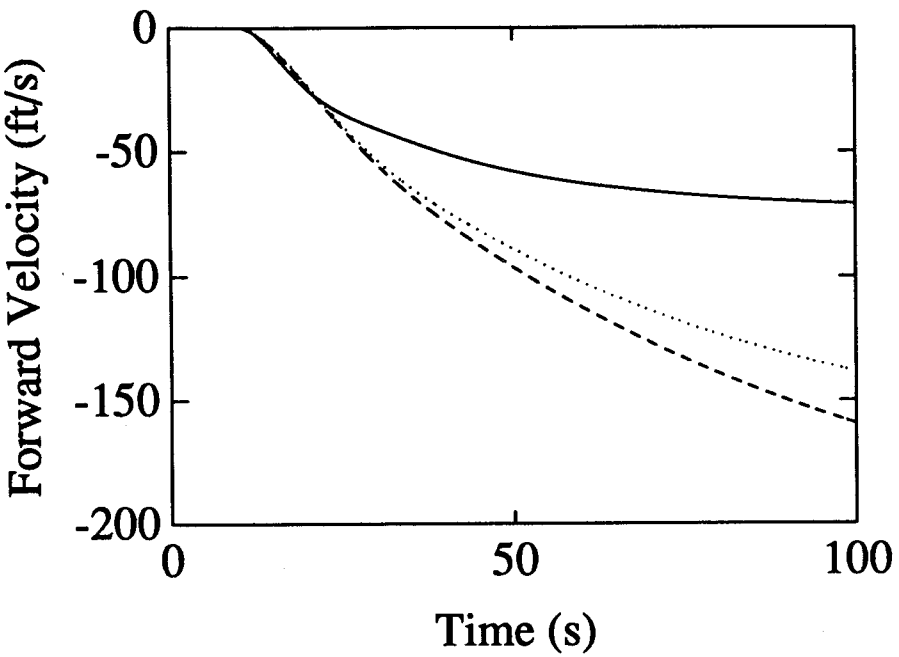
Forward Velocity (ft/s)
0
-50
-100
-150
-200
0
50
100
Time (s)

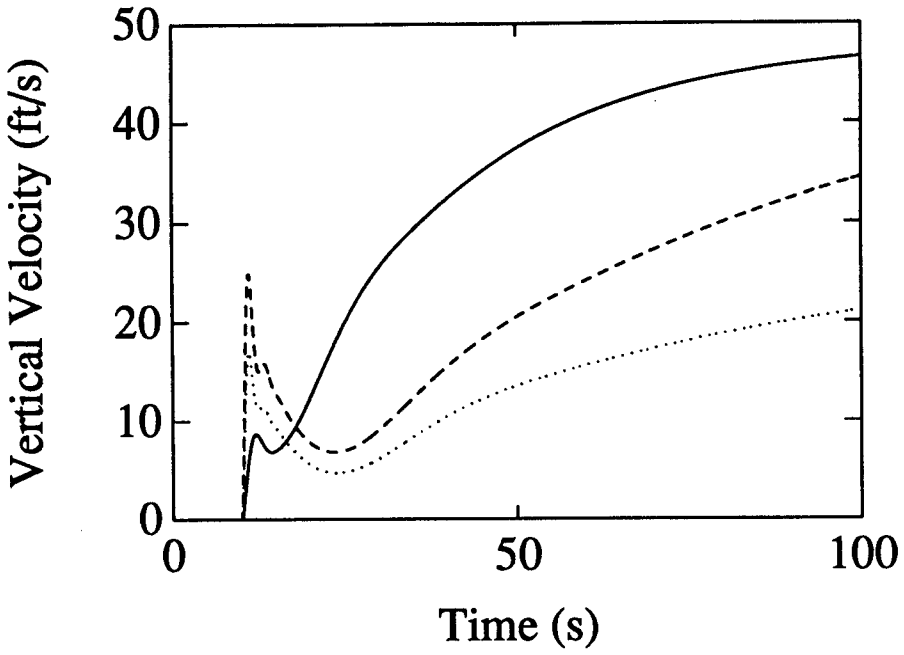
Vertical Velocity (ft/s)
50
40
30
20
10
0
0
50
100
Time (s)

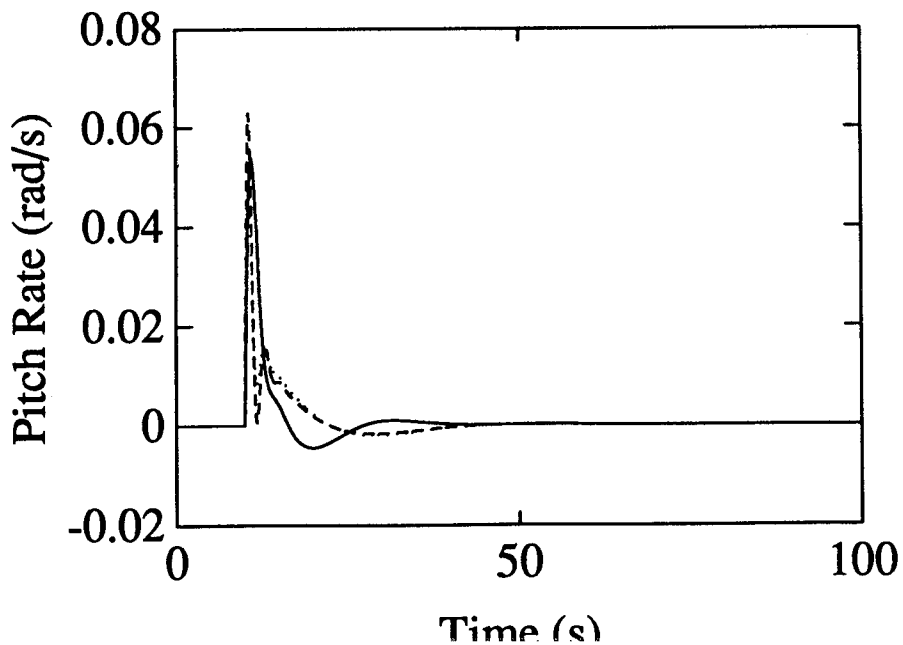
Pitch Rate (rad/s)
0.08
0.06
0.04
0.02
0
-0.02
0
50
100
Time (s)

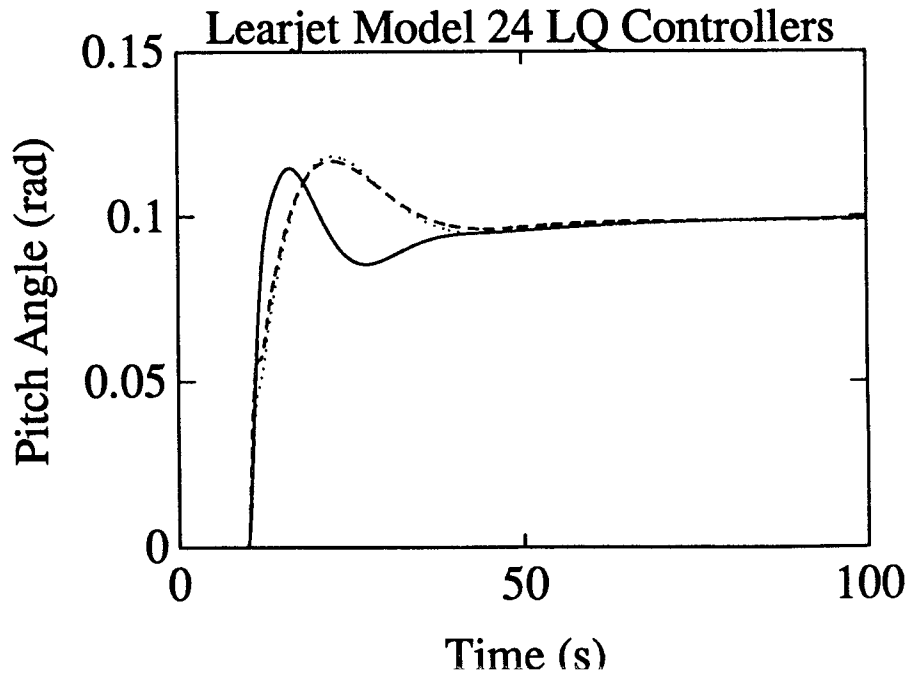
Learjet Model 24 LQ Controllers
Pitch Angle (rad)
0.15
0.1
0.05
0
0
50
100
Time (s)

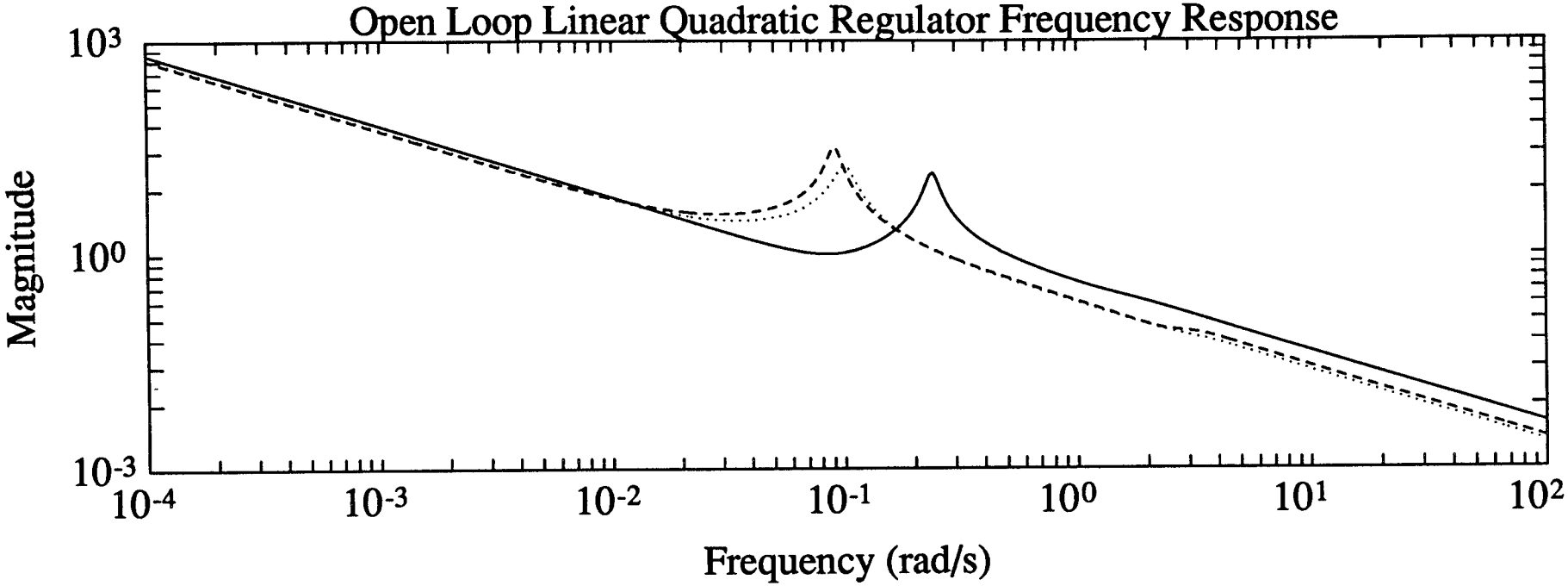
Open Loop Linear Quadratic Regulator Frequency Response
Magnitude
10^3
10^0
10^{-3}
10^{-4}
10^{-3}
10^{-2}
10^{-1}
10^0
10^1
10^2
Frequency (rad/s)

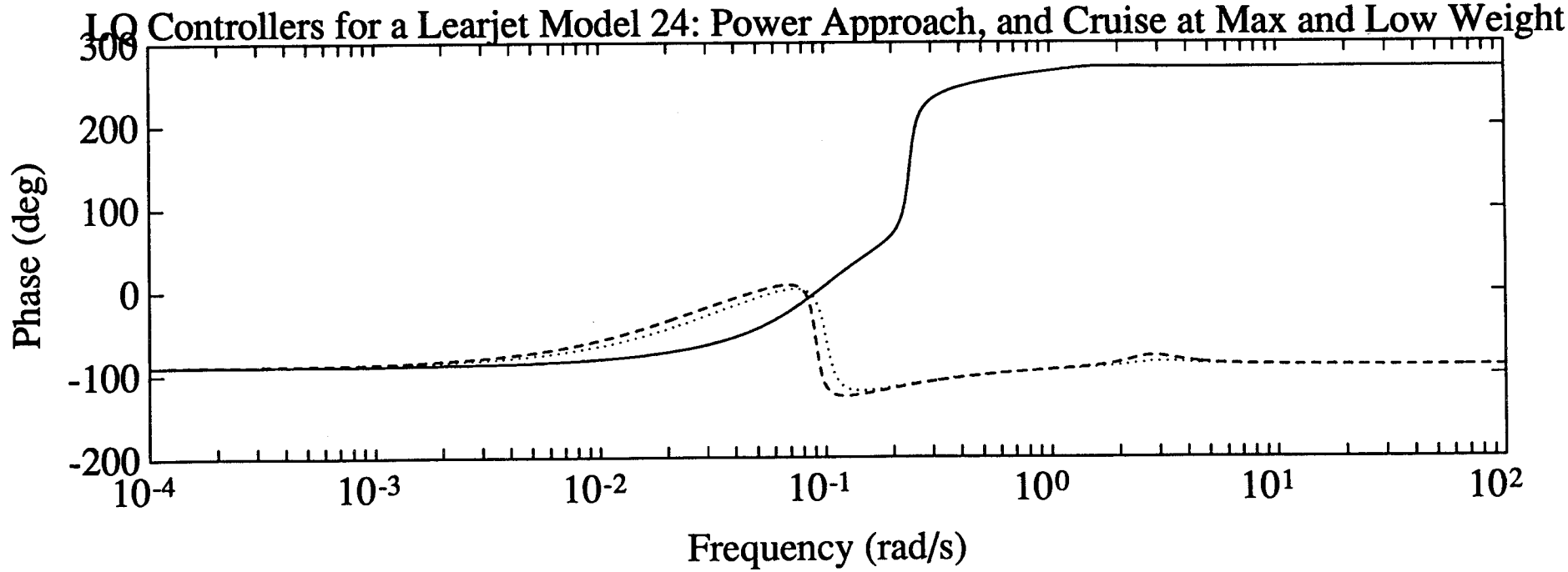
LQ Controllers for a Learjet Model 24: Power Approach, and Cruise at Max and Low Weight
Phase (deg)
300
200
100
0
-100
-200
10^{-4}
10^{-3}
10^{-2}
10^{-1}
10^0
10^1
10^2
Frequency (rad/s)

```
%LINEAR QUADRATIC REGULATOR SOLUTION TO AIRCRAFT TURN CONTROL

%Copy aircraft dynamics

format short e
Aaug=Ala;
Baug=Bla;
Caug=Cla(2:3,:);
Daug=Dla(2:3,:);
evaug=eig(Aaug)

%Compute feedback gains for the aircraft dynamics using
%the steady-state solution for the linear, quadratic regulator.

%Weight only the sideslip and yaw rate states. Use
%weightings in the workspace (a.k.a. stack), if they exist.

if exist('Qaug')*exist('Raug')~=1,
  Qaug=diag([1 0 1 0 0])
  Raug=diag([1 1]);
end;

%Compute feedback gains for the augmented dynamics and the
%selected error and control weightings, using the function "lqr".

[Kr,S]=lqr(Aaug,Baug,Qaug,Raug);
Kr
[vcl,evcl]=eig(Aaug-Baug*Kr);
evcl=diag(evcl)
[Wncl,Zcl]=damp(evcl);
[Wncl,Zcl]
abs(vcl)

%Compute and plot open loop frequency response.
%Note that Col and Dol have minus signs so that "bode"
%evaluates GH rather than -GH (see block diagram).
%The loop is broken twice: once at the aileron command
%and once at the rudder command.

[Aol,Bol,Col,Dol]=linmod('RollyawOLa');
[mgola,phola]=bode(Aol,Bol,-Col,-Dol,1,om);
clg;
subplot(221);
if exist('mgolalast')*exist('mgola0')==1,
  loglog(om,[mgola,mgolalast mgola0]);
elseif exist('mgolalast')==1,
  loglog(om,[mgola,mgolalast]);
else
  loglog(om,mgola);
end;
title('Open Loop LQR FR: Aileron');
xlabel('Frequency (rad/s)');ylabel('Magnitude');
subplot(223);
if exist('pholalast')*exist('phola0')==1,
  semilogx(om,[phola,pholalast phola0]);
elseif exist('pholalast')==1,
  semilogx(om,[phola,pholalast]);
else
```

```
  semilogx(om,phola);
end;
xlabel('Frequency (rad/s)');ylabel('Phase (deg)');
[Aol,Bol,Col,Dol]=linmod('RollyawOLr');
[mgolr,pholr]=bode(Aol,Bol,-Col,-Dol,1,om);
subplot(222);
if exist('mgolrlast')*exist('mgolr0')==1,
  loglog(om,[mgolr,mgolrlast mgolr0]);
elseif exist('mgolrlast')==1,
  loglog(om,[mgolr,mgolrlast]);
else
  loglog(om,mgolr);
end;
title('Open Loop LQR FR: Rudder');
xlabel('Frequency (rad/s)');ylabel('Magnitude');
subplot(224);
if exist('pholrlast')*exist('pholr0')==1,
  semilogx(om,[pholr,pholrlast pholr0]);
elseif exist('pholrlast')==1,
  semilogx(om,[pholr,pholrlast]);
else
  semilogx(om,pholr);
end;
xlabel('Frequency (rad/s)');ylabel('Phase (deg)');
```

```
Learjet Model 24 3 deg/s turn in flight condition 3

Open loop eigenvalues
-2.7189e-02+  2.2741e+00i
-2.7189e-02-  2.2741e+00i
-2.2733e+00
-8.5389e-04
-5.0717e-20

»diag(Qaug)'=
 1.0000e-01             0   1.0000e+05             0             0

Raug =
   1.0001e+03   1.0256e+02
   1.0256e+02   2.6065e+03

Feedback gains
Kr =
   6.4222e-03   8.6736e-02   1.0996e+00   2.7898e-01   7.3053e-03
   1.8039e-03   4.1943e-02  -6.1807e+00   7.1804e-02   1.8803e-03

Closed loop eigenvalues
-1.8701e+01
-1.3476e+00+  1.5102e+00i
-1.3476e+00-  1.5102e+00i
-2.6708e+00
-1.1946e-11

Closed loop natural frequencies and damping ratios
   1.8701e+01   1.0000e+00
   2.0240e+00   6.6579e-01
   2.0240e+00   6.6579e-01
   2.6708e+00   1.0000e+00
   1.1946e-11   1.0000e+00

Closed loop eigenvectors
   9.9837e-01   9.9044e-01   9.9044e-01   9.7748e-01   4.1873e-11
   4.7360e-02   1.2365e-01   1.2365e-01   1.9765e-01   3.1258e-13
   3.1748e-02   4.8493e-04   4.8493e-04   6.5683e-05   1.1942e-11
   2.5325e-03   6.1092e-02   6.1092e-02   7.4003e-02   2.6177e-02
   1.6977e-03   2.3958e-04   2.3958e-04   2.4593e-05   9.9966e-01
```

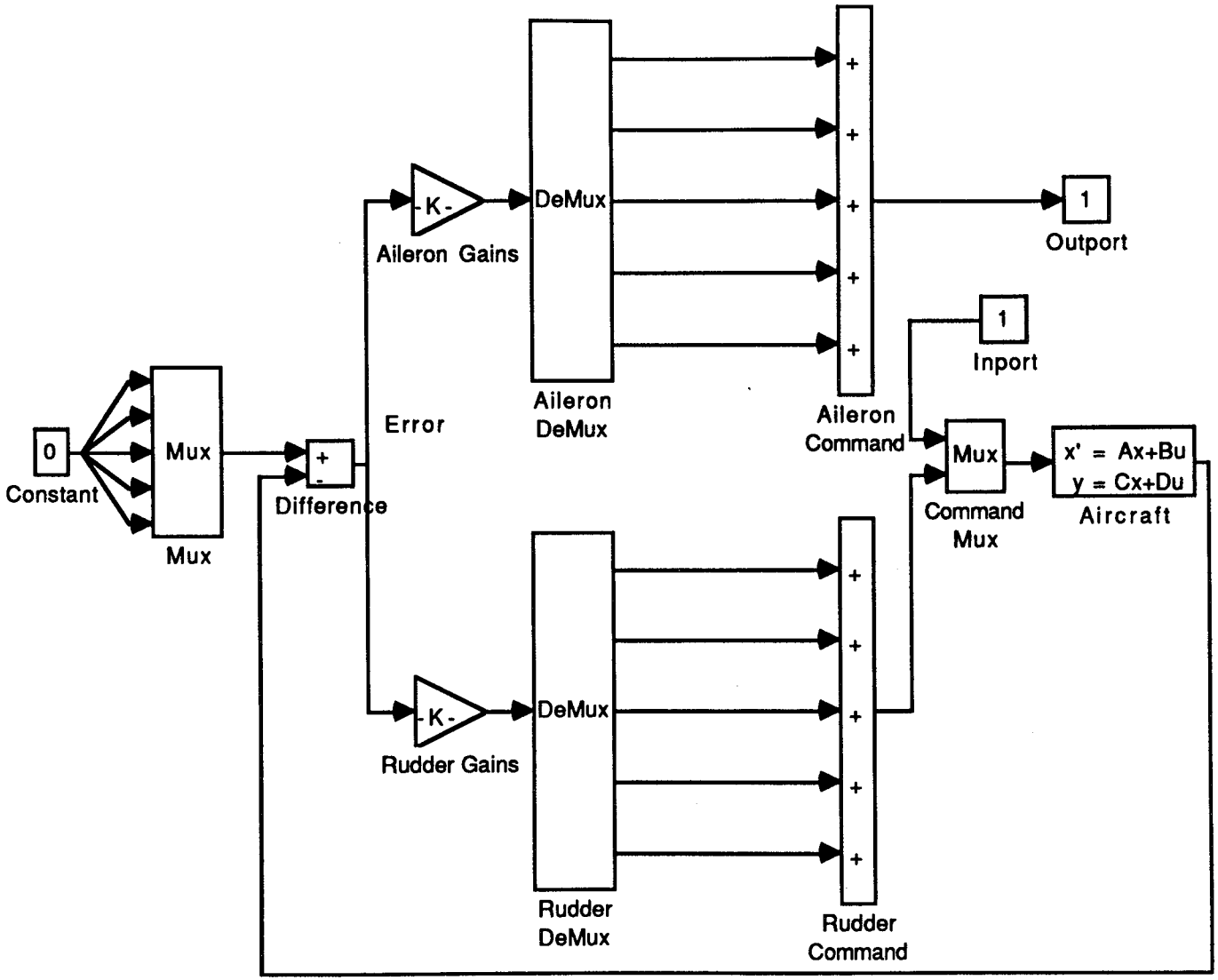

OPEN LOOP ANALYSIS OF A LINEAR, QUADRATIC REGULATOR FOR AIRCRAFT LATERAL DYNAMIC

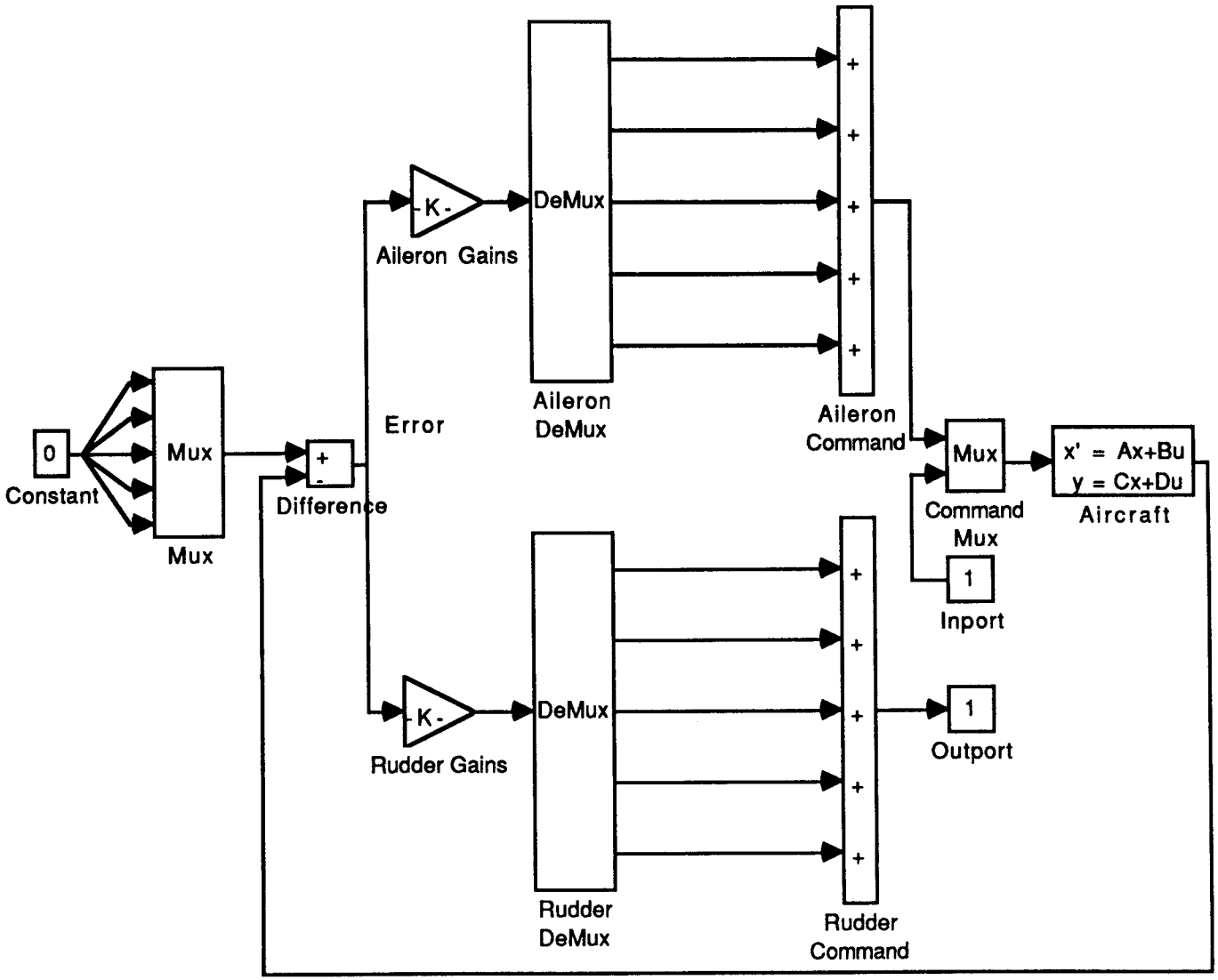

OPEN LOOP ANALYSIS OF A LINEAR, QUADRATIC REGULATOR FOR AIRCRAFT LATERAL DYNAMIC

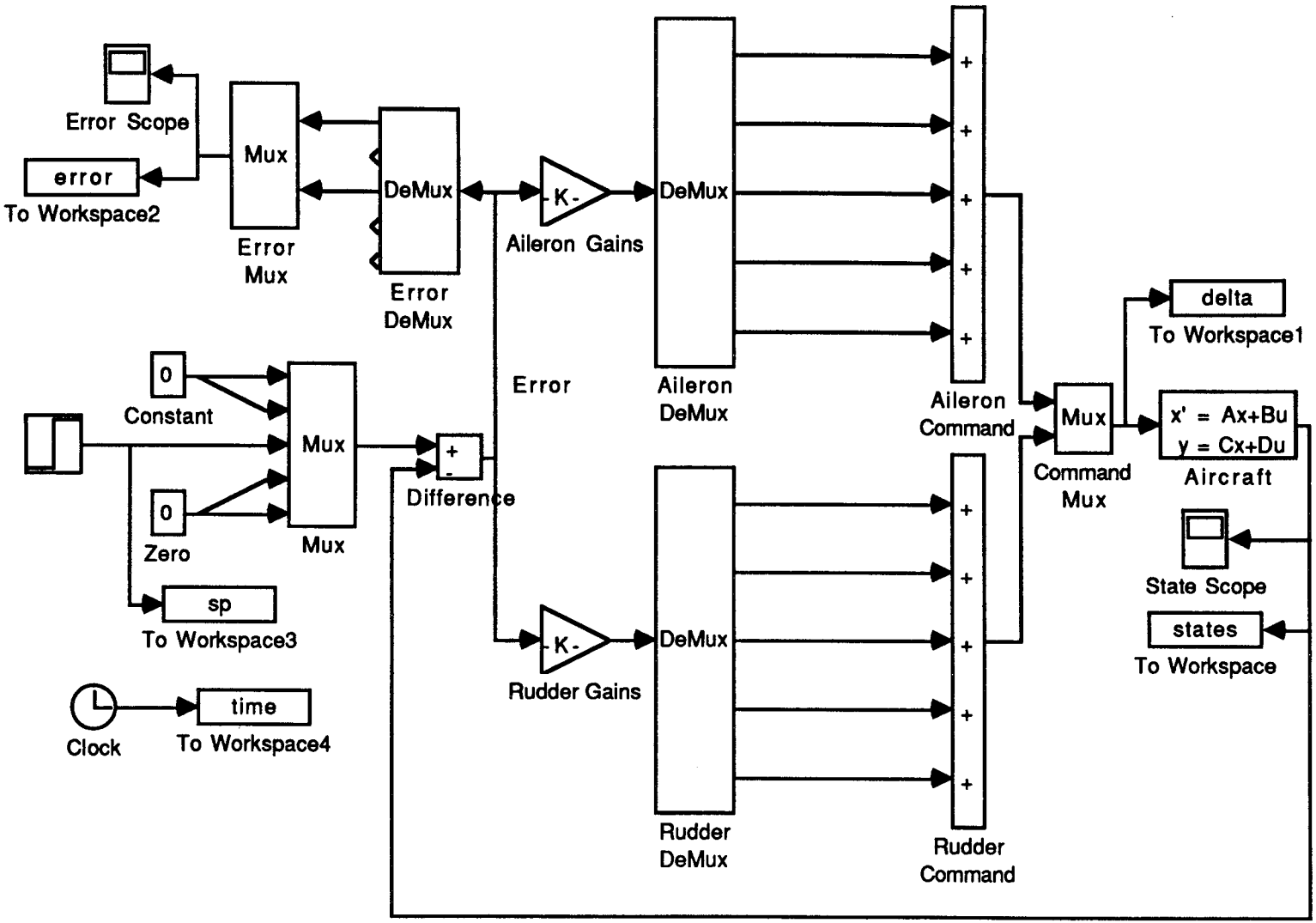

SIMULATION OF A LINEAR-QUADRATIC REGULATOR FOR AIRCRAFT LATERAL DYNAMICS

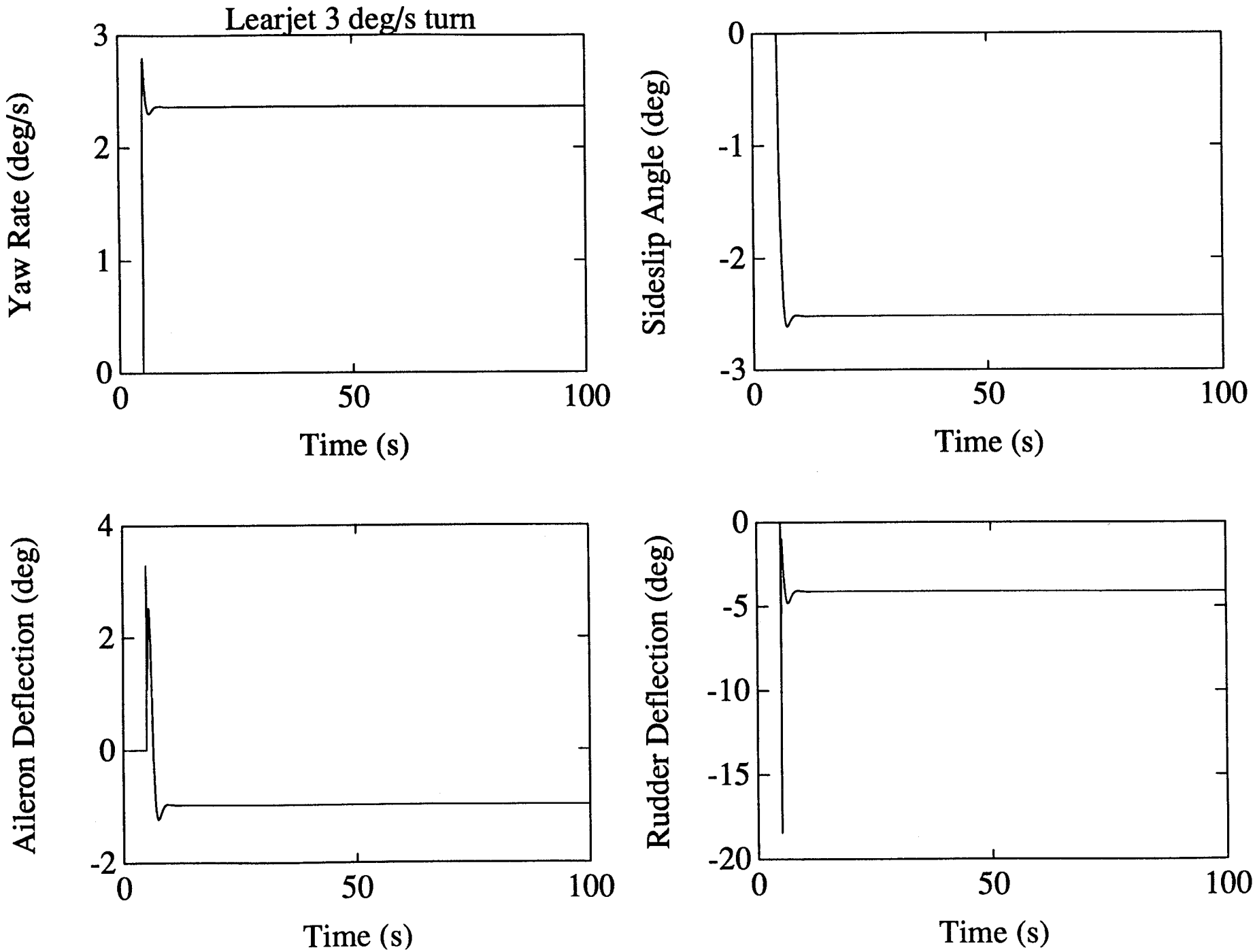
Learjet 3 deg/s turn
Yaw Rate (deg/s)
3
2
1
0
0
50
100
Time (s)
Sideslip Angle (deg)
0
-1
-2
-3
0
50
100
Time (s)
Aileron Deflection (deg)
4
2
0
-2
0
50
100
Time (s)
Rudder Deflection (deg)
0
-5
-10
-15
-20
0
50
100
Time (s)

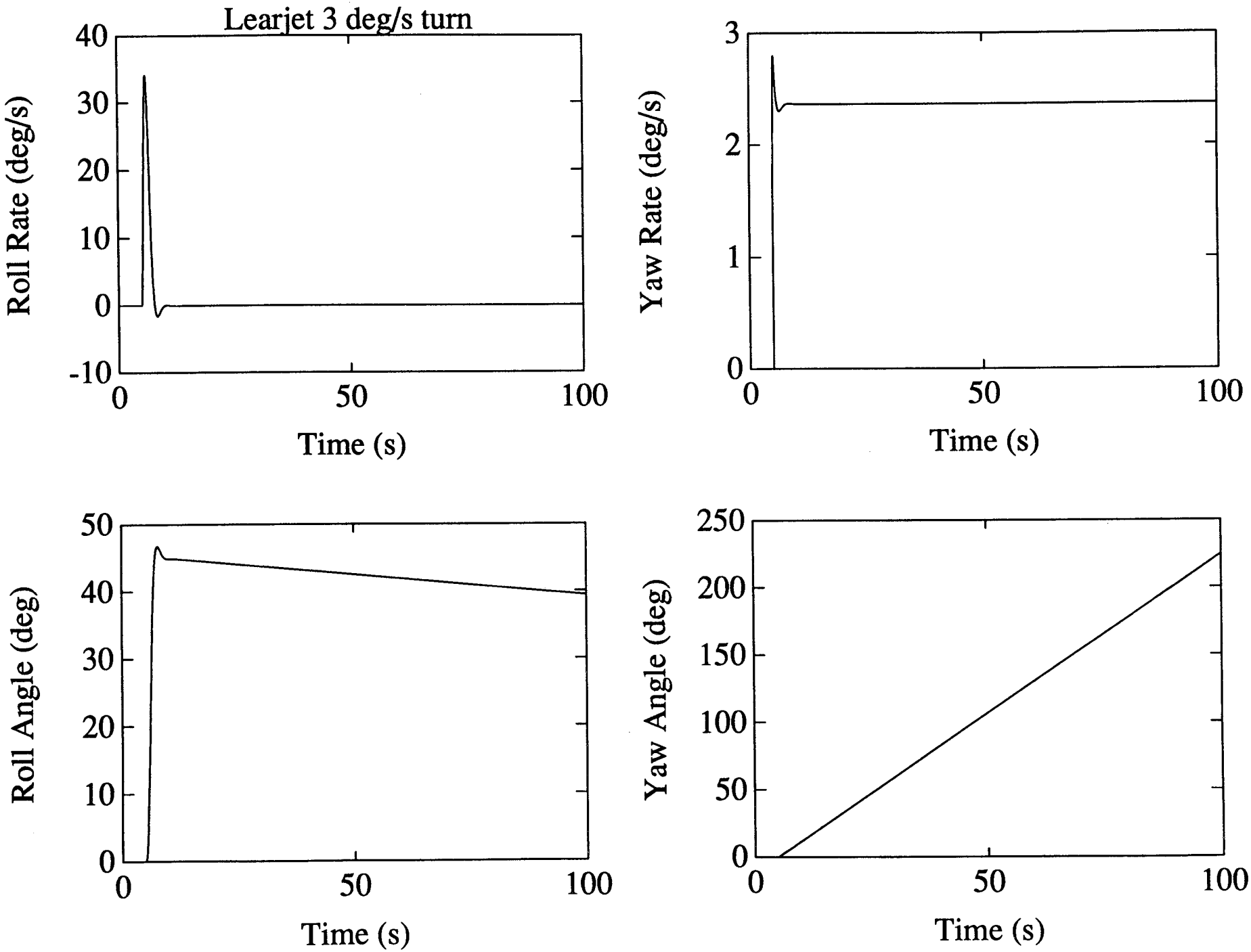
Learjet 3 deg/s turn
Roll Rate (deg/s)
40
30
20
10
0
-10
0
50
100
Time (s)
Yaw Rate (deg/s)
3
2
1
0
0
50
100
Time (s)
Roll Angle (deg)
50
40
30
20
10
0
0
50
100
Time (s)
Yaw Angle (deg)
250
200
150
100
50
0
0
50
100
Time (s)

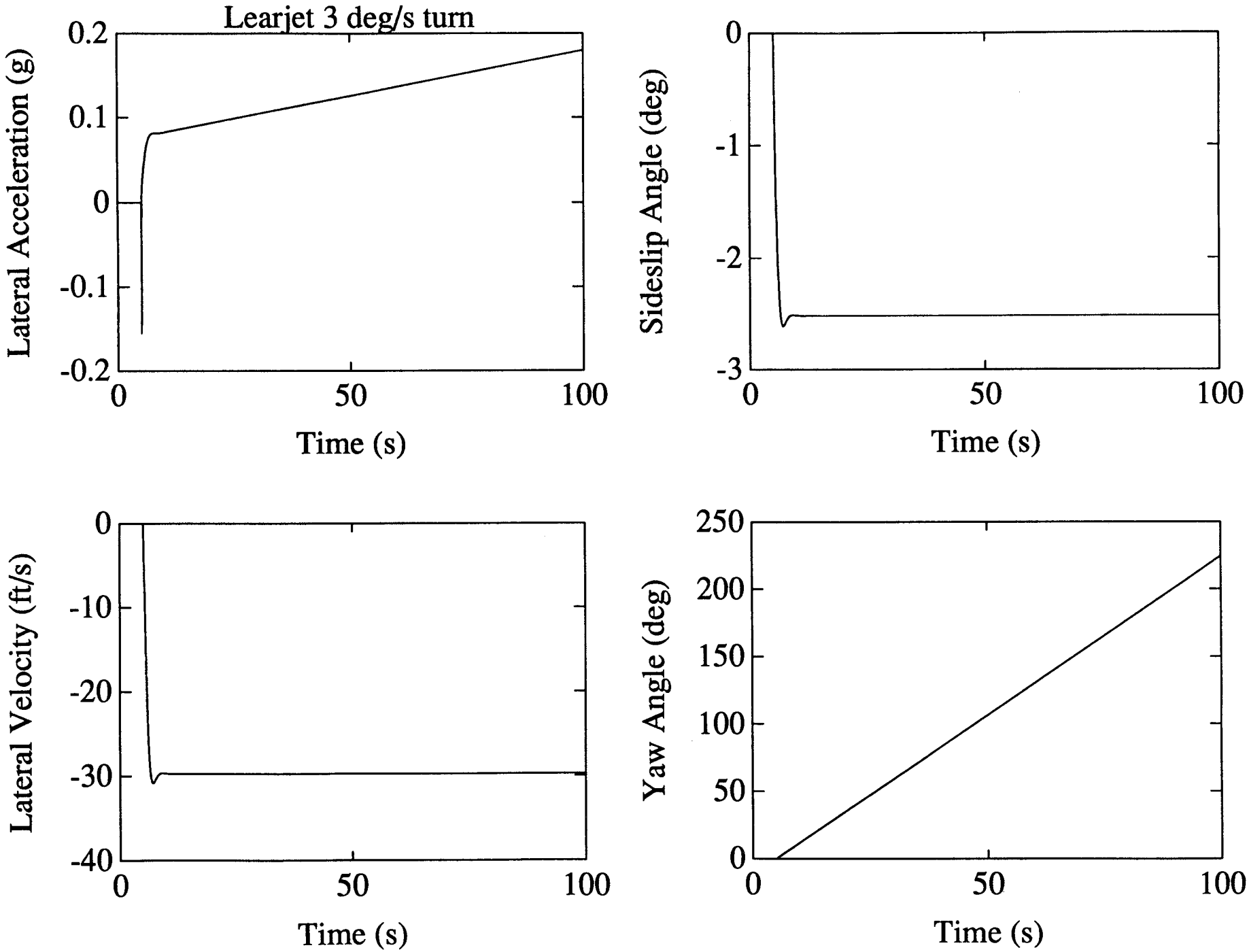
Learjet 3 deg/s turn
Lateral Acceleration (g)
0.2
0.1
0
-0.1
-0.2
0
50
100
Time (s)
Sideslip Angle (deg)
0
-1
-2
-3
0
50
100
Time (s)
Lateral Velocity (ft/s)
0
-10
-20
-30
-40
0
50
100
Time (s)
Yaw Angle (deg)
250
200
150
100
50
0
0
50
100
Time (s)

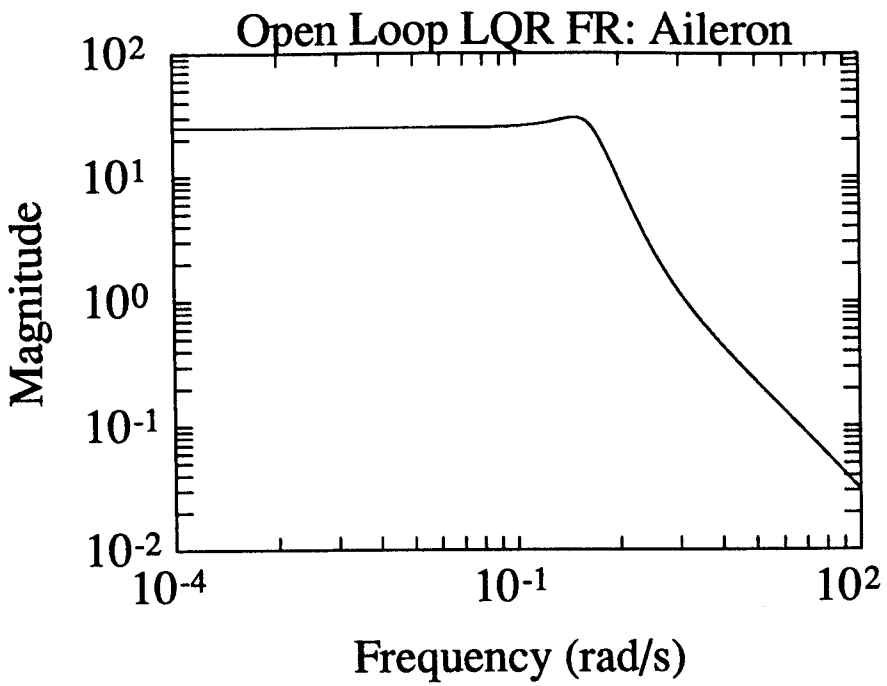
Open Loop LQR FR: Aileron
Magnitude
10^2
10^1
10^0
10^{-1}
10^{-2}
10^{-4}
10^{-1}
10^2
Frequency (rad/s)

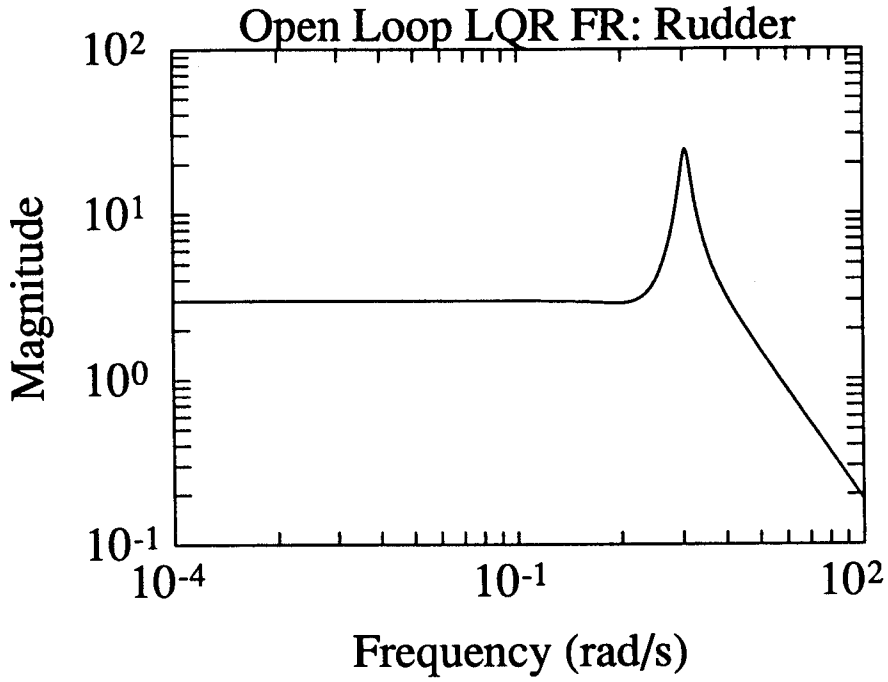
Open Loop LQR FR: Rudder
Magnitude
10^2
10^1
10^0
10^{-1}
10^{-4}
10^{-1}
10^2
Frequency (rad/s)

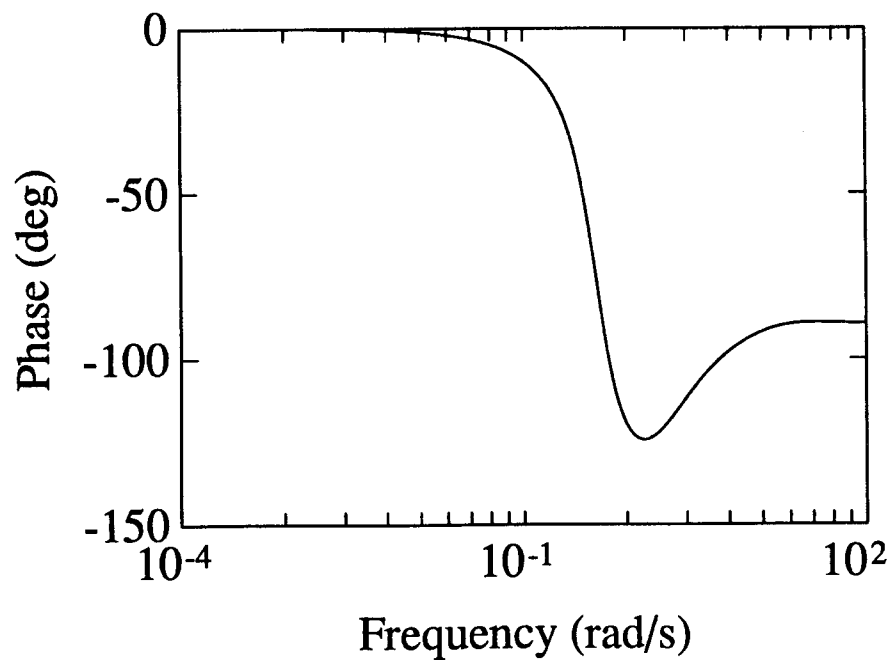
Phase (deg)
0
-50
-100
-150
10^{-4}
10^{-1}
10^2
Frequency (rad/s)

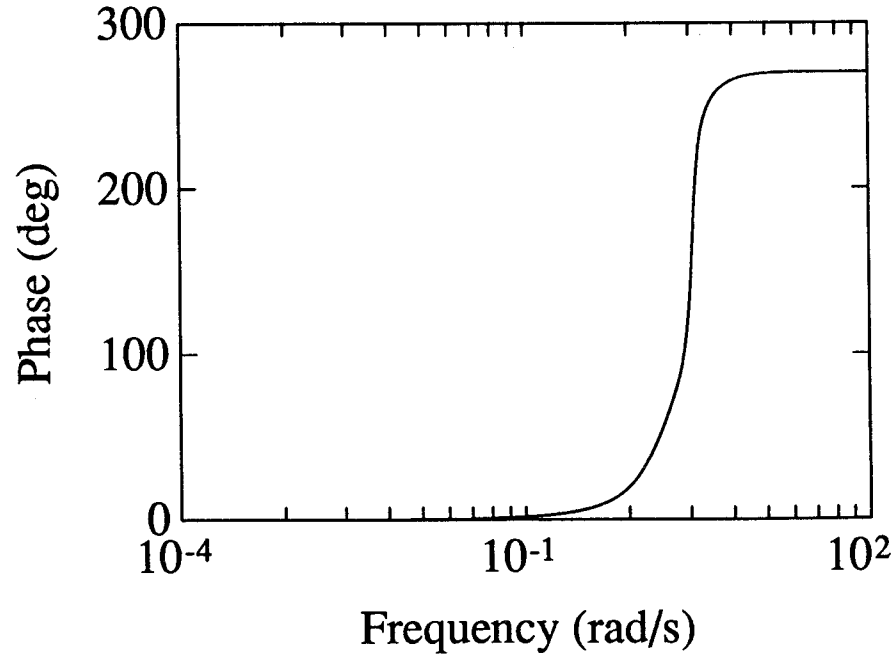
Phase (deg)
300
200
100
0
10^{-4}
10^{-1}
10^2
Frequency (rad/s)